

This work is protected by copyright and other intellectual property rights and duplication or sale of all or part is not permitted, except that material may be duplicated by you for research, private study, criticism/review or educational purposes. Electronic or print copies are for your own personal, non-commercial use and shall not be passed to any other individual. No quotation may be published without proper acknowledgement. For any other use, or to quote extensively from the work, permission must be obtained from the copyright holder/s.

The sedimentological characteristics of basal ice  
and their preservation within the proglacial  
environment

Stephanie Lauren Cutts

This thesis is submitted for the degree of Master  
of Philosophy

December 2016

Keele University

## Abstract

---

The identification of distinctive sedimentological characteristics within the basal ice layer (BIL), and their potential preservation within the proglacial environment, is crucial to enhancing our understanding of glaciological conditions beneath ice masses. Though much work has focussed on understanding the nature and formation of basal ice, its diagnostic sedimentological characteristics and the circumstances in which they might be preserved remain unclear.

Field work at Svínafellsjökull in southeast Iceland was carried out to establish whether specific sedimentological characteristics from the BIL could be identified within the proglacial environment. This involved sampling the basal ice and proglacial sedimentology at seven key sites for grain size analysis. Particle size data collected from the BILs of six glaciers from around the world were also used to provide a broader global context.

Six key basal ice types were identified at Svínafellsjökull along with two distinct proglacial landforms (moraines and minor outwash fans) and other proglacial sediments. The findings suggest that basal ice is most easily recognised within the proglacial environment through the transfer of the high volume of silt contained within some basal ice facies (<50%) and the formation of minor outwash fans. The grain size data from Svínafellsjökull and six other glaciers has provisionally defined the envelope for the sedimentology of basal ice: a low sand content (>15%), a high silt content (between 50% and 80%) and a low to medium clay content between 15% and 30%.

The results indicate that whilst basal ice sediments are sedimentologically distinct, these distinctive characteristics are not always clearly distinguishable within the proglacial sediments. Future research should therefore utilise a broader range of sedimentological criteria derived from a greater number of sites in order to identify diagnostic criteria more frequently preserved within the proglacial environment.

## Acknowledgements

---

Firstly, thank you to my wonderful parents who have supported me both emotionally and financially throughout my time at university. I know I'm incredibly lucky to have parents who have always allowed me to walk the path I wanted to and have helped me in doing so, regardless of the cost to them.

To my family, thank you for always keeping my spirits up and keeping me grounded. I couldn't have done any of this without you all. Special thanks to my Aunty Karen and Grammy, who have provided a listening ear and support whenever I've stumbled.

Huge thanks to Ian Wilshaw and Rich Burgess. You guys are amazing! Thank you for your support with all things technical! Most people who know me are aware that I practically repel technology so I most definitely wouldn't have been able to do this without you both.

Thank you to Spikey and all the staff who I've worked with at the KPA! Frankie, Bea, T, Alice, Nat, Jules, Dan, JJ, Rob, Niall, Jo Lea, Arun, Luke and to my regulars, Elliot, Daz, Prof, Dr. Dan and Matty! You've all been absolute stars and many of you have cheered me up when I've felt a bit down and offered me encouragement to see this thesis through. Thank you all!

To my office lot and fellow postgrads, Liam, Amy, Luke, Amir, Adam and Frankie thanks for providing support, advice and laughter over these last two years! To Liam, my kindred spirit, thanks for hours of laughter and quoting our favourite shows, 'Thank God it's Friday!!'

Thank you to my two fantastic wives, Nat and Lyane. I couldn't have asked to find two better lasses who have supported me the entire way through this masters, whether it's been offering advice, cheering me up when I've felt low, encouraging me when I felt like giving up or providing hours of laughter and enjoyment away from it all, you two are the absolute bee's knees.

Thanks to Simon Cook for providing samples from Storglaciären and for offering advice and insight into all things Svínafellsjökull, much appreciated!

To my two absolutely magnificent supervisors Rich and Peter, thank you for everything. Not only have you put up with me for nigh on 6 years now, you've supported me through several trying times throughout these last two years, with what seems like endless amounts of patience. I couldn't have asked for two better individuals who have provided me with guidance, support, and a push in the right direction whenever I've got stuck in the mud along the way. Not to mention the opportunities to get out to Iceland for field work!

Thank you to my wonderful Leopold who has been my rock throughout this Masters. You've picked me up when I've stumbled, pushed me when I needed it and listened when I've ranted. I've spent countless days laughing (Stormtrooper?!) and enjoying myself with you, without which I probably wouldn't have made it through this Masters project! Not to mention the hours you've spent in the last few weeks proof reading for me and being a general excel wizard. You've been a light for me in some dark places throughout this journey. Thank you for everything.

Finally, thank you to my absolutely amazing partner Pete. You may not have been with me throughout the original project, but you're the one who has helped me to get over the final hurdle and complete my corrections. I couldn't have done it without you, or the endless support you have provided, despite the countless times I told myself I couldn't do it. You truly are my brightest star.

The thesis is dedicated to the memory of my Grandad,  
Norman Gouland.

‘Despair is only for those who see the end beyond all doubt.’

*-Gandalf*

*(J.R.R. Tolkien, The Fellowship of the Ring)*

## Table of Contents

<a href="#">1. INTRODUCTION</a>	1
<a href="#">1.1 Rationale</a>	1
<a href="#">1.2 Aim</a>	3
<a href="#">1.3 Specific Objectives</a>	3
<a href="#">2. LITERATURE REVIEW</a>	5
<a href="#">2.1 The basal ice layer</a>	5
<a href="#">2.1.1 Characteristics</a>	5
<a href="#">2.1.2 Processes of formation</a>	6
<a href="#">2.2 Sedimentology of basal ice</a>	8
<a href="#">2.2.1 Introduction</a>	8
<a href="#">2.2.2 Sediment Concentration</a>	13
<a href="#">2.2.3 Clast Shape and roundness</a>	15
<a href="#">2.2.4 Particle size distribution</a>	17
<a href="#">2.3 Preservation within proglacial landforms</a>	20
<a href="#">2.3.1 Moraines</a>	20
<a href="#">2.3.2 Minor outwash fans</a>	21
<a href="#">2.4 Preservation within glacial sediments</a>	22
<a href="#">2.5 Summary</a>	27
<a href="#">3. FIELD WORK SITE AND METHODS</a>	29
<a href="#">3.1 Fieldwork Location</a>	29
<a href="#">3.2 Bedrock Geology</a>	31
<a href="#">3.3 Site selection and description</a>	32
<a href="#">3.4 Sampling Method</a>	33
<a href="#">3.5 Collection of samples for grain-size analysis</a>	34
<a href="#">3.5.1 Sample Preparation</a>	35
<a href="#">3.5.2 Laser Granulometry Analysis</a>	35
<a href="#">3.6 Data Presentation</a>	36
<a href="#">3.7 Secondary Data Use</a>	37
<a href="#">4. THE SEDIMENTOLOGICAL CHARACTERISTICS OF BASAL ICE AND THEIR PRESERVATION AT SVÍNAFELLSJÖKULL</a>	38
<a href="#">4.1 Introduction</a>	38
<a href="#">4.2 Field Sites, Svínafellsjökull</a>	38
<a href="#">4.2.1 Facies Classification</a>	40

<a href="#">4.2.2 The Proglacial Environment at Svínafellsjökull</a>	44
<a href="#">4.2.3 Site 1 (63°59'50.67N, 16°52'37.32W)</a>	46
<a href="#">4.2.4 Site 1 grain size analysis</a>	48
<a href="#">4.2.5 Site 2 (63°59'43.49N, 16°52'41.18W)</a>	50
<a href="#">4.2.6 Site 2 grain size analysis</a>	52
<a href="#">4.2.7 Site 3 (63°59'40.67N, 16°52'30.66W)</a>	54
<a href="#">4.2.8 Site 3 grain size analysis</a>	59
<a href="#">4.2.9 Site 9 (63°59'40.95N, 16°52'25.89W)</a>	60
<a href="#">4.2.10 Site 4 grain size analysis</a>	63
<a href="#">4.2.11 Site 5 (63°59'40.14N, 16°52'24.38W)</a>	66
<a href="#">4.2.12 Site 5 grain size analysis</a>	69
<a href="#">4.2.13 Site 6 (63°59'35.77N, 16°52'21.77W)</a>	71
<a href="#">4.2.14 Site 6 grain size analysis</a>	74
<a href="#">4.2.15 Site 7 (63°59'25.11N, 16°52'04.60W)</a>	76
<a href="#">4.2.16 Site 7 grain size analysis</a>	78
<a href="#">4.2.17 Site 8 (63°59'23.22N, 16°51'59.68W)</a>	80
<a href="#">4.2.18 Site 8 grain size analysis</a>	83
<a href="#">4.2.19 Summary of grain size data for all ice types</a>	84
<a href="#">4.3 Ternary Plots</a>	86
<a href="#">4.3.1 Svínafellsjökull basal ice samples</a>	87
<a href="#">4.3.2 Svínafellsjökull proglacial samples</a>	90
<a href="#">4.3.3 Comparison of basal ice and proglacial samples</a>	91
<a href="#">4.4 Spatial Analysis</a>	92
<a href="#">4.5 Summary</a>	96
<a href="#">5. SEDIMENTOLOGY OF BASAL ICE: A GLOBAL PERSPECTIVE</a>	100
<a href="#">5.1 Introduction</a>	100
<a href="#">5.2 Analysis of the data</a>	101
<a href="#">5.2.1 Ferpècle Glacier, Switzerland</a>	103
<a href="#">5.2.2 Storglaciären, Sweden</a>	105
<a href="#">5.2.3 Root Glacier, Alaska</a>	107
<a href="#">5.2.4 Matanuska Glacier, Alaska</a>	110
<a href="#">5.2.5 Russell Glacier, Greenland</a>	112
<a href="#">5.2.6 Skeiðarárjökull, Iceland</a>	115
<a href="#">5.3 Comparison of basal ice data from all glaciers</a>	118

<a href="#">5.4 Summary</a>	120
<a href="#">6.0 DISCUSSION</a>	122
<a href="#">6.1 Synthesis</a>	122
<a href="#">6.2 The sedimentological characteristics of basal ice at Svínafellsjökull</a>	125
<a href="#">6.3 Global variations in the sedimentology of basal ice</a>	127
<a href="#">6.4 Preservation within the proglacial environment</a>	129
<a href="#">6.4.1 Introduction</a>	129
<a href="#">6.4.2 Moraines</a>	129
<a href="#">6.4.3 Ice-marginal Sediments</a>	131
<a href="#">6.4.4 Minor outwash fans</a>	132
<a href="#">6.5 Wider Implications</a>	135
<a href="#">6.6 Scope for future research</a>	137
<a href="#">7.0 CONCLUSIONS</a>	139
<a href="#">7.1 Key findings</a>	139
<a href="#">7.2 Focus for future research</a>	142
<a href="#">REFERENCES</a>	144
<a href="#">APPENDICES</a>	152
<a href="#">Appendix A: Raw Grain Size Data</a>	152
<a href="#">Appendix B: Cumulative Volume Graphs</a>	286

## List of Figures

Figure 2.1	Scale of roundness (Powers, 1953).	16
Figure 2.2	A ternary plot highlighting the various textural groupings of the facies at Matanuska. Almost all of the facies exhibited a preference for grain size distribution, aside from the solid subfacies (Lawson, 1979).	19
Figure 3.1	Map showing location of Svínafellsjökull.	30
Figure 3.2	Map showing bedrock geology of Svínafellsjökull (modified from Skaftafell Bedrock Geology map).	31
Figure 4.1	Google Earth image showing the locations of the sample sites around the Svínafellsjökull margin (Google Earth, 2014).	40
Figure 4.2	(a) ice type A, (b) ice type B, (c) ice type C, (d) ice type E, (e) ice type D, (f) frazil ice.	43
Figure 4.3	Image showing the southern margin and the proglacial area at Svínafellsjökull.	44
Figure 4.4	The exposure at site 1. 'A' highlights the location of the facies which forms crudely stratified laminations. 'B' marks the location of the larger clasts dispersed throughout the facies which are between 5 and 10 cm in diameter. Person for scale.	47
Figure 4.5	A view of the wider proglacial area at site 1. Box highlights exposure. Dashed line indicates the edge of the ice margin and the start of the proglacial environment. Ice axe for scale is approximately 0.5 m.	48
Figure 4.6	Grain size distribution plot for site 1.	49
Figure 4.7	(a) Image showing the exposure which features two distinct facies. Walking pole for scale is approximately 1 m. (b): A close up image of the ice types. Dashed line highlights the boundary between ice type D on the left and ice type B on the right. (c): Image showing a thin section of ice carved from ice type B at site 2. Dashed lines highlight the presence of crude laminations of sediment aggregates within the ice.	51
Figure 4.8	An image of the basal ice exposure at site 2. Dashed line indicates the edge of the margin. 'A' highlights the area that was sampled for grain size analysis. Walking pole (1 m) for scale.	52
Figure 4.9	Grain size distribution plot for site 2.	53
Figure 4.10	(a): An image of the exposure at site 3 highlighting the fracture at the ice margin and the boundary between the facies and englacial ice. Spade for scale is approximately 1 m. (b): A close up image of the hollow that features in the facies at site 3. Coin	56

	for scale is 2 cm in diameter. (c): An image depicting the ‘clots’ of fine-grained sediment within the hollow, with lenses of clear englacial ice. Coin for scale is 2 cm in diameter.	
Figure 4.11	The proglacial environment at site 3. ‘A’ highlights area where melt-out sediments were sampled, ‘B’ identifies location of minor outwash fans sampled and ‘C’ marks the edge of a moraine (approx. 10 m high). Person for scale.	57
Figure 4.12	(a): Pit dug out of minor outwash fan sampled at site 3. (b): Cross section of minor outwash fan sampled at site 3. (c): Minor outwash fan. Note the drainage from supraglacial material into the fan.	58
Figure 4.13	Grain size distribution plot for site 3.	59
Figure 4.14	A view of the exposure at site 4. ‘A’ indicates the exposure, ‘B’ highlights sediments that are sampled. Pole is approximately 1m for scale.	61
Figure 4.15	The exposure and glacier margin at site 4. ‘A’ indicates supraglacial material located on surface of glacier and ‘B’ highlights the melt-out sediments sampled. Person for scale.	62
Figure 4.16	Grain size distribution plot for site 4.	63
Figure 4.17	(a) An image of site 5 highlighting the location of the two ice types. The red arrow indicates the area where ice type B was sampled and the yellow area indicates the sampling site for ice type A. (b): Ice type B featured at site 5. This facies has crudely stratified layers of silt and sand. Trowel for scale is approximately 25 cm. (c): Ice type A featured at site 5. This facies also features laminations of sediment within the ice, but they are more distinct and the sediment is primarily finer grained (silt and clay).	67
Figure 4.18	Image depicting the proglacial environment at site 5. ‘A’ indicates proglacial lakes, ‘B’ shows the location of a minor outwash fan and ‘C’ highlights a group of small moraines approximately 1-1.5 m high. Person for scale.	68
Figure 4.19	Grain size distribution plot for site 5.	69
Figure 4.20	(a): The exposure at site 6. Person for scale (b): The three ice types featured at site 6. (c): A close up image of ice type E. These are pockets within the ice, infilled with high concentrations of silt.	72
Figure 4.21	Proglacial environment at site 6. Box indicates location of exposure. ‘A’ highlights the moraine situated directly in front of the exposure approximately 1.5 m high. Rucksack for scale	73

	is approximately 0.5 m.	
Figure 4.22	Grain size distribution plot for site 6.	74
Figure 4.23	(a): The exposure at site 7. Ice axe is approximately 0.65 m. (b): The facies at site 7. Interlocking lines within the ice resemble a herringbone pattern, which is only seen at this sampling site. Ice axe pick visible is approximately 5 cm in length.	77
Figure 4.24	(a): The proglacial environment at site 7 features a small moraine and an outwash fan flowing out from the exposure. (b): A cross section through one of the minor outwash fans at site 7. These are dominated by silt and small amounts of clay but also feature occasional sand partings of ~1 mm in thickness.	78
Figure 4.25	Grain size distribution plot for site 7.	79
Figure 4.26	An image of the frazil ice section found at the edge of the main meltwater channel at Svínafellsjökull. Person for scale.	81
Figure 4.27	A closer view of the large interlocking plates which form the frazil ice section. The ice contains very fine sediment, compacted between the ice plates.	82
Figure 4.28	Grain size distribution for Site 8.	83
Figure 4.29	Summary graph of grain size characteristics of all ice types identified across the eight sampling sites	85
Figure 4.30	Ternary plot showing the composition of samples taken from basal ice facies around the margin of Svínafellsjökull.	87
Figure 4.31	Ternary plot showing the composition of samples collected from the proglacial environment around the margin of Svínafellsjökull.	90
Figure 4.32	Ternary plot showing the composition of samples taken from basal ice facies and proglacial features around the margin of Svínafellsjökull.	91
Figure 4.33	Diagram highlighting the distribution of different ice types around the margin of Svínafellsjökull and the local geomorphology in the surrounding proglacial environment.	93
Figure 4.34	Silt content within each ice type and proglacial feature on a site by site basis.	94
Figure 5.1	Location map of the glacier sites used for basal ice layer sampling.	102
Figure 5.2	Grain size distribution plot of basal ice at Ferpècle.	104

Figure 5.3	Ternary plot of the basal ice samples collected at Ferpècle.	104
Figure 5.4	Grain size distribution plot of the basal ice samples from Storglaciären.	106
Figure 5.5	Ternary plot of basal ice samples from Storglaciären.	106
Figure 5.6	Grain size distribution plot of the samples taken from the Root glacier.	108
Figure 5.7	Ternary plot of Root glacier samples.	109
Figure 5.8	Grain size distribution plot of Matanuska samples.	110
Figure 5.9	Ternary Plot of samples from Matanuska glacier.	111
Figure 5.10	Grain size distributions of the samples collected at the Russell Glacier, Greenland.	113
Figure 5.11	Grain size distributions of the samples collected at the Russell Glacier, Greenland.	113
Figure 5.12	Ternary plot of samples collected from Russell Glacier, Greenland.	114
Figure 5.13	Grain size distributions of the samples collected at Skeiðarárjökull, Iceland.	116
Figure 5.14	Ternary plot of Skeiðarárjökull samples, Iceland.	117
Figure 5.15	Comparison ternary plot showing all samples.	119

## List of Tables

Table 2.1	Sedimentological characteristics of basal ice facies identified in the literature.	9-12
Table 2.2	A table showing the varying attributes of the different facies at Matanuska, Alaska including grain size distributions and sediment concentrations (Lawson, 1979).	14
Table 4.1	Descriptions of the basal ice facies identified around the margin at Svínafellsjökull.	41-42
Table 4.2	Summary data table for site 1. (PS = Poorly Sorted, VPS = Very Poorly Sorted)	50
Table 4.3	Summary data table for site 2. (PS = Poorly Sorted, VPS = Very Poorly Sorted)	54
Table 4.4	Summary data table for site 3. (PS = Poorly Sorted, VPS = Very Poorly Sorted)	60
Table 4.5	Summary data table for site 4. (PS = Poorly Sorted, VPS = Very Poorly Sorted)	65
Table 4.6	Summary data table for site 5. (PS = Poorly Sorted, VPS = Very Poorly Sorted)	70
Table 4.7	Summary data table for site 6. (PS = Poorly Sorted, VPS = Very Poorly Sorted)	75
Table 4.8	Summary data table for site 7. (PS = Poorly Sorted, VPS = Very Poorly Sorted)	80
Table 4.9	Summary data table for frazil ice. (PS = Poorly Sorted, VPS = Very Poorly Sorted)	84
Table 5.1	Summary data table for Ferpècle. (PS = Poorly Sorted, VPS = Very Poorly Sorted)	105
Table 5.2	Summary data table for Storglaciären. (PS = Poorly Sorted, VPS = Very Poorly Sorted)	107
Table 5.3	Summary data table for the Root glacier. (PS = Poorly Sorted, VPS = Very Poorly Sorted)	109
Table 5.4	Summary data table for Matansuka (PS = Poorly Sorted, VPS = Very Poorly Sorted)	112
Table 5.5	Summary data table for Russell glacier (PS = Poorly Sorted, VPS = Very Poorly Sorted)	115
Table 5.6	Summary data table for Skeiðarárjökull. (PS = Poorly Sorted, VPS = Very Poorly Sorted)	118

Table 5.7	The mean percentage of sand, silt and clay of three sample sets	120
-----------	-----------------------------------------------------------------	-----



# 1. INTRODUCTION

---

## 1.1 Rationale

---

There has been a great deal of research conducted on the basal ice layer (BIL) of glaciers worldwide. This has focussed primarily on the various theories of its formation, the processes that operate within the subglacial zone and the sedimentology of the BIL.

Research into the basal ice layer has involved the study of its complex sedimentology and extended to the identification and classification of the different types of basal ice facies based on their visual and sedimentological characteristics (Hubbard and Sharp, 1989, Knight, 1997). The use of microtextures, debris volume, clast shape and roundness or till fabric can ascertain which characteristics are associated with the various sources for basal ice sediments (Whalley and Krinsley, 1974, Reheis, 1975, Boulton, 1978) or to distinguish between facies created by different formation processes (Cook et al., 2011).

Despite this, there is still limited knowledge surrounding whether sediments can be preserved once they have been disturbed, whether sedimentary characteristics are being preserved in or contributing to specific landforms or types of sediments, and a lack of sedimentological criteria to establish and identify the preservation of such sediments. Glaciologists' understanding of sediment transfer pathways, especially those that are active between the basal ice layer and the proglacial environment, is also far from complete.

Initial research has examined whether basal ice displays distinctive sedimentological characteristics of the basal ice types that make them distinctive. If so, these sedimentological distinctions could provide a basis from which to establish a set of

diagnostic criteria in an attempt to track their transfer to proglacial sediments and landforms, and establish if they are being preserved here.

Previous work has looked at potential preservation of basal ice sediments within subglacial melt-out tills (Goodchild, 1875, Lawson, 1979, Paul and Eyles, 1990), moraines (Knight et al., 2000, Adam and Knight, 2003) and proglacial sediments (Lawson, 1979, Cook et al., 2011), examining a range of parameters such as particle size distributions, fractal dimensions or surface microtextures. Much of the previous work has also been restricted to identifying specific sedimentological characteristics and criteria for preservation at individual sites. Whilst this is useful on a site by site basis, it does mean that it has yet to be established if a distinctive characteristic can be found in the basal ice layers of all glaciers that feature one. A study which compares particle size distributions across several glaciers would be useful in determining whether basal ice is truly distinctive sedimentologically, and whether criteria for the identification of these sediments could be applied to more than one glacier.

The basal ice layer is crucial to glacier dynamics, rheology and thermal regimes and is subject to processes that are active at the bed (Knight, 1997). As such, deposits from the basal ice layer can provide information on the behaviour, local geology, sediment sources of entrained material and the active processes that are influencing the glacier.

Better knowledge of sediment transfer pathways and specific sedimentological characteristics of the BIL, along with establishing what occurs after they are deposited by the glacier, will help to better understand how the BIL works, aid in reconstructing past basal ice patterns, and allow for more accurate palaeoglacial models to be produced.

This study determines whether particle size characteristics are the key to identifying a distinctive sedimentological characteristic within basal ice facies, whether this is

transferred to the proglacial environment and if preservation fares better within a specific geomorphological setting. This would provide not only a better indication of what to look for when trying to identify basal ice sediments, but also the formations or deposits that hold the most potential for their preservation.

## 1.2 Aim

---

To determine whether basal ice displays distinctive sedimentological characteristics and to examine whether these sedimentological signatures are transferred to and preserved within the proglacial environment.

## 1.3 Specific Objectives

---

1. Identify, map and describe the different basal ice exposures present at Svínafellsjökull, with particular focus on the sedimentology of these sequences
2. To collect basal ice sediment and proglacial sediment samples for grain-size analysis
3. To determine whether the basal ice facies found at Svínafellsjökull have any distinguishing sedimentological characteristics
4. To determine whether any of these characteristics are preserved within the proglacial sediments

5. To determine whether the presence of particular basal ice facies are associated with the development of distinctive geomorphological features
6. To determine the extent to which the grain-size characteristics of basal ice are universal or site specific

## 2. LITERATURE REVIEW

---

### 2.1 The basal ice layer

---

The basal ice layer is of great significance not only to glaciologists, but also to Quaternary scientists. It is physically and chemically distinctive from the englacial ice above (Hubbard and Sharp, 1989) as it forms and interacts at the bed of a glacier. It can be in excess of tens of metres thick and is considerably different from the ice above which forms due to firnification processes (Paterson, 1981). Due to these differences, it plays a role in glacier movement, erosion, glacier hydrology, sediment transport and deposition.

It also directly influences the local glacial geomorphology, with the resulting landforms providing further information of both past and present glacial regimes. An understanding of basal ice sedimentology is crucial as basal ice sediments open a window to what is otherwise an often inaccessible subglacial zone (Knight, 1997). It is also vital to developing accurate and realistic models of ice sheet behaviour (Knight, 1997) and glacial land systems as a whole (Evans et al., 2006, Cook et al., 2011).

#### 2.1.1 Characteristics

---

Basal ice forms at the bed of a glacier and is therefore subject to the conditions and processes that operate at the ice-bed interface (Knight, 1997). The BIL can vary from a few millimetres to several metres in thickness. Basal ice is characterised by its ability to entrain debris and sediment at the bed which can form distinct facies in the ice, depending on the

nature and concentration of sediment that is available. This means that it is physically and sedimentologically distinct from glacier ice. As it forms at the bed, it is also isotopically and chemically distinct from other zones within the glacier (Knight, 1997). This has paved the way for oxygen isotope and co-isotopic analysis of basal ice, in order to determine its origin (Lawson and Kulla, 1978, Lawson, 1979, Jouzel and Souchez, 1982).

Initial work by Chamberlin (1895) and Salisbury (1896) introduced the concept of englacial shearing to explain the BIL; the notion that fragments of rock from the bed were being thrust upwards into the ice to create a basal layer that was debris-rich. Englacial shearing was considered to be the main method of formation for the BIL until the theories of regelation (Weertman, 1957, Lliboutry, 1986) and freeze-on (Weertman, 1961).

### 2.1.2 Processes of formation

---

The basal ice layer and the processes by which it forms have been the subject of much debate and controversy within the discipline. A range of processes have been suggested, such as regelation, freeze-on and glaciohydraulic supercooling. These are reviewed in this section.

Regelation is the process whereby melting and refreezing of the meltwater present at the base of the glacier takes place, which results in the formation of superimposed ice onto the base of the glacier, entraining sediment from the bed with it. Weertman (1957, 1964) proposed that small obstacles up to 1 m in length at the bed cause a redirection in the pressure melting point on the up-flow side of the obstacle, which results in the ice melting, flowing around it and then refreezing once the pressure melting point stabilises on the down-flow of the obstacle. As the water refreezes, it can entrain sediment that has been eroded by the bed of the glacier. This was considered a likely process of basal ice

formation, though typically only for thin sequences, and was supported by Kamb and LaChapelle (1964), who observed the process at the Blue glacier in Washington. Boulton (1970) also agreed with the theory of regelation, but argued that it could only account for the preliminary entrainment of sediment into the ice, and also that the process is limited due to the small critical obstacle size required for the process to work effectively.

The freeze-on hypothesis (Weertman, 1961) presented an alternative theory which argued that meltwater at the base of the glacier, generated by geothermal heat and friction from movement by basal sliding, would freeze eventually, entraining whatever was present subglacially at the time (Weertman, 1961). This process also allows for the accretion of extensive amounts of sediment and thus the formation of thick basal ice sequences which have often been observed in the field (Lawson, 1979, Sugden et al., 1987, Knight, 1988). Boulton (1970) also argued that this process was important as it could account for basal ice formation at both temperate and polar glaciers, though this varies with the amount of meltwater available (Hubbard and Sharp, 1989).

Another formation process is that of glaciohydraulic supercooling (Röthlisberger, 1968, 1972, Hooke and Pohjola, 1994). This is the process whereby meltwater underneath a glacier can remain in liquid form below 0°C due to the overburden pressure, before freezing. This is thought to be linked to glaciers that have formed in subglacial overdeepenings, which generate the required adverse slope needed to form supercooled ice (Cook and Swift, 2012). It is also now widely accepted to be involved in the basal ice formation at specific glaciers, such as Svínafellsjökull in Iceland (Cook et al., 2007, Cook et al., 2011) and the Matanuska glacier in Alaska (Lawson, 1979, Lawson et al., 1998). The process has often been linked to the generation of ice facies that are predominantly silt, but it is still unclear as to whether this is a process signature (Cook et al., 2011).

The various processes attributed to basal ice formation can affect the distribution and concentration of sediment within the BIL. Formation is also dependent upon the nature of the bed and whether this is rigid (bedrock) or soft (unconsolidated). This can affect the type of material that becomes entrained within the BIL.

Links between basal ice characteristics and glacial sediments need to be explored in order to better understand methods of sediment entrainment, deposition and the possible preservation of BIL sedimentary characteristics in the proglacial environment.

## 2.2 Sedimentology of basal ice

---

### 2.2.1 Introduction

---

Previous research has demonstrated that basal ice facies are associated with varied sedimentological characteristics (Table 2.1). It is therefore difficult to generalise the sedimentology of the basal ice layer, as during its formation it can often entrain whatever material is present within the subglacial zone; this is especially true of the freeze-on process (Boulton, 1970).

The development of the BIL largely depends on the availability and nature of the subglacial sediment. Since this varies across glaciers worldwide, due to differing thermal regimes and different substrates, it is hard to ascertain a common set of characteristics for the sedimentology of basal ice.

Ice Facies	Thickness	Bubble Characteristics	Ice Crystal Size	Debris Concentration	Grain Size
<b>Classification scheme of Knight</b> (Knight, 1987, Knight et al., 1994)					
Clotted Ice (Knight, 1987 and Knight et al., 1994)	Can be several tens of metres	Bubble-poor	Between 2 and 5 cm	Maximum 4-8% by weight and minimum 0.001% by weight	Predominantly silt and clay, occur in clots up to 8 cm in diameter
Banded Ice (Knight, 1987 and Knight et al., 1994)	Total sequences can be up to 20 m thick and debris bands can be up to 10 cm thick	Bubble-poor	Ice crystals within debris bands mainly described as interstitial	Between 5 and 75% by weight.	Predominantly sand and fine gravel, no clay present.
Solid Ice (Knight, 1987 and Knight et al., 1994)	Up to 5 m thick	Bubble-poor	Generally too small to observe or interstitial	Between 14 and 34% by weight	Varies.
<b>Classification scheme of Sharp</b> (Sharp et al., 1994)					
Basal diffused (Sharp et al., 1994)	Up to 0.65 cm thick	Bubble-rich	Up to 8 cm in diameter	Averaged 0.3% by volume	Predominantly medium to coarse silt
Basal stratified, debris- rich laminae (Sharp et al., 1994)	Up to 0.3 cm thick	Rare, but could be found concentrated along planes parallel to the lamination which lay immediately above the upper surface of debris-rich layers	Up to 0.1 cm in diameter	Average of 10.9% by volume	Debris predominantly consisted of sand and silt. Some coarser clasts occasionally protrude from upper surface of the laminae into overlying clear ice.
Basal stratified, clear ice (Sharp et al., 1994)	Up to 2 cm thick	Not identified	Generally less than 0.3 cm in diameter	Average of 10.9% by volume	N/A
Basal stratified, clear sub-facies (Sharp et al., 1994)	Could be decimetres thick	Low bubble content	Up to 4 cm in diameter	Averaged 0.4% by volume	Debris consisted of scattered coarse clasts dispersed

					throughout.
Basal stratified, solid sub-facies (Sharp et al., 1994)	Up to 80 cm thick	Not identified	Not identified	Averaged 36% by volume	Silt-rich layers with clasts of up to 26 cm in length
<b>Classification scheme of Hubbard</b> (Hubbard et al., 1996)					
Clear facies (Hubbard et al., 1996)	Decimetres to metres	Occasional groups of flattened bubbles	Not identified	Mean concentration is 4.1 g	Mean grain size of 1.0 $\phi$
Laminated facies (Hubbard et al., 1996)	Laminae are tenths of a millimetre to a millimetre thick	Bubble-free	Not identified	Mean concentration of 262 g-1 <sup>1</sup>	Mean grain size of - 0.1 $\phi$
Interfacial facies (Hubbard et al., 1996)	Layers of sub-facies ice spaced millimetres to centimetres apart	Sub-vertical bubble lineations	Not identified	No debris samples recovered from the facies	No debris samples recovered from the facies
Dispersed facies (Hubbard et al., 1996)	Some decimetres thick	Bubble-free	Not identified	Mean concentration of 47 g-1 <sup>1</sup>	Generally coarse with a mean grain size of 0.7 $\phi$
Solid facies (Hubbard et al., 1996)	Centimetres to metres thick	Not identified	Not identified	Mean concentration of 4410 g-1 <sup>1</sup>	Sediment textures vary greatly, indicating a high number of possible sources
Stratified facies (Hubbard et al., 1996)	Decimetres to metres thick	Bubble-free	Not identified	Mean concentration of 45 g1-1 <sup>1</sup>	Mean particle size of 0.2 $\phi$
Planar facies (Hubbard et al., 1996)	Can extend for some metres	Bubble-free	Not identified	Not identified	Mean particle size of 4.0 $\phi$

<b>Classification scheme of Waller (Waller et al., 2000)</b>					
Solid sub-facies (Waller et al., 2000)	Usually occurs in layers or lenses between 1-2 cm and 100 cm thick	Bubble-poor	Fine crystal structure	Mean debris content of 47% by volume	Predominant sand-sized matrix. Abundance of small clasts up to 2 cm in length and occasional boulders up to 30 cm in length
Discontinuous sub-facies (Waller et al., 2000)	0.5-2 mm thick	Bubble-poor	Fine crystal structure	Mean debris content of 22% by volume	Fine-grained
Suspended sub-facies (Waller et al., 2000)	Not identified	Bubble-poor	Fine crystal structure	Mean debris content of 30% by volume	High proportion of debris aggregates between 1-2 mm in diameter. Fine-grained.
Dispersed facies (Waller et al., 2000)	Not identified	Bubble-rich	Not identified	Less than 1% by volume	Coarse grained.
<b>Classification scheme of Cook (Cook et al., 2007)</b>					
Basal Ice Facies, sub-facies A (Cook et al., 2007)	0.12-2.0 m	Bubble-free	1.8 cm	Mean = 5.7%	Muddy sandy gravel Gravel= 32.2%, Sand= 45.9%, Mud= 21.9%
Basal Ice Facies, sub-facies B (Cook et al., 2007)	0.02-1.75 m	Bubble-poor	2.2 cm	Mean = 3.7%	Gravelly muddy sand Gravel= 18.1%, Sand= 63.4%, Mud= 18.5%
Basal Ice Facies, sub-facies C (Cook et al., 2007)	0.2-1.9 m	Occasional but rare spherical bubbles	0.4 cm	Mean = 27.63%	Gravelly mud Gravel= 10.6%, Sand= 37.9%, Mud= 51.5%

Basal Ice Facies, sub-facies D (Cook et al., 2007)	0.02-0.2 m	Not identified	Interstitial ice	Mean = 80.8%	Gravelly muddy sand Gravel= 17.0%, Sand= 56.2%, Mud= 26.9%
Basal Ice Facies, sub-facies E (Cook et al., 2007)	0.2-4.0 m	Not identified	0.5 cm	Mean= 36.6%	Slightly gravelly mud Gravel= 0.2%, Sand= 4.2%, Mud= 95.7%
<b>Classification scheme of Cook</b> (Cook et al., 2011)					
Regelation facies, sub-facies A (Cook et al., 2011)	Up to 2 m	Not Identified	Not Identified	Less than 6% by volume	Alternating debris-rich and debris-poor layers. Mean particle size between 3.1 $\phi$ and 2.6 $\phi$ (very fine sand to fine sand)
Regelation facies, sub-facies B (Cook et al., 2011)	Not Identified	Not Identified	Not Identified	Less than 4% by volume	Dispersed particles and debris aggregates within a clean ice matrix
Supercool facies, sub-facies C (Cook et al., 2011)	0.9 m	Not Identified	Not Identified	Mean= 28% by volume	Angular aggregates of predominantly silt-sized material. Mean particle size between 3.9-5.4 $\phi$ (very fine sand to coarse silt)

Table 2.1: Sedimentological characteristics of basal ice facies identified in the literature.

### 2.2.2 Sediment Concentration

---

Sediment concentration can vary in the BIL and often reflects the type of substrate that is present within the zone of entrainment. The amount of sediment available for entrainment depends on the local geology and the processes of erosion that are active at the glacier bed.

Boulton (1978) and Hubbard (1991) suggested that three factors could influence differences found in sediment concentrations across BILs at different glaciers. These are: the type of material that is available for entrainment, the nature of sediment transfer pathways, and the method of BIL formation. Hubbard (1991) considered that the freezing rate could influence the debris concentration of basal ice. He argued that low rates of freezing would promote the expulsion of debris and thus result in a fairly low debris concentration. Sediment concentrations also appear to decrease as you move upwards through the varying facies of the BIL, such as in the clotted facies at the Russell glacier (Knight, 1994) and the facies at Matanuska (Lawson, 1979, Hart, 1995). This could be linked to increased deformation in the upper parts of the BIL, or perhaps sediment diffusion through the crystal vein network (Knight and Knight, 1994).

Large volumes of unconsolidated sediment and debris can lead to the formation of more extensive sequences of basal ice (up to tens of metres thick), whereas fine grained sediments are entrained more easily as they can retain water and adhere to glacier sole freezing (Tison et al., 1989).

Different facies tend to exhibit varying sediment concentrations; such variations were noted in the facies at Matanuska by Lawson (1979). He stated that the debris concentration of the dispersed facies ranged from 0.04 to 8.4%, whereas the concentration of stratified facies could range anywhere between 0.02 to 74% (Table 2.2).

ZONE	Thickness (m)	Features	ICE			DEBRIS			
			Grain diameter (cm)	Color	Debris content (vol %)	Internal distribution and features	Texture (Max. - $\Phi$ ) (Mean, $\sigma$ - $\Phi$ )	Pebble roundness	Fabric
Ice Facies Sub facies Superglacial	0-0.2	Ice surface cover					Gravel to sandy gravel M: -3.1 $\sigma$ : 1.5-3.3	Very angular to angular	
Englacial Diffused	Estimated at 300	Ice massive to foliated; minor sedimentary layering	2-10	White to blue	0.002 (rarely 0.1)	Uniform, occasional increase in debris to form layering	Silt to sand M: 2-4 $\sigma$ : 1.5-3	Angular	
Banded	0.02-0.5	Random distribution in diffused facies; gentle to steep upglacier dip; lateral extent variable	Variable	White	<50-75	Apparently random; massive	Silt to gravel M: -1.6 $\sigma$ : 1.5-3	Very angular to angular	
Basal Dispersed	0.2-8	Uniform in appearance; upper contact distinct and planar; horizontal to upglacier dip	1-4	White at surface; black to clear at depth	0.04-8.4	Uniform, massive	Sandy gravel to gravelly sand M: -1.1 $\sigma$ : 1.5-3	Subangular to angular with minor sub-rounded to round	
Stratified	3-15	Stratification, often showing internal deformation; downglacier to steep upglacier dip; irregular, sharp upper contact; subfacies interlayered	<0.4 (exceptionally 1)	Black at surface; clear at depth	0.02-74	Layers, lenses, zones compose strata; thin and thicken rapidly; lateral extent limited	Silt to sand to gravel	Rounded to subrounded	Strong single mode; mean axis (V1) parallels local ice flow; S1 >0.8
discontinuous	0.05-2				Variable (0.02-36); dependent on sampling technique	Lenses, layers, platelets, aggregates aligned subparallel to stratification; debris streaming	Silt to sandy silt M: 3.5-6.5 $\sigma$ : 1.3-1.9		
suspended	0.001-1.2				0.02-60	Suspended particles and aggregates without orientation	Silt to silty sand M: 4.3-6 $\sigma$ : 1.3-2.5		
solid	0.01-1.7				>60	Well-defined layers; may show sedimentary structures	Silt to gravel M: -2.5-5 $\sigma$ : 1-2.6		

Table 2.2: A table showing the varying attributes of the different facies at Matanuska, Alaska including grain size distributions and sediment concentrations (Lawson, 1979).

### 2.2.3 Clast shape and roundness

---

The morphology of clasts throughout the literature is often described using both particle shape, which is the relative dimensions of the particle, and particle roundness, which is the overall smoothness of the particle outline. Benn and Ballantyne (1993) noted the continued usefulness of analysing the morphology of sediment particles and clasts, as they provide important information linked to their provenance, transport pathways and depositional environments. Their research on Slettmarkbreen in Norway (Benn and Ballantyne, 1993) focussed on the distinctions in particle shape between supraglacial and subglacial sediment sources. They found that the supraglacial clasts were often platy and elongated in comparison to the subglacial samples, which had a higher percentage of compact clasts.

The analysis of clast shape and roundness can also offer a way to distinguish between basal ice facies (Slatt, 1971, Lawson, 1979) and provide information on the transport history of the sediments, as well as the characterisation of depositional environments (Graham and Midgley, 2000). The roundness of clasts is usually estimated using the Powers Scale (1953, Figure 2.1). Shape analysis has been represented by the Sneed and Folk (1958) diagram and has since been developed into a spreadsheet method to aid the production of such diagrams (Graham and Midgley, 2000).

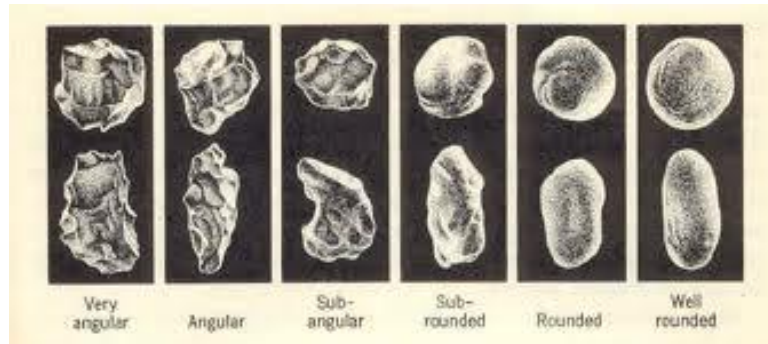


*Figure 2.1: Scale of roundness (Powers, 1953).*

The shape of a clast can shed light as to the origins of material within the BIL and on transport and pathway processes that are occurring at the bed of a glacier. An abundance of rounded or sub-rounded clasts could indicate a high rate of comminution (Boulton, 1978, Lawson, 1979). Both found evidence to suggest that clasts found within basal ice facies were worn down, abraded and striated. Boulton (1979) surmised that clasts should be spheroidal and plate shaped, unless they came into contact with the bed, in which case worn down and abraded material would be found. Lawson (1979) found similar evidence of this in the stratified facies at Matanuska which was primarily rounded to sub-rounded and had undergone major reworking in the basal zone.

Reheis (1975) recognised that it is possible to distinguish material that is from an englacial source by using the degree of roundness and the presence of striations. This material had been entrained into alpine glaciers subglacially and then deposited. He then used these characteristics to separate this material from debris and sediment that had been deposited onto the glacier by rock falls and avalanches.

Recognising these distinctions could potentially aid in identifying basal ice sediments within the proglacial environment, and help deduce the source of material and the processes that they have undergone. Well-rounded particles for example, could indicate

that there is a large amount of comminution occurring at the base of the glacier. However, previous work that has used this method suggests that it only allows for a clear identification of subglacial sediments, rather than being able to isolate those solely generated by basal ice. Accurate observations of these distinctions bodes well not only for present day observations of the preservation of sedimentological characteristics, but may also inform researchers about past glacial deposition, flow and subglacial processes.

#### 2.2.4 Particle size distribution

---

The variation of textures within glacial sediments has become significantly important to the discipline in recent years as research into the distinct characteristics of glacial sediments has become more popular. Textural differences can potentially allow for the recognition of basal ice sediments, proglacial sediments and glacial deposits on the whole. Observations of sediment texture differences can be made in the field, and more in depth analysis can be conducted on samples brought back to laboratories, using a laser granulometer.

Boulton (1978) linked grain size to the transport of sediment through the glacier. He examined basal ice samples from three different glaciers which were all sliding over rigid beds. From this he found that they were enriched in fine material. Lawson (1979) also noted that the sediment within the stratified basal ice of Matanuska was almost all fine grained (less than 2 mm). This could support Boulton's theory or just reflect the nature of the material that is available at the site, which consists mainly of silt and clays.

Hubbard et al. (1996) used fractal dimensions to characterise the sedimentology of alpine facies in terms of their grain size/mean size and distribution. They found that there were high fractal dimensions, meaning that there were a high percentage of fines within the

samples. These results could indicate that the sediments were subject to high energy comminution, which would reduce overall particle size distribution of the sediment.

Lawson (1979) argued that textural variations could be identified in the sediment and that the facies themselves were texturally distinct from each other. He argued that fine-grained sediment was transported almost exclusively within the stratified facies of the basal ice layer, whereas silt was usually moved within the discontinuous and suspended sub-facies. The majority of coarse-grained sediment and larger clasts could then be located in the supraglacial zone and the dispersed facies. It is plausible then to attribute preservation within proglacial sediments from basal ice facies to any textural distinctions observed in the facies first.

Grain-size frequency curves by Lawson (1979) highlight the polymodal nature of the sediment found at the Matanuska glacier, Alaska and showed that facies contain a restricted range of particle sizes and highlighted 'textural groupings' (Figure 2.2). He noted that there was a much wider grain size distribution at Matanuska than glaciers with active margins (Boulton, 1976).

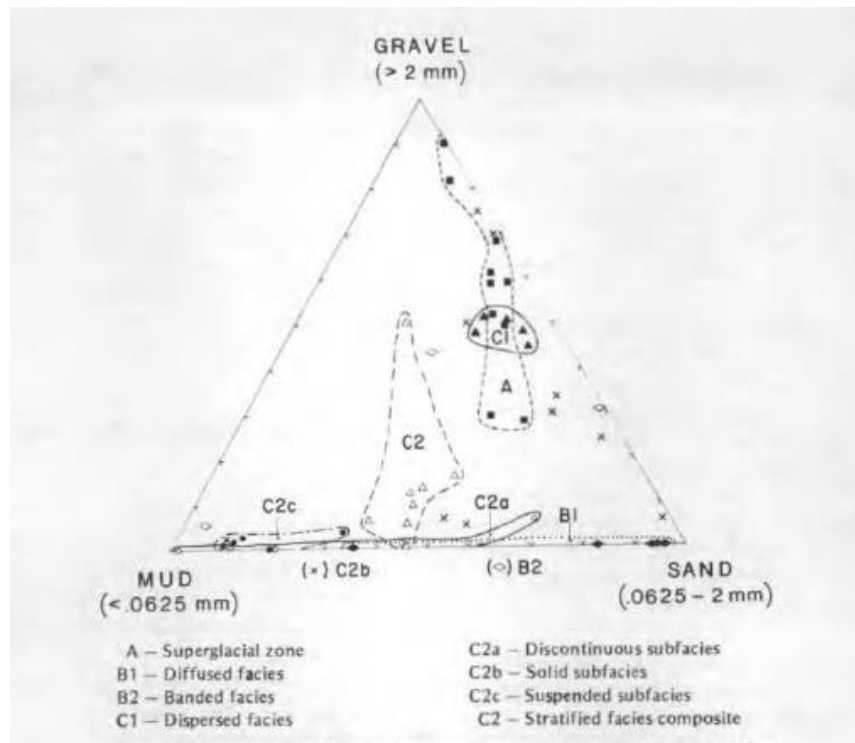


*Figure 2.2: A ternary plot highlighting the various textural groupings of the facies at Matanuska. Almost all of the facies exhibited a preference for grain size distribution, aside from the solid subfacies (Lawson, 1979).*

His data suggests that during and after the deposition of material from the glacier that mixing occurred. Therefore, he concluded that the sediment is not transported by the glacier as a ‘heterogeneous dispersal that contains particles of all sizes present in the ice’ (Lawson, 1979, p.12), but rather in sections that are texturally distinct from each other. The differences highlighted in the texture of the facies and the sub-facies at Matanuska suggest that the similarity between textures of any of the tills must be a product of deposition rather than the transport of material (Goldthwait, 1971). Analysis of the processes that occur during deposition within the terminus region of the Matanuska glacier, show that the majority of the debris underwent significant homogenization before its final release from the glacier, and that only melt-out tills show differing amounts of preservation of ice and sediment properties.

Particle size analysis has shown that it is possible to distinguish between certain facies at different glaciers, as they exhibit clear textural groupings as shown in Figure 2.2.

## 2.3 Preservation within proglacial landforms

---

### 2.3.1 Moraines

---

Much of the work conducted into the preservation of sedimentological characteristics from the BIL has focussed on their preservation within moraines. Although moraines can contain sediment from an array of different sources (subglacial, supraglacial), it is possible that in certain environments they are not reworked and thus may be able to preserve distinctive characteristics of basal ice, even though structures such as laminae and englacial debris fabrics are not maintained (Knight et al., 2000).

Work executed at the Russell glacier in Greenland by Knight et al. (2000) showed that the dispersed facies was the main source for fine-grained material, and that they could use the variations in particle size to reconstruct the spatial distribution for the dispersed facies. They argued that this method could most likely be used in situations where specific structures are not preserved and in conditions where there are distinctive particle size differences. It was noted that the same results may not be found at other sites, especially in more temperate glaciers where there is a high fluvial dominance.

Their work in Greenland showed that it is possible to identify specific basal ice facies in the proglacial sediments, specifically in ice marginal moraines, though there would need to be a high degree of particle sorting and distinctive characteristics present in the facies. Though the approach may be limited to areas that experience the same aeolian and fluvial

conditions, moraine sediments can be used to infer the presence or absence of a particular facies, and then possibly used to reconstruct patterns of ice flow or the subglacial thermal regime in glaciers.

In a similar study to Knight et al. (2000), Adam and Knight (2003) confirmed that certain sedimentological characteristics of the basal ice sequences could be used to track the melt-out of them into ice marginal moraines. They found that there were distinct patterns and characteristics, attributed to two distinct facies, which could be identified after melt-out from the BIL. They suggested that this preservation could have been successful due to little aeolian and fluvial input at the field site, which meant that melt-out from the BIL occurred mainly *in situ*, which led to a better state of preservation within the moraines. Adam and Knight (2003) found that there were distinctive particle size characteristics found in the stratified and dispersed facies which helped identify the facies within the moraines.

### 2.3.2 Minor outwash fans

---

Outwash fans have been well researched and well documented for many years. Since the 1970s there has also been an advance into the research of minor outwash fans, also termed Hochsandur fans (Gripp, 1975), within proglacial environments (Heim, 1983, 1992, Krüger, 1997, Kjaer et al., 2004). Their formation is linked to the transference of supraglacial sediments via streams, which could also enable the transfer of basal ice sediments into these structures as they flow over exposed sections of basal ice.

Minor outwash fans have a semi-conical shape and are dominated by finer gravels and sand, with the occasional shallow braided stream network. They are linked to advancing or stationary glaciers which favour supraglacial drainage rather than subglacial. Much of the work on these fans has been undertaken in Iceland as the climate and temperate glaciers

here provide the perfect environment for their formation, as meltwater is required to feed the streams. Minor outwash fans could have large impacts upon local glacial geomorphology in Iceland and be vital to understanding proglacial sedimentation. Krüger (1997) noted that minor outwash fans usually consist of material such as sand and do not extend far from the glacier margin, which means that they could play a significant role in the preservation of sediments which melt out from the BIL. Even though it is thought that the formation of the fans is due to supraglacial drainage rather than subglacial, it is also thought that the sedimentary structures found within the minor outwash fans are due to a changing influx of sediments from varying sources, one of which could be melt-out from the BIL. Minor outwash fans do not continue to develop when a glacier is in retreat (Krüger, 1997, Kjaer et al., 2004) meaning that they could be used to identify periods of glacier flow and retreat and be an ideal feature for the preservation of BIL facies, though this would depend on the amount of resedimentation taking place.

#### 2.4 Preservation within glacial sediments

---

Another recent focus on the preservation of BIL sedimentologies has attempted to establish whether distinctive sediment characteristics can be identified within the proglacial and ice marginal sediments formed by direct melt-out, rather than focussing purely on glacial landforms. Cook et al. (2011) recognised that it is possible to identify BIL deposits which were produced by two different methods of basal ice formation. They noted that particular features of the sediments can be attributed to the different processes of BIL formation and that they could identify these within proglacial sediments. Cook et al. (2011) argued that there have been lots of studies conducted into identifying basic sedimentary features that are present within the BIL, but that not enough has been done on distinguishing

sedimentary characteristics of proglacial sediments. They also pointed out that there was a lack of focus on attributing sedimentary characteristics to BIL formation processes in the literature.

Work was conducted at Svínafellsjökull, an ideal site as the basal ice formations have already been well documented (Cook et al., 2006, 2007). Cook et al. (2011) focussed on regelation and supercooling sediments in order to distinguish between facies and identify these within the proglacial material. Regelation sediments were found to be predominantly composed of worked clasts, with occasional sharp-edged fracture planes, as well as supercooled sediments which tended to be angular aggregates of predominantly silt-sized material. After testing several sites at known basal ice exposures, Cook et al. (2011) concluded that it was difficult to identify regelation sediments, however they found that ice marginal sediments could preserve layering that was indicative of supercooling. This was usually recognised by copious amounts of silt being present in the sediment. It was possible to identify two distinct facies by their sedimentological characteristics, but only one of them was then preserved and easily recognised within ice marginal sediments.

This is similar to the research done in Greenland mentioned previously (Knight et al., 2000, Adam and Knight, 2003) where two distinct facies were identified in ice marginal moraines, though the studies used two different methods of approach (particle size distribution and sediment characteristics attributed to different processes of BIL formation). The preservation of sedimentary characteristics within proglacial sediments could lead to possible reconstruction of glacier flow using post-glacial sediments.

Research that considers the possible preservation of basal ice sediments within the subglacial and supraglacial environment is also important. Much of the early work on the preservation of specific basal ice sedimentological characteristics within the proglacial

environment focussed on the identification of different types of tills. Melt-out tills are one of the principal sediment types that have been related to the potential transference and preservation of sedimentological characteristics from the BIL. Melt-out tills are formed by the release of debris by melting ice either at the glacier base or surface (Lowe and Walker, 1997). This means that such tills can have either a subglacial or supraglacial origin (Boulton, 1976).

One of the first researchers to identify and describe melt-out tills was Goodchild (1875), who discussed the formation of such features as it melted out *in situ* from debris-rich stagnant ice. Goodchild (1875) also highlighted the difficulty involved when trying to establish how much reworking of the depositional sediment is allowed (if any), before it cannot be classed as a 'true' melt-out till anymore.

Establishing these boundaries was considered an especially important task by Lawson (1979) who highlighted the need to distinguish between deposits that had come directly from the glacier and from those that had been reworked and resedimented. Lawson (1979, p.viii) defined till as 'sediment released directly from the glacial ice that has not undergone subsequent disaggregation and resedimentation.'

Paul and Eyles (1990) picked up on this issue in their paper, which looked at the formation of melt-out tills generated by the down wasting of stagnant ice at the margin. They argued that within the terrestrial glacial environment the opportunity for till to form *in situ* and be preserved can be very restricted. They put forward the idea that this could be due to a high pore-water pressure. If high, this could create a drag force on the individual particles, which could allow them to overcome frictional forces, which would then allow particles to move relative to one another. This could lead to the clast and matrix fabric of tills being disturbed and destroying melt-out tills. They do highlight that although it must occur in

specific and restricted conditions, the preservation and formation of melt-out tills can occur by passive *in situ* aggregation from thawing englacial debris.

The formation of melt-out tills via the melt-out of stagnant ice was also investigated by Haldorsen and Shaw (1982). Stagnant ice sections contain much of the former basal ice zone, where debris is highly concentrated, which presents the ideal opportunity to study the characteristics of preservation from the basal ice zone in melt-out tills. Through research undertaken at Omnsbreen in Norway they discovered that englacial cavities often contained sorted sediments that were melting out *in situ* from the stagnant ice zone. The structures were also linked to the current drainage directions and highlighted that deposition can be a rapid process, though it is relative to the melting rate of the underlying ice.

Haldorsen and Shaw (1982) noted that the differential thickness of ice can cause disruption of sediments upon the final melting of the ice and also noted that usually there was a sharp contact present between the ice and the sediment. They observed that this sharp contact often led to production of delicate sedimentary structures and bed forms, from the melt-out which could be preserved at the point of contact. Their work highlighted problems yet again when attempting to distinguish melt-out tills from flow tills. However, they concluded that the most important criteria for interpreting melt-out tills involves the presence of unlithified, sorted and stratified sediments within tills that are parallel to the direction of ice flow. Tills that contain similar textural properties to the englacial ice are also significant (Haldorsen and Shaw, 1982). This is in agreement with the point made by Mickelson (1973) who had previously shown that fabrics are relatively sensitive to very subtle changes in ice flow direction and they will often reflect this.

Lawson (1979) argued that the sediments produced by the *in situ* melting of the basal ice zone are 'true tills.' These have been termed melt-out tills by Boulton (1970). Boulton (1970) argued that melt-out tills form when ice melts under a stable overburden pressure, whereas lodgement tills form subglacially. These would form when debris-rich basal ice stagnated and then melted out either *in-situ*, due to frictional drag between particles, or pressure melting of the ice which occurred against bedrock obstructions.

As these deposits are formed by *in situ* melting, they inherit their properties directly from their basal ice source, which means that under ideal conditions, the debris and sedimentary characteristics from the BIL would be preserved in the till. Despite the strict conditions needed for the preservation of basal ice characteristics, Lawson (1979) did find evidence of preservation within a melt-out till. The stratigraphic sequence had been exposed by stream erosion near the ice margin at the time that the origin of the melt-out sediment was indicated by the contact of the strata in the ice and the sediment. The vast majority of the till was fundamentally identical to that of the ice source which Lawson (1979) argued was likely due to the fact that the ice contact was very close and without cavities, which ensured that the characteristics of the texture of the sediment were preserved in the till. He argued that this was because the overburden pressure caused the sediment to compact as it was released, which meant that only a limited amount of mixing between different debris types within the strata of the ice took place. He also noted that a slow rate of melt-out may enhance the amount of preservation taking place.

Lawson's (1979) study at Matanuska was of vital importance to research concerning the identification of different tills and their properties, as well as being one of the first to establish some of the processes needed to establish preservation of basal ice sediments within them. He surmised that although the depositional processes present at Matanuska gave the sediments distinct properties which allowed for their identification of their origins

within tills, that a single property was not enough to accurately identify their source. He noted that an assemblage of properties was required and that re sedimentation processes must be taken into account, most of which are extremely complex.

## 2.5 Summary

---

Much of the research on basal ice has focussed on identifying the various formation methods and on the processes that operate within the subglacial zone of a glacier, as well as the sedimentological characteristics that make the BIL sediments distinctive. Research has shown that basal ice facies can be sedimentologically distinct from each other (Lawson, 1979) and can be located in some proglacial sediments (Cook et al., 2011), within landforms such as moraines (Knight et al., 2000) and have the potential to be preserved within melt-out tills if specific conditions are met (Haldorsen and Shaw, 1982, Paul and Eyles, 1990).

Despite this, it is still unclear as to which sedimentological characteristics of basal ice are transferred and preserved within the proglacial environment. Previous studies also often focus on a specific glacier so it is difficult to tell whether the findings are site specific. A key sedimentological characteristic that could be identified across the BILs of the majority of glaciers around the world has yet to be established.

The geomorphological features or proglacial sediments in which they might best be preserved are also still unknown. Much of the previous research has focussed on proglacial sediments or melt-out tills as potential sinks for basal ice sediments, whilst little has been done to explore the geomorphological settings in which sedimentological attributes are best preserved.

The ability to recognise and identify basal ice sediments within the proglacial environment of active glaciers, and in the relict deposits left by ice masses in the past, would allow a greater understanding of ice sheet behaviour and enable the production of more accurate ice sheet models. This project aims to continue the effort in attempting to identify what makes basal ice sedimentologically distinct, and explore the potential for these characteristics to be preserved within the proglacial environment.

### 3. FIELD WORK SITE AND METHODS

---

This chapter outlines the field site where sampling took place for this project. It also presents the field methods used in order to collect the samples and the laboratory techniques used in data collection, in order to complete specific objectives 1 and 2. The analysis of these will be presented in the next chapter in order to achieve specific objectives 3, 4 and 5.

#### 3.1 Fieldwork Location

---

Fieldwork was carried out at Svínafellsjökull, a temperate outlet valley glacier that drains from the Vatnajökull ice cap in southern Iceland (Figure 3.1).

Svínafellsjökull was chosen for study as the basal ice layer is well documented (Cook et al., 2006, 2007, 2011) and the margin was accessible for fieldwork. Initial work has suggested that specific characteristics of basal ice types have the potential to be preserved in the proglacial environment, but this, and the mechanisms of sediment transfer in proglacial environments, has yet to be studied in greater detail. Cook et al. (2011) suggested that it was possible to identify two distinct basal ice facies formed via different processes.

This study aims to identify whether the basal ice at Svínafellsjökull contains any distinctive and identifiable sedimentological characteristics, with a focus on identifying any distinctive proglacial geomorphology which may have the potential to preserve these.

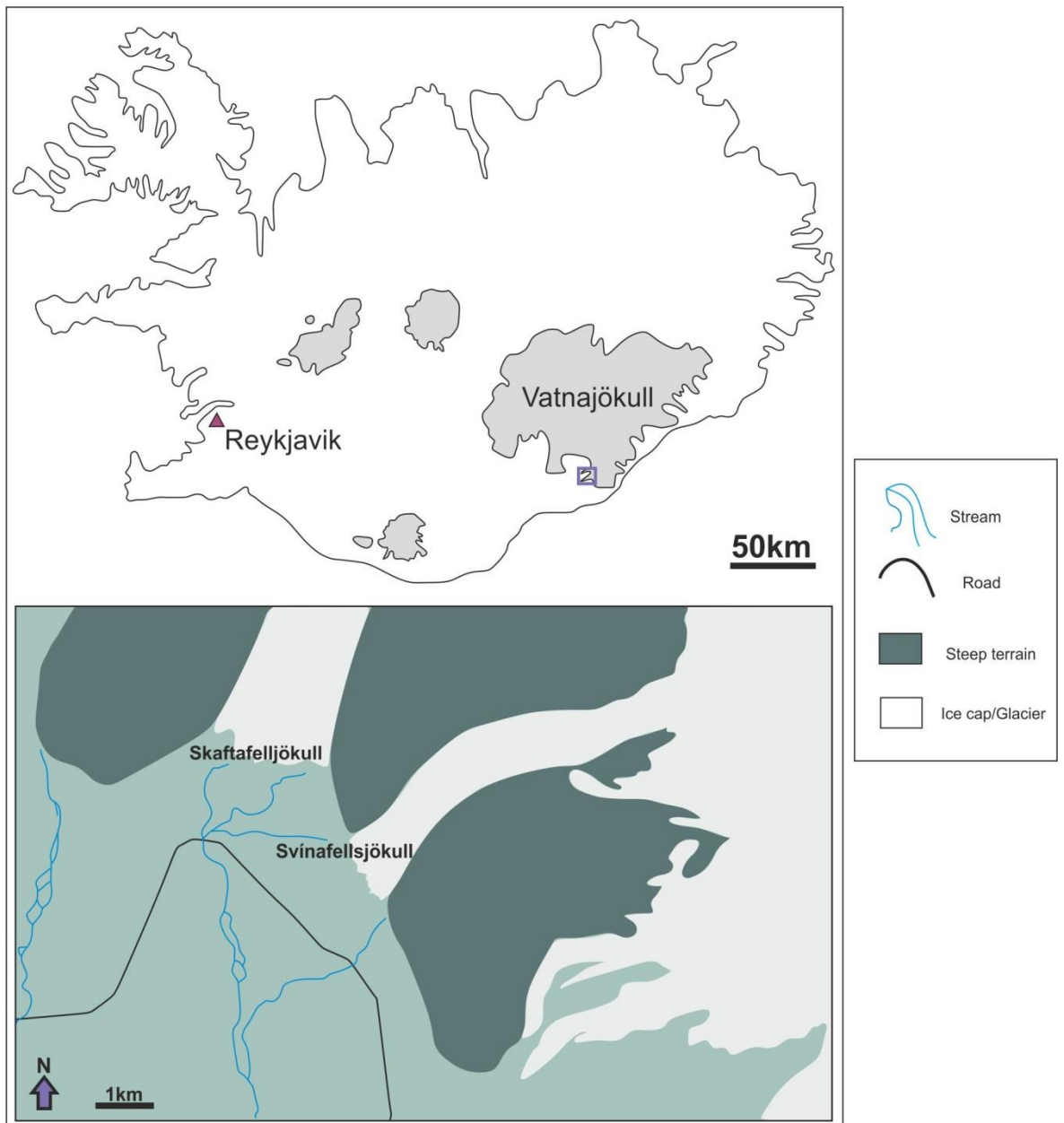
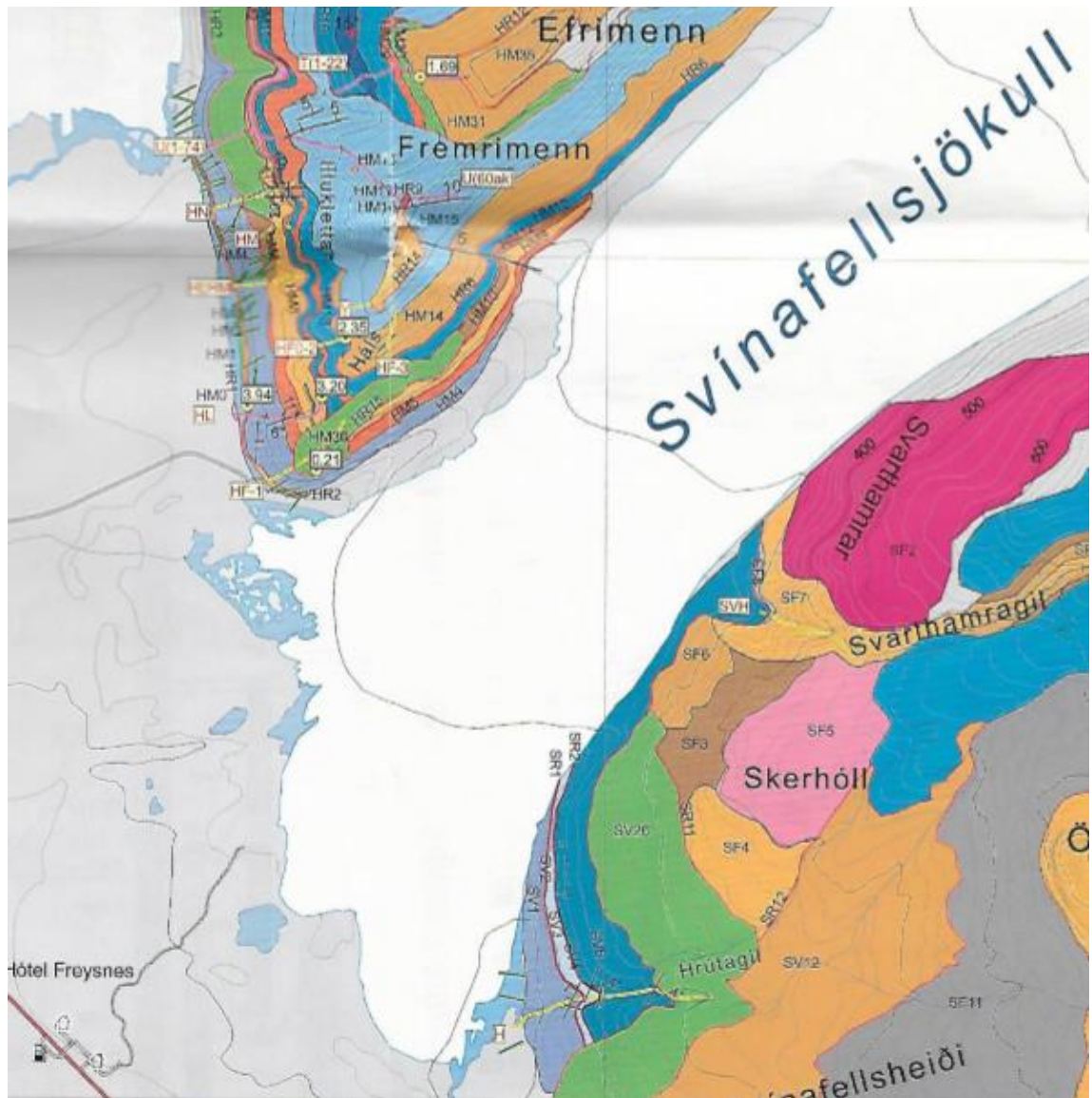


Figure 3.1: Map showing location of Svínafellsjökull.

### 3.2 Bedrock Geology



#### KEY

##### **Lower Formations:**

- SV1 (light blue): Tholeiite basalt lavas, probably R-polarity.
- SV5 (dark blue): Tholeiite basalt lavas. R-polarity.
- SV26 (green): Porphyritic basalt lavas. Normal-polarity.
- HM4 (light blue): Tholeiite basalt lavas. R-polarity.
- HM5 (orange): Olivine and porphyritic basalt lavas. R-polarity.

##### **Upper Formations:**

- SF2 (pink): Subglacially erupted cube jointed rock of intermediate composition
- SF6 (light brown): Subglacially erupted, fine-grained, cube jointed rock.
- SF7 (pale orange): Subglacially erupted cube jointed rock and breccia.

*Figure 3.2: Map showing bedrock geology of Svínafellsjökull (modified from Skaftafell Bedrock Geology map).*

Figure 3.2 depicts the varied geology present at the fieldwork site. The bedrock geology of Svínafellsjökull, and the wider area of Skaftafell where it is located, is highly variable (Helgason and Duncan, 2001) as it contains volcanic, intrusive and sedimentary rocks. Volcanic activity has occurred either on ice-free land or beneath glaciers, the latter of which has resulted in geology that is linked to subglacial volcanism. Lava flows from subglacial eruptions can sometimes merge to become large continuous sheets of uniform magma, such as in Skaftafell where cliffs are formed from piles of lava. Subglacial eruptions have also resulted in the formation of palagonite ridges in the Svínafellsjökull area surrounding the field site (Helgason and Duncan, 2001).

Figure 3.2 highlights that the bedrock geology on the southern edge of Svínafellsjökull is divided into upper and lower formations. The lower formations closest to southern margin of the glacier are composed of tholeiite basalt lavas (reverse polarity), and porphyritic basal lavas of normal polarity (SV1, SV5 and SV26). The upper formations are a mix of subglacially erupted cube jointed rock, some of which is described as fine-grained and of intermediate composition (SF2, SF6 and SF7). The lower formations on the northern margin of Svínafellsjökull are again composed of tholeiite basalt lavas, with an addition of olivine and porphyritic basalt lavas (HM4, HM5). The extent in the foreland of Svínafellsjökull is unknown as it is obscured below the more recent glacial sediments.

### 3.3 Site selection and description

---

Initial reconnaissance of the frontal ice margin was undertaken to identify the location of accessible basal ice exposures that formed the basis for further investigation. Both the exposure and the adjacent proglacial environment had to be accessible for sampling. The margin was mapped using a handheld GPS (Global Positioning System), marking a

waypoint at estimated ten metre intervals, enabling the construction of a basic site map with the areas containing basal ice exposures highlighted.

Eight sites were identified around the margin at Svínafellsjökull. Initial observations of the exposures were recorded upon arrival at each site and their locations were marked and recorded using a handheld GPS. A bag of water was then used to sluice the section of the exposure and remove the surface sediment. The sites were then sketched and photographed. Ice crystal size, debris content and distribution within the facies, clast shape and roundness, bubble content and the length and width of the exposure were recorded at each location. Facies and sub-facies were identified and distinguished using a descriptive and facies-based method similar to Lawson (1979).

### 3.4 Sampling Method

---

A paired sampling strategy was the key to this project. Sites that contained an exposed section of basal ice were initially identified around the margin. At each site, samples were then taken from the basal ice facies present and then from features within the adjacent proglacial environment, in order to try and ascertain whether the sedimentological characteristics were being transferred from one environment to the other. The paired sampling method was used for all sites except site 8, which only contains samples from an ice type.

A total of 55 samples were collected in the field for analysis back in the laboratory; 37 from the different basal ice facies and 18 from the proglacial features identified across all eight sites.

### 3.5 Collection of samples for grain-size analysis

---

Basal ice exposures were sampled using an ice axe to carve out a small sample (enough to fill 100 ml sample bottle) which was placed into a sealed bag or container. Once the ice had melted, the water and entrained sediment was poured into labelled sample bottles for analysis at a later date in the laboratory. Multiple samples were taken at exposures where the ice contained more than one type of facies.

Samples were also collected from the adjacent proglacial environment. The focus for sampling was on ice-marginal sediments or geomorphological features that appeared to be linked to the ablation of the exposure at that site. This included proglacial sediments, moraines and minor outwash fans.

Samples taken from proglacial sediments close to the exposure of the basal ice layer were sampled with a trowel.

At certain sites moraines had formed and samples were extracted from these. A spade was used to dig a trial pit 1 m deep through the moraine and then three samples were collected; 30 cm, 60 cm, and 90 cm retrospectively.

Sites 3, 4, 5 and 7 contained features which resembled minor outwash fans, these were also sampled. A trowel was used to dig a 30 cm pit, showing the cross section through the sediments, this was then sampled.

### 3.5.1 Sample Preparation

---

Sediment samples from the basal ice were already saturated with meltwater and consisted largely of fine grained material less than 2 mm in size, therefore the samples did not require any preparation prior to grain size analysis.

The proglacial samples were sorted into marked containers and left to dry out in the laboratory over a three week period. These samples contained large clasts so a sample was taken from each using a trowel and then dry sieved through a 2 mm sieve. A 2 g sample of the material that was less than 2 mm in size was then weighed out into a sample bottle and 20 ml of calgon solution was added in order to separate any particles that may have adhered to each other. This was done for every proglacial sample collected. The sample bottles were then vigorously shaken and left to soak overnight.

No method was employed to eliminate organic matter in any of the samples as they were taken directly from the ice, so it was considered unlikely that there would have been any significant amount of organic material within the samples. This is standard practice with this procedure when using basal ice samples.

### 3.5.2 Laser Granulometry Analysis

---

Particle size analysis on all samples less than 2 mm was conducted within the laboratory at Keele University using a Coulter® LS230 laser granulometer. The laser granulometer uses laser diffraction in order to obtain an accurate particle size distribution of sediment that is < 2 mm in size. Samples are automatically run three times in order to produce an average.

The data exported include the particle size distribution of the sediment, including both cumulative and differential volume, as well as plus or minus two standard deviation of the three runs combined. The laser granulometer also records the average, mean, mode, median, skewness and kurtosis of each sample which was exported into an excel file.

A 2 mm sieve especially designed for use with the laser granulometer was used in order to make sure that no particles larger than 2 mm entered the machine. Each sample bottle of sediment was held on a small vortex shaker for approximately 30 seconds, immediately before processing a proportion of the sample through the laser granulometer. This was to ensure that the particles had been disaggregated prior to analysis. An enlarged pipette, which allowed for slightly coarser granules to pass through, was then used to try and gain a representative sample from the sediment bottle. The pipette was used to disturb the sediment continuously for a short period of around 20 seconds, at which point a sample was extracted and then added to the water-filled vessel within the granulometer. Sediment was added until the laser granulometer detected an 8-10% obscuration and 40-60% PIDS (Polarisation Intensity Differential Scattering) within the vessel inside it. The same process was followed for each of the samples, both basal and proglacial.

### 3.6 Data Presentation

---

The grain size data (all raw grain size data can be found in Appendix A) from both basal ice and proglacial samples have been presented within line graphs, a scatter graph, summary data tables and ternary plots within chapters 4, 5 and 6. The line graphs provide an overview of the grain size distribution of each sample. These highlight the differential volume of the sample at each interval set by the laser granulometer between 0.4-2000  $\mu\text{m}$ . Cumulative volume graphs for each sample site can be found in Appendix B. The

summary data tables include the values for D50, standard deviation, mean particle size, minimum and maximum particle size, skewness, kurtosis, sorting and percentage silt content for each sample. The ternary plots highlight the distribution of each sample in sand, silt and clay. The ternary plots were produced using the TRI-PLOT programme provided by Graham and Midgley (2000). The GRADISTAT programme was used to calculate sorting for each of the samples (Blott and Pye, 2001).

### 3.7 Secondary Data Use

---

In addition to samples collected at Svínafellsjökull, this project has also involved compiling a data set of grain size analysis from the basal ice layer of glaciers around the world.

The grain size data analysed within chapter 5 uses data from samples collected by Dr Richard Waller from Ferpècle (Switzerland), Skeiðarárjökull (Iceland), and the Root, Matanuska (Alaska) and Russell (Greenland) glaciers. It also uses grain size data from samples collected from the Storglaciären glacier in Sweden by Dr Simon Cook.

## **4. THE SEDIMENTOLOGICAL CHARACTERISTICS OF BASAL ICE AND THEIR PRESERVATION AT SVÍNAFELLSJÖKULL**

---

### 4.1 Introduction

---

This chapter presents the findings of the specific case study based on fieldwork at the Icelandic glacier, Svínafellsjökull. Section 4.2.1 provides a table identifying the main characteristics associated with the six ice types identified and a detailed description of each, complete with photographs. This is presented first in order to document and describe both the basal ice at Svínafellsjökull and the local glacial geomorphology and landforms associated with the exposures. Section 4.2.2 provides some context on the proglacial geomorphology at Svínafellsjökull. An in-depth grain size analysis is then provided throughout section 4.2 and in 4.3 which offers a detailed look at the sedimentological characteristics of the basal ice facies, and the noted landforms and sediments present in the proglacial environment. Section 4.4 finishes with a visual focus on the spatial variability of the various facies and landforms identified around the margin.

### 4.2 Field Sites, Svínafellsjökull

---

Initial reconnaissance of the frontal margin of Svínafellsjökull (refer to Figure 3.1) led to the identification of seven sites appropriate for description and sampling of both the basal ice layer and the proglacial landforms and sediments (Figure 4.1). Another site was included (site 8) however this only contains data for some frazil ice sampled at the meltwater channel, rather than a basal ice exposure at the margin. As such, it does not contain any proglacial data and was included to provide comparison with the other ice

types identified. This addresses specific objectives 1 and 3 which are to identify, map and describe the basal ice sequences present at Svínafellsjökull, in order to collect samples from the basal ice and immediate proglacial environment for grain-size analysis. A paired sampling technique was essential to this project in order to look for and establish any potential link between the possible transference of basal ice sediments to the proglacial environment.

A description of the basal ice and the proglacial environment close to the identified exposure are presented for each of the eight locations. Observations of the basal ice focused on the physical characteristics of the sediment present within the ice, such as the distribution and angularity of clasts and the features of the ice itself, such as ice crystal size. The proglacial descriptions primarily focus on the geomorphology of the immediate area and any distinctive landforms that are present. Six key ice types were identified at Svínafellsjökull, the classifications of which can be found in Table 4.1.

The findings from the particle size analysis of the basal ice and proglacial sediment samples collected are presented individually after the initial description. This addresses specific objectives 2 and 3 which involved the collection of samples from the research site and the subsequent analysis of the sediment with a laser granulometer, in order to determine the particle size characteristics of the samples. Grain size distribution graphs for each site are presented and described first, followed by a summation of the results. Summary data tables for each sample have also been compiled. These include parameters such as mean particle size, silt content and standard deviation.

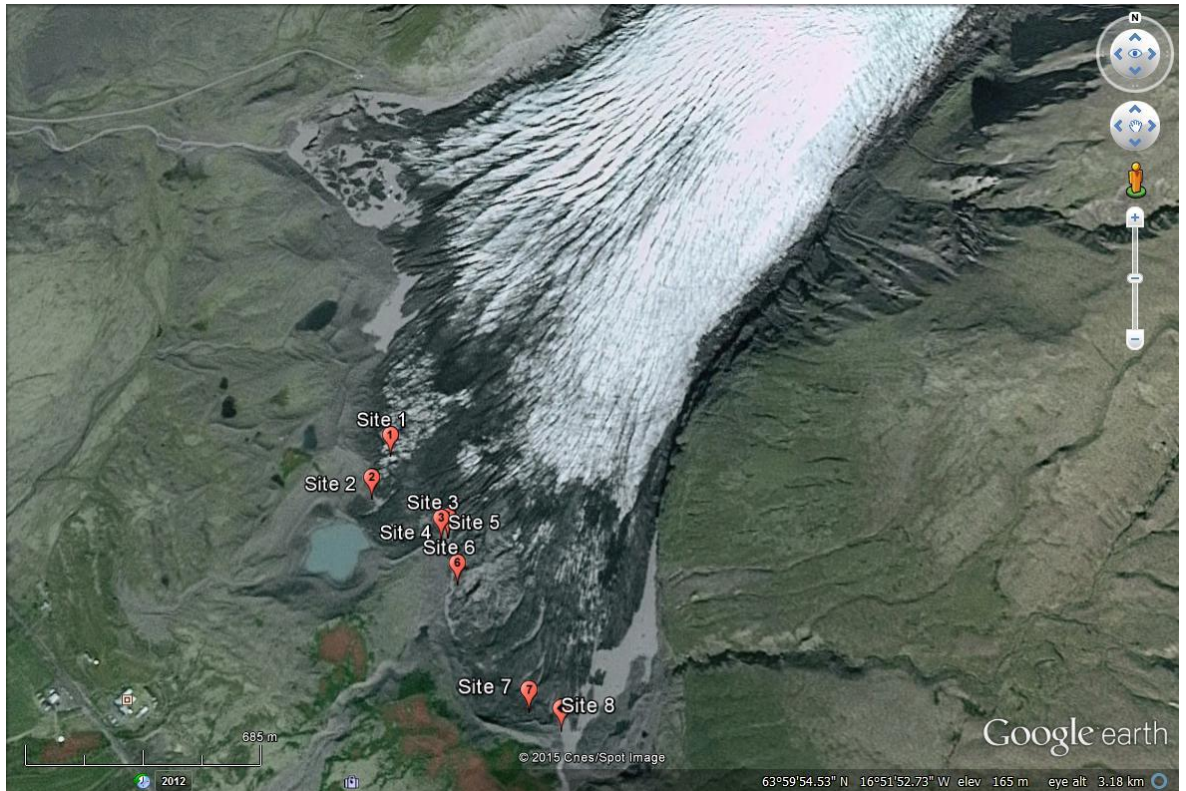


*Figure 4.1: Google Earth image showing the locations of the sample sites around the Svínafellsjökull margin (Google Earth, 2014).*

#### 4.2.1 Facies Classification

---

Visual observation of the basal ice at each sampling site allowed for the identification of six visually distinct facies. Some facies occurred at several sites whereas others were only at a singular sampling location. The six facies have been described based on their visual characteristics observed in the field, the results of which are shown in Table 4.1. The table has been presented prior to the site by site descriptions in order to highlight the various ice types that were present at particular sites. Figure 4.2 provides images of the six facies identified.

ICE TYPE	DESCRIPTION
A	<p>Ice type A typically comprised very fine sediment, which was less than 2 mm in diameter, with very few larger clasts present. The fine-grained sediment featured within crude laminations in exposures that were approximately 2-3 m thick in some places. There were no visible ice crystal boundaries present within this facies type.</p> <p>This ice type was thought to be of a supercooled origin as it shares similarities with the supercooled facies described by Lawson (1979) at Matanuska and Cook et al. (2007, 2011) at Svínafellsjökull. It predominantly contained very fine material, indicating potential silt dominance, which both Lawson (1979) and Cook et al. (2007, 2011) note could be a possible signature of the supercooling process.</p>
B	<p>Ice type B featured crude laminations that gave it a stratified appearance. It predominantly comprised material 1-5 mm in diameter which mainly featured within the laminations. Some larger, sub-rounded clasts up to 15 cm in diameter could be found dispersed throughout the facies. There were no visible ice crystal boundaries present within this facies type.</p> <p>The crudely stratified ice type B shares similarities with the basal stratified, debris-rich laminae described by Sharp et al. (1994) which predominantly comprised sand and silt, with some small clasts that could be found protruding into the clear ice above. It could also be linked to the regelation and stratified facies identified at Svínafellsjökull by Cook et al. (2011) which contained alternating debris-rich and debris-poor layers that were composed mainly of sand.</p>
C	<p>Ice type C typically comprised fine-grained sediment less than 2 mm in diameter. This facies type was very debris-rich and the sediment formed within a distinctive herringbone surface texture and crystal structure. Larger, sub-angular clasts which were between 1-5 cm in diameter, were dispersed throughout. The ice crystals that were visible ranged between 1-2 cm in diameter.</p> <p>The distinct herringbone pattern that featured within this ice type shares similarities with the observations of supercooled ice created under laboratory conditions by Knight and Knight (2005) and Cook et al. (2012), and also with basal ice sub-facies E identified at Svínafellsjökull by Cook et al. (2007). Knight and Knight (2005) describe their ice type as having a distinctive ‘herringbone’ crystal structure whilst Cook et al. (2007) note a ‘herringbone-like’ texture within their observed sub-facies.</p>
D	<p>Ice type D featured one or multiple bands that were mainly infilled with sediment typically 1-5 mm in diameter. The bands also contained sub-angular clasts between 10-20 cm in diameter and sometimes small boulder between 30-60 cm in diameter either within the band, or surrounding them. At one site, ice type D featured between two sections of ice type B.</p> <p>Debris bands have been described within basal ice sections at many locations and can vary largely in thickness and width. Waller et al. (2000)</p>

	<p>described a series of debris bands that could vary between 10 – 200 cm in thickness, located at one of their sites at the Russell glacier. Similar to ice type D identified here, the debris bands at the Russell glacier also contained a variety of grain sizes, ranging from fine-grained sediments to clasts that could be 200 cm in length. Lawson (1979) also identified a debris band that featured within the diffused ice facies at Matanuska, similar to ice type D which at one site separated two sections of another ice type.</p>
E	<p>Ice type E was located within or around areas dominated by ice type B. It typically comprised very fine-grained material less than 2 mm in diameter, ‘spidery’ aggregates and formed a type of ‘silt pocket’. There were no visible ice crystals within this ice type.</p> <p>Ice type E could be linked to the suspended facies described by Lawson (1979) which contained sediment particles that had no clear orientation and was silt-dominated. It also could share resemblance to the basal ice sub-facies C noted by Cook et al. (2007) which contained angular and ‘spidery’-shaped debris aggregates.</p>
FRAZIL	<p>The frazil ice type featured large, interlocking plates of ice with visible ice crystals approximately 2 cm in length. There were no clear debris structure within it, but it did feature some fine-grained material between 1-5 mm in diameter within clots which were embedded within the plates.</p> <p>This ice type is similar to that of the frazil identified in by Knight and Knight (2005) and Cook et al. (2007). Both described frazil as ice that featured large interlocking plates, needles or lozenge shaped crystals. Knight and Knight (2005) also added that debris was trapped between the plates.</p>

*Table 4.1: Descriptions of the basal ice facies identified around the margin at Svínafellsjökull.*



Figure 4.2: (a) ice type A, (b) ice type B, (c) ice type C, (d) ice type E, (e) ice type D, (f) frazil ice.

#### 4.2.2 The proglacial environment at Svínafellsjökull



*Figure 4.3: Image showing the southern margin and the proglacial area at Svínafellsjökull.*

The proglacial environment at Svínafellsjökull is characterised by various geomorphological features. Samples for each site are taken from the basal ice exposure identified and from the immediate proglacial environment. In some cases, this only includes proglacial sediments directly in front of the exposure. However, at some sites this includes samples from proglacial geomorphology, at times up to approximately 3 m in front of the relative basal ice facies.

The wider proglacial geomorphology at Svínafellsjökull is characterised by a series of larger moraines, which are between 5 and 10 m in height, with steep gradients (highlighted by 'A' in Figure 4.3). This is often where the ice margin has advanced into the moraines and become hidden beneath them. Some other sites feature systems of smaller moraines which are up to 1.5 m in height at most sites, but can be up to 2 m. In addition, some of the sites that feature the smaller moraines also contain an intra-moraine network of minor outwash fans (highlighted by 'B' in Figure 4.3). These are fed by supraglacial streams that often flow over the exposed basal ice. Many of the sites have small, but sometimes fast-flowing, meltwater streams that are caused by the melting of the ice at the margin. As a result, they are often highly turbid. Much of the margin at Svínafellsjökull has retreated into a proglacial lake, which is already the case on the northern side of the margin where it is inaccessible. This can be seen in the figure where pools have formed both in front and within sections of the glacier (shown by 'C' in Figure 4.3).

Unconsolidated diamicton can also be found in most places around the margin. At certain sites, small mounds of unconsolidated proglacial sediment are located directly in front of the exposed basal ice. Samples from these are included within this research, to test whether they contain sediments that have melted out from the exposure. Much of the ice margin also features a layer of supraglacial sediment.

#### 4.2.3 Site 1 (*63°59'50.67N, 16°52'37.32W*)

---

The exposure at site 1 (Figure 4.4) is located in the central part of the glacier margin (Figure 4.1). It features a basal ice exposure approximately 3 m wide and 1.5 m high and comprises one distinct facies (Ice type B, Table 4.1). A layer of englacial ice (approximately 0.5 m) can be observed above the exposure. The facies is debris-rich and bubble poor, with ice crystals that range from 1-2 cm in length. The facies is characterised by debris aggregates comprised predominantly of silt and clay (approximately 60% silt and 40% clay). These aggregates tend to occur in discrete layers providing a crudely stratified appearance to the facies. Sporadic clasts up to 10 cm in diameter are primarily sub-rounded and found predominantly within the laminations, but can also occur in a dispersed pattern. The facies also contains abundant granule-gravel between 1-5 mm long. There are some small hollows within the exposure, which appear to have formed as larger clasts fell out as the ice as it melted.

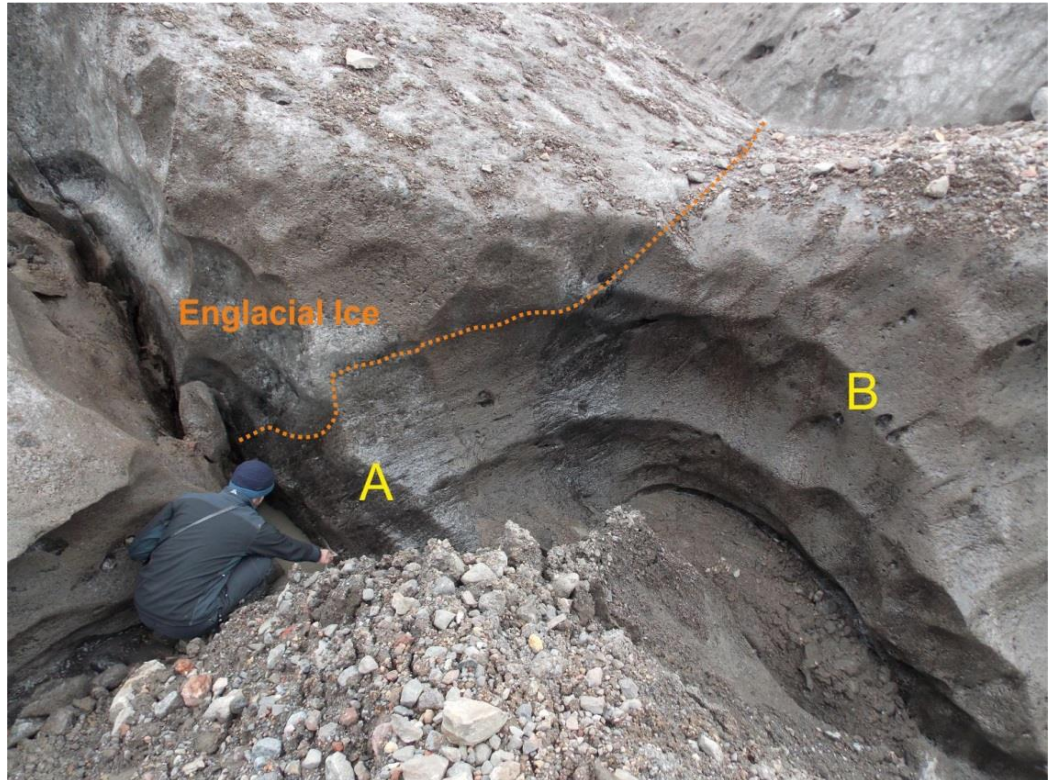


*Figure 4.4: The exposure at site 1. 'A' highlights the location of the facies which forms crudely stratified laminations. 'B' marks the location of the larger clasts dispersed throughout the facies which are between 5 and 10 cm in diameter. Person for scale.*

The proglacial area at site 1 (Figure 4.5) features a large, ice-cored moraine directly in front of the exposure (approximately 2 m high). The material that forms the moraine is unconsolidated diamicton, the surface of which consists predominantly of sub-angular clasts between 5 and 20 cm in size.

The proglacial area is characterised by sections of buried ice where the ice margin meets the moraines and has become hidden beneath them. Though the focus for sampling at this site is on the edge of the moraine closest to the facies, the visible section of the moraine continues on a steep gradient away from the exposure, rising to about 10 m in height. The basal ice exposure produces a small stream of melt-water which flows for about 2 m parallel to the margin and then flows underground. The melt-out stream has a very high turbidity and the basal ice can be observed melting directly into it. Material melting from

the basal ice facies forms small mounds in front of the exposure which have not yet entered the stream. Samples for this site are taken from both the moraine and melt-out from the exposure.



*Figure 4.5: A view of the wider proglacial area at site 1. Box highlights exposure. Dashed line indicates the edge of the ice margin and the start of the proglacial environment. Ice axe for scale is approximately 0.5 m.*

#### 4.2.4 Site 1 grain size analysis

---

Figure 4.6 illustrates the particle-size distributions of the six samples collected from ice type B, as well as the sample collected from the moraine at site 1. The grain size distributions for the basal ice samples are almost identical. The distributions range from  $0.4 \mu\text{m}$  to  $c.100 \mu\text{m}$  and therefore primarily comprise silt and clay ( $<63 \mu\text{m}$ ). Ice type B samples display peaks between  $15 \mu\text{m}$  (fine silt) and  $50 \mu\text{m}$  (coarse silt) and they all contain very small concentrations of material between  $63-100 \mu\text{m}$ , which is very fine sand. They are also negatively skewed towards the coarse end of their distribution. Table 4.2

shows that the mean particle size for the basal ice ranges from 12 to 18  $\mu\text{m}$ , which is fine to medium silt. All of the samples are poorly sorted.

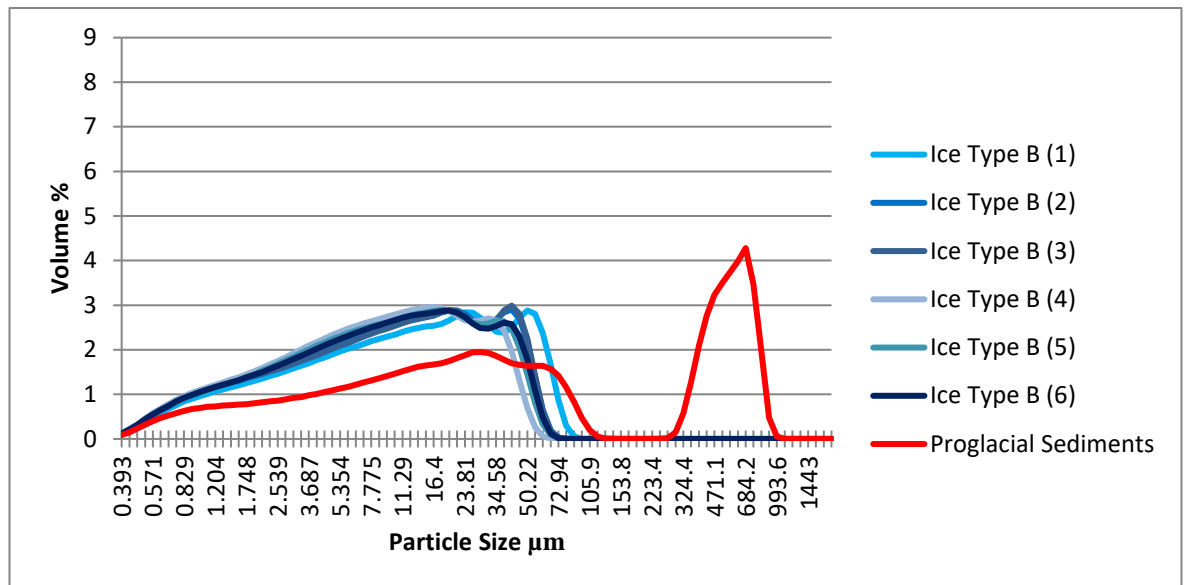


Figure 4.6: Grain size distribution plot for site 1.

The proglacial sample has a bi-modal character, is very poorly sorted, and denotes a major peak at 500  $\mu\text{m}$  (sand), which is a complete contrast to the basal samples, which do not contain any sand. It lacks any material ranging between approximately 150-220  $\mu\text{m}$  (fine sand) and shows an increase in material between 15-100  $\mu\text{m}$ , which is medium silt to very fine sand. Table 4.2 shows that the mean particle size for the samples is 198  $\mu\text{m}$ , which is medium sand. It contains 43.5% silt, less than all of the basal ice samples.

Site 1	D50 (µm)	Mean (µm)	Standard Deviation (µm)	Max Particle Size (µm)	Min Particle Size (µm)	Silt (%)	Sorting (µm)	Kurtosis (µm)	Skewness (µm)
Ice B	11.78	18.82	18.68	96.49	0.393	60.2	19.59 PS	0.43	1.16
Ice B	10.11	15.55	14.98	80.07	0.393	56.8	15.72 PS	0.38	1.13
Ice B	10.08	15.53	15.01	80.07	0.393	56.7	15.74 PS	0.32	1.11
Ice B	8.54	12.88	12.22	72.94	0.393	52.6	12.82 PS	0.65	1.19
Ice B	9.23	14.21	13.71	80.07	0.393	54.6	14.38 PS	0.70	1.21
Ice B	9.47	14.63	14.22	80.07	0.393	55.3	14.91 PS	0.66	1.21
Moraine	31.8	198.2	271.3	993.6	0.393	43.5	284.5 VPS	-0.52	1.05

*Table 4.2: Summary data table for site 1.  
(PS = Poorly Sorted, VPS = Very Poorly Sorted)*

#### 4.2.5 Site 2 (63°59'43.49N, 16°52'41.18W)

Site 2 is also located in the central part of the glacier margin, south of site 1 (Figure 4.1). The basal ice exposure is composed of two distinct facies (Figure 4.7a) identified as ice types B and D (Table 4.1). The exposure is approximately 2 m wide and 1.5 m high.

The section of the exposure containing ice type B is approximately 0.5 m high and 25 cm wide. It features ice crystal boundaries that are too small to observe and is debris-rich but bubble poor. The facies features debris aggregates which predominantly comprise silt (70%) and have formed layers which give it a crudely stratified appearance (Figure 4.7b, 4.7c). The facies comprised mainly granule-gravel clasts of 1-5 mm in size and features sub-rounded clasts that range from 5-15 cm and are dispersed throughout the facies.

The exposure featuring ice type D is 120 cm long and up to 30 cm wide. In places it runs horizontally through the exposed section and separates two sections of ice type B. The material featuring within the debris band is similar to that in the stratified facies, but comprises slightly smaller clasts from 5-10 cm in diameter that are mainly sub-angular. Ice type D is much more debris-rich, with only interstitial ice. There are also larger boulders located in and around the exposure, ranging from 30-60 cm in length.

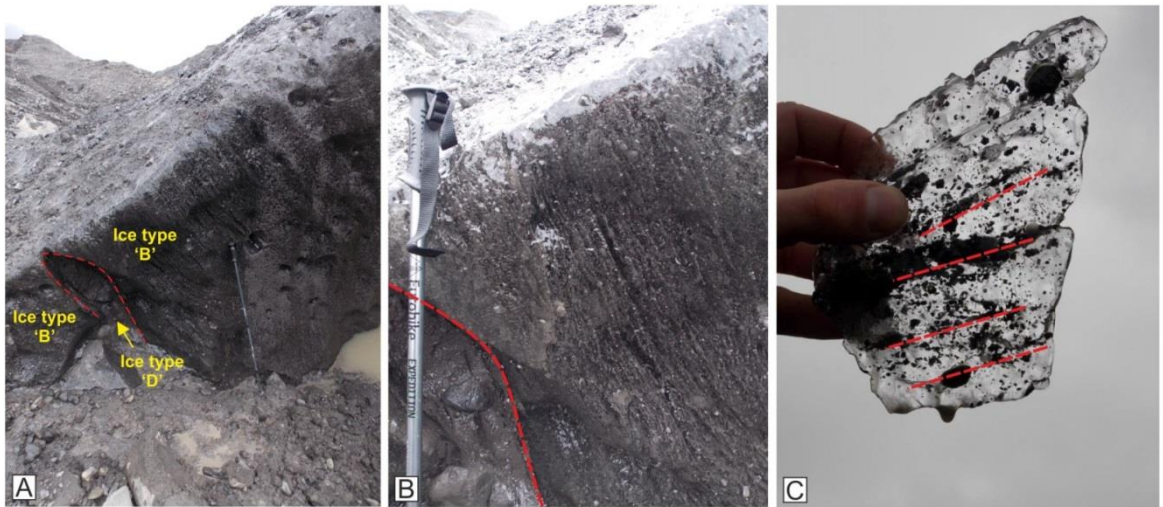


*Figure 4.7: (a) Image showing the exposure which features two distinct facies. Walking pole for scale is approximately 1 m. (b): A close up image of the ice types. Dashed line highlights the boundary between ice type D on the left and ice type B on the right. (c): Image showing a thin section of ice carved from ice type B at site 2. Dashed lines highlight the presence of crude laminations of sediment aggregates within the ice.*

Much of the margin at site 2 has started to retreat into a proglacial lake. There is a large, steep moraine approximately 5 m high, located about 2 m in front of the exposure. The material around site 2 consists largely of sub-angular to angular clasts, which range from around 5 to 10 cm in size, and larger rounded boulders which can reach up to 60 cm in length. The exposure consists of two different facies which can be observed melting out to produce an unconsolidated till surrounding the exposure. This has no clear structure to it and is the basis for the proglacial samples taken at this site (Figure 4.8).



*Figure 4.8: An image of the basal ice exposure at site 2. Dashed line indicates the edge of the margin. 'A' highlights the area that was sampled for grain size analysis. Walking pole (1 m) for scale.*

#### 4.2.6 Site 2 grain size analysis

---

The basal ice samples from site 2 are sampled from two distinct facies within the exposure (ice types B and D). The grain size distribution plot (Figure 4.9) indicates that there is some variation between the two.

The plot indicates that the sediment from ice type B consists of material that is less than 110  $\mu\text{m}$  in diameter, which is anything from very fine sand to clay. It also displays a peak at around 30  $\mu\text{m}$  indicating that a large proportion of the sample consists of medium silt.

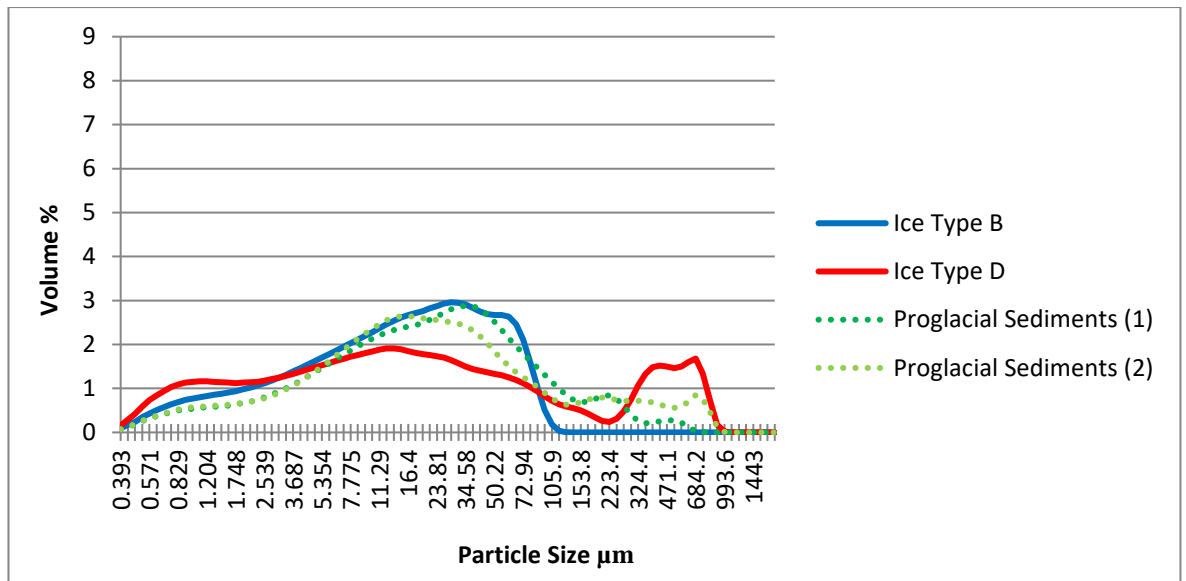


Figure 4.9: Grain size distribution plot for site 2.

In contrast, the sample from ice type D has a bi-modal distribution with approximately 20% of the sediment ranging between 220 μm and 1000 μm in diameter (fine to very coarse sand), with a peak around 680 μm (coarse sand). The key distinction between the two samples is the distinct peak in coarse sand in ice type D, in contrast to the sample from ice type B which only contains a small amount of very fine sand. This is highlighted by Table 4.3 as ice type B has a mean of approximately 23 μm which is medium silt, whereas ice type D has a mean particle size of approximately 107 μm, which is very fine sand. Ice type B also contains a much higher percentage of silt (67%) and is poorly sorted, in contrast to ice type D which only contains 43% silt and is very poorly sorted.

The plot shows that the proglacial sediment samples which are both sampled from proglacial sediments at the exposure, have similar grain size distributions. The samples contain a small percentage of sand but at least 80% of the sample is less than 100 μm in diameter, which is silt and clay. The peaks within the proglacial sediment samples also

closely match the peak shown in the ice type B sample. Table 4.3 shows that the mean particle size for the two samples is between 47 and 75 $\mu\text{m}$ , which is coarse silt to very fine sand. Both samples contain a high percentage of silt (59 and 65%). The samples are not unimodal and both are very poorly sorted, similar to that of ice type D.

Site 2	D50 ( $\mu\text{m}$ )	Mean ( $\mu\text{m}$ )	Standard Deviation ( $\mu\text{m}$ )	Max Particle Size ( $\mu\text{m}$ )	Min Particle Size ( $\mu\text{m}$ )	SILT (%)	Sorting ( $\mu\text{m}$ )	Kurtosis ( $\mu\text{m}$ )	Skewness ( $\mu\text{m}$ )
Ice B	15.51	23.37	22.63	127.6	0.393	67.3	23.73 PS	0.71	1.19
Ice D	15.42	107.6	198.2	993.6	0.393	43.8	207.8 VPS	3.33	2.11
Proglacial Sediments	21.60	47.29	77.44	751.1	0.393	65.61	81.32 VPS	17.84	3.77
Proglacial Sediments	19.53	74.96	149.4	993.6	0.393	59.8	156.7 VPS	10.05	3.16

*Table 4.3: Summary data table for site 2.  
(PS = Poorly Sorted, VPS = Very Poorly Sorted)*

#### 4.2.7 Site 3 (63°59'40.67N, 16°52'30.66W)

---

Site 3 is located towards the eastern part of the margin, south-east of site 2 (Figure 4.1). It features a conspicuous layer of debris-rich basal ice, which infills an ice-marginal fracture (Figure 4.10a). The layer dips up-glacier and tapers in thickness from ~1 m in thickness at the base of the exposure to ~20 cm at the top of the exposure. The facies (ice type A) is debris-rich and bubble poor, with ice crystals ranging from 2-10 mm in width. The

exposure is characterised almost exclusively by a dense distribution of very fine material (1-2 mm). No larger clasts are present within the exposure.

The down-glacier margin of the fracture fill features an irregularly-shaped lens of basal ice approximately 30 cm in diameter. A small hollow has formed within the fracture-fill itself which also contains ice type A, characterised by its very high debris concentration of fine-grained material (approximately 85% silt by volume) (Figure 4.10b). There are no laminations present within the hollow itself, but there are smaller lenses of coarser-grained material dispersed within the infill. Small clots of very fine-grained material ( $<63 \mu\text{m}$ ) (Figure 4.10c) can be observed below the infill, between patches of clear ice.

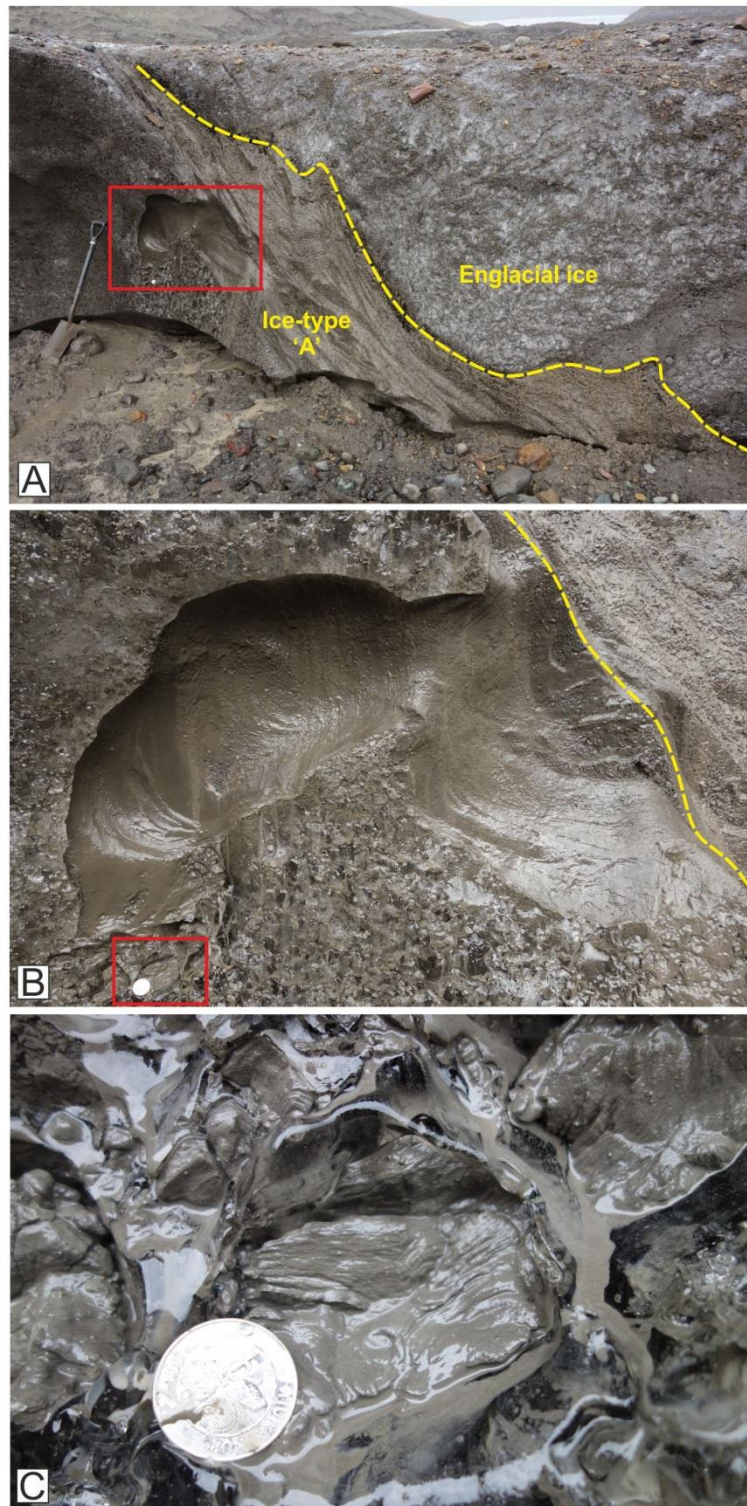


Figure 4.10: (a): An image of the exposure at site 3 highlighting the fracture at the ice margin and the boundary between the facies and englacial ice. Spade for scale is approximately 1 m. (b): A close up image of the hollow that features in the facies at site 3. Coin for scale is 2 cm in diameter. (c): An image depicting the 'clots' of fine-grained sediment within the hollow, with lenses of clear englacial ice. Coin for scale is 2 cm in diameter.

The proglacial environment at site 3 is characterised by small moraine ridges up to 1.5 m in height, and small outwash fans which infill the intervening depressions between the moraine ridges (Figure 4.11). The moraines consist of unsorted and unconsolidated material, which consists of anything from very fine sand and silt, to smaller, sub-angular clasts between 5-20 cm in size, and larger, rounded boulders which can range between 20 and 60 cm in size.



*Figure 4.11: The proglacial environment at site 3. 'A' highlights area where melt-out sediments were sampled, 'B' identifies location of minor outwash fans sampled and 'C' marks the edge of a moraine (approx. 10 m high). Person for scale.*

In contrast, the minor outwash fans which have formed in the intra-moraine areas comprise very fine silt and clay. A cross-section (Figures 4.12a, 4.12b) dug into one of the minor outwash fans highlights alternating layers of coarser (sand-rich) and finer (silt-rich) material. The transfer of ablated material from both supraglacial and basal ice sources into

some of the fans can be observed within the field (Figure 4.12c). Larger clasts up to 10 cm in diameter that are predominantly sub-rounded and have been deposited by the moraines, sometimes feature around the edges of the fans. The moraines, proglacial sediments situated next to the exposure and the minor outwash fans are sampled at this site (Figures 4.11, 4.12).



Figure 4.12: (a): Pit dug out of minor outwash fan sampled at site 3. (b): Cross section of minor outwash fan sampled at site 3. (c): Minor outwash fan. Note the drainage from supraglacial material into the fan.

#### 4.2.8 Site 3 grain size analysis

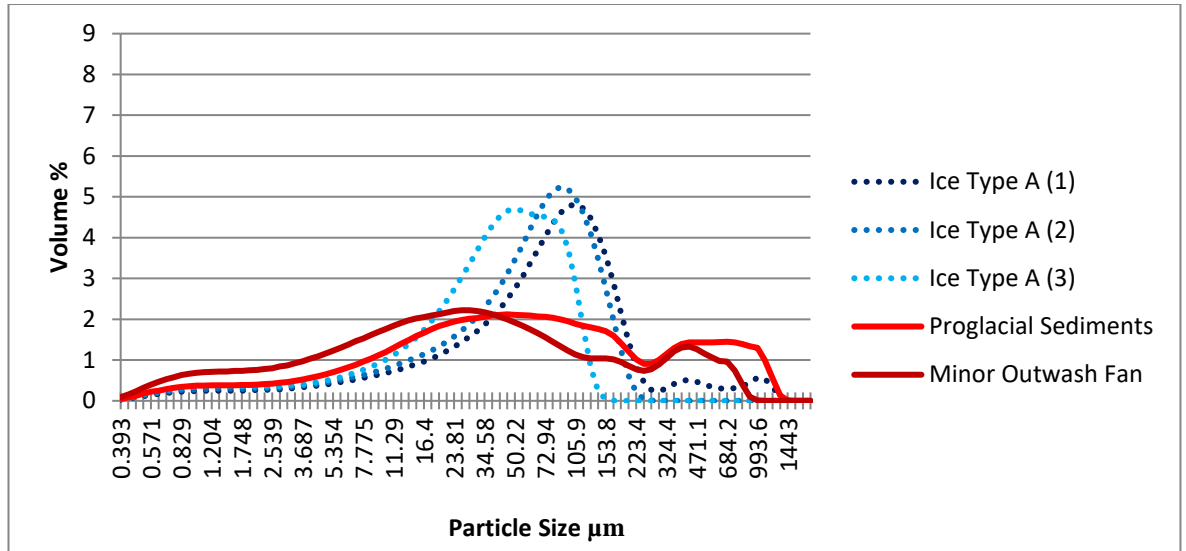


Figure 4.13: Grain size distribution plot for site 3.

The graph (Figure 4.13) illustrates that the samples taken from the facies of ice type A have very similar grain size distributions, as they all consist almost entirely of sediment less than 150  $\mu\text{m}$  in size, which is fine sand to clay. The samples contain a minimal amount of sand at approximately 1-2% in each, and the peaks between 40-80  $\mu\text{m}$  indicate that the ice predominantly comprises silt in all three samples, as each contains at least 85% (Table 4.4). Table 4.4 also shows that the mean particle sizes are all around 45  $\mu\text{m}$ , which is coarse silt. They all have a fine negative skew and are poorly sorted with unimodal distributions.

The proglacial samples are obtained from sediments in front of the exposure and from the minor outwash fan pictured in Figure 4.12c. Both samples also have similar grain size

distributions and comprise large volumes of silt, approximately 76% in the proglacial sediments and 53% for the minor outwash fan (Table 4.4). Similar to the samples from ice type A, they are poorly sorted and are very closely matched in their distributions, despite being sampled from two different features. Table 4.4 shows that the mean particle size for the proglacial sediments is 67  $\mu\text{m}$  which is very fine sand, whereas the mean particle size for the minor outwash fan is 116  $\mu\text{m}$ , which is also very fine sand.

Site 3	D50 ( $\mu\text{m}$ )	Mean ( $\mu\text{m}$ )	Standard Deviation ( $\mu\text{m}$ )	Mean ( $\mu\text{m}$ )	Max Particle Size ( $\mu\text{m}$ )	Min Particle Size ( $\mu\text{m}$ )	SILT (%)	Sorting ( $\mu\text{m}$ )	Kurtosis ( $\mu\text{m}$ )	Skewness ( $\mu\text{m}$ )
Ice A	39.66	45.07	32.13	45.07	168.9	0.393	86.6	33.69 PS	-0.28	0.65
Ice A	39.27	43.65	30.06	43.65	153.8	0.393	87.41	31.52 PS	-0.52	0.52
Ice A	40.15	45.10	31.43	45.10	168.9	0.393	87.41	32.96 PS	-0.40	0.58
Proglacial Sediments	62.17	67.61	47.91	67.61	269.2	0.431	76.70	50.25 PS	-0.23	0.60
Minor Outwash Fan	76.24	116.3	173.6	116.3	1443	0.393	65.70	181.9 PS	18.16	4.02

*Table 4.4: Summary data table for site 3.  
(PS = Poorly Sorted, VPS = Very Poorly Sorted)*

#### 4.2.9 Site 9 ( $63^{\circ}59'40.95\text{N}$ , $16^{\circ}52'25.89\text{W}$ )

---

Site 4 is located in close proximity to site 3, towards the eastern side of the margin (Figure 4.1). The exposure is approximately 2 m wide and 1 m high, and is associated with a fracture orientated approximately parallel to the ice margin (Figure 4.14). The exposure features two distinct ice types (A and B) which consist of two different types of crude

laminations. There is a layer of englacial ice above the basal ice exposure which is ~10cm thick with debris and clasts on the surface of the glacier.

Ice type A is debris-rich and bubble poor, with ice crystals that are too small to observe in the field. It contains a high concentration of silt which has formed crude laminations. Clasts are typically sub-rounded or rounded, between 2-5 cm in length and dispersed within the facies.

Ice type B is debris-rich and bubble poor but features lenses of debris-poor ice, which often cut through the laminations. The facies contains granule-gravel material which has formed crude but distinct laminations. Large, typically sub-angular, clasts up to 10 cm in length feature either within the laminations or dispersed around them.

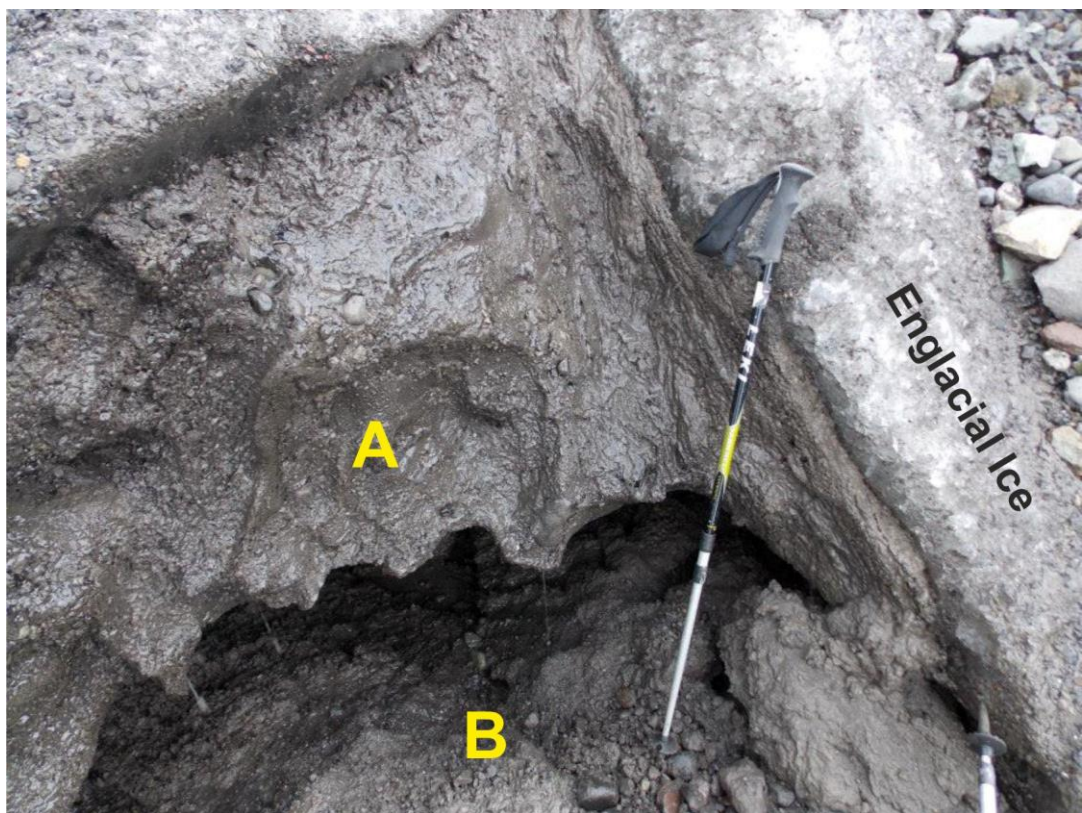


*Figure 4.14: A view of the exposure at site 4. 'A' indicates the exposure, 'B' highlights sediments that are sampled. Pole is approximately 1m for scale.*

This area of the margin is situated on a shallow slope featuring a small meltwater stream flowing from the exposure, which runs down-slope and into a proglacial lake. This meltwater stream contributes to the sediment supply of the saturated and immediate proglacial environment directly in front of the exposure, which features unconsolidated diamicton. There are larger clasts which are well-rounded and between 5 and 15 cm in length. Whilst at the site, several of these clasts were observed falling out of the faces as the ice ablated, leaving hollows in the exposure. These proglacial sediments are the source for one of the samples (Figure 4.15).

A series of small moraines has formed directly in front of the exposure. These are approximately between 1 and 1.5 m high and consist of unconsolidated and unsorted material. The closest moraine to the exposure is approximately 2 m away and this is the source for the other sample taken at this site.



Figure 4.15: The exposure and glacier margin at site 4. 'A' indicates supraglacial material located on surface of glacier and 'B' highlights the melt-out sediments sampled. Person for scale.

#### 4.2.10 Site 4 grain size analysis

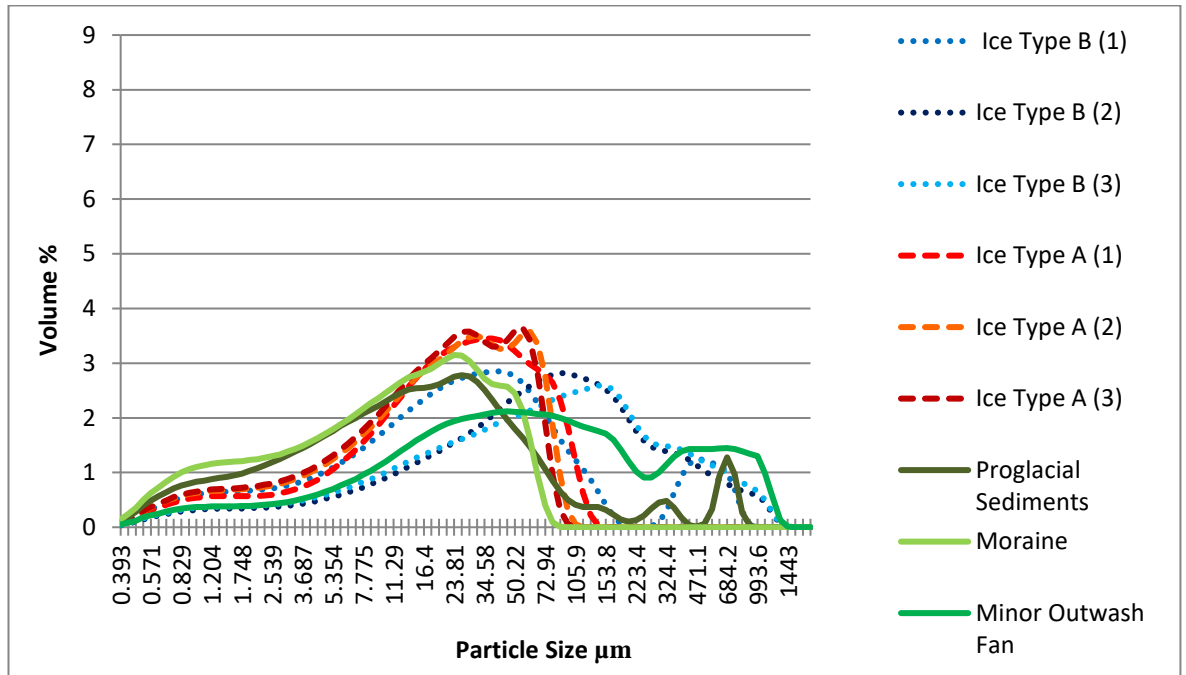


Figure 4.16: Grain size distribution plot for site 4.

Figure 4.16 indicates that the samples taken from ice type B have a similar grain size distribution. Two of the samples from ice type B have a slightly larger grain size distribution as they contain approximately 35% sand, 55% silt and 10% clay. The other sample varies slightly (ice type B1) as it contains only 12% sand, 65% silt and 22% clay. The mean particle size ranges from approximately 82-157 μm which is very fine to fine sand (Table 4.5). Samples 1 and 2 have fine negative skews and are unimodal, in contrast to sample 1 which is bi-modal. All of the samples are very poorly sorted.

Likewise, ice type A samples also share very similar grain size distributions, but in contrast are notably finer grained than the sediment found within ice type B. All three samples

consist almost entirely of sediment that is less than 100  $\mu\text{m}$  in size, which is very fine sand to clay. Each sample contains at least 75% silt (Table 4.5) and they share a peak between 20-60  $\mu\text{m}$ , which is medium to coarse silt. Mean particle size ranges from approximately 24-3  $\mu\text{m}$ , which is medium to coarse silt (Table 4.5). The samples have a fine negative skew and are poorly sorted.

The proglacial samples vary slightly in grain size distribution, but they do share peaks at approximately 20  $\mu\text{m}$  (medium silt). Whilst they share similar distributions in fine-grained material, they differ in the volume of sand they contain. The sample taken from the moraine does not contain any sand and has approximately 60% of silt and the remaining 40% in clay. It has a fine positive skew and is poorly sorted. The sample collected from the proglacial sediments at the exposure does contain a small volume of sand (7%) but still has its highest peak in silt (58%). The samples collected from the minor outwash fan and the proglacial sediments are both very poorly sorted.

Table 4.5 highlights the differences in mean particle size for each feature. The minor outwash fan has a mean particle size of 177  $\mu\text{m}$  (fine sand), the moraine has a mean particle size of 17  $\mu\text{m}$  (medium silt) and the proglacial sediments have a mean particle size of 54  $\mu\text{m}$  (coarse silt).

Site 4	D50 (µm)	Mean (µm)	Standard Deviation (µm)	Max Particle Size (µm)	Min Particle Size (µm)	SILT (%)	Sorting (µm)	Kurtosis (µm)	Skewness (µm)
Ice B	26.01	82.3 8	159.1	993.6	0.393	65.8	166. 8 VPS	7.27	2.85
Ice B	71.23	145. 6	202.9	1443	0.393	55.2	212. 8 VPS	7.30	2.57
Ice B	72.67	156. 2	216.1	1443	0.393	51.2	226. 6 VPS	5.72	2.33
Ice A	23.42	31.4 7	27.39	153.8	0.393	79.3	28.7 3 PS	0.52	1.08
Ice A	20.64	26.8 5	22.66	116.3	0.393	75.6	23.7 6 PS	-0.15	0.86
Ice A	19.33	24.8 0	20.68	105.9	0.393	74.4	21.6 9 PS	-0.18	0.84
Minor Outwash Fan	55	177	265.5	1443	0.393	53.6	278. 4 VPS	3.36	2.01
Moraine	11.98	17.5 6	16.83	96.49	0.393	61	17.6 6 PS	0.56	1.14
Proglacial Sediments	14.52	54.3 5	137.1	905.1	0.393	57.9 9	143. 6 VPS	16.4 7	4.07

*Table 4.5: Summary data table for site 4.  
(PS = Poorly Sorted, VPS = Very Poorly Sorted)*

#### 4.2.11 Site 5 (*63°59'40.14N, 16°52'24.38W*)

---

Site 5 is located in close proximity to site 4, towards the eastern side of the margin (Figure 4.1) and comprises two distinct facies, ice types A and B (Figure 4.17a).

The exposure featuring ice type A is 40 cm high and 30 cm wide. The facies is debris-rich, bubble poor and contains no visible ice crystal boundaries. It contains an abundance of fine-grained material (less than 2 mm) which has formed distinct but crude laminations. There are few larger clasts featured in this part of the exposure, as the material is fine-grained (0.5-1 mm) and looks to mainly comprise sand and silt (Figure 4.17c).

The exposure that featured ice type B is approximately 50 cm wide and 20 cm high. It contains granule-gravel material which has formed crude laminations, giving it a stratified structure. The ice is sediment laden, bubble poor and has no visible crystal boundaries (assumed to be mm in size). Large clasts are predominantly sub-rounded and range between 5 and 10 cm in length. These can be found within the laminations (Figure 4.17b).



*Figure 4.17: (a) An image of site 5 highlighting the location of the two ice types. The red arrow indicates the area where ice type B was sampled and the yellow area indicates the sampling site for ice type A. (b): Ice type B featured at site 5. This facies has crudely stratified layers of silt and sand. Trowel for scale is approximately 25 cm. (c): Ice type A featured at site 5. This facies also features laminations of sediment within the ice, but they are more distinct and the sediment is primarily finer grained (silt and clay).*

Site 5 features the same geomorphological signature as site 3 with a network of small moraines and minor outwash fans (Figure 4.18). A small moraine, approximately 1.5 m in height, has formed adjacent to the exposure. On the far side of the moraine a minor outwash fan has formed, flowing away from the margin. The fan comprises predominantly fine material which is less than 2 mm in size, with no larger clasts or boulders being present. Melt-out from ice type B has led to the formation proglacial sediments and a turbid melt-out stream, which flows directly into the proglacial sediments. The stream flows parallel to the margin, down a shallow slope and into a proglacial lake. Samples for this site are taken from numerous features which include the moraine, outwash fan, proglacial sediments, supraglacial material and the sediment rich stream.



*Figure 4.18: Image depicting the proglacial environment at site 5. 'A' indicates proglacial lakes, 'B' shows the location of a minor outwash fan and 'C' highlights a group of small moraines approximately 1-1.5 m high. Person for scale.*

#### 4.2.12 Site 5 grain size analysis

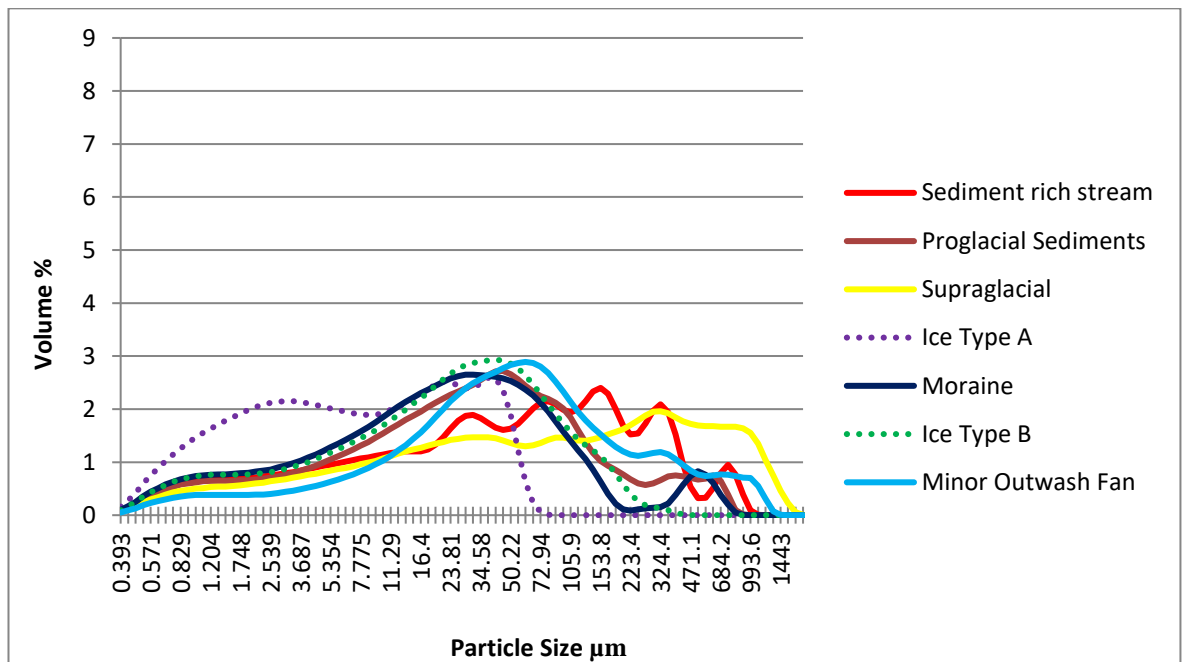


Figure 4.19: Grain size distribution plot for site 5.

Figure 4.19 illustrates the differences in grain size distributions between all of the samples. Ice type B has a distribution that ranges from 0-500 μm which is clay to medium sand, with a peak at approximately 40 μm (coarse silt). The mean particle size is 40 μm which is coarse silt (Table 4.6). The sample is very poorly sorted with a fine positive skew.

Ice type A in contrast, only contains material up to 70 μm (very fine sand) and contains two broader, less distinct peaks at approximately 50 μm (coarse silt) and 3 μm (clay). The mean particle size is approximately 13 μm, which is fine silt (Table 4.6). It also contains a very minimal amount of sand in comparison to the sample from ice type B and is poorly sorted.

The other samples are taken from various landforms and proglacial sediments around the exposure. In contrast to the two ice type samples, they all contain sand, with the

supraglacial and sediment rich stream containing the largest volume (between 30-40%). The sediment-rich stream comprises approximately 30% sand, 48% silt and 22% clay. The proglacial sediments forming at the margin consist of ~15% sand, 63% silt and 22% clay. The moraine contains approximately 8% sand, 65% silt and 27% clay and the minor outwash fan in contrast comprises approximately 25% sand, 62% silt and 13% clay.

The samples taken from the minor outwash fan, proglacial sediments and moraine are the closest grain size match to those taken from the ice and they are very poorly sorted. The samples for the supraglacial and sediment rich stream are also very poorly sorted, however the grain size distributions are not at all similar to the ice type A and B samples.

Site 5	D50 (µm)	Mean (µm)	Standard Deviation (µm)	Max Particle Size (µm)	Min Particle Size (µm)	Silt (%)	Sorting (µm)	Kurtosis (µm)	Skewness (µm)
Ice B	24.21	40.93	49.31	517.2	0.393	67.7	51.74 VPS	7.90	2.40
Ice A	7.189	13.93	15.02	87.9	0.393	48.3	15.75 PS	0.76	1.28
Proglacial Sediments	30.67	77.84	132.1	905.1	0.393	62.8	138.5 VPS	9.55	3.01
Minor Outwash Fan	50.17	129.7	209.6	1443	0.393	61.8	219.8 VPS	8.29	2.81
Moraine	22.13	57.79	115.1	905.1	0.393	64.86	120.7 VPS	15.12	3.83
Sed.Rich Stream	48.84	117.8	167.7	1091	0.393	47.9	175.8 VPS	6.37	2.39
Supraglacial	75.8	232.6	322.3	1909	0.393	39.4	337.7 VPS	2.71	1.79

*Table 4.6: Summary data table for site 5.  
(PS = Poorly Sorted, VPS = Very Poorly Sorted)*

#### 4.2.13 Site 6 (*63°59'35.77N, 16°52'21.77W*)

---

Site 6 is located due south of site 5 and in the eastern part of the margin (Figure 4.1). The exposure here features 3 distinct ice types and is approximately 2 m high and 1.5 m wide.

The key feature at this site is the large fracture-filled debris band (ice type D) running vertically through the exposure (Figure 4.20). The fracture is approximately 2 m high and 15 cm at its widest. It is predominantly filled with sand and gravel, with some larger, sub-angular or sub-rounded clasts ranging from 5-10 cm in length.

At the base of the exposure and to the right of the fracture is another facies (ice type B, Figure 4.20b). This facies is debris-rich and bubble poor with no visible ice crystal boundaries. It predominantly comprises silt and granular material between 1-5 mm in length which has formed crude laminations, giving it a stratified structure. Within the laminations there are also lines infilled with fine sediment moving across the section. Some larger clasts up to 5 cm in length can be found within the laminations. These are typically sub-rounded.

Located above ice type B is another facies, identified as ice type E. This facies is also sediment laden, bubble poor and contains ice crystal boundaries too small to observe in the field. It contains an abundance of fine-grained and silted material (less than 2 mm) which has formed 'pockets' close to the other two ice types. There are no larger clasts featured within this ice type (Figure 4.20c).

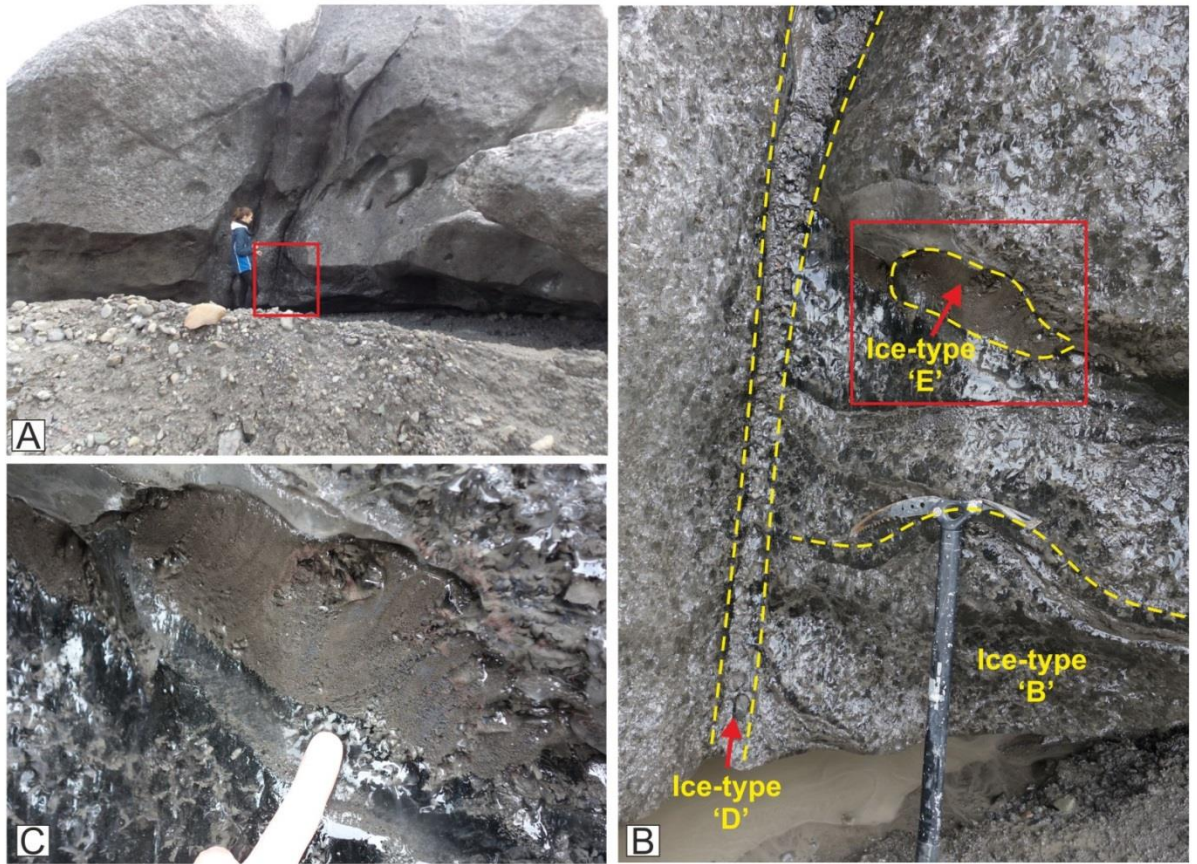


*Figure 4.20: (a): The exposure at site 6. Person for scale (b): The three ice types featured at site 6. (c): A close up image of ice type E. These are pockets within the ice, infilled with high concentrations of silt.*

The proglacial environment at site 6 (Figure 4.21) consists of a small melt-out stream which has formed as the facies and surrounding englacial ice ablated. There is also a moraine approximately 1.5 m high with a gentle slope on the proximal side and a more steep-sided distal slope. A small mound of proglacial sediments has accreted at the margin directly in front of the exposure. The proglacial sediments and the moraine consist of unconsolidated and unsorted material, featuring fine-grained material such as clay, silt and sand. Larger and more angular clasts between 5 and 15 cm in size and some larger, more rounded clasts which could be up to 30 cm in size can also be observed. The shallower

slope of the moraine has horizontal grooves in the sediment, which run parallel to the glacier margin. The till and the moraine are the basis for the samples taken at this site.



*Figure 4.21: Proglacial environment at site 6. Box indicates location of exposure. 'A' highlights the moraine situated directly in front of the exposure approximately 1.5 m high. Rucksack for scale is approximately 0.5 m.*

#### 4.2.14 Site 6 grain size analysis

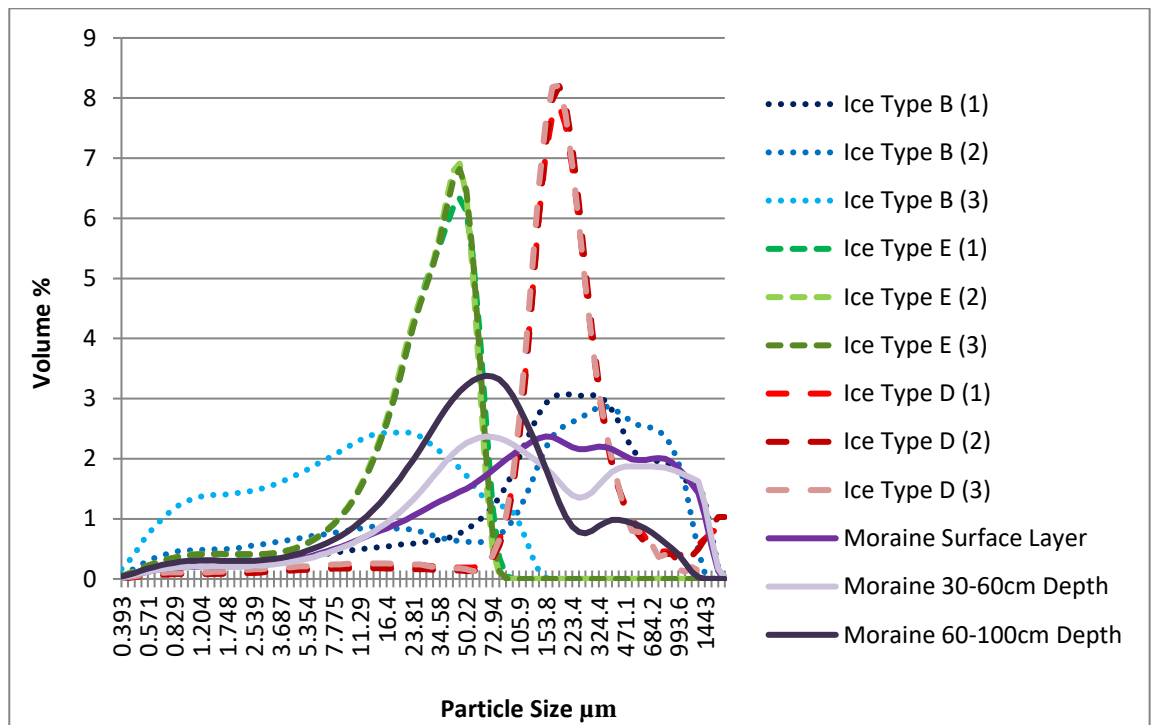


Figure 4.22: Grain size distribution plot for site 6.

Figure 4.22 illustrates the grain size distributions for three different ice types collected at site 6: ice types B, D and E. The samples collected from ice type E all share a peak at around 40 μm (coarse silt), do not contain anything above 80 μm (very fine sand) and are poorly sorted. The mean particle size ranges from 29-30 μm which is coarse silt and they all contain approximately 86% silt (Table 4.7). They all have unimodal distributions and a fine negative skew.

Those collected from ice type D also share a peak at approximately 220 μm (fine sand) and contain minimal amounts of both silt and clay. The mean particle size ranges from 212-280 μm (fine to medium sand) and they contain between 4 and 16% silt (Table 4.7). In contrast

to ice type E, this sample contains much coarser material. It is negatively skewed and poorly sorted.

Site 6	D50 (µm)	Mean (µm)	Standard Deviation (µm)	Max Particle Size (µm)	Min Particle Size (µm)	Silt (%)	Sorting (µm)	Kurtosis (µm)	Skewness (µm)
Ice B	205.8	335	363.2	1909	0.393	55.8	380.3 VPS	1.92	1.56
Ice B	192.5	291.1	311	1584	0.393	23.9	326.1 VPS	0.69	1.19
Ice B	10.54	20.74	25.71	168.9	0.393	56.57	26.94 VPS	3.69	1.94
Ice D	191.4	276.9	318.1	1909	0.393	4.7	293.1 PS	11.78	3.34
Ice D	194	280.6	325.3	1909	0.393	14	294.6 PS	12.05	3.41
Ice D	182.3	212.9	159.6	1739	0.393	16.9	167.3 PS	13.47	2.83
Ice E	29.52	30.58	18.54	96.49	0.393	86.9	19.44 PS	-0.72	0.25
Ice E	29	29.57	17.54	87.9	0.393	86.6	18.40 PS	-0.82	0.16
Ice E	29.51	30.14	17.96	87.9	0.393	86.8	18.84 PS	-0.82	0.17
Moraine 0-30cm	152.3	305.2	361.2	1909	0.393	37.7	378.3 VPS	1.82	1.57
Moraine 30-60cm	106.1	290.9	376.2	1909	0.393	46.6	394.2 VPS	1.89	1.64
Moraine 60-100cm	56.75	121.1	183.9	1443	0.393	66.3	192.9 VPS	9.09	2.90

*Table 4.7: Summary data table for site 6.  
(PS = Poorly Sorted, VPS = Very Poorly Sorted)*

Those from ice type B do not have distinct peaks like the ones that can be seen in the other types, show more variation between samples, and are very poorly sorted. Two are shown to have a large volume of sand (approximately 60%) with 25% silt and the remaining percentage is clay. The mean particle size for these two samples is between 291 and 335  $\mu\text{m}$  which is medium sand (Table 4.7). One sample in contrast (ice type B3) contains almost no sand and instead has its largest peak in silt at 60% and 40% in clay. The mean particle size for this sample is 20  $\mu\text{m}$ , which is medium silt.

The three samples taken from a moraine in the proglacial environment share similar grain size distributions, but it is clear that the surface layer comprises the coarsest material. The only distinct peak is within the sample taken from 60-100 cm depth which is at approximately 80  $\mu\text{m}$  (very fine sand). All three samples are very poorly sorted and do not closely match any of the samples taken from either of the three ice types. The mean particle size ranges from 121-305  $\mu\text{m}$ , which is very fine to medium sand (Table 4.7).

#### 4.2.15 Site 7 (*63°59'25.11N, 16°52'04.60W*)

---

The exposure at site 7 is located at the very southern edge of the margin of Svínafellsjökull (see Figure 4.1) and features a distinct facies with a herringbone-like structure (Ice type C), that is only found in this one location. The basal ice exposure is located in between two sections of englacial ice and is approximately 1 m in width and 1.5 m in height (Figure 4.23a). The facies is debris-rich and bubble poor with ice crystals that range from 1-2 cm in width. The facies comprises very fine material which is predominantly less than 2 mm, with some granular material between 2 and 5 mm, and very few slightly larger clasts (1-5 cm) which are dispersed throughout. The sediment laden ice has produced a distinct pattern

(Figure 4.23b) of small linear features which are orientated in different directions to each other within the facies. This closely resembles the herringbone structure found in supercooling experiments by Knight and Knight (2005) and Cook et al. (2012).

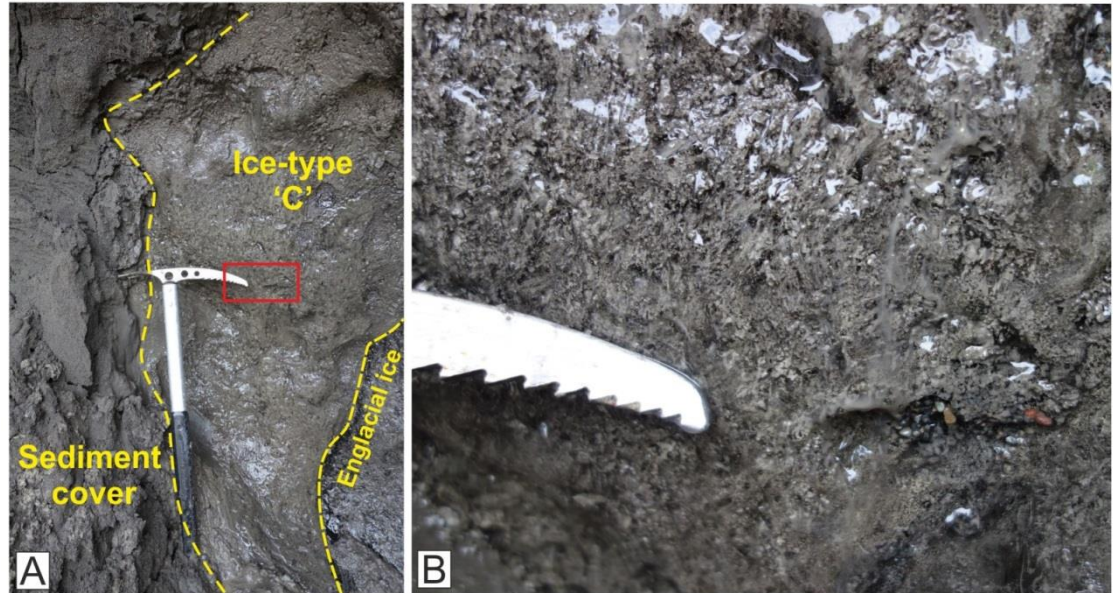


*Figure 4.23: (a): The exposure at site 7. Ice axe is approximately 0.65 m. (b): The facies at site 7. Interlocking lines within the ice resemble a herringbone pattern, which is only seen at this sampling site. Ice axe pick visible is approximately 5 cm in length.*

The exposure at site 7 has produced several small melt-out streams as the sediment laden ice ablates. The melt-out streams from the exposure flow directly into several minor outwash fans that are present around this site. They have formed within intra-moraine networks and are the main geomorphological feature in the proglacial zone of this site. Similar to those found at some of the other sites, the fans comprise material less than 2 mm in size with no larger clasts or boulders present. A cross-section through one of the fans when they were excavated (Figure 4.24b) showed that they appeared to consist of two alternating layers, one of very fine-grained material (silt-rich) and one of slightly coarser material (sand-rich).

The moraines at this site are approximately 1-1.5 m in height and consist of unconsolidated and unsorted material. This surface layer of the moraines predominantly comprises small, sub-angular clasts which are between 5 and 10 cm in diameter. Some larger boulders such as the one seen in Figure 4.24a are found around the edges of the moraines. These are primarily well-rounded and can reach 30 cm in diameter.

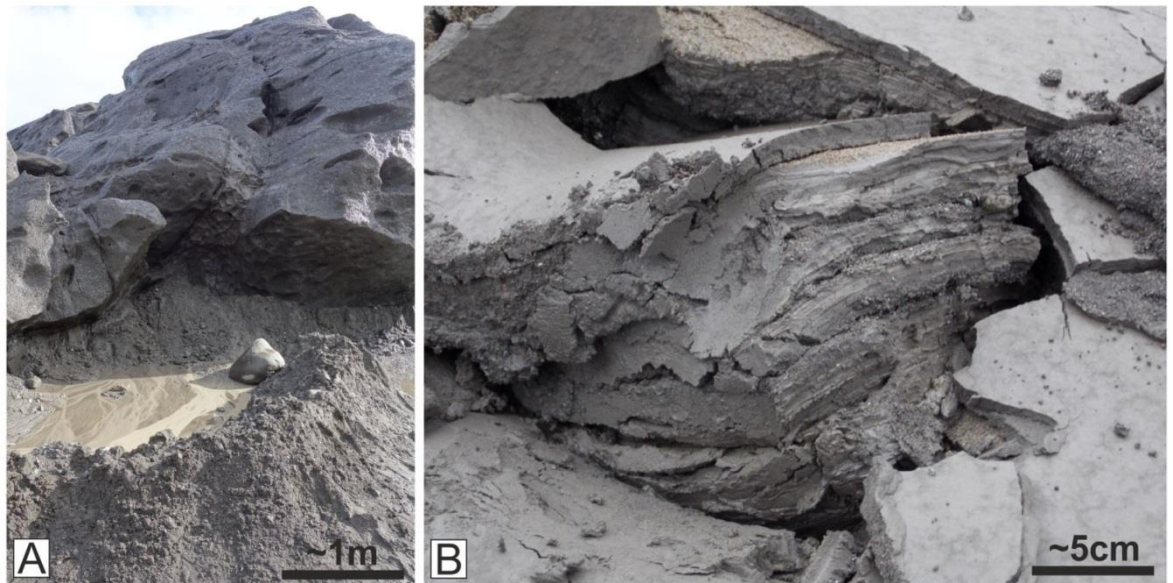


*Figure 4.24: (a): The proglacial environment at site 7 features a small moraine and an outwash fan flowing out from the exposure. (b): A cross section through one of the minor outwash fans at site 7. These are dominated by silt and small amounts of clay but also feature occasional sand partings of ~1 mm in thickness.*

#### 4.2.16 Site 7 grain size analysis

---

Figure 4.25 indicates that the samples taken from ice type C all share similar grain size distributions. Most of them contain a broad peak between 10 and 30  $\mu\text{m}$  which is fine to medium silt, contain minimal amounts of sand and are poorly sorted. Ice type C (3) in contrast has a peak at around 65  $\mu\text{m}$ , almost on the border between coarse silt and very fine

sand. The mean particle size ranges from 10-23 $\mu$ m which is fine to medium silt and the silt content for all samples ranges between 45 and 66% (Table 4.8).

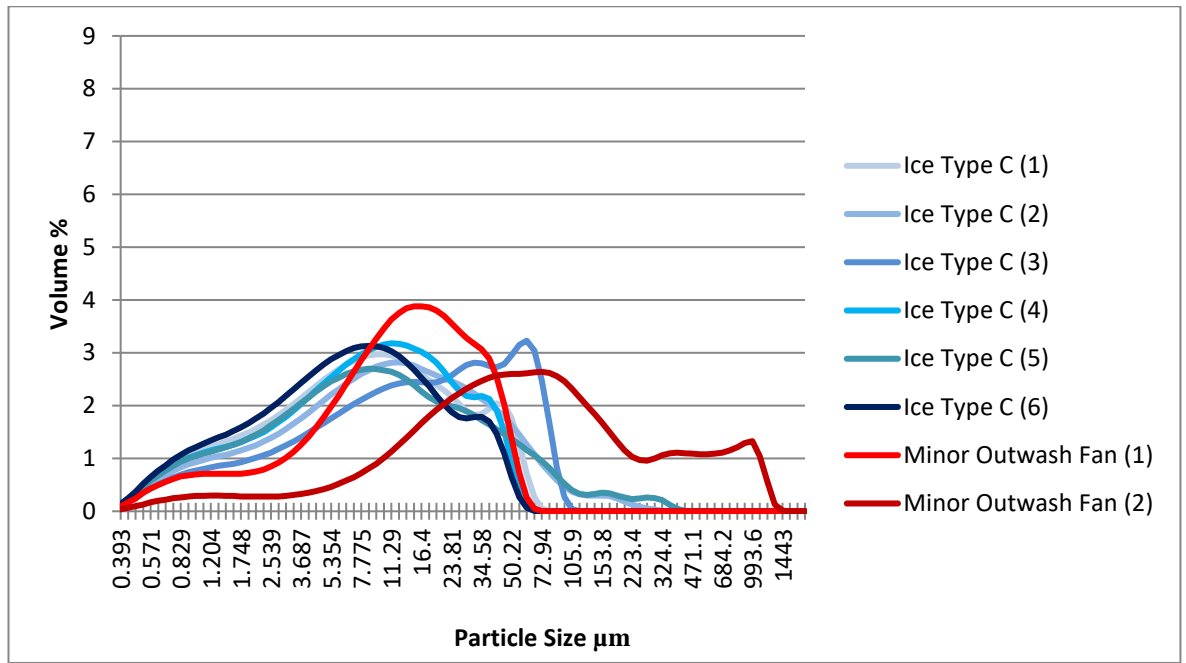


Figure 4.25: Grain size distribution plot for site 7.

The samples taken from the two minor outwash fans have two different distributions. Minor outwash fan 1 shows a peak at approximately 20  $\mu$ m (medium silt), whereas minor outwash fan 2 has a much broader peak between 30-100  $\mu$ m (medium silt to very fine sand). Fan 1 also only contains material up to approximately 65  $\mu$ m (very fine sand), has a fine negative skew and is poorly sorted. Fan 2 contains material up to 1500  $\mu$ m (coarse to very coarse sand), has a negative skew and is also poorly sorted. The fans do not share similar distributions with any of the samples taken from ice type C. The two fans also have different mean particle sizes (Table 4.8). Fan 1 has a mean particle size of 16  $\mu$ m (medium silt) in contrast to that of fan 2 which is 165  $\mu$ m (fine sand). Despite this, they share similar percentages of silt, at 67% and 60% (Table 4.8)

Site 7	D50 (µm)	Mean (µm)	Standard Deviation (µm)	Mean (µm)	Max Particle Size (µm)	Min Particle Size (µm)	Silt (%)	Sorting (µm)	Kurtosis (µm)	Skewness (µm)
Ice C	8.58	12.76	12.27	12.76	72.94	0.393	53.1	12.86 PS	1.26	1.35
Ice C	10.64	20.86	30.07	20.86	429.2	0.393	57.15	31.54 PS	19.40	3.71
Ice C	15.3	23.8	22.76	23.8	116.3	0.393	66.9	23.86 PS	0.01	1.04
Ice C	8.11	13.49	14.17	13.49	80.07	0.393	51.2	14.87 PS	1.68	1.52
Ice C	8.89	22.96	42.25	22.96	471.1	0.393	50.63	44.32 PS	23.92	4.40
Ice C	6.84	10.93	11.27	10.93	72.94	0.393	45.7	11.83 PS	2.18	1.61
Minor Outwa sh Fan	12.77	16.2	13.02	16.2	72.94	0.393	67.8	13.66 PS	0.37	0.99
Minor Outwa sh Fan	57.73	165.3	255.9	165.3	1443	0.393	60.7	268.4 PS	4.60	2.28

*Table 4.8: Summary data table for site 7.  
(PS = Poorly Sorted, VPS = Very Poorly Sorted)*

#### 4.2.17 Site 8 (63°59'23.22N, 16°51'59.68W)

The frazil ice was found within the main meltwater channel at Svínafellsjökull, which is located at the southern end of the margin (see Figure 4.1). The frazil ice was floating close to the edge of the channel. Though this ice did not feature or form part of a basal ice exposure, a sample was collected in order to compare grain size with samples collected at the other exposures.

The section of ice has large interlocking plates and ice crystals of around 2 cm in length (Figures 4.26 and 4.27). There are some fine material clots embedded within the ice which appear to be between 1-5 mm long and appear to predominantly comprise silt or fine clay.



*Figure 4.26: An image of the frazil ice section found at the edge of the main meltwater channel at Svínafellsjökull. Person for scale.*



*Figure 4.27: A closer view of the large interlocking plates which form the frazil ice section. The ice contains very fine sediment, compacted between the ice plates.*

#### 4.2.18 Site 8 grain size analysis

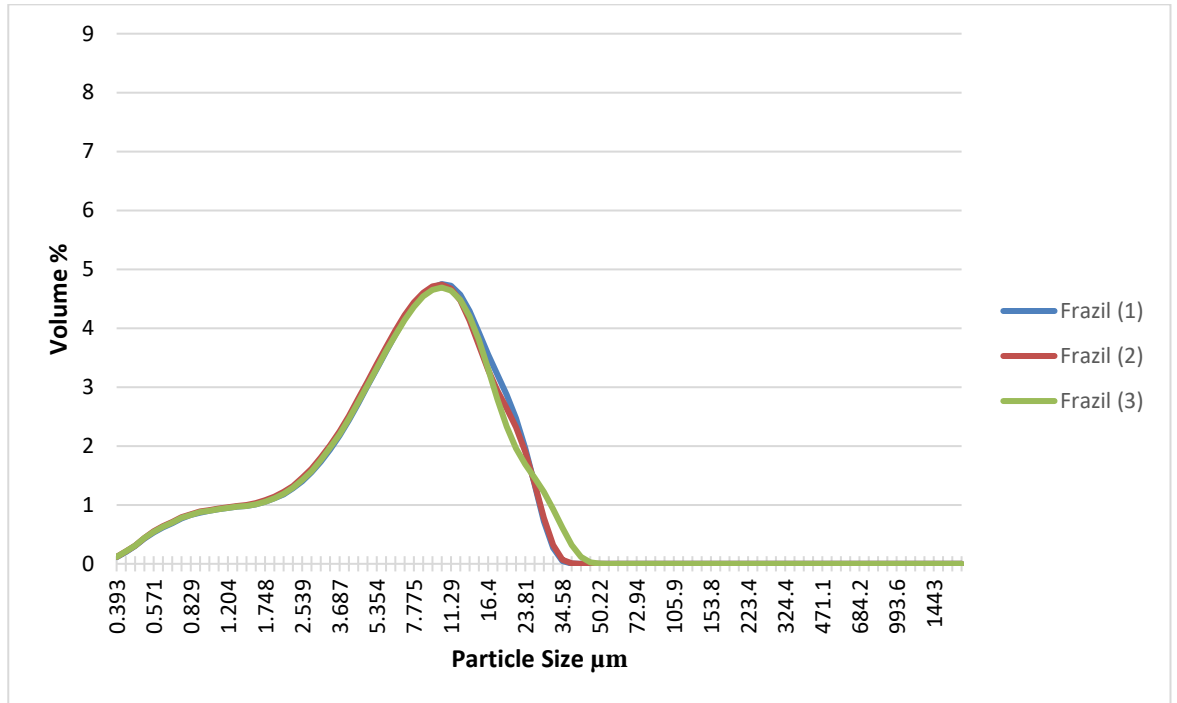


Figure 4.28: Grain size distribution for Site 8.

Figure 4.28 illustrates that the samples taken from the frazil ice all share similar grain size distributions. They all share a peak at approximately 10 µm (fine silt) and do not contain any material larger than 50 µm (coarse silt). Table 4.9 indicates that all of them contain around 50% silt with a mean particle size between 7-8 µm which is very fine silt. The samples have a unimodal distribution and are poorly sorted with a fine positive skew.

Site 8	D50 (µm)	Mean (µm)	Standard Deviation (µm)	Max Particle Size (µm)	Min Particle Size (µm)	Silt (%)	Sorting (µm)	Kurtosis (µm)	Skewness (µm)
Frazil 1	7.81	9.11	6.57	37.97	0.393	50.1	6.89 PS	0.31	0.88
Frazil 2	7.61	8.95	6.57	41.68	0.393	48.8	6.89 PS	0.53	0.96
Frazil 3	7.77	9.40	7.35	55.13	0.393	49.8	7.71 PS	1.82	1.29

*Table 4.9: Summary data table for frazil ice.  
(PS = Poorly Sorted, VPS = Very Poorly Sorted)*

#### 4.2.19 Summary of grain size data for all ice types

---

Figure 4.29 shows the grain size data for all of the ice types identified at each of the eight sampling sites. The graph illustrates that the samples taken for ice types C, D and the frazil ice all have fairly unanimous grain size distributions, with each displaying a distinct peak. It's worth noting that the samples for these ice types are only found at one sampling site, excluding ice type D, which is identified at two. As such, it is expected that they would have a similar grain size distribution. The samples taken from ice types A and C also have very similar grain size patterns, though they do vary more in their distributions. The ice type A samples do contain identifiable peaks between 50 and 130 µm. The samples taken from ice type B show the most variance in grain size distribution. There are no distinct peaks and the samples contain sediment which varies from clay to coarse sand. This ice type is the most common identified, occurring at five out of the eight sites.

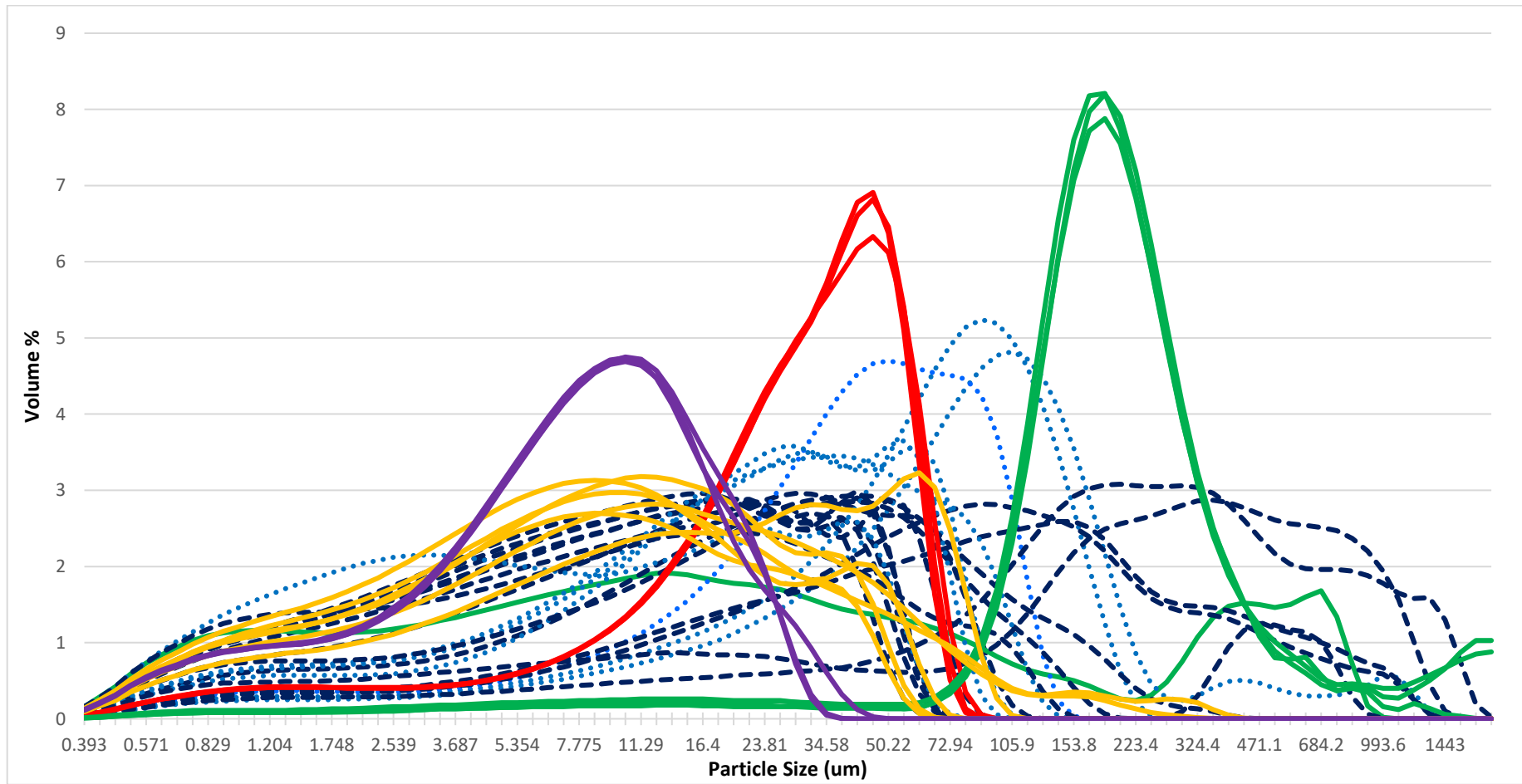


Figure 4.29: Summary graph of grain size characteristics of all ice types

identified across the eight sampling sites



### 4.3 Ternary Plots

---

This section addresses specific objective 2 (chapter 1, section 1.3) by providing a summary of the particle size characteristics of the basal ice at Svínafellsjökull. Ternary plots showing the composition of the collected samples are examined in this section, facilitating a comparison of the samples taken from the basal ice facies with those from the proglacial environment at Svínafellsjökull. The samples have not been separated site by site, but rather by a distinguishing facies identified in the previous section (see Table 4.1). This in order to determine whether the various ice types are sedimentologically distinctive, as well as whether they occur within distinct envelopes on the plot. This would indicate if basal ice or a specific facies has a distinctive and definitive characteristic. Figure 4.31 illustrates the samples taken from specific features found in the proglacial environment (moraine, minor outwash fan, proglacial sediments).

### 4.3.1 Svínafellsjökull basal ice samples

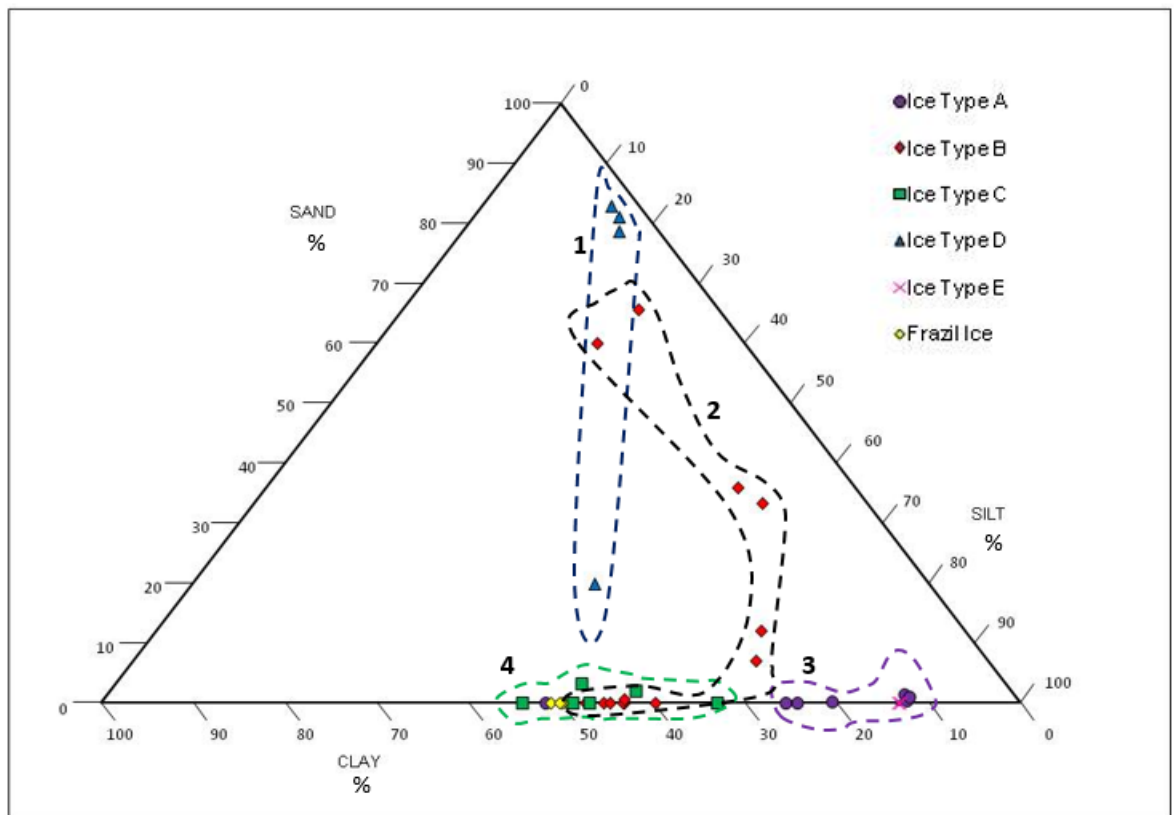


*Figure 4.30: Ternary plot showing the composition of samples taken from basal ice facies around the margin of Svínafellsjökull.*

The ternary diagram (Figure 4.30) illustrates four distinct sedimentological envelopes, based on the six different ice types identified at Svínafellsjökull. The samples with constrained distributions are contained within small sedimentological envelopes, whilst others have a much wider distribution and therefore a larger envelope. The envelopes can also overlap, which indicates that some of the samples share similar sedimentological traits.

- Envelope 1 mainly features samples from ice type D, with a sample from ice type B. It also overlaps with envelope 2.

- Envelope 2 comprises mainly samples from ice type B, with some from ice type C. It also overlaps with envelope 4.
- Envelope 3 contains almost all of the samples for ice type A, and all of the samples for ice type E.
- Envelope 4 predominantly comprises ice types C and frazil ice, with a sample from ice type A, as well as overlap from envelope 2.

The envelopes highlight that some of the samples have distinctive sedimentological signatures, shown by the fact that they only feature within one envelope (such as ice type E in envelope 3) or are mostly within one envelope (such as ice type A, which is mainly contained in envelope 3, with one sample in envelope 4). However, some ice types do not appear to have a distinctive signature, and feature within a much larger envelope overlapping with the others (such as ice type B). In terms of their composition:

- Three samples from ice type A are grouped very closely together, with over 80% of the sample composed of silt, around 1% in sand and the rest in clay. The other two samples similarly do not contain much sand but contain a higher percentage of clay.
- For ice type B, many of the samples are grouped together as they contain no sand but contain roughly 50% clay and 50% silt, though in some cases the silt content is slightly higher at around 65% and 35% for clay. In contrast, two of the samples contain very high percentages in sand (60-65%) with 20-25% silt and 10-15% clay.

- All samples from ice type C are very similar in their composition. All samples contain either no sand or a very small percentage of sand (1-4%), around or just over 50% silt and the rest is clay.
- Similarly, out of the four samples taken from ice type D, three are grouped very closely together. These three samples each contain around 80% sand, approximately 15% silt and about 3-4% clay. The anomaly from this ice type in contrast contains approximately 20% sand, 40% silt and 35% clay.
- Samples from ice type E are also comparable in composition. They each contain no sand, around 85% silt and 15% clay.
- Likewise, the three samples from the frazil ice are alike in composition, again containing no sand and around 50% silt and 50% clay.

### 4.3.2 Svínafellsjökull proglacial samples

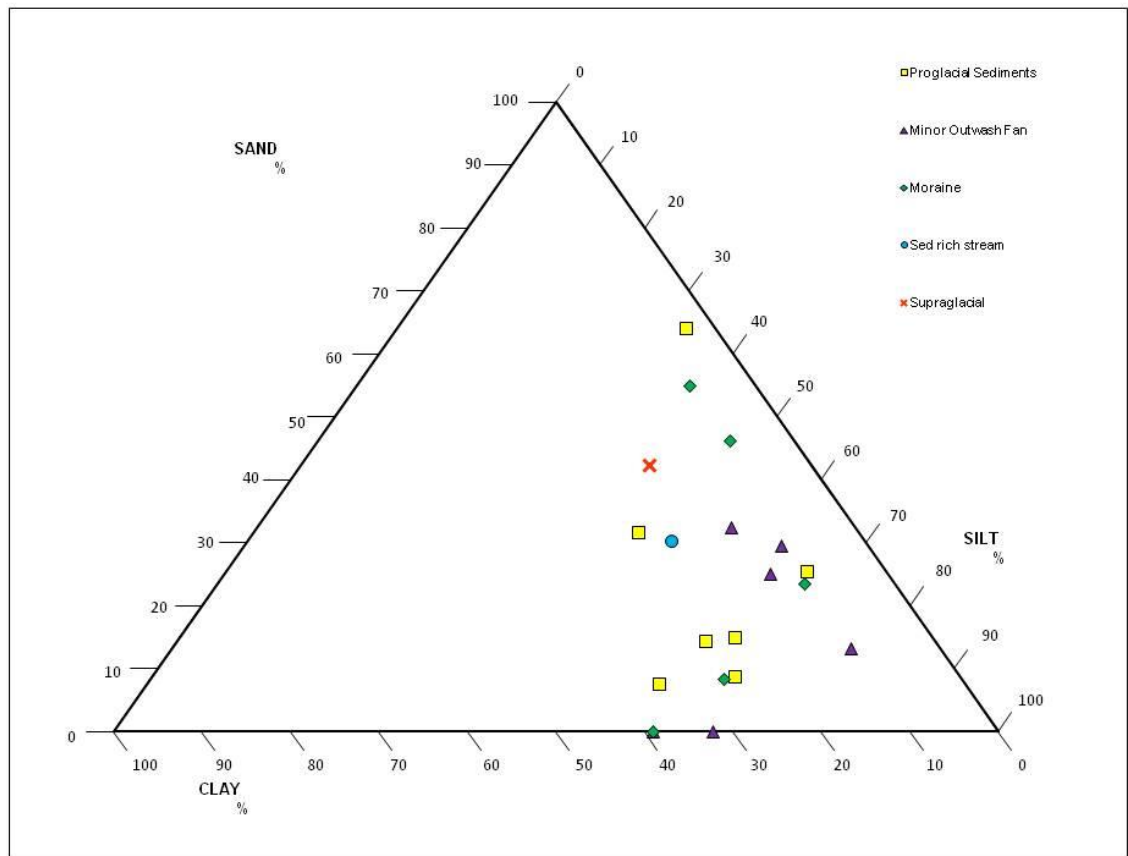


Figure 4.31: Ternary plot showing the composition of samples collected from the proglacial environment around the margin of Svínafellsjökull.

Samples taken from proglacial sediments from the various exposures show some grouping by composition with a few differences (Figure 4.31). Around four of the samples contain approximately 10-15% sand, 60% silt and 25% clay. Two of the other samples contain a greater percentage of sand (30% and 65%) a smaller percentage of silt (30-40%) and little in the way of clay.

The minor outwash fan samples also show some similarities in their composition. Three of them contain between 15-30% sand, 60-70% silt and a small percentage in clay. In contrast, one contains no sand, and approximately 70% silt and 30% clay.

The moraine samples do not have many likenesses in their composition. Of the five samples taken, they range from 0-55% sand, 35-60% silt and 8-40% clay. Three of the samples do however contain very similar amounts of silt (between 61 and 66%).

There is only one sample each for a sediment rich stream and a supraglacial sample, both taken from site 5. The sediment rich stream contains approximately 30% sand, 48% silt and 22% clay and the supraglacial sample has 42% sand, 40% silt and 18% clay.

#### 4.3.3 Comparison of basal ice and proglacial samples

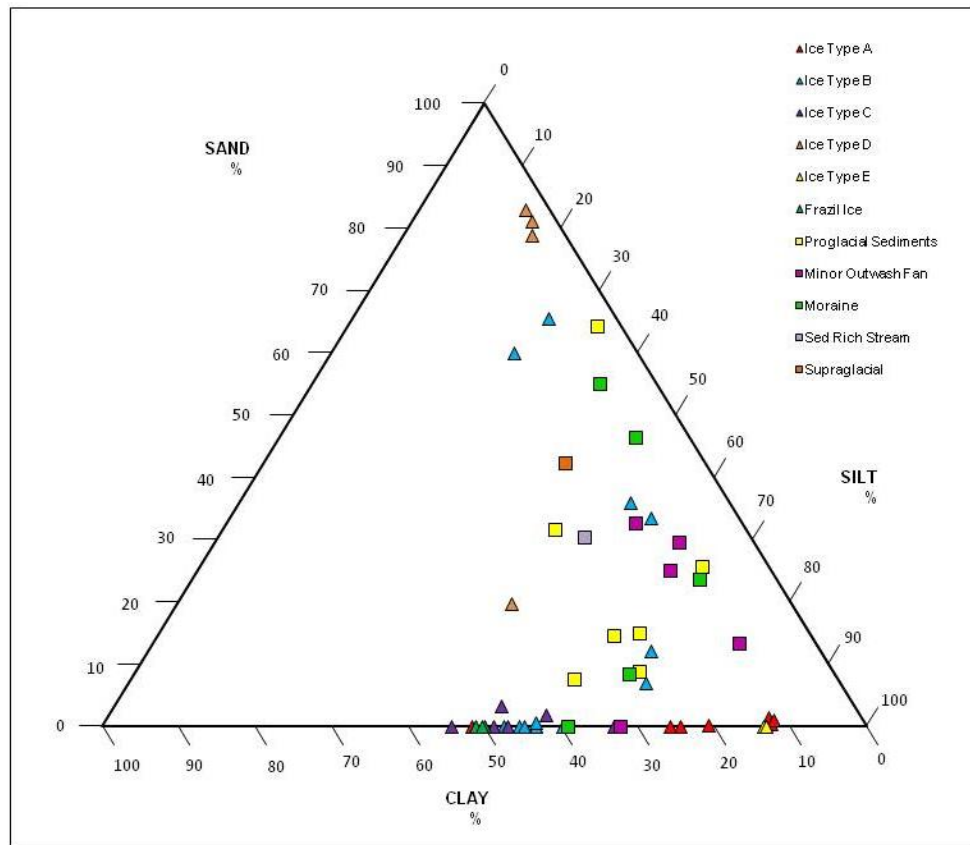


Figure 4.32: Ternary plot showing the composition of samples taken from basal ice facies and proglacial features around the margin of Svínafellsjökull.

If basal ice sediments are being preserved within the proglacial environment, then the plot would be expected to show similarities in the sedimentologies of both the basal ice and proglacial samples. Figure 4.32 shows a comparison between both the basal ice (represented by triangles) and proglacial samples (represented by squares).

Figure 4.32 illustrates that many of the basal ice samples are clustered together, whilst the samples from proglacial features are more dispersed. The plot does highlight some instances where the basal ice and proglacial samples overlap, most notably in the case of the proglacial sediments and minor outwash fans. The samples from these two features match the grain size distributions of the basal ice samples more closely, in that they contain minimal sand, and a relatively high percentage of silt and/or clay. This could suggest that these are the two features most likely to preserve basal ice sediments within them. Since the basal ice samples overlap so much, it is not possible to suggest which facies would be most likely to be preserved, although some samples from ice type B share a very close distribution with some samples taken from proglacial sediments.

#### 4.4 Spatial Analysis

---

The purpose of this section is to determine whether the presence of basal ice is associated with the formation of specific local geomorphology, and to consider whether a particular landform or type of proglacial sediment could be linked to the preservation of basal ice in the proglacial environment (specific objectives 6 and 7, chapter 1, section 1.3). Figure 4.33 shows the distribution of the facies and proglacial features around the margin of Svínafellsjökull, and figure 4.34 illustrates the silt content of each ice facies and proglacial feature on a site by site basis.

Figure 4.33 illustrates that the various ice facies and proglacial features identified are unevenly distributed around the margin of Svínafellsjökull. Whilst some of the ice types are identified at several sampling sites (such as ice type B), some are only found in a singular location (such as ice type E). Similarly, with the proglacial features, the moraines and proglacial sediments can be found at each site (though these were not always sampled) whereas the minor outwash fans have only formed at sites 3,4 5 and 7.

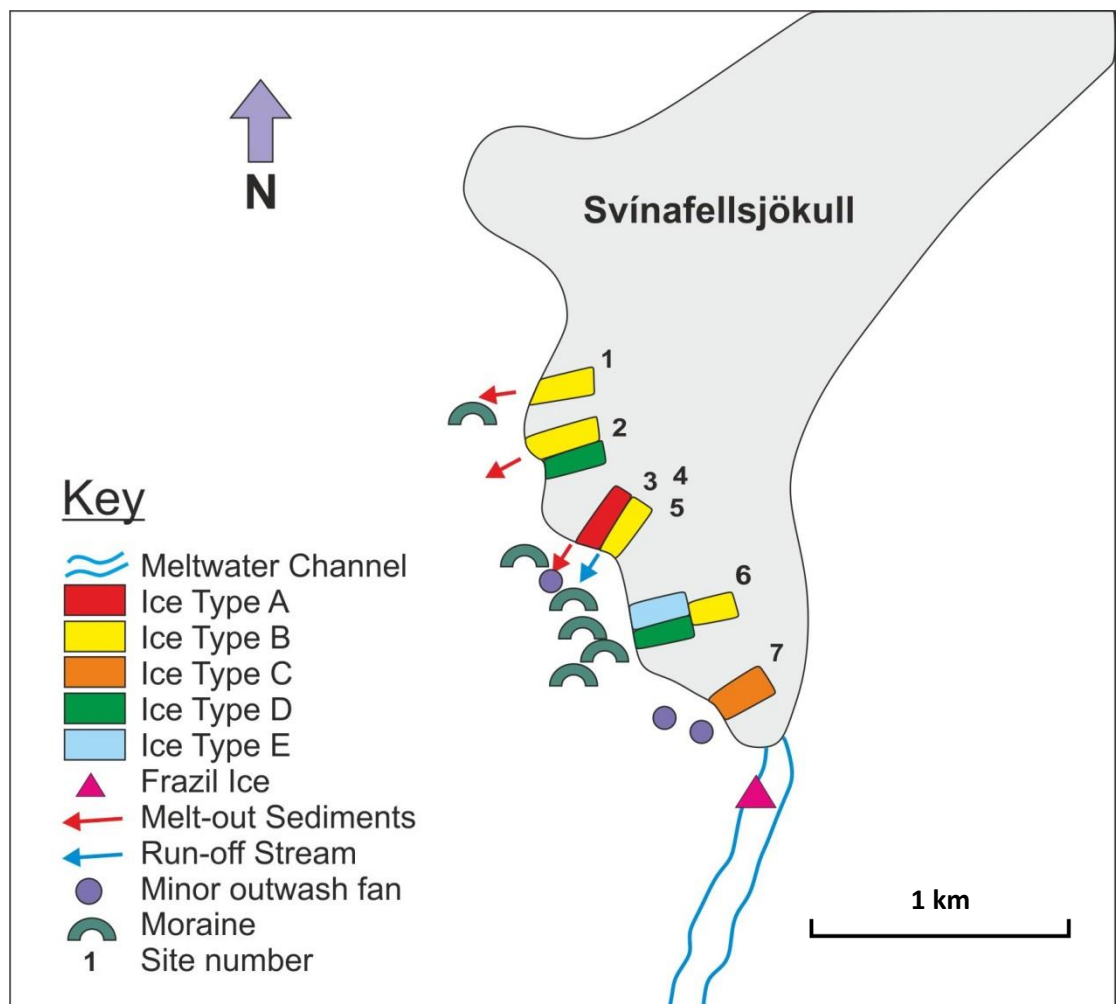


Figure 4.33: Diagram highlighting the distribution of different ice types around the margin of Svínafellsjökull and the local geomorphology in the surrounding proglacial environment.

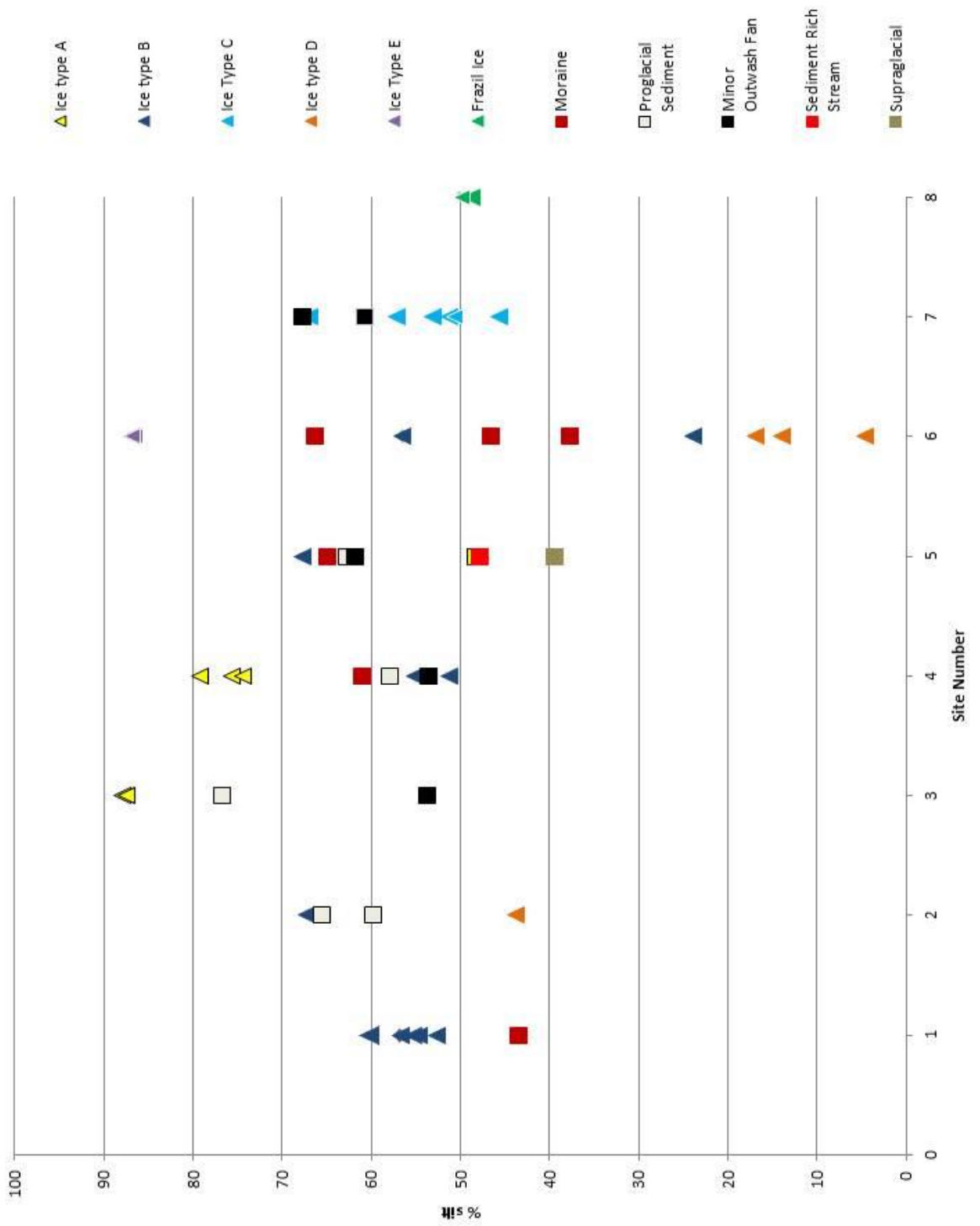


Figure 4.34: Silt content within each ice type and proglacial feature on a site by site basis.

Figure 4.34 is intended to show whether any distinct spatial variations within the basal ice are transferred to the proglacial samples. Basal ice samples are again represented by triangles and proglacial samples by squares. Overall, the graph shows that for many of the sites, the silt content variations seen within the basal ice samples are not reflected in the proglacial features. This is especially clear at site 6, where there are samples from three different ice types as well as samples taken from a moraine. They all contain very different silt percentages, ranging from less than 10% up to approximately 85%. None of the basal ice samples overlap with the samples from the moraine, which shows that the spatial variation within the basal ice samples at this site has not been transferred to the proglacial environment.

Despite this, at site 7 there is some overlap between the samples taken from ice type C and the minor outwash fans sampled at this site. The same can also be seen at site 4, where samples from ice type B overlap with a minor outwash fan and proglacial sediments. The graph overall does not present a clear link between the spatial variations of silt seen within the basal ice samples and those within the proglacial samples. However, the small overlap of the two sample sets at sites 4 and 7 could suggest that there is scope for a spatial relationship between the sediment source (basal ice) and transference to a sediment sink (proglacial fans and sediments).

## 4.5 Summary

---

The visual descriptions of the sample sites, grain size distribution graphs, ternary plots and spatial analysis figures all indicate that the basal ice at Svínafellsjökull is distinctive, both visually and sedimentologically. The proglacial features are more diverse in their grain-size distributions and are also sedimentologically distinct. A clear link between the sedimentological characteristics identified within the basal ice and the transference and preservation of these to the proglacial environment cannot be established based on these results.

*1. The basal ice at Svínafellsjökull is characterised by a range of visually distinctive ice types*

Initial observations at the field site has led to the identification of six distinctive ice types. Some ice types are only found at one sample site whilst others, predominantly ice types A and B, can be found across numerous sites, especially ice type B. Visually, the ice types vary, in terms of the size of the ice crystals, the structure of the debris and sediment within, the ice formation patterns (herringbone and frazil), and the size and shape of the clasts featured in or around the facies.

*2. The ice types and proglacial features are sedimentologically distinct*

The ternary plot that separates the samples according to ice type, rather than site, suggests that some of the ice types are sedimentologically distinct from each other as they fall within small, distinct envelopes. Others have much wider distributions and therefore fall within a larger sedimentological envelope, which suggests a lack of a distinctive sedimentological signature.

There are also similarities that feature across the whole sample set. For the most part, the basal ice samples contain less than 10% sand, aside from the samples from ice type D which each contain around 80% sand and two of the samples from ice type B. Many of the ice type samples also comprise over 50% silt.

In contrast, the proglacial samples contain a substantial amount of sand, mainly between 10 and 30% with only one or two containing no sand at all. Similar to the basal ice samples, those that contain less sand, have a high percentage of silt (over 50%) and little clay. This pattern can be seen for samples taken from the three main proglacial features (proglacial sediments, minor outwash fans and moraines).

*3. Basal ice and proglacial samples are all either poorly or very poorly sorted*

Poorly and very poorly sorted samples are not entirely unexpected in samples taken from basal ice that has formed due to the entrainment of subglacial sediments, due to the variance in material available. Poorly or very poorly sorted samples taken from proglacial sediments or features, could be explained by the potential for numerous sediment sources to be contributing to their formation.

Some of the ice types that are thought to have a supercooling origin are often poorly sorted rather than very poorly sorted (Ice types A and C). The slightly higher level of sorting within these samples could be due to the fluvial input from glaciohydraulic supercooling, if they are indeed formed as a result of this process.

*4. A high silt content (over 50%) is common in many ice types and this is reflected the most within proglacial sediments and minor outwash fans*

Where samples from the ice have a relatively high percentage of silt (50% or more), which is the most common in ice types A, B and C, this appears to be reflected in samples taken in the proglacial area. This can be seen in the main three features sampled, proglacial

sediments, minor outwash fans and moraines, though appears to be most commonly associated with the proglacial sediments.

Moraines can be found close to every site around the margin but these were not always sampled. All of the exposures feature proglacial sediments, though these can differ slightly visually across the sites. In contrast, minor outwash fans only form at certain sites (3, 4, 5 and 7). This appears to be wherever the ice has a very high sediment content that is very fine grained (silt and clay), a fluvial input from the melt-out streams and an intra-moraine network that they can form within.

*5. The different ice types and proglacial features identified are unevenly distributed around the margin of Svínafellsjökull*

Figure 4.30 shows that the different ice types and proglacial features do not all occur at each sampling site. Some ice types (A and B) can be found at several sites, whilst others (C and E) can only be found at one site. Similarly, the moraines and proglacial sediments can be found at numerous sites but the minor outwash fans have only formed at four of the sites. This could suggest that different subglacial processes are active at different parts of the margin, which is affecting the formation of different ice types in different locations. This could in turn be affecting the resulting proglacial formations, producing distinct geomorphology at particular sites.

*6. Spatial variations in silt content within the basal ice samples are not reflected within the proglacial features*

There is not enough evidence to suggest a clear link between spatial variations seen within the basal ice facies and proglacial features sampled at Svínafellsjökull on a site by site basis. Though there does appear to be a genetic link between some of the facies and the minor outwash fans at some of the sites, the sedimentological characteristics of the two do

not reflect each other closely enough to fully determine if there is a sediment supply, transfer and preservation relationship occurring.

## 5. SEDIMENTOLOGY OF BASAL ICE: A GLOBAL PERSPECTIVE

---

### 5.1 Introduction

---

One of the objectives of this research project (specific objective 6, chapter 1, section 1.3), is to analyse and compare sedimentological data collected from the basal ice layers of several glaciers, from numerous locations. These include the Russell glacier in Greenland, the Matanuska and Root glaciers in Alaska, Ferpècle in Switzerland, Storglaciären in Sweden and Skeiðarárjökull in Iceland.

The site specific case study was conducted at Svínafellsjökull in order to assess whether a particular sedimentary characteristic of basal ice could be identified and then applied to the proglacial environment in one location. However, a comparison study of the BIL of other glaciers is imperative when trying to ascertain whether basal ice is indeed sedimentologically distinctive. If the basal ice layers of different glaciers are distinct from one another then this would suggest that the sedimentological characteristics and patterns found within the BIL are site specific. However, if a specific characteristic can be identified across a set of data that compares several glaciers from a range of different environments, this would suggest that it is indeed possible to use this one sedimentological signature to identify the presence of basal ice anywhere in the world.

The ability to recognise basal ice layer sedimentologies anywhere in the world would have a significant impact upon the discipline and the work of quaternary scientists. The basal ice layer provides information on the largely inaccessible subglacial zone (Knight, 1997). The sediments from basal ice can therefore be used to infer the active subglacial processes,

conditions such as the basal thermal regime and the bedrock geology. The ability to recognise such sediments would provide a much greater insight into current and former glaciated areas, and allow for more accurate reconstructions of glacial masses.

Though much of the previous literature has often focussed in detail on the basal ice layer of an individual glacier, a comparison of the characteristics of the BILs from several glaciers is rarely undertaken. An assessment of basal ice facies characteristics across glaciers from various locations, which are subject to different environments and thus changing site specific conditions, could greatly improve our understanding of the variability in basal ice sedimentologies, and their potential for preservation and identification. In turn, this could potentially lead to the key criteria enabling the identification of basal ice sediments within the proglacial environment. This would be especially useful for identifying BIL deposits in areas that have been previously glaciated. Unless it is possible to identify a distinctive characteristic that relates to most, if not all basal ice layers, then there is little prospect of recognising their imprint in the palaeoglaciological record.

## 5.2 Analysis of the data

---

The grain size data analysed in this chapter is taken from several different glaciers: Ferpècle in Switzerland, the Root and Matanuska glaciers in Alaska, Russell glacier in Greenland and Skeiðarárjökull in Iceland (Figure 5.1).

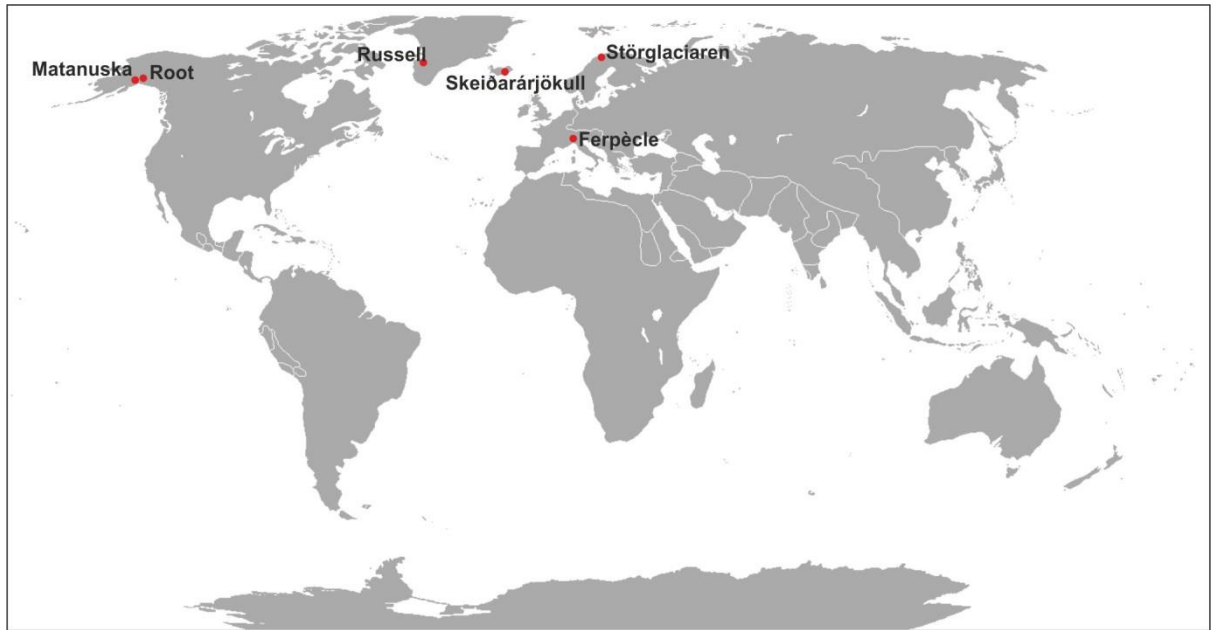


*Figure 5.1: Location map of the glacier sites used for basal ice layer sampling.*

**Ferpècle, Switzerland** ( $46^{\circ}01'13.31''N$   $7^{\circ}34'35.84''E$ )

Ferpècle is a 6.5km long valley glacier located in the Pennine Alps, Switzerland. The grain size data provided in this chapter for Ferpècle is analysed from samples collected from its basal ice layer by Dr Richard Waller.

**Storglaciären, Sweden** ( $67^{\circ}54'11.79''N$   $18^{\circ}34'14.48''E$ )

Storglaciären is a glacier located in the Tarfala Valley in the Scandinavian Alps. It is a polythermal valley glacier. The grain size data provided in this chapter for Storglaciären is analysed from samples collected from its basal ice layer by Dr Simon Cook.

**Matanuska Glacier, Alaska** ( $61^{\circ}40'06.87''N$   $147^{\circ}34'43.60''W$ )

The Matanuska glacier is a valley glacier located in the Chugach mountain range in Alaska. Its terminus feeds into the Matanuska River. The grain size data provided in this chapter for the Matanuska glacier is analysed from samples collected from its basal ice layer by Dr Richard Waller.

**Root Glacier, Alaska** (61°34'52.31"N 142°54'19.16"W)

The Root glacier is a valley glacier located in Wrangell-St. Elias national park in Alaska. The grain size data provided in this chapter for the Root glacier is analysed from samples collected from its basal ice layer by Dr Richard Waller.

**Russell glacier, Greenland** (67°05'44.59"N 50°13'00.08"W)

The Russell glacier is located in the Qeqqata municipality in south west Greenland. It is a polar outlet glacier of the west Greenland ice sheet. The grain size data provided in this chapter for the Russell glacier is analysed from samples collected from its basal ice layer by Dr Richard Waller.

**Skeiðarárjökull, Iceland** (64°01'01.74"N 17°14'59.08"W)

Skeiðarárjökull is a large outlet glacier which drains from the southern edge of the Vatnajökull ice cap. The grain size data provided in this chapter for Skeiðarárjökull is analysed from samples collected from its basal ice layer by Dr Richard Waller.

5.2.1 Ferpècle Glacier, Switzerland

---

Figure 5.2 illustrates that the samples collected from the basal ice layer of Ferpècle share similar particle size distributions. All of the samples are either poorly or very poorly sorted and have a fine negative skew. The most defined peak is at approximately 30 µm (medium silt) in the F2 sample. The samples do not contain material coarser than 300 µm which is medium sand.

Figure 5.3 also highlights the similarities in grain size distributions as the samples are clustered together, indicating similar percentages of sand, silt and clay within each. Table

5.1 shows that the mean particle size ranges from approximately 28-37  $\mu\text{m}$  which is medium to coarse silt. Silt content is also high and is between 65-75% for all five samples.

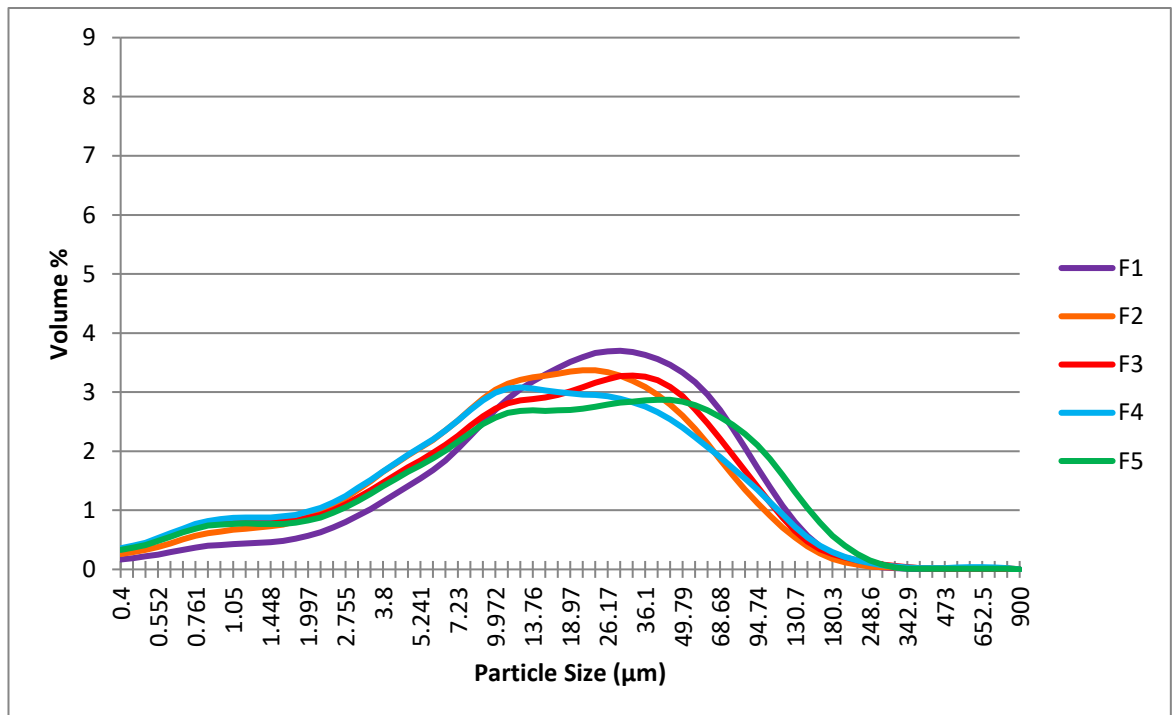


Figure 5.2: Grain size distribution plot of basal ice at Ferpècle.

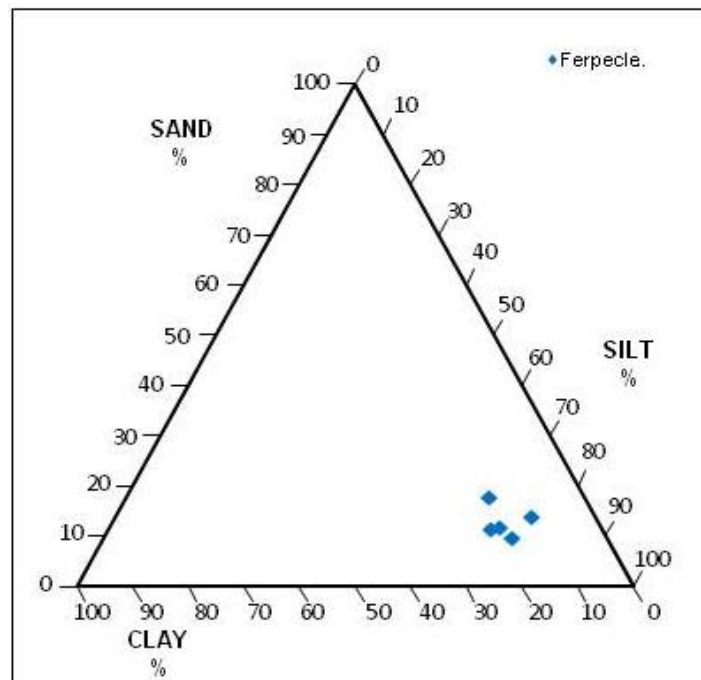


Figure 5.3: Ternary plot of the basal ice samples collected at Ferpècle.

Sample	D50 (µm)	Mean (µm)	Standard deviation (µm)	Minimum (µm)	Maximum (µm)	Silt Content (%)	Sorting (µm)	Kurtosis (µm)	Skewness (µm)
F1	22.6	34.54	38.70	0.4	808.5	75	39.18 PS	60.03	4.62
F2	16.3	28.38	40.39	0.4	808.5	73.51	40.44 PS	99.74	7.11
F3	17.91	30.96	39.54	0.4	726.3	70.34	39.90 PS	37.93	4.16
F4	15.13	30.11	46.69	0.4	808.5	68.87	46.66 PS	76.20	6.47
F5	19.87	37.28	47.05	0.4	808.5	65.25	46.62 VPS	31.83	3.62

*Table 5.1: Summary data table for Ferpècle.  
(PS = Poorly Sorted, VPS = Very Poorly Sorted)*

### 5.2.2 Storglaciären, Sweden

Figure 5.4 shows that all three samples taken from the BIL at Storglaciären have similar particle size distributions. All three samples are negatively skewed, contain peaks in silt between 67-73% and lack anything coarser than c. 100 µm. The samples are all poorly sorted.

The ternary plot (Figure 5.5) shows that the samples are clustered together and highlights that the samples contain a negligible amount of sand, with each comprising approximately 70% silt and 30% clay. One of the most noticeable aspects of the samples for Storglaciären is that they only contain a very small amount of sand (less than 0.1%). Table 5.2 indicates

that the mean particle size ranges between 15 and 22  $\mu\text{m}$ , which is fine to medium silt. Silt content is also high across all three samples as it ranges between 67 and 73%.

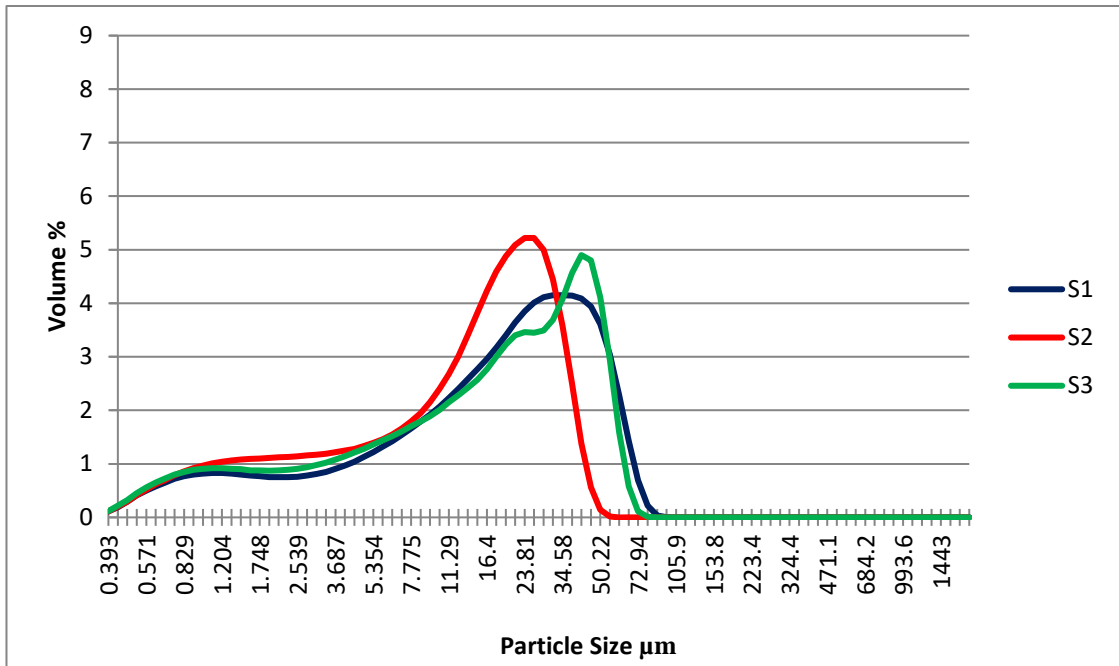


Figure 5.4: Grain size distribution plot of the basal ice samples from Storglaciären.

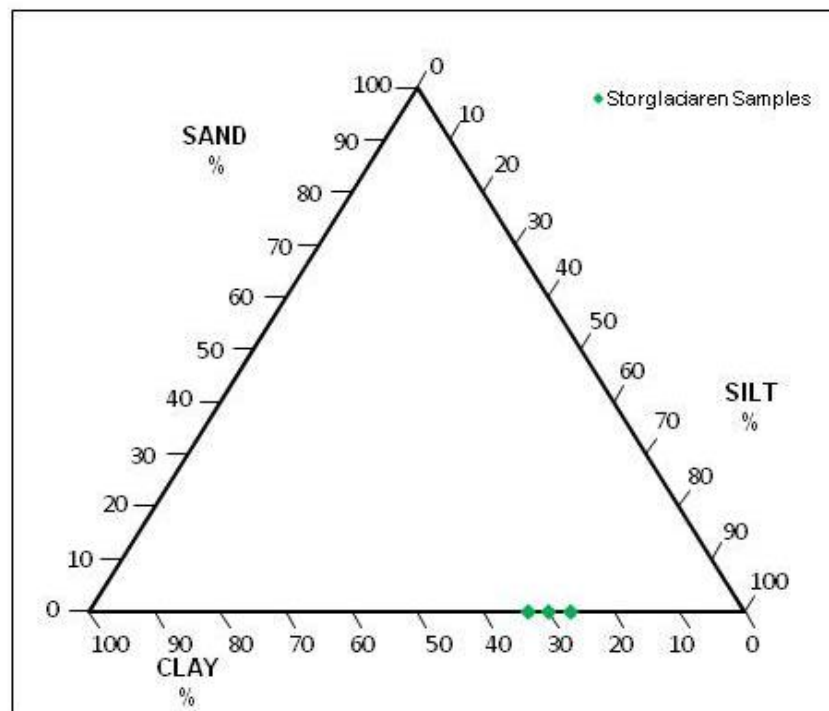


Figure 5.5: Ternary plot of basal ice samples from Storglaciären.

Sample	D50 (µm)	Mean (µm)	Standard deviation (µm)	Minimum (µm)	Maximum (µm)	Silt Content (%)	Sorting (µm)	Kurtosis (µm)	Skewness (µm)
S1	19.29	22.78	18.11	0.4	96.49	73.5	19.00 PS	-0.29	0.71
S2	14.5	15.53	11.44	0.4	60.52	67.1	12.00 PS	-0.70	0.46
S3	17.97	21.53	17.33	0.4	80.07	70.1	18.18 PS	-0.75	0.58

*Table 5.2: Summary data table for Storglaciären.  
(PS = Poorly Sorted, VPS = Very Poorly Sorted)*

### 5.2.3 Root Glacier, Alaska

---

The samples taken from the basal ice layer of the Root glacier comprise very different particle size distributions (Figure 5.6). The samples are very poorly or poorly sorted and are multi-modal. The R1 sample contains around 50% silt, 40% sand and 10% clay, with no visible peaks in either classification and is very strongly positively skewed. The R2 sample also has a fine positive skew and contains a large volume of clay (70%), around 30% silt and no sand. The R3 sample in contrast has a fine negative skew and contains approximately 10% clay and 45% in both sand and silt.

The ternary plot reflects these broader distributions (Figure 5.7) and how diverse the samples are. Table 5.3 indicates that the mean particle size ranges between 3 and 115  $\mu\text{m}$ , which is clay to very fine sand. Silt content ranges between approximately 30-50%.

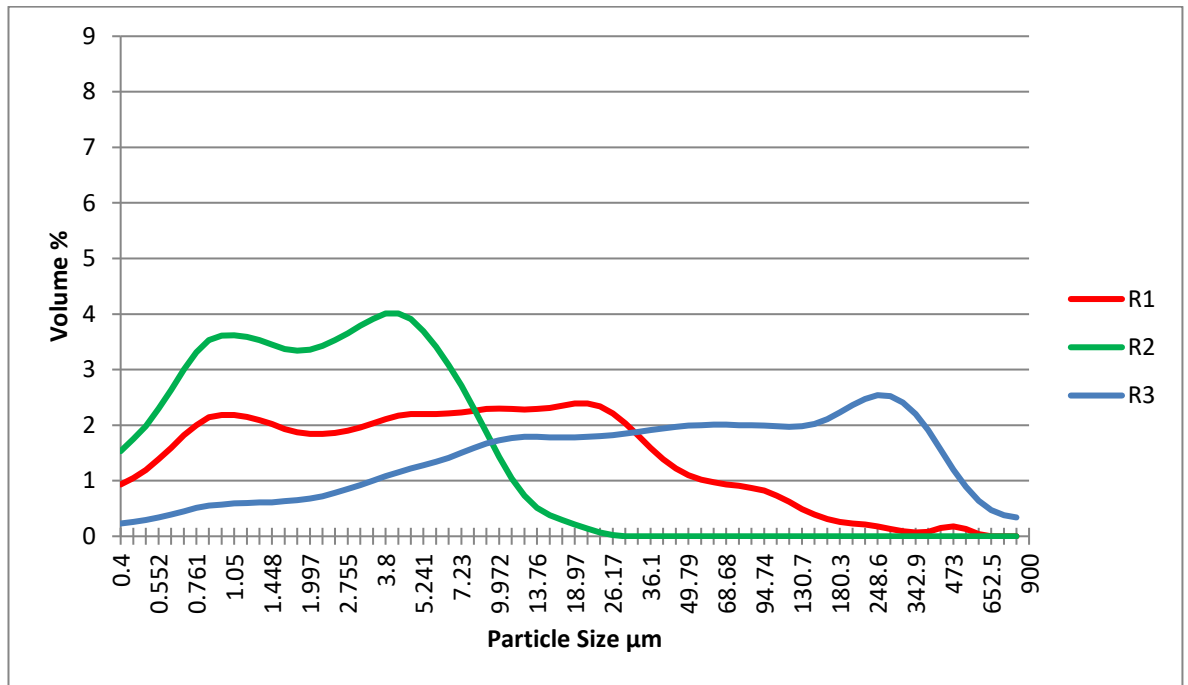


Figure 5.6: Grain size distribution plot of the samples taken from the Root glacier.

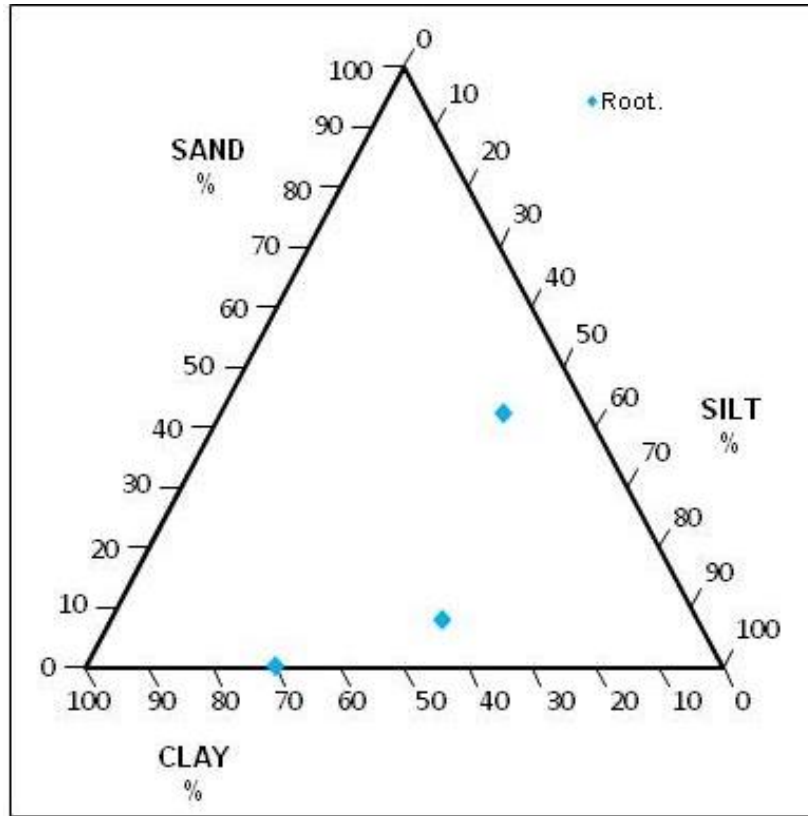


Figure 5.7: Ternary plot of Root glacier samples.

Sample	D50 ( $\mu\text{m}$ )	Mean ( $\mu\text{m}$ )	Standard deviation ( $\mu\text{m}$ )	Minimum ( $\mu\text{m}$ )	Maximum ( $\mu\text{m}$ )	Silt Content (%)	Sorting ( $\mu\text{m}$ )	Kurtosis ( $\mu\text{m}$ )	Skewness ( $\mu\text{m}$ )
R1	6.87	23	51.81	0.4	586.2	52.05	51.81 VPS	47.30	6.01
R2	45.06	115.8	153.3	0.4	808.5	44.54	153.6 VPS	3.77	1.90
R3	2.38	3.479	3.294	0.4	26.17	29.8	3.30 PS	6.13	2.06

Table 5.3: Summary data table for the Root glacier.  
(PS = Poorly Sorted, VPS = Very Poorly Sorted)

#### 5.2.4 Matanuska Glacier, Alaska

Figure 5.8 indicates that the samples taken from the BIL at Matanuska all share similar particle size distributions. The samples are all poorly sorted and have fine positive skews. The peaks of all the samples are between approximately 7-20  $\mu\text{m}$  which is very fine silt to medium silt.

Figure 5.9 illustrates that the samples have formed two clusters on the ternary plot, which means they contain similar percentages of sand, silt and clay. Table 5.4 shows that silt content is high across all samples which range between approximately 68 and 78%. Many of the samples contain less than 5% sand, meaning that the remaining percentage is clay. The mean particle size across all the samples is between 8 and 25  $\mu\text{m}$ , which is fine silt to medium silt.

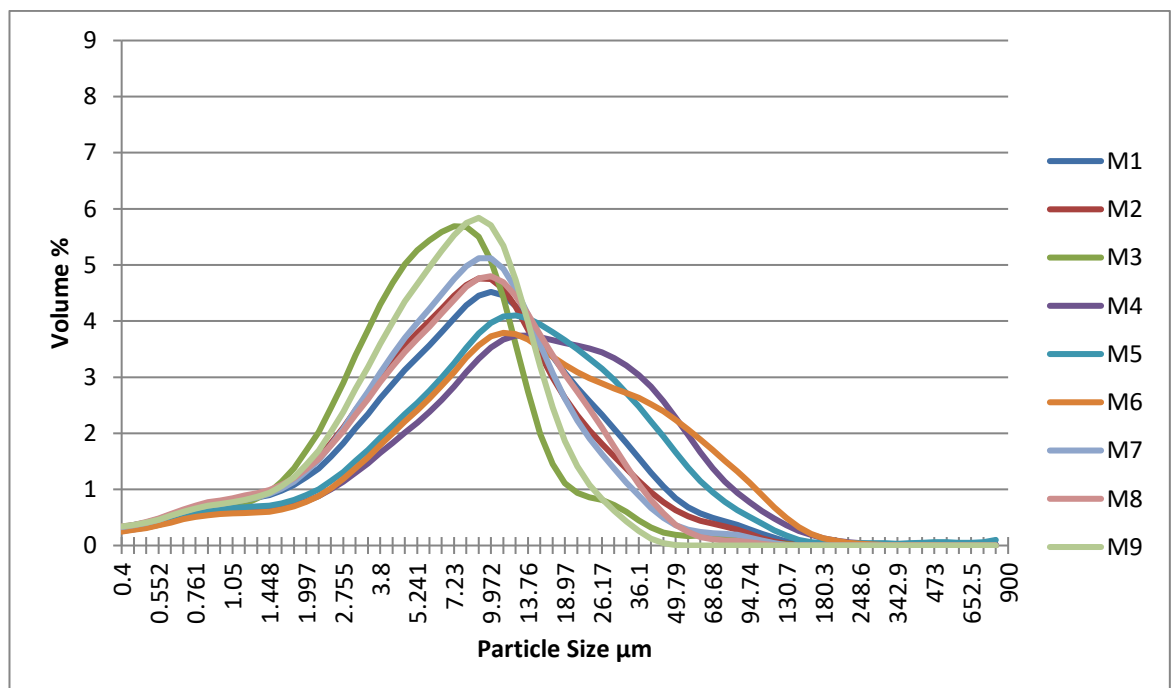


Figure 5.8: Grain size distribution plot of Matanuska samples.

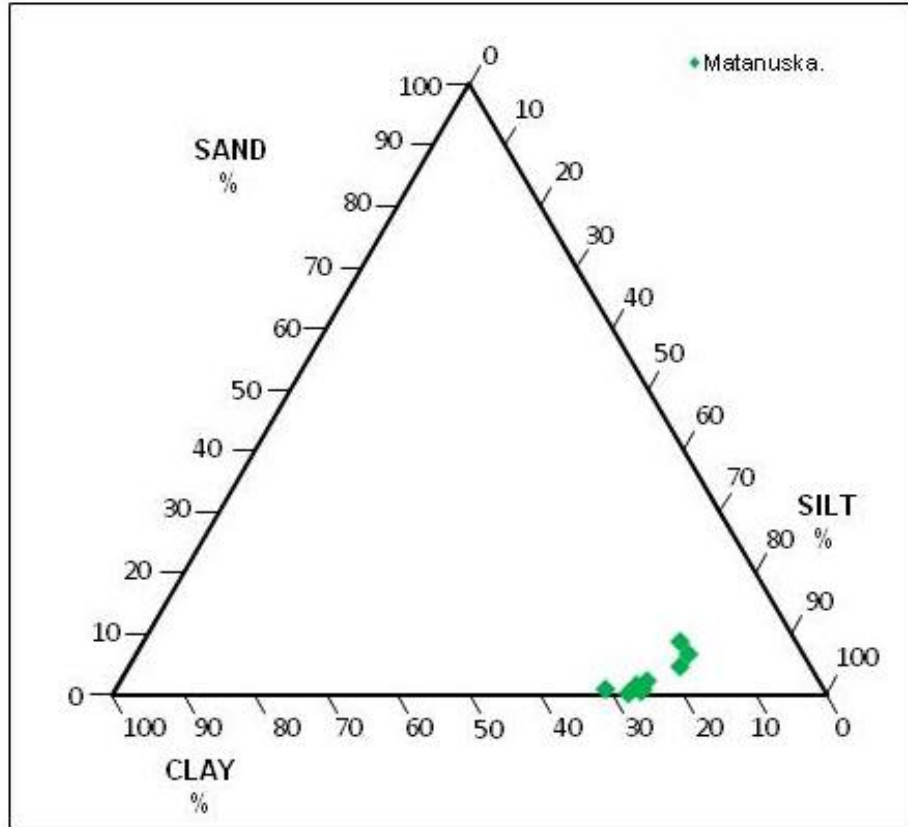


Figure 5.9: Ternary Plot of samples from Matanuska glacier.

Sample	D50 ( $\mu\text{m}$ )	Mean ( $\mu\text{m}$ )	Standard deviation ( $\mu\text{m}$ )	Minimum ( $\mu\text{m}$ )	Maximum ( $\mu\text{m}$ )	Silt Content (%)	Sorting ( $\mu\text{m}$ )	Kurtosis ( $\mu\text{m}$ )	Skewness ( $\mu\text{m}$ )
M1	9.30	14.45	16.77	0.4	161.9	74.52	16.74 PS	13.37	3.08
M2	8.26	12.81	16.42	0.4	276.8	72.77	16.46 PS	49.87	5.18
M3	6.40	9.99	25.75	0.4	161.9	68.7	26.65 PS	327.90	16.63
M4	14.92	25.09	36.35	0.4	808.5	77.32	36.80 PS	127.30	8.22
M5	12.57	22.91	49.51	0.4	808.5	77.39	50.10 PS	149.70	10.88
M6	14.02	25.51	31.62	0.4	473	75.38	31.29	23.90	3.42

							PS		
M7	8.09	11.34	12.28	0.4	130.7	73.83	12.26 PS	19.32	3.56
M8	8.38	11.48	11.11	0.4	117.4	74.03	11.07 PS	12.18	2.64
M9	7.12	8.52	6.437	0.4	49.79	72.4	6.45 PS	3.90	1.62

*Table 5.4: Summary data table for Matansuka  
(PS = Poorly Sorted, VPS = Very Poorly Sorted)*

### 5.2.5 Russell Glacier, Greenland

---

The samples taken from the basal ice layer of the Russell glacier contain a diverse range of particle size distributions (Figures 5.10 and 5.11). The R1 sample (Figure 5.10) is very different to all the others as it contains a distinct peak at approximately 130  $\mu\text{m}$  which is fine sand. In contrast, the remaining samples have broader distributions and contain peaks between 10 and 25  $\mu\text{m}$ , which is fine to medium silt. All of the samples are either poorly or very poorly sorted and are negatively skewed, though the R1 sample has a much stronger negative skew than the others.

The samples on the ternary plot are clustered together and in a linear fashion, reflecting the similar percentages of silt across the majority of the samples, and the diverse range in the amount of clay and sand within each (Figure 5.12).

Table 5.5 shows that silt content is high for the majority of the samples, as all but one of them contain between 55 and 75%. The R1 sample in contrast only contains approximately 23%. The volume of clay and sand in each sample can vary between 15-20% for clay and 5-30% for sand. Mean particle size ranges between 18 and 142  $\mu\text{m}$ , which is medium silt to fine sand.

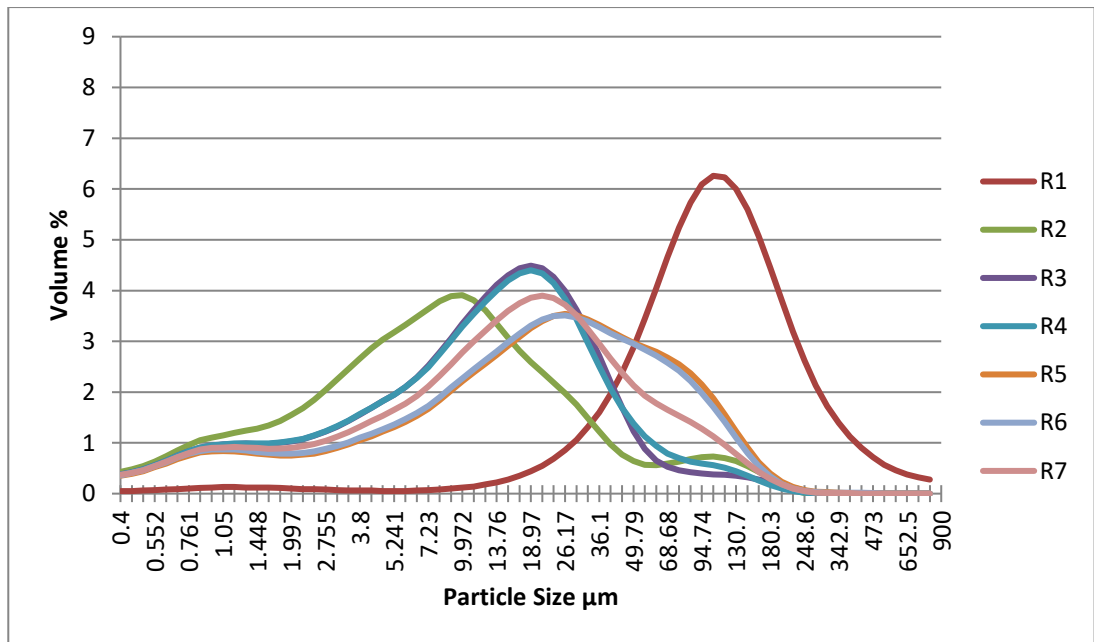


Figure 5.10: Grain size distributions of the samples collected at the Russell Glacier, Greenland.

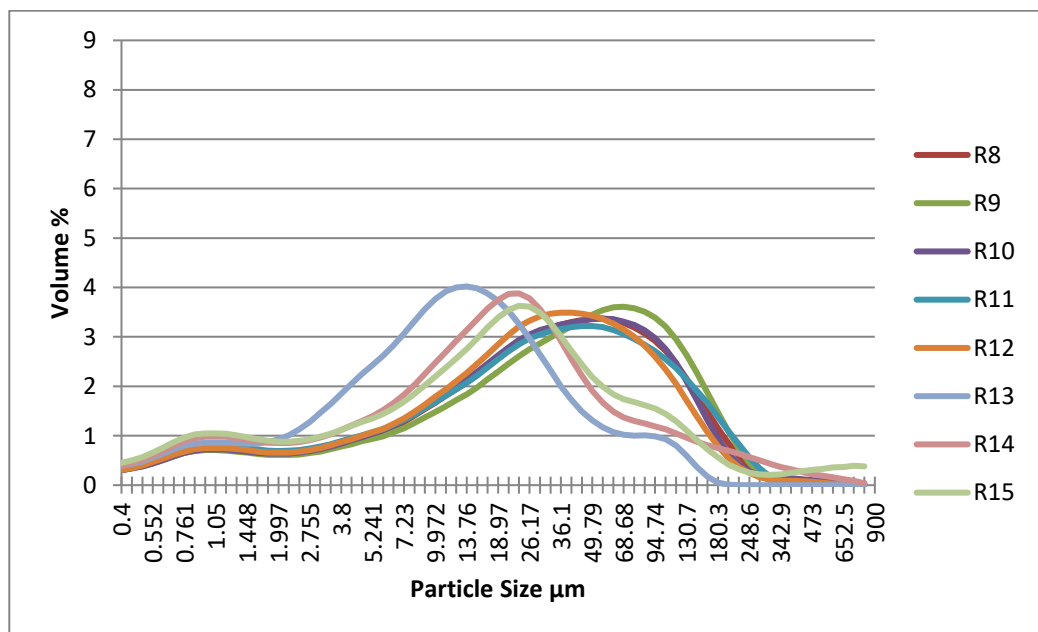


Figure 5.11: Grain size distributions of the samples collected at the Russell Glacier, Greenland.

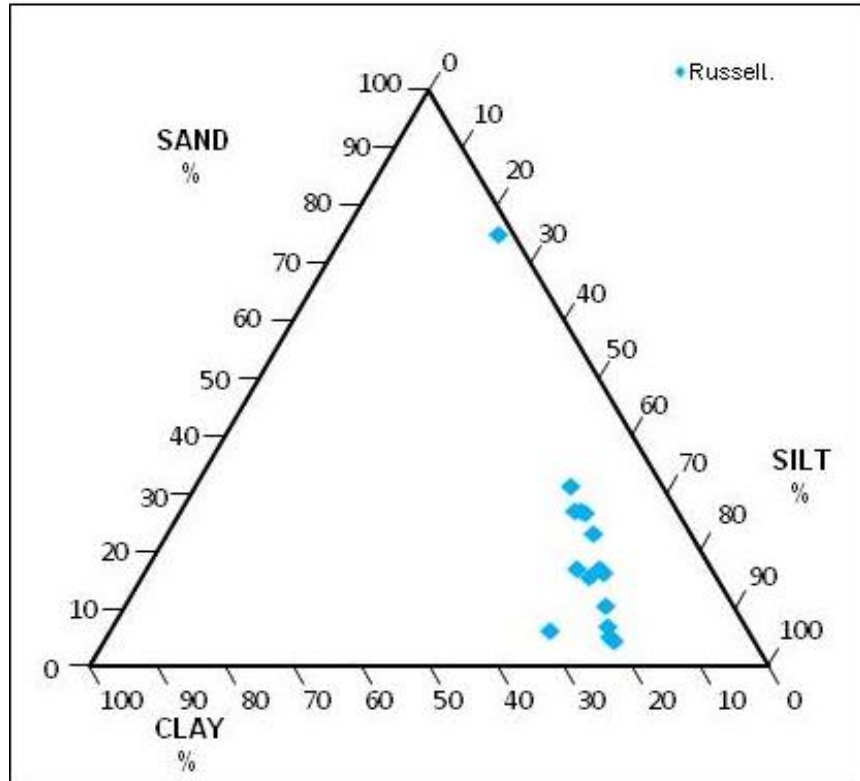


Figure 5.12: Ternary plot of samples collected from Russell Glacier, Greenland.

Sample	D50 ( $\mu\text{m}$ )	Mean ( $\mu\text{m}$ )	Standard deviation ( $\mu\text{m}$ )	Minimum ( $\mu\text{m}$ )	Maximum ( $\mu\text{m}$ )	Silt Content (%)	Sorting ( $\mu\text{m}$ )	Kurtosis ( $\mu\text{m}$ )	Skewness ( $\mu\text{m}$ )
R1	111.6	142.8	120.2	0.4	808.5	23.03	120.4 PS	7.92	2.33
R2	8.43	18.27	30.35	0.4	248.6	64.89	30.39 PS	14.18	3.54
R3	13.89	20.89	27.65	0.4	308.1	76.84	27.60 PS	22.96	4.09
R4	13.97	21.49	27.03	0.4	248.6	74.09	26.92 PS	14.83	3.30
R5	22.87	36.54	40.12	0.4	281.8	66.91	40.28 VPS	5.79	2.02
R6	21.72	35	39.52	0.4	473	67.48	39.51 VPS	11.06	2.44
R7	17.11	28.48	34.93	0.4	381.8	70.94	34.77 PS	11.60	2.75
R8	32.39	51.78	59.74	0.4	808.5	59.11	59.40 VPS	17.86	2.94

R9	38.06	56.27	57.78	0.4	526.6	55.49	57.67 VPS	4.90	1.76
R10	32.05	52.34	66.37	0.4	808.5	59.82	66.10 VPS	29.59	4.08
R11	31.3	51.69	57.63	0.4	381.8	58.23	57.61 VPS	3.73	1.81
R12	29.35	46.83	56.28	0.4	808.5	62.89	56.62 VPS	24.06	3.52
R13	12.37	21.57	27.38	0.4	200.6	72.91	27.39 PS	7.68	2.61
R14	19.07	44.41	87.84	0.4	808.5	66.23	82.20 VPS	24.85	4.39
R15	20.3	51.17	108.7	0.4	808.5	63.58	108.8 VPS	26.20	4.83

*Table 5.5: Summary data table for Russell glacier  
(PS = Poorly Sorted, VPS = Very Poorly Sorted)*

#### 5.2.6 Skeiðarárjökull, Iceland

---

The samples taken from the basal ice layer at Skeiðarárjökull contain a diverse range of particle size distributions (Figure 5.13). Samples 1-8 are poorly sorted and negatively skewed, with several distinct peaks at various volumes. These are at approximately 20  $\mu\text{m}$  (medium silt), 30  $\mu\text{m}$  (medium silt), 50  $\mu\text{m}$  (coarse silt) and 90  $\mu\text{m}$  (very fine sand). Samples 9 and 10 in contrast are very poorly sorted and do not contain any distinct peaks, but range between 0.4 to 350  $\mu\text{m}$ , which is clay to medium sand.

Figure 5.14 highlights the diverse nature of the samples. The three clusters are all plotted towards the bottom right of the plot, which illustrates the dominance of silt in many of them, with small volumes of sand and clay. Two of the samples do contain a greater volume of sand which are plotted away from the other two clusters.

Table 5.6 shows that the mean particle size is between 25 and 85  $\mu\text{m}$  which is medium silt to very fine sand. It also indicates that the silt content is relatively high for many of the samples as they all contain between 45 and 75%.

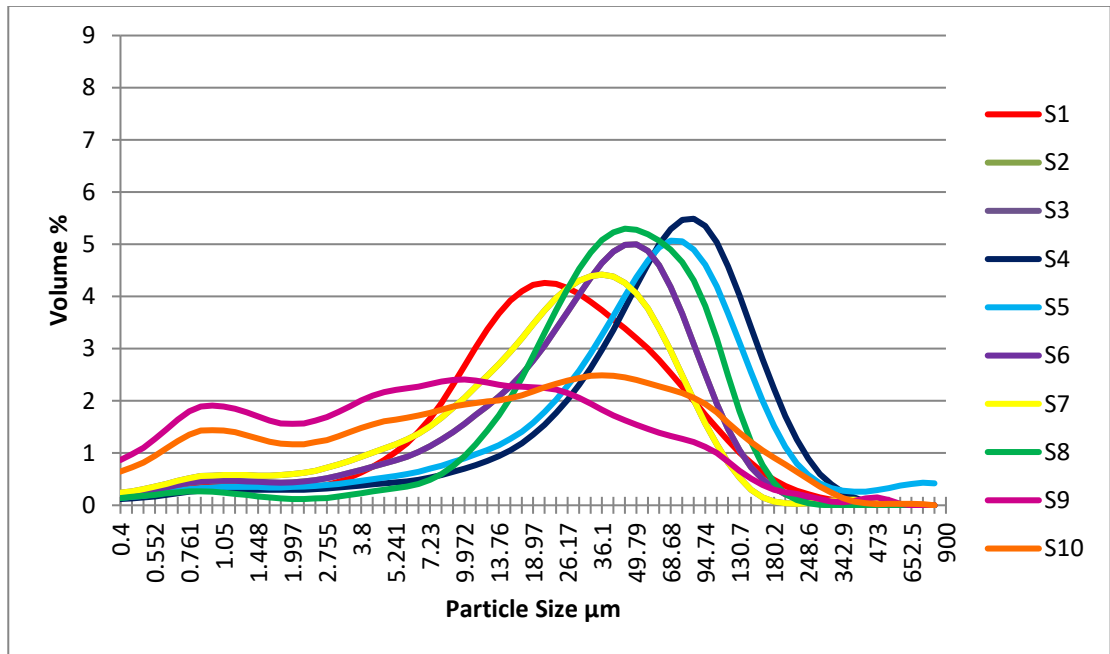


Figure 5.13: Grain size distributions of the samples collected at Skeiðarárjökull, Iceland.

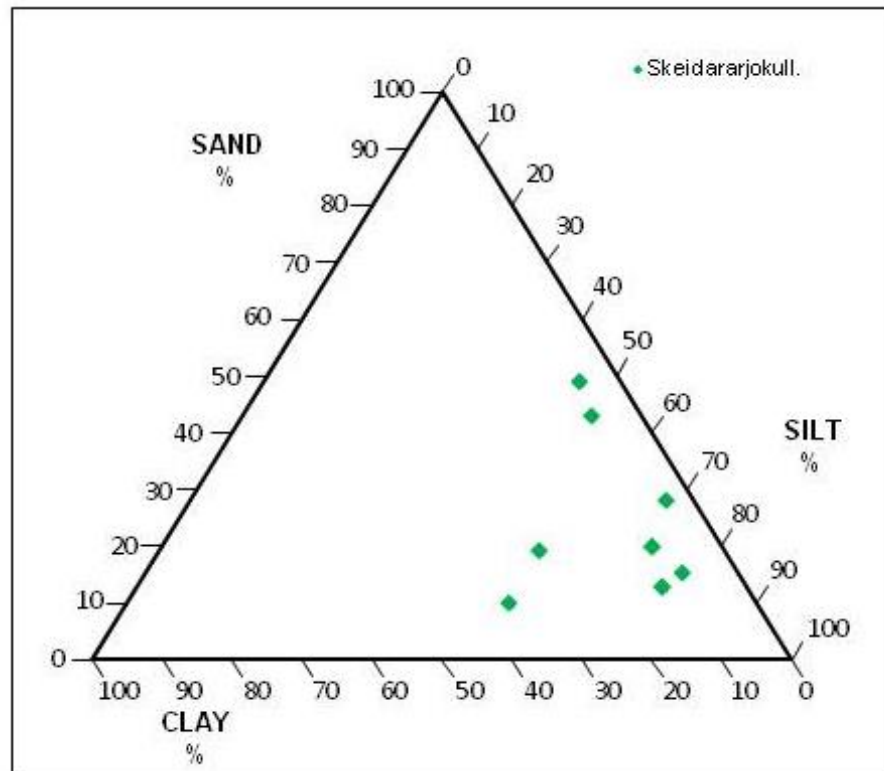


Figure 5.14: Ternary plot of Skeiðararjökull samples, Iceland.

Sample	D50 ( $\mu\text{m}$ )	Mean ( $\mu\text{m}$ )	Standard deviation ( $\mu\text{m}$ )	Minimum ( $\mu\text{m}$ )	Maximum ( $\mu\text{m}$ )	Silt Content (%)	Sorting ( $\mu\text{m}$ )	Kurtosis ( $\mu\text{m}$ )	Skewness ( $\mu\text{m}$ )
S1	24.40	38.47	42.94	0.4	424.9	76.42	43.10 PS	12.02	2.84
S2	35.18	43.42	37.58	0.4	308.1	70.48	37.55 PS	4.50	1.65
S3	26.08	35.7	40.82	0.4	526.6	74.91	40.67 PS	41.24	4.83
S4	67.33	80.43	64.97	0.4	473	45.03	65.03 PS	3.34	1.47
S5	58.93	85.18	112	0.4	808.5	49.93	112.0 PS	20.12	4.03
S6	28.92	43.08	69.09	0.4	308.1	70.48	69.38 PS	63.78	7.22
S7	30.14	38.68	40.25	0.4	308.1	74.91	40.67 VPS	42.60	4.74
S8	43.68	52.89	38.63	0.4	276.8	67.84	38.75 VPS	1.81	1.22

S9	8.533	25.95	51.02	0.4	586.2	54.55	50.88 VPS	40.79	5.36
S10	16.91	40.68	60.84	0.4	726.3	54.27	60.39 VPS	20.08	3.41

*Table 5.6: Summary data table for Skeiðarárjökull.  
(PS = Poorly Sorted, VPS = Very Poorly Sorted)*

### 5.3 Comparison of basal ice data from all glaciers

---

Figure 5.15 displays the composition of all samples taken from the basal ice layer across a range of glaciers from different environments, combined with the basal ice data collected at Svínafellsjökull. Many of these samples are clustered together on the plot, highlighting a dominance of silt across many of them (at least 50% and above). Percentages of sand and clay vary in each sample, though many of them contain less than 10% sand. Some data sets, such as those taken from Storglaciären contain less than 0.1%.

- Envelope 1 only contains the samples from the Root glacier, and overlaps with envelopes 2 and 4.
- Envelope 2 comprises samples from Svínafellsjökull, Storglaciären, and the Russell and Matanuska glaciers. It overlaps with all of the other envelopes.
- Envelope 3 predominantly comprises samples from the Russell glacier, with some from Svínafellsjökull, Ferpècle and Matanuska.
- Envelope 4 contains samples from Skeiðarárjökull and Ferpècle, and overlaps with envelopes 2 and 3.

Apart from envelope 1, which only contains samples from the Root glacier, all 3 of the other envelopes encompass samples from multiple sites. Some of the envelopes are

dominated by a set of samples from one site, such as Svínafellsjökull in envelope 2 and Skeiðarárjökull in envelope 4. Similar to the ice types previously identified at Svínafellsjökull, some sample sets exhibit much wider distributions and therefore fall within a larger envelope (such as those contained within envelope 2), while some dominate one envelope (with some variations). The overlap between the envelopes and the samples suggests that it is possible to identify a universal and distinctive sedimentological characteristic that can be applied to all BILs.

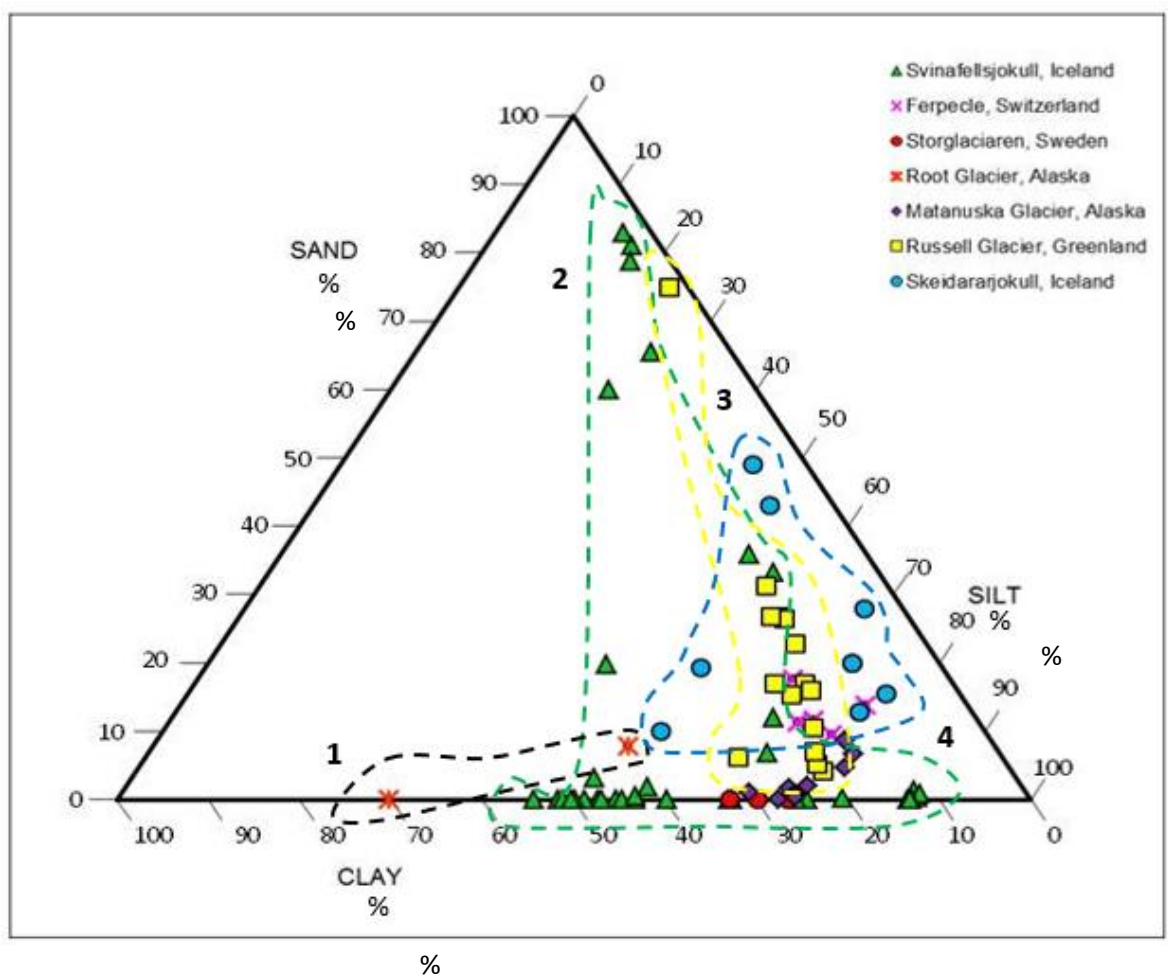


Figure 5.15: Comparison ternary plot showing all samples.

Table 5.7 shows the mean percentage of sand, silt and clay which would feature in an average sample from three sample sets. An average sample from the basal ice at Svínafellsjökull contains 57% silt, which is identical to the proglacial sample set and very

close to the 62% silt found in an average sample across all of the basal ice data from Svínafellsjökull and the other six glaciers. There is a contrast in the average percentage of sand across the three sample sets. Whilst the two basal ice sample sets share similar averages of sand (14% and 13%), the proglacial samples contain an average of 24% sand, indicating that the sample set is noticeably coarser than the others.

	<i>SAND</i> (%)	<i>SILT</i> (%)	<i>CLAY</i> (%)
<b>Basal ice samples from Svínafellsjökull and other glaciers</b> n=81	14	62	24
<b>Basal ice samples from Svínafellsjökull</b> n=37	13	57	30
<b>Proglacial samples from Svínafellsjökull</b> n=18	24	57	19

*Table 5.7: The mean percentage of sand, silt and clay of three sample sets*

#### 5.4 Summary

---

1. Grain size analysis shows that the samples fall within specific envelopes, which suggests that it is possible to define a universal envelope for the sedimentology of basal ice.
2. Though the BILs of the various glaciers sampled do exhibit differences on a site by site basis, many of them feature basal ice facies that contain a high volume of silt (over 50%).
3. This suggests that whilst site specific conditions may influence the characteristics of basal ice there may be a distinctive characteristic that can be found across all BILs.

4. This initial data highlights the need for future research to analyse and compare the sedimentological characteristics of BILs across a broader range of glaciers in different environments and locations (temperate and polar).

## 6.0 DISCUSSION

---

### 6.1 Synthesis

---

The ability to interpret glacial sediments and identify those that are a result of basal ice formation is critical to our understanding and reconstruction of glaciological conditions beneath current and past ice masses (Knight, 1997). If a distinct sedimentological characteristic from the BIL can be preserved and identified, this in turn allows us to infer the basal ice characteristics of that glacier, the processes operating at the bed and the characteristics of that ice mass as a whole.

The aim of this project was therefore to identify a distinctive sedimentological characteristic within the basal ice layer at Svínafellsjökull, which could then be used to ascertain whether basal ice sediments can indeed be preserved within the proglacial sedimentology. Since the original work of Goodchild in 1875 on melt-out tills, much work has focussed on attempting to establish whether the distinct facies of basal ice layers can be preserved within proglacial sediments or landforms. Despite numerous amounts of research investigating the potential for this, the links between basal ice characteristics and proglacial sedimentology still remain unclear.

The project at Svínafellsjökull identified seven key sites around the margin that were accessible for the sampling of the BIL and the proglacial area. The initial visual description of the sites and subsequent particle size analysis of the samples have shown that the BIL at Svínafellsjökull is distinctive, both visually and sedimentologically. Six key types of ice

facies were identified and although some facies could be identified at several of the sampling sites, others could only be observed in one location.

One of the objectives of this project was to determine whether the basal ice was sedimentologically distinctive (chapter 1, section 1.3). Grain-size analysis of the basal ice samples has shown that the facies are dominated by silt (between 50-80%) with a smaller volume of clay (between 20-30%), with little or no sand in all of the samples. Samples from the same ice type do appear to occur within distinct envelopes within the grain size ternary plot, however there is little grouping of samples taken from the same landforms within the proglacial area. That said, this is not the case for sites that contain ice type D, which is significantly coarser than all the other ice types. Ice type D samples contain a very high percentage of sand (approximately 80%) unlike all the other ice types that often do not contain any sand at all. Visually, this ice type was also very different to the others. There were debris bands that had formed at the exposure and could be seen to contain much coarser material than the other facies.

From the proglacial environment, three key features were identified for sampling to determine whether any of them were sediment sinks for basal ice sediments. These were moraine, proglacial sediments and minor outwash fans. The proglacial samples, in contrast to those from the basal ice, often contain sand (between 10 and 30%) and can fluctuate between high and low volumes of silt within the samples (30-75%). Overall, the proglacial samples are coarser than those sampled from the BIL and thus have a larger grain size distribution on average. Though moraines and proglacial sediments could be observed at each site, minor outwash fans could only be found at a few of the sites, typically where the partnering basal ice contained a high volume of fine-grained sediment.

Grain size data from Svínafellsjökull was subsequently combined with data obtained from basal ice samples from glaciers around the world. This led to the development of a global dataset collected from a diverse range of glaciers in a range of different geological contexts. Particle size analysis of this wider dataset highlighted that many of the samples do not contain sand, or only contain small percentages of it, and many of them contain a high percentage of silt (over 50%). The ternary plot comparing all of the samples (refer to Figure 4.27, chapter 4, section 4.3.1) does display some grouping of basal ice samples taken from the same glacier, which could suggest that site specific differences are too big of an influence to isolate a single distinctive sedimentological characteristic. Overall though, there is considerable overlap between many of the samples from each glacier. Since the samples were collected from various BIL facies of different glaciers in diverse environments, this does suggest that silt content could be a potential indicator for the distinctive sedimentological characteristic.

Key findings of this study suggest that facies with a high proportion of silt (50% and over) may have the potential to be transferred and subsequently preserved within the proglacial environment at Svínafellsjökull. This could indicate that the formation of these facies may be process specific, as not all of the identified facies contained a high volume of silt (such as ice type D). It may be that the presence of facies that contain a high volume of silt is also influencing the formation of the proglacial geomorphology. While moraines and melt-out sediments could be found at all of the sampling sites, the minor outwash fans were only present in certain areas. Their formation appears to be linked to areas where the ice contained a very high volume of fine-grained material.

Minor outwash fans were therefore identified as the geomorphological features most likely to be associated with the preservation of basal ice signatures. They were only present at sites where the basal ice contained a high silt content (between 50% and 80%). There also

appeared to be a genetic link between supraglacial and basal sediments as sources for the sediment input into the fans which could be observed within the field. Of the five minor outwash fans that were sampled, only one contained less than 50% silt. Typically, they also contained a higher percentage of sand (10-30%) than the ice types sampled at the same sites. The presence of sand within the minor outwash fans and lack of it within the basal ice facies highlights the need to consider that there may be multiple sediment sources contributing to their formation, but the potential for the basal ice to be one of these is clear. The potential link between distinct facies and the subsequent formation of distinct geomorphology associated with these is a definitive avenue for further research.

## 6.2 The sedimentological characteristics of basal ice at Svínafellsjökull

---

Previous research has frequently focussed on attempting to identify the distinctive characteristics of basal ice and whether these can be transferred and preserved within the proglacial environment. Despite numerous attempts that have focussed on various characteristics such as clast fabrics, clast shape and roundness and textural variations (Lawson, 1981, Ham and Mickelson, 1994, Knight et al., 2000, Adam and Knight, 2003), there has still yet to be a definitive characteristic identified. The aim of this project was to continue this effort and establish whether a specific characteristic within the basal ice could be identified and then traced to the proglacial sediments. Six distinct ice types were identified around the margin at Svínafellsjökull and sampled. These underwent grain size analysis and were subsequently plotted on a ternary diagram in order to see if they fell within distinct envelopes.

The samples from ice types A, C, D, E and frazil ice were grouped close together on the plot, whereas ice type B had a more varied grain size distribution. Despite this, the ice

types identified at Svínafellsjökull (apart from ice type D) are all plotted in a similar area on the diagram (refer to Figure 4.27, chapter 4, section 4.3.1), as many contain high volumes of silt and clay. This is similar to the findings from the facies at Matanuska found by Lawson (1979) which also formed distinct textural groupings (refer to Figure 2.2), though the ones from this project are not as defined. In contrast, the textural groupings of the facies at Matanuska are more defined, but the clusters themselves are more diverse, indicating that there is less chance that the basal ice has a distinctive and recognisable characteristic. Lawson's (1979) grain size analysis also included gravel which is larger than 2 mm in diameter, whereas this project focussed solely on the material below that size.

Previous work at Svínafellsjökull by Cook et al. (2006, 2007, 2011) has already identified basal ice exposures that have been formed by glaciohydraulic supercooling. This process is often credited with the formation of silt-rich basal ice facies (Alley et al., 1997, Lawson et al., 1998). It has been suggested the process therefore leaves a distinctive and recognisable signature within the sedimentary record.

Cook et al. (2011) attempted to identify distinctive sedimentological characteristics within the basal ice and proglacial sediments. In contrast to this project, they focussed on attempting to distinguish between sediments that were the result of two different methods of basal ice formation, and their proglacial sampling was limited to sediments directly in front of the basal ice exposure, with little focus on the geomorphological context. They concluded that it is possible to isolate and identify evidence for the preservation of basal ice facies that were formed by two different processes, regelation and glaciohydraulic supercooling. Those sediments derived from regelation facies were shown to have a sediment matrix dominated by coarse sand which is inconsistent with any of the facies identified during this project. The majority of the basal ice sampled in this project was

found to have either little or no sand at all, with an exception for samples taken from ice type D. The supercooling sediments identified by Cook et al. (2011) however share similarities with several of the facies sampled in this project as they have a silt-dominated matrix. This is consistent with many of the ice types identified which almost always contained high concentrations of silt.

The samples taken from the ice types and the proglacial features identified at Svínafellsjökull do indicate that silt dominance may be key to locating the basal ice sediments within the geological record, however there is nothing to suggest that this is definitively a process signature of supercooling BIL formation. Whilst research has shown supercooling to be an active process at Svínafellsjökull, the findings of this project suggest that silt dominance may be an indication of basal ice sediments in general and not just the facies formed by supercooling. Of the six ice types identified in this project, five of them contain high volumes of silt (over 50%) and they are all distinctively different in visual appearance, suggesting that they may have formed by different processes. Similar to the conclusions made by Cook et al. (2007, 2011) this project indicates that more research needs to focus on assessing whether silt dominance is indeed a process signature of glaciohydraulic supercooling, and whether high silt concentrations can be found in the basal ice layers of glaciers where supercooling is not known to be an active process.

### 6.3 Global variations in the sedimentology of basal ice

---

As mentioned previously, much research has focussed on attempting to identify a distinctive characteristic within the BIL, but usually at a specific glacier. There has not been an attempt to do so across multiple BILs of different glaciers.

This is crucial to our ability to identify basal ice layer sediments. If basal ice contains a distinctive characteristic that applies to the majority of glaciers then it would mean that once identified, it could be used in various locations. If however, site specific conditions are more influential during its formation, then it is likely that the basal ice layers differ so much from each other according to external influences and factors- such as local bedrock geology- that there will not be one distinctive characteristic, but perhaps several that could apply to different glaciers.

The grain size characteristics of the samples collected at Svínafellsjökull, and those from several glaciers around the world, were highlighted in Figure 5.15 (chapter 5, section 5.3). Considering that the data has come from a range of facies, from several BILs of glaciers that are subject to various conditions at each location, the samples do show a significant level of clustering within the plot. Many of the samples are clustered together in the bottom right of the ternary diagram. Table 5.7 (chapter 5, section 5.3) showed that the average sediment sample of the entire data set would consist of approximately 14% sand, 62% silt and 24% clay. This could potentially be the sedimentological envelope for the basal ice layer of glaciers. Similar to the ice facies at Svínafellsjökull they do appear to show a preference for high volumes of silt and sometimes clay.

That said, many of the samples do fall into distinct envelopes according to where they are sampled from which suggests that site specific conditions are influential. Differences in the sedimentology of basal ice layers could be explained by variations in local lithologies and the types of processes that affect sediment entrainment during basal ice formation.

This is the first attempt at a project that has included and compared the basal ice grain size data of several glaciers. Though the results are not conclusive to suggest that silt is definitely the distinctive characteristic or that site specific conditions are too influential to

isolate one characteristic, it does indicate that further research into a large scale project of this type would be beneficial for the search for a distinctive characteristic across all BILs.

## 6.4 Preservation within the proglacial environment

---

### 6.4.1 Introduction

---

Previous studies often have not looked at the geomorphological settings of the sediments examined. As identified in previous work (Knight et al., 2000, Adam and Knight, 2003), the potential for the preservation of any signature is better in some depositional settings than others. The focus of this project was not only on proglacial sedimentologies, but also in classifying and identifying any distinct geomorphology in the proglacial environment at Svínafellsjökull. There were three distinct features identified at the seven sites around the margin of Svínafellsjökull: moraines, minor outwash fans and proglacial sediments situated on the boundary between glacial and proglacial. Similar to the samples collected from various facies, the proglacial samples were plotted on a ternary diagram after grain-size analysis according to the feature they were sampled from to see if they plotted within distinct envelopes (refer to Figure 4.28, chapter 4, section 4.3.2).

### 6.4.2 Moraines

---

Moraines could be considered an unlikely feature for the preservation of basal ice sedimentologies, due to the fact that they are often formed of sediment from several sources (subglacial, supraglacial, basal) and can often be reworked by the glacier itself or

external processes. Despite this they have been the focus of several studies that have tried to identify whether basal ice sediments were being transferred and preserved within them. Work conducted in Greenland by Knight et al. (2000) and Adam and Knight (2003) concluded that if certain conditions are met in the proglacial area and the facies were distinctive enough, they could be identified within ice marginal moraines.

The moraines sampled at Svínafellsjökull were found to exhibit the most varied grain size distribution. However, at sites where they were sampled they were most similar to the particle size distributions of ice type B, which was found in the partnering basal ice at all sites where moraines were sampled. This can be seen most definitively at site 6 (refer to Figure 4.20, chapter 4, section 4.2.12). Three samples at different depths of the same moraine were sampled and three different facies in the ice were also analysed. Though the grain size distributions of the moraine are distinctly different from ice types D and E, they are very similar to those of ice type B.

Knight et al. (2000) noted that the basal ice at Kangerlussuaq exhibited a high degree of particle-size sorting and very distinctive facies. The dispersed facies, which they concluded could be identified within the moraines had an abundance of silt and clay sized material, is similar to many of the facies identified at Svínafellsjökull. The visual observations and the grain size analysis of the basal ice facies at Svínafellsjökull has shown that the basal ice is distinctive and has produced several distinctive facies, many of which share a high volume of silt. The samples taken from the moraines at Svínafellsjökull do not show as much potential for the preservation of a specific facies as they do in the previous work in Greenland. However, in areas where moraines can form under more rigid environmental conditions with little fluvial and aeolian processes present, there is less reworking of the sediment taking place, so they could be key for the preservation of one particular type of facies.

### 6.4.3 Ice-marginal Sediments

---

Much of the previous research has focussed on melt-out tills as the key formation best adapted to preserving basal ice sediments (Goodchild, 1875, Paul and Eyles, 1990). Melt-out tills have often been considered the best possible place to identify BIL sediments due to the method of their formation. A ‘true’ melt-out till has been described as the *in situ* melting of debris-rich ice in the basal zone without any reworking of the sediment (Lawson, 1979). Since these deposits are formed *in situ* they should inherit their sedimentological properties directly from their basal ice source, resulting in the sedimentological characteristics of the BIL being preserved. Formations regarded as ‘true’ melt-out tills have strict formation requirements, which means that it is highly unlikely that these conditions could be met at most glaciers that have a BIL, and thus are not the best place to look for the preservation of basal ice sediments within the proglacial environment.

The initial visual observations taken at each of the sites at Svínafellsjökull support this. It was often noted that the sediment deposits directly in front of the margin were being reworked almost constantly by melt-out streams, and thus the sediments could have been deposited via various other subglacial processes. When plotted according to the grain size of the samples, some of them featured quite large grain size distributions containing high volumes of sand, whereas others were more clustered together and contained higher percentages of silt and sand. These samples were termed ‘proglacial sediments’ and could be formed as a result of melt-out from the basal ice layer, but could also include supraglacial material or indeed subglacial material that has been exposed due to the retreat

of the glacier. There were no formations that could be identified as true melt-out tills and therefore the reliance upon these as potential preservation sinks in previous literature does not apply to Svínafellsjökull.

#### 6.4.4 Minor outwash fans

---

One of the features identified around the margin at Svínafellsjökull were minor outwash fans. The fans may provide a promising archive for basal ice sediments as they are formed by supraglacial drainage, which indicates a clear potential process link between sediment supply (basal ice) and product (minor outwash fan).

The fans identified at Svínafellsjökull share many similarities with those described by Krüger (1997) and Kjær et al. (2004). According to Krüger (1997), minor outwash fans are formations that consist of fine-grained material, predominantly sand, which has been deposited by supraglacial streams that have a low transport capacity. These have also been termed Hochsandur fans by Gripp (1975). They are similar in appearance to the more common glacial outwash fans but are devoid of the larger boulders and coarser material that form the first stages of such features. In contrast, they are entirely made up of the much finer material that you find in the latter stages of the larger outwash fans. The minor outwash fans described in the previous literature are also supraglacially fed, which could mean that the transfer of basal ice sediments could occur via passageway of supraglacial streams.

Minor outwash fans were sampled at sites 3, 4, 5 and 7. They were not present within the proglacial environment at the other three sites. The visual observations undertaken at each site highlighted that minor outwash fans formed in areas where the basal ice facies were very debris-rich and contained high volumes of fine-grained material, specifically silt and

clay. The fans formed within intra-moraine networks and were usually dominated by a high percentage of silt. They comprised at least 50% silt with small volumes of sand between 10 and 30% and the rest in clay. Since they only formed at certain sites it can be inferred then that they require specific conditions in which to form.

This project identified several sites around the margin of Svínafellsjökull that have substantial exposures of the basal ice layer which contain debris-rich facies. If the streams that are transferring the sediment to the fans are indeed supraglacial, then the basal ice layer sediments could be entrained and deposited as the streams flow over these exposures. Since the fans form within intra moraine networks this could suggest that any coarser supraglacial material could be trapped within the moraines whilst the finer grained silt and clay can flow through and form the minor outwash fans, leading to the preservation of sediments from certain facies.

The supraglacial source as an initial input for the formation of the fans could also explain why much of the BIL facies contain little or no sand, whereas the fans sampled at Svínafellsjökull often contained between 10 to 30% sand. This does suggest that the minor outwash fans may have multiple sediment sources including that which is entrained from the basal ice, but if a distinctive sedimentological can be identified from a facies then sediment preserved from the BIL could be isolated and recognised within them.

Evidence of a supraglacial and basal sediment source for one of the minor outwash fans sampled can be seen at site 3 (refer to Figure 4.10c, chapter 4, section 4.2.6). The image taken at this site shows a clear relationship between a supraglacial and basal sediment source contributing directly to the formation of a minor outwash fan. The grain size analysis at this site showed that whilst the fan did contain a small volume of sand which could have potentially been transferred by the supraglacial source, the distribution was

completely different to that of the facies at this site. Despite the fact that there was a clear link between source and the formation of distinct geomorphology, the grain size distribution of the fan was not a reflection of those taken from the ice.

This does not mean that minor outwash fans are not capable of preserving a facies sedimentological signature however. Certainly the visual evidence, which points to a clear link between the ablation and transfer of basal ice sediments into these fans, is enough to suggest that this relationship should be a focus for future research. It also highlights the need to consider that recognising and identifying distinctive proglacial geomorphology may be the key to identifying where basal ice sediments are best preserved, rather than focussing on proglacial sedimentology alone.

Previous literature has focused on the structure and formation of minor outwash fans in the proglacial environment of Icelandic glaciers (Krüger, 1997, Kjær et al., 2004) but there has been little work in marking these as potential sediment sinks for preservation of basal ice facies. The results of this study indicate minor outwash fans may form within intra moraine networks in areas where the exposed basal ice facies contains a high silt content. Furthermore, the fans may be crucial to the preservation of distinct basal ice facies as the material is entrained through supraglacial melt out. This project and previous literature have focussed on the development and formations of minor outwash fans based on glaciers around Iceland; further research needs to establish whether these fans can form at other glaciers outside of Iceland and establish what conditions are required for their formation. The minor outwash fans are potentially distinctive landform-sediment assemblages which could hold the key to identifying preserved sediments from ice facies. The key findings of this project suggest that it is not the melt-out sediments that should be the focus for sampling within the proglacial area in order to isolate BIL sediments, but specific

geomorphological formations. These could vary due to site specific conditions and the type of facies exposed.

## 6.5 Wider Implications

---

The ability to identify basal ice sediments in the proglacial geomorphology of current glaciers or in relict deposits left by past ice masses would be greatly beneficial to Quaternary scientists. The basal ice layer of a glacier is subject to the processes that operate at the bed of an ice mass (Knight, 1997) and as such can provide information about the thermal regime, the subglacial processes and conditions, and the type and characteristics of the sediments available for entrainment. For example, the basal thermal regime of an ice mass is a key control on its dynamic behaviour. The ability to reconstruct basal processes and thermal regimes could help to test the predictions of numerical ice-sheet models.

This project has not only defined an initial envelope for the sedimentary characteristics of basal ice, but it has also highlighted specific glacial features and geomorphology that may be the key to preserving these. This is essential in order to provide Quaternary scientists with ideal locations for the transfer and preservation of basal ice sediments. If we know that a specific type of proglacial formation is ideal for preserving the definitive sedimentological characteristics of basal ice facies, then future researchers will be able to focus their study on identifying these parameters and establishing the links between basal ice and the resulting geomorphological formations in the field. Similarly, when searching for the presence of basal ice characteristics from relict ice masses, it may be possible to identify deposits where these would have been best preserved.

This project has indicated the need to consider both the sedimentological and geomorphological context of proglacial environments, rather than focussing on just one aspect. The results of this study has indicated that the presence of a particular facies could be linked to the development of specific geomorphology, such as minor outwash fans that only formed in areas where the basal ice contained a high volume of silt (between 50% and 80%). Preservation of basal ice sediments then may only occur at certain glaciers where a specific facies is formed, in combination with the right conditions for the formation of local geomorphology that enables the characteristics of the facies to be preserved.

It has also illustrated a clear relationship between the formation of minor outwash fans via visible supraglacial streams which flowed over ablating basal ice. Though this demonstrates that the fans are not merely a sink for just basal ice sediments, the link between the transference of such to specific geomorphological features, highlights the need for future research to explore and consider not only what makes basal ice distinctive, but also the importance of distinctive proglacial geomorphology.

Melt-out tills have been the focus of several studies in the past (Goodchild, 1875, Boulton 1970, Haldorsen and Shaw, 1982, Paul and Eyles, 1990) for the potential preservation of basal ice sediments. Since they require such specific conditions in which to form (Lawson, 1979), it is unlikely that any 'true' melt-out tills would be able to form at many of the active glacier margins and therefore this lessens the potential for them to be features that can preserve basal ice sediments. Even when looking at particle size alone, there is no clear link between the sedimentology of the basal ice and that of the immediate proglacial sediments.

Instead, this study argues for a greater focus on specific proglacial geomorphology, specifically minor outwash fans. Though the potential for minor outwash fans to be

formations that preserve basal ice sedimentologies may be restricted to Icelandic glaciers, or indeed glaciers where they have the right conditions to form, it does suggest that the local geomorphology of a glacier may be crucial to the identification of distinctive facies characteristics.

## 6.6 Scope for future research

---

The results of this project have shown that it is possible to identify a clear and definitive envelope for the sedimentology of basal ice, by analysing grain size data from the BILs of several glaciers around the world. Whilst this provides a substantial basis to potentially identify sediments that have been sourced from basal ice layers, additional research is needed to further define this envelope and to explore the best features for preservation of these within the proglacial environment.

A similar study focussing on the grain size characteristics of basal ice from several glaciers using a facies by facies approach could further our understanding of basal ice sedimentology. Whilst this project compared grain size data from various facies at different glaciers, a more refined approach which separated distinctive facies, could identify if specific facies produce distinctive characteristics or indeed whether high silt content was still a significant aspect. Another study with more samples from a wider range of glaciers would ascertain whether silt content is indeed a diagnostic characteristic for the presence of basal ice sediments and further refine the sedimentological envelope for basal ice.

One of the most important aspects for BIL sedimentology is the sediment supply that is available. The bedrock geology and sediment supply beneath a glacier determines what sort of material the glacier can entrain and thus affects the processes that operate at the bed, and therefore the formation and visual aspects of the basal ice facies. Iceland is dominated by basalt which can be easily eroded by glaciers. Due to the location of Iceland, the glaciers are temperate and can supply the high amounts of meltwater needed to encourage glacio-fluvial erosion, which could explain the silt dominance within the facies at Svínafellsjökull. Future work should focus on identifying whether site specific conditions are the most influential upon basal ice formation, in order to establish whether silt dominance is a distinctive characteristic that can be used to identify basal ice sedimentology within the geological record, or if site specific conditions mean that a distinctive characteristic could vary from site to site.

This project has also focussed on grain size analysis as the sole method for identifying a distinctive sedimentological characteristic. It could be that in order to truly identify a distinctive characteristic that could be applied to the majority of glaciers with basal ice layers, that other sedimentological characteristics should be explored and combined. In order to further narrow down the search for such a characteristic, future research should focus on other methods of analysis for basal ice and proglacial sedimentologies.

Scanning electron microscopy (SEM) has been shown to isolate basal ice sediments that were derived from different sources (subglacial, supraglacial etc) in a study by Whalley and Krinsley (1974). Thus SEM analysis of various basal ice facies and proglacial features could isolate microtextures that are distinctive within either and allow for their identification within proglacial sedimentologies. It is possible also that shape characteristics of sediments could be key to identifying basal ice sediments. The shape of a sediment particle can offer information on the source and transfer of sediments, highlight

differences between basal ice facies, and provide details on their depositional environments (Graham and Midgley, 2000).

## 7.0 CONCLUSIONS

---

### 7.1 Key findings

---

The key findings of this study are presented with reference to the relevant specific objectives (chapter 1, section 1.3).

***To determine whether the basal facies found at Svínafellsjökull have any distinguishing sedimentological characteristics.***

1. It is possible to define a sedimentological envelope for basal ice. Grain size data taken from Svínafellsjökull and six other glaciers in various locations suggests that this is: a low sand content (<15%), a high silt content (between 50 and 80%) and a low to medium clay content between 15% and 30%.
2. It is possible that a high silt content (between 50 and 80%) is the distinctive characteristic which indicates the presence of basal ice sediments within the proglacial environment.

***To determine whether any of these characteristics are preserved within the proglacial sediments.***

1. Whilst it has been shown that the basal ice does indeed possess distinctive sedimentological aspects it is unclear as to where these are best preserved at Svínafellsjökull.
2. Grain-size analysis has shown that proglacial features at Svínafellsjökull often contain more sand than the basal ice samples (between 10 and 30%). Many of them also contain over 50% silt. Despite this, the sedimentologies of the basal ice and proglacial features do not reflect each other when examined on a site by site basis.
3. Spatial analysis based on the silt content of the samples did not present a clear link between the basal ice facies and the proglacial features at each site.

***To determine whether the presence of particular basal ice facies are associated with the development of distinctive geomorphological features.***

1. The formation of distinctive proglacial geomorphology may be linked to the presence of particular ice types and be the best chance at preserving basal ice sediments.
2. There appears to be a genetic link between supraglacially fed minor outwash fans which could also be preserving sediments transferred from ablating basal ice via supraglacial streams. Minor outwash fans forming in areas where the basal ice contains a high volume of fine-grained material could therefore be a potential sink for the preservation of both supraglacial and basal ice sediments. However, even where there appears to be a clear genetic link at specific sites, the sedimentological signature is different.
3. This could mean that moraines and proglacial sediments in general could be discounted as the best features for the preservation of basal ice sediments.

*To determine the extent to which the grain-size characteristics of basal ice are universal or site specific.*

1. Grain-size analysis of the basal ice layers of six glaciers other than Svínafellsjökull has indicated that sedimentological characteristics of basal ice could be universal.
2. Basal ice samples from all of the sites are characterised by a low sand content (<15%), a high silt content (between 50 and 80%) and a low to medium clay content between 15% and 30%.
3. However, the tendency of some of the samples to delineate site-specific clusters highlights the role played by site specific factors. This could indicate variations in controls such as bedrock geology and subglacial entrainment processes.

The aim of this project was to determine whether basal ice displays distinctive sedimentological characteristics and to examine whether these sedimentological signatures are transferred to and preserved within the proglacial environment. The results indicate that basal ice layers at Svínafellsjökull, and those at the other six glaciers compared within this study, all display some distinctive sedimentological characteristics.

This means that there is a potential for basal ice to contain a distinctive and universal sedimentological characteristic. However, it should be noted that difference in facies type and site may influence basal ice sedimentology. The ice types at Svínafellsjökull do display some differences in sedimentology when compared on a facies by facies basis, but their sedimentological envelopes often overlap. Similarly, the samples taken from basal ice layers of the other glaciers do show clustering on a site by site basis, which suggests that even though the basal ice is distinctive, site specific controls do influence the sedimentology and this should be considered in future work.

Whilst this research project has highlighted a potential link between the formation of specific basal ice facies and distinct geomorphology within the proglacial area, the results do not show a clear spatial link between their sedimentologies. As such, it cannot be concluded that basal ice sediments are being transferred and preserved at Svínafellsjökull, but it has highlighted a potential connection between the presence of particular basal ice facies and the formation of minor outwash fans. The possible supply of basal ice sediments to minor outwash fans via supraglacial streams should be explored further. It has also indicated that future studies should focus on both the sedimentological and geomorphological aspect of proglacial environments, when investigating the potential transference and preservation of basal ice sediments.

## 7.2 Focus for future research

---

Future work should focus on:

1. More systematic collection of grain size data of basal ice samples from glaciers around the world, in order to confirm sedimentological variability and determine the influence of site-specific controls such as bedrock geology.
2. Exploring the potential links of sediment transfer and preservation from basal ice facies to minor outwash fans. A more process-based study that focuses on sites where the basal ice layer is exposed, and minor outwash fans are forming, would be able to sample both the basal ice and supraglacial sediments as well as the meltwater drainage linking the two. The results would potentially indicate whether the fans are an amalgamation of the two sediment sources.

3. The use of a broader range of techniques to determine the sedimentology of basal ice. Future work could potentially combine grain size analysis with SEM work, or the shape and roundness of particles, in order to identify the characteristics that make basal ice distinctive. The focus should still be on examining the links between basal ice and minor outwash fans, but could benefit from additional methods of sediment analysis, other than grain size.

## REFERENCES

---

Adam, W.G. and Knight, P.G. (2003) Identification of basal layer debris in ice-marginal moraines, Russell Glacier, West Greenland. *Quaternary Science Reviews*, 22(14), p.1407-1414.

Alley, R.B., Cuffey, K.M., Evenson, E.B., Strasser, J.C., Lawson, D.E. and Larson, G.J.. (1997). How glaciers entrain and transport basal sediment: Physical constraints. *Quaternary Science Reviews*. 16 (9), p.1017-1038.

Blott, S.J. and Pye, K. (2001) GRADISTAT: A grain size distribution and statistics package for the analysis of unconsolidated sediments. *Earth Surface Processes and Landforms*, 26, p.1237-1248

Boulton, G. S. (1970) On deposition of subglacial and melt-out tills at the margins of certain Svalbard glaciers. *Journal of Glaciology*, 9, p.231-246

Boulton, G. S. (1976) A genetic classification of tills and criteria for distinguishing tills of different origins. In: Tills – genesis and Diagenesis. *Geografia*, 12, p.65-80

Boulton, G. S. (1978) Boulder shapes and grain size distribution of debris as indicators of transport paths through a glacier and till genesis. *Sedimentology*, 25, p.773-799

Boulton, G. S. (1979) Processes of glacier erosion on different substrates. *Journal of Glaciology*, 23, p.15-38

Chamberlin, T. C. (1895) Recent Glacial studies in Greenland. *Bulletin of the Geological Society of America*. 6, p.199-220

- Cook, S.J. and Swift, D.A. (2012). Subglacial basins: Their origin and importance in glacial system and landscapes. *Earth-Sciences Reviews* 115, p.332-372
- Cook, S.J., Waller, R.I. and Knight, P.G. (2006). Glaciohydraulic supercooling: the process and its significance. *Progress in Physical Geography*, 30(5), p.577-588.
- Cook, S.J., Knight, P.G., Waller, R.I., Robinson, Z.P. and Adam, W.G. (2007). The geography of basal ice and its relationship to glaciohydraulic supercooling: Svínafellsjökull, southeast Iceland. *Quaternary Science Reviews*, 26(19-21), p.2309-2315.
- Cook, S.J., Graham, D.J., Swift, D.A., Midgley, N.G. and Adam, W.G. (2011). Sedimentary signatures of basal ice formation and their preservation in ice-marginal sediments. *Geomorphology*, 125(1), p.122-131.
- Cook, S.J., Knight, P.G., Knight, D.A. and Waller, R.I., 2012. Laboratory observations of sediment entrainment by freezing supercooled water. *Geografiska Annaler: Series A, Physical Geography*, 94(3), p.351-362.
- Evans, D.J.A., Rea, B.R., Hiemstra, J.F. and Ó Cofaigh, C. (2006). A critical assessment of subglacial mega-floods: a case study of glacial sediments and landforms in south-central Alberta, Canada. *Quaternary Science Reviews*, 25(13-14), p.1638-1667
- Goldthwait, R. P. (1971) Introduction to till today. *In Till: A symposium*, p.3-26
- Goodchild, J.G. (1875) The glacial phenomena of the Eden Valley and the western part of the Yorkshire Dales district. *Quarterly Journal of the geological society of London*, 31, p.55-99
- Google Earth (2015). *Svínafellsjökull, Iceland. 63°59'54.53"N, 16°51'52.73"W elev. 165m*. Online. [https://www.google.co.uk/intl/en\\_uk/earth/](https://www.google.co.uk/intl/en_uk/earth/) Accessed 20<sup>th</sup> November 2015

- Graham, D.J., Midgley, N.G. (2000) Graphical representation of particle shape using triangular diagrams: An Excel spreadsheet method. *Earth Surface Processes and Landforms* 25, p.1473-1477
- Gripp, K. (1975) Hochsander-Satzmorane-Endmoränenvertreter. *Z. Geomorphol., Neue Folge* 19, p.490-496
- Halderson, S. and Shaw, J. (1982) The problem of recognising melt-out till. *Boreas*. 11, p.261-277
- Ham, N. R. and Mickelson, D. M. (1994) Basal till fabric and deposition at Burroughs Glacier, Glacier, Alaska. *Geological Society of America Bulletin*, 106, p.1552-1559
- Hart, J. K. (1995) An investigation of the deforming layer/ debris-rich basal ice continuum, illustrated from three Alaskan Glaciers. *Journal of Glaciology*, 41, p.619-633
- Heim, D. (1983) Glaziäre Entwässerung und Sanderbildung am Kotlujokull, Sudisland. *Polarforschung*, 53, p.21-36
- Heim, D. (1992) Sanderogenese und Gletcherentwässerung am Kotlujokull (Hofdabrekkujokull), Sudisland. *Polarforschung*, 62, p.95-128
- Helgason, J. and Duncan, R.A. (2001) Glacial-interglacial history of the Skaftafell region, southeast Iceland. *Geology*, 29, p.179-182
- Hooke, R. LeB. and Pohjola, V. A. (1994) Hydrology of a segment of a glacier situated in an overdeepening, Storglaciären, Sweden. *Journal of Glaciology*, 40, p.140-148
- Hubbard, B. (1991) freezing rate effects on the physical characteristics of basal ice formed by net adfreezing. *Journal of Glaciology*, 37, p.339-347

- Hubbard, B. and Sharp, M.J., (1989) Basal ice formation and deformation: A review. *Progress in Physical Geography* 13, p.529-558
- Hubbard, B., Sharp, M.J. and Lawson, W.J. (1996). On the sedimentological character of Alpine basal ice facies. *Annals of Glaciology*. 22, 187-193.
- Hubbard, B., Cook, C. and Coulson, H. (2009) Basal ice facies: a review and unifying approach. *Quaternary Science Reviews* 28, p.1956-1969
- Jouzel, J. and Souchez, R. A. (1982) Melting-refreezing at the glacier sole and the isotopic composition of the ice. *Journal of Glaciology*, 28, p.35-42
- Kamb, B. and LaChapelle, E. (1964) Direct observation of the mechanism of glacier sliding over bedrock. *Journal of Glaciology*, 5, p.159-172
- Kjaer, K. H., Sultan L., Kruger J. and Schomacker A. (2004) Architecture and sedimentation of outwash fans in front of the Myrdalsjokull ice cap, Iceland. *Sedimentary Geology*, 172, p.139-163.
- Knight, P.G. (1987) Observations at the edge of the Greenland ice sheet; boundary condition implications for modellers. *International Association of Hydrological Sciences Publication*, 170, p.359-366
- Knight, P.G. (1988) The basal ice and debris sequence at the margin of an equatorial ice cap; El Cotopaxi, Ecuador. *Geografiska Annaler* 70A, p.9-13
- Knight, P.G. (1994). Two-facies interpretation of the basal layer of the Greenland ice sheet contributes to a unified model of basal ice formation. *Geology*, 22(11), p.971.
- Knight, P.G. (1997) The basal ice layer of glaciers and ice sheets. *Quaternary Science Reviews*, 16(9), p.975-993.

- Knight, P.G. and Knight, D.A., (1994) Glacier sliding, regelation water flow and development of basal ice. *Journal of Glaciology*, 40, p.600-601
- Knight, P. G. and Knight, D. A. (2005) Laboratory observations of debris-bearing ice facies frozen from supercooled water. *Journal of Glaciology*, 51, p.337-339
- Knight, P.G., Patterson, C.J., Waller, R.I., Jones, A.P. and Robinson, Z.P. (2000) Preservation of basal-ice sediment texture in ice-sheet moraines. *Quaternary Science Reviews*, 19(13), p.1255-1258.
- Knight, P.G., Sugden, D.E. and Minty, C. (1994) Ice flow around large obstacles as indicated by basal ice exposed at the margin of the Greenland ice sheet. *Journal of Glaciology*, 40, p.359-367
- Krüger, J. (1997) Development of minor outwash fans at Kotlujokull, Iceland. *Quaternary Science Reviews*, 16, p.649-659
- Lawson, D. E. (1979) Sedimentological analysis of the western terminus region of the Matanuska Glacier, Alaska. *U.S. Army Cold Regions Research and Engineering Laboratory, Report 79-9*, 103p
- Lawson, D.E. (1981) Distinguishing Characteristics of diamictons at the margin of the Matanuska Glacier, Alaska. *Annals of Glaciology* 2, p.78-84.
- Lawson, D.E. and Kulla, J. (1978) An Oxygen Isotope Investigation of the Origin of the Basal Zone of the Matanuska Glacier, Alaska. *The Journal of Geology*, 86(6), p.673-685
- Lawson, D. E., Strasser, J. C., Evenson, E. B., Alley, R. B., Larson, G. J., Arconci, S. A. (1998) Glaciohydraulic supercooling a freeze-on mechanism to create stratified debris-rich basal ice: I Field evidence. *Journal of Glaciology*, 44, p.547-562

- Lliboutry, L. (1986) A discussion of Robin's 'Heat Pump' effect by extending Nye's model for the sliding of a temperate glacier. Hydraulic effects at the bed and related phenomena *Mitteilungen Nr.90 der Versuchsanstalt für Wasserbau, Hydrologie, und Glaziologie*, ETH-Zurich, p.74-77
- Lowe, J.J. and Walker, M.C.J. (1997). *Reconstructing Quaternary Environments* (2<sup>nd</sup> edition). (Prentice-Hall, Essex).
- Mickelson, D.M. (1973) Nature and rate of basal till deposition in a stagnating ice mass, Burroughs Glacier, Alaska. *Arctic and Alpine Research*, 5, p.17-27
- Paterson, W.S.B. (1994). *The Physics of Glaciers* (3<sup>rd</sup> edition). (Butterworth-Heinemann, Oxford).
- Paul, M.A. and Eyles, N. (1990) Constraints on the preservation of diamict facies (melt-out tills) at the margins of stagnant glaciers. *Quaternary Science Reviews*, 9, p.51-69
- Powers, M. C. (1953) A new roundness scale for sedimentary particles. *Journal of Sedimentary Petrology*, 23, p.117-119
- Reheis, M. J. (1975) Source, transportation and deposition of debris on Arapaho Glacier, Front Range, Colorado, U.S.A. *Journal of Glaciology*, 14(72), p.407-420
- Röthlisberger, H. (1968) Erosive processes which are likely to accentuate or reduce the bottom relief of valley glaciers. *IAHS Publication*. 79, p.87-97
- Röthlisberger, H. (1972) Water pressure in intra and subglacial channels. *Journal of Glaciology*, 11, p.177-203
- Salisbury, R. D. (1896) Salient points regarding the glacial geology of north Greenland. *Journal of Geology* 4, p.769-810

- Sharp, M., Jouzel, J., Hubbard, B. and Lawson, W. (1994) The character, structure and origin of the basal ice layer of a surge-type glacier. *Journal of Glaciology*, Vol. 40, 135, p.327-340
- Slatt, R. M. (1971) Texture of ice-cored deposits from ten Alaskan Valley Glaciers. *Journal of Sedimentary Petrology*, 11, p.828-834
- Sneed, E.D. and Folk, R.L. (1958). Pebbles in the lower Colorado River, Texas, a study in particle morphogenesis, *Journal of Geology* 66(2), p.114-150.
- Sugden, D. E., Clapperton, C. M., Gemell, J. C. and Knight, P.G. (1987) Stable isotopes and debris in basal glacier ice, South Georgia, Southern Ocean. *Journal of Glaciology*, 33 (115), p.324-329
- Tison, J.-L., Souchez, R. and Lorrain, R. (1989) On the incorporation of unconsolidated sediments in basal ice: present-day examples. *Zeitschrift für Geomorphologie*, 72, p.173-183
- Waller, R.I., Hart, J.K. and Knight, P.G. (2000) The influence of tectonic deformation on facies variability in stratified debris-rich basal ice. *Quaternary Science Reviews*, 19, p.775-786
- Weertman, J. (1957) On the sliding of Glaciers. *Journal of Glaciology*, 3, p.965-978
- Weertman, J. (1961) Mechanism for the formation of inner moraines found near the edge of cold ice caps and ice sheets. *Journal of Glaciology*, p.965-978
- Weertman, J. (1964) The theory of glacier sliding. *Journal of Glaciology*, 5, 287-303

Whalley, B. and Kinsley, D. H. (1974) A scanning electron microscope study of surface textures of quartz grains from glacial environments. *Journal of Sedimentology*, p.21, 87-105

## APPENDICES

---

### Appendix A: Raw Grain Size Data

---

#### APPENDIX A: RAW GRAIN SIZE DATA

##### Site 1: Moraine

<b>Channel Diameter</b>	<b>Diff.</b>	<b>-2 S.D.</b>	<b>+2 S.D.</b>	<b>Cum. &lt;</b>
<b>µm</b>	<b>Volume</b>	<b>Diff.</b>	<b>Diff.</b>	<b>Volume</b>
	<b>%</b>	<b>Volume</b>	<b>Volume</b>	<b>%</b>
		<b>%</b>	<b>%</b>	
0.393	0.087	0.085	0.089	0
0.431	0.15	0.15	0.16	0.087
0.474	0.23	0.22	0.23	0.24
0.52	0.32	0.31	0.33	0.47
0.571	0.4	0.39	0.41	0.79
0.627	0.47	0.46	0.48	1.19
0.688	0.53	0.51	0.54	1.66
0.755	0.58	0.57	0.6	2.19
0.829	0.63	0.62	0.65	2.77
0.91	0.67	0.65	0.68	3.4
0.999	0.69	0.68	0.71	4.07
1.097	0.72	0.7	0.73	4.76
1.204	0.73	0.72	0.75	5.48
1.321	0.75	0.73	0.76	6.21
1.451	0.76	0.74	0.78	6.96
1.592	0.77	0.76	0.79	7.72
1.748	0.78	0.77	0.8	8.49
1.919	0.8	0.79	0.82	9.28
2.107	0.82	0.8	0.84	10.1
2.313	0.84	0.82	0.86	10.9
2.539	0.86	0.84	0.88	11.7
2.787	0.89	0.87	0.91	12.6
3.059	0.92	0.89	0.94	13.5
3.358	0.94	0.92	0.97	14.4
3.687	0.98	0.95	1	15.3
4.047	1.01	0.98	1.04	16.3
4.443	1.05	1.01	1.09	17.3

4.877	1.09	1.04	1.13	18.4
5.354	1.13	1.08	1.18	19.5
5.878	1.17	1.12	1.23	20.6
6.452	1.22	1.16	1.28	21.8
7.083	1.27	1.2	1.33	23
7.775	1.31	1.24	1.39	24.2
8.536	1.36	1.28	1.44	25.6
9.37	1.41	1.32	1.5	26.9
10.29	1.46	1.37	1.56	28.3
11.29	1.52	1.42	1.62	29.8
12.4	1.57	1.47	1.67	31.3
13.61	1.62	1.51	1.72	32.9
14.94	1.65	1.54	1.76	34.5
16.4	1.67	1.56	1.78	36.2
18	1.7	1.6	1.81	37.8
19.76	1.75	1.66	1.84	39.5
21.69	1.81	1.74	1.89	41.3
23.81	1.88	1.83	1.94	43.1
26.14	1.94	1.9	1.97	45
28.7	1.95	1.93	1.98	46.9
31.5	1.93	1.89	1.96	48.9
34.58	1.86	1.8	1.92	50.8
37.97	1.78	1.69	1.87	52.7
41.68	1.7	1.59	1.81	54.4
45.75	1.66	1.54	1.77	56.1
50.22	1.64	1.54	1.74	57.8
55.13	1.64	1.58	1.71	59.4
60.52	1.64	1.59	1.68	61.1
66.44	1.57	1.53	1.62	62.7
72.94	1.42	1.33	1.51	64.3
80.07	1.16	1	1.32	65.7
87.9	0.83	0.6	1.05	66.9
96.49	0.47	0.22	0.72	67.7
105.9	0.2	0.013	0.38	68.2
116.3	0.052	0	0.14	68.4
127.6	0.0072	0	0.026	68.4
140.1	0.00041	0	0.0018	68.4
153.8	0	0	0	68.4
168.9	0	0	0	68.4
185.4	0	0	0	68.4
203.5	0	0	0	68.4
223.4	0	0	0	68.4
245.2	0.00096	0	0.0043	68.4
269.2	0.02	0	0.064	68.4

295.5	0.15	0	0.35	68.5
324.4	0.57	0.19	0.94	68.6
356.1	1.27	0.84	1.7	69.2
390.9	2.09	1.79	2.38	70.4
429.2	2.76	2.57	2.95	72.5
471.1	3.23	2.93	3.53	75.3
517.2	3.5	3.06	3.94	78.5
567.7	3.74	3.22	4.26	82
623.3	3.99	3.4	4.59	85.8
684.2	4.28	3.54	5.01	89.7
751.1	3.47	2.8	4.15	94
824.5	1.96	1.55	2.38	97.5
905.1	0.48	0.37	0.59	99.5
993.6	0.052	0.04	0.065	99.9
1091	0	0	0	100
1197	0	0	0	100
1314	0	0	0	100
1443	0	0	0	100
1584	0	0	0	100
1739	0	0	0	100
1909	0	0	0	100

**Site 1: Ice Type B (1)**

<b>Channel Diameter</b>	<b>Diff.</b>	<b>-2 S.D.</b>	<b>+2 S.D.</b>	<b>Cum. &lt;</b>
<b>µm</b>	<b>Volume</b>	<b>Diff.</b>	<b>Diff.</b>	<b>Volume</b>
	<b>%</b>	<b>Volume</b>	<b>Volume</b>	<b>%</b>
		<b>%</b>	<b>%</b>	
0.393	0.11	0.11	0.11	0
0.431	0.19	0.19	0.19	0.11
0.474	0.28	0.28	0.28	0.3
0.52	0.4	0.4	0.4	0.58
0.571	0.5	0.5	0.51	0.98
0.627	0.59	0.59	0.6	1.48
0.688	0.68	0.67	0.68	2.07
0.755	0.76	0.75	0.77	2.74
0.829	0.84	0.83	0.85	3.51
0.91	0.9	0.89	0.91	4.34
0.999	0.96	0.95	0.97	5.24
1.097	1.01	1	1.03	6.21
1.204	1.07	1.05	1.08	7.22
1.321	1.11	1.1	1.13	8.29
1.451	1.16	1.15	1.17	9.4

1.592	1.2	1.19	1.22	10.6
1.748	1.25	1.24	1.27	11.8
1.919	1.3	1.29	1.32	13
2.107	1.35	1.34	1.37	14.3
2.313	1.41	1.39	1.42	15.7
2.539	1.46	1.45	1.48	17.1
2.787	1.52	1.51	1.54	18.5
3.059	1.58	1.57	1.6	20.1
3.358	1.64	1.63	1.66	21.6
3.687	1.7	1.69	1.72	23.3
4.047	1.77	1.75	1.79	25
4.443	1.83	1.81	1.85	26.8
4.877	1.89	1.87	1.92	28.6
5.354	1.96	1.93	1.98	30.5
5.878	2.02	1.99	2.04	32.4
6.452	2.07	2.04	2.11	34.5
7.083	2.13	2.09	2.17	36.5
7.775	2.19	2.14	2.23	38.7
8.536	2.24	2.19	2.29	40.9
9.37	2.29	2.24	2.34	43.1
10.29	2.34	2.29	2.39	45.4
11.29	2.4	2.35	2.44	47.7
12.4	2.45	2.41	2.49	50.1
13.61	2.49	2.46	2.53	52.6
14.94	2.52	2.49	2.54	55.1
16.4	2.54	2.5	2.57	57.6
18	2.58	2.53	2.63	60.1
19.76	2.66	2.59	2.73	62.7
21.69	2.76	2.68	2.85	65.4
23.81	2.84	2.77	2.91	68.1
26.14	2.83	2.81	2.86	71
28.7	2.72	2.7	2.75	73.8
31.5	2.55	2.49	2.61	76.5
34.58	2.41	2.36	2.45	79.1
37.97	2.38	2.36	2.39	81.5
41.68	2.5	2.41	2.59	83.8
45.75	2.72	2.59	2.85	86.3
50.22	2.88	2.79	2.96	89.1
55.13	2.8	2.73	2.86	91.9
60.52	2.37	2.13	2.62	94.7
66.44	1.66	1.27	2.06	97.1
72.94	0.87	0.52	1.22	98.8
80.07	0.3	0.11	0.5	99.6
87.9	0.053	0.0074	0.098	99.9

96.49	0.0036	0	0.008	99.996
105.9	0	0	0	100
116.3	0	0	0	100
127.6	0	0	0	100
140.1	0	0	0	100
153.8	0	0	0	100
168.9	0	0	0	100
185.4	0	0	0	100
203.5	0	0	0	100
223.4	0	0	0	100
245.2	0	0	0	100
269.2	0	0	0	100
295.5	0	0	0	100
324.4	0	0	0	100
356.1	0	0	0	100
390.9	0	0	0	100
429.2	0	0	0	100
471.1	0	0	0	100
517.2	0	0	0	100
567.7	0	0	0	100
623.3	0	0	0	100
684.2	0	0	0	100
751.1	0	0	0	100
824.5	0	0	0	100
905.1	0	0	0	100
993.6	0	0	0	100
1091	0	0	0	100
1197	0	0	0	100
1314	0	0	0	100
1443	0	0	0	100
1584	0	0	0	100
1739	0	0	0	100
1909	0	0	0	100
				100

**Site 1: Ice Type B (2)**

<b>Channel Diameter</b>	<b>Diff.</b>	<b>-2 S.D.</b>	<b>+2 S.D.</b>	<b>Cum. &lt;</b>
<b>µm</b>	<b>Volume</b>	<b>Diff.</b>	<b>Diff.</b>	<b>Volume</b>
	<b>%</b>	<b>Volume</b>	<b>Volume</b>	<b>%</b>
		<b>%</b>	<b>%</b>	
0.393	0.12	0.11	0.12	0
0.431	0.2	0.2	0.21	0.12

0.474	0.3	0.3	0.31	0.32
0.52	0.43	0.42	0.44	0.62
0.571	0.54	0.53	0.55	1.05
0.627	0.64	0.63	0.65	1.6
0.688	0.73	0.72	0.75	2.24
0.755	0.83	0.81	0.84	2.97
0.829	0.91	0.89	0.93	3.79
0.91	0.98	0.96	1	4.7
0.999	1.04	1.02	1.06	5.68
1.097	1.1	1.08	1.12	6.72
1.204	1.16	1.13	1.18	7.82
1.321	1.21	1.18	1.24	8.98
1.451	1.26	1.23	1.29	10.2
1.592	1.3	1.27	1.33	11.4
1.748	1.36	1.32	1.39	12.7
1.919	1.41	1.37	1.44	14.1
2.107	1.46	1.43	1.5	15.5
2.313	1.52	1.48	1.56	17
2.539	1.58	1.54	1.62	18.5
2.787	1.65	1.61	1.69	20.1
3.059	1.72	1.68	1.75	21.7
3.358	1.78	1.74	1.82	23.4
3.687	1.85	1.81	1.89	25.2
4.047	1.92	1.88	1.96	27.1
4.443	1.99	1.95	2.04	29
4.877	2.06	2.02	2.1	31
5.354	2.13	2.09	2.17	33.1
5.878	2.19	2.15	2.24	35.2
6.452	2.26	2.21	2.3	37.4
7.083	2.32	2.27	2.37	39.6
7.775	2.38	2.33	2.43	42
8.536	2.43	2.38	2.48	44.3
9.37	2.48	2.43	2.53	46.8
10.29	2.54	2.48	2.59	49.2
11.29	2.6	2.54	2.66	51.8
12.4	2.65	2.59	2.71	54.4
13.61	2.69	2.63	2.75	57
14.94	2.73	2.65	2.8	59.7
16.4	2.77	2.68	2.87	62.4
18	2.84	2.73	2.94	65.2
19.76	2.88	2.8	2.97	68
21.69	2.88	2.85	2.91	70.9
23.81	2.8	2.76	2.85	73.8
26.14	2.67	2.6	2.75	76.6

28.7	2.57	2.55	2.6	79.3
31.5	2.57	2.47	2.66	81.9
34.58	2.68	2.45	2.91	84.4
37.97	2.84	2.56	3.12	87.1
41.68	2.9	2.73	3.07	89.9
45.75	2.7	2.58	2.82	92.8
50.22	2.18	1.75	2.61	95.5
55.13	1.4	0.7	2.1	97.7
60.52	0.66	0.036	1.28	99.1
66.44	0.19	0	0.53	99.8
72.94	0.03	0	0.11	99.97
80.07	0.0019	0	0.0085	99.998
87.9	0	0	0	100
96.49	0	0	0	100
105.9	0	0	0	100
116.3	0	0	0	100
127.6	0	0	0	100
140.1	0	0	0	100
153.8	0	0	0	100
168.9	0	0	0	100
185.4	0	0	0	100
203.5	0	0	0	100
223.4	0	0	0	100
245.2	0	0	0	100
269.2	0	0	0	100
295.5	0	0	0	100
324.4	0	0	0	100
356.1	0	0	0	100
390.9	0	0	0	100
429.2	0	0	0	100
471.1	0	0	0	100
517.2	0	0	0	100
567.7	0	0	0	100
623.3	0	0	0	100
684.2	0	0	0	100
751.1	0	0	0	100
824.5	0	0	0	100
905.1	0	0	0	100
993.6	0	0	0	100
1091	0	0	0	100
1197	0	0	0	100
1314	0	0	0	100
1443	0	0	0	100
1584	0	0	0	100

1739	0	0	0	100
1909	0	0	0	100

**Site 1: Ice Type B (3)**

<b>Channel Diameter</b>	<b>Diff.</b>	<b>-2 S.D.</b>	<b>+2 S.D.</b>	<b>Cum. &lt;</b>
<b>µm</b>	<b>Volume</b>	<b>Diff.</b>	<b>Diff.</b>	<b>Volume</b>
	<b>%</b>	<b>Volume</b>	<b>Volume</b>	<b>%</b>
		<b>%</b>	<b>%</b>	
0.393	0.12	0.12	0.12	0
0.431	0.22	0.21	0.22	0.12
0.474	0.32	0.31	0.32	0.34
0.52	0.45	0.45	0.46	0.65
0.571	0.57	0.56	0.58	1.11
0.627	0.67	0.66	0.68	1.68
0.688	0.77	0.76	0.78	2.35
0.755	0.87	0.85	0.88	3.12
0.829	0.95	0.94	0.96	3.98
0.91	1.02	1.01	1.04	4.94
0.999	1.09	1.07	1.1	5.96
1.097	1.14	1.13	1.16	7.05
1.204	1.2	1.18	1.21	8.19
1.321	1.25	1.23	1.26	9.39
1.451	1.29	1.27	1.3	10.6
1.592	1.33	1.31	1.35	11.9
1.748	1.37	1.35	1.39	13.3
1.919	1.42	1.4	1.44	14.6
2.107	1.46	1.44	1.48	16
2.313	1.51	1.49	1.53	17.5
2.539	1.56	1.54	1.59	19
2.787	1.62	1.6	1.65	20.6
3.059	1.68	1.66	1.71	22.2
3.358	1.75	1.72	1.77	23.9
3.687	1.81	1.78	1.84	25.6
4.047	1.88	1.85	1.91	27.4
4.443	1.95	1.92	1.98	29.3
4.877	2.02	1.99	2.05	31.3
5.354	2.09	2.06	2.11	33.3

5.878	2.15	2.13	2.18	35.4
6.452	2.22	2.2	2.25	37.5
7.083	2.29	2.27	2.32	39.8
7.775	2.36	2.33	2.38	42
8.536	2.42	2.39	2.44	44.4
9.37	2.47	2.45	2.5	46.8
10.29	2.54	2.5	2.57	49.3
11.29	2.6	2.56	2.64	51.8
12.4	2.66	2.61	2.7	54.4
13.61	2.7	2.65	2.74	57.1
14.94	2.73	2.67	2.79	59.8
16.4	2.77	2.7	2.84	62.5
18	2.84	2.76	2.91	65.3
19.76	2.88	2.83	2.93	68.1
21.69	2.87	2.83	2.9	71
23.81	2.76	2.7	2.83	73.9
26.14	2.61	2.54	2.67	76.6
28.7	2.49	2.48	2.51	79.2
31.5	2.5	2.41	2.58	81.7
34.58	2.65	2.47	2.84	84.2
37.97	2.88	2.66	3.1	86.9
41.68	2.99	2.84	3.13	89.8
45.75	2.8	2.7	2.9	92.7
50.22	2.24	1.96	2.53	95.5
55.13	1.4	0.95	1.85	97.8
60.52	0.62	0.23	1.02	99.2
66.44	0.16	0	0.37	99.8
72.94	0.021	0	0.065	99.98
80.07	0.00091	0	0.0041	99.999
87.9	0	0	0	100
96.49	0	0	0	100
105.9	0	0	0	100
116.3	0	0	0	100
127.6	0	0	0	100
140.1	0	0	0	100
153.8	0	0	0	100
168.9	0	0	0	100
185.4	0	0	0	100
203.5	0	0	0	100
223.4	0	0	0	100
245.2	0	0	0	100
269.2	0	0	0	100
295.5	0	0	0	100
324.4	0	0	0	100

356.1	0	0	0	100
390.9	0	0	0	100
429.2	0	0	0	100
471.1	0	0	0	100
517.2	0	0	0	100
567.7	0	0	0	100
623.3	0	0	0	100
684.2	0	0	0	100
751.1	0	0	0	100
824.5	0	0	0	100
905.1	0	0	0	100
993.6	0	0	0	100
1091	0	0	0	100
1197	0	0	0	100
1314	0	0	0	100
1443	0	0	0	100
1584	0	0	0	100
1739	0	0	0	100
1909	0	0	0	100

**Site 1: Ice Type B (4)**

<b>Channel Diameter</b>	<b>Diff.</b>	<b>-2 S.D.</b>	<b>+2 S.D.</b>	<b>Cum. &lt;</b>
<b>µm</b>	<b>Volume</b>	<b>Diff.</b>	<b>Diff.</b>	<b>Volume</b>
	<b>%</b>	<b>Volume</b>	<b>Volume</b>	<b>%</b>
		<b>%</b>	<b>%</b>	
0.393	0.12	0.12	0.13	0
0.431	0.22	0.21	0.23	0.12
0.474	0.32	0.31	0.34	0.34
0.52	0.46	0.44	0.48	0.67
0.571	0.58	0.56	0.6	1.13
0.627	0.68	0.67	0.7	1.71
0.688	0.78	0.77	0.78	2.39
0.755	0.87	0.87	0.87	3.16
0.829	0.95	0.94	0.97	4.03
0.91	1.03	1	1.06	4.99
0.999	1.09	1.05	1.14	6.01
1.097	1.15	1.09	1.21	7.11
1.204	1.21	1.14	1.28	8.26
1.321	1.27	1.2	1.34	9.47

1.451	1.33	1.25	1.4	10.7
1.592	1.38	1.32	1.45	12.1
1.748	1.45	1.39	1.51	13.4
1.919	1.52	1.48	1.56	14.9
2.107	1.59	1.57	1.62	16.4
2.313	1.67	1.66	1.68	18
2.539	1.75	1.74	1.77	19.7
2.787	1.83	1.8	1.86	21.4
3.059	1.92	1.88	1.96	23.3
3.358	2.01	1.95	2.06	25.2
3.687	2.09	2.04	2.14	27.2
4.047	2.17	2.12	2.23	29.3
4.443	2.25	2.2	2.3	31.4
4.877	2.33	2.29	2.37	33.7
5.354	2.4	2.37	2.43	36
5.878	2.47	2.46	2.48	38.4
6.452	2.53	2.53	2.54	40.9
7.083	2.59	2.56	2.62	43.4
7.775	2.64	2.58	2.7	46
8.536	2.69	2.6	2.78	48.7
9.37	2.74	2.62	2.85	51.4
10.29	2.79	2.66	2.92	54.1
11.29	2.84	2.7	2.97	56.9
12.4	2.88	2.74	3.02	59.7
13.61	2.92	2.78	3.05	62.6
14.94	2.95	2.81	3.08	65.5
16.4	2.96	2.85	3.07	68.5
18	2.93	2.87	3	71.4
19.76	2.86	2.85	2.87	74.4
21.69	2.76	2.7	2.81	77.2
23.81	2.66	2.65	2.68	80
26.14	2.63	2.54	2.71	82.6
28.7	2.65	2.41	2.89	85.3
31.5	2.7	2.36	3.04	87.9
34.58	2.66	2.37	2.94	90.6
37.97	2.43	2.36	2.49	93.3
41.68	1.96	1.69	2.24	95.7
45.75	1.32	0.73	1.91	97.7
50.22	0.69	0.027	1.35	99
55.13	0.26	0	0.71	99.7
60.52	0.064	0	0.23	99.9
66.44	0.0088	0	0.038	99.99
72.94	0.00046	0	0.002	100
80.07	0	0	0	100

87.9	0	0	0	100
96.49	0	0	0	100
105.9	0	0	0	100
116.3	0	0	0	100
127.6	0	0	0	100
140.1	0	0	0	100
153.8	0	0	0	100
168.9	0	0	0	100
185.4	0	0	0	100
203.5	0	0	0	100
223.4	0	0	0	100
245.2	0	0	0	100
269.2	0	0	0	100
295.5	0	0	0	100
324.4	0	0	0	100
356.1	0	0	0	100
390.9	0	0	0	100
429.2	0	0	0	100
471.1	0	0	0	100
517.2	0	0	0	100
567.7	0	0	0	100
623.3	0	0	0	100
684.2	0	0	0	100
751.1	0	0	0	100
824.5	0	0	0	100
905.1	0	0	0	100
993.6	0	0	0	100
1091	0	0	0	100
1197	0	0	0	100
1314	0	0	0	100
1443	0	0	0	100
1584	0	0	0	100
1739	0	0	0	100
1909	0	0	0	100

**Site 1: Ice Type B (5)**

<b>Channel Diameter</b>	<b>Diff.</b>	<b>-2 S.D.</b>	<b>+2 S.D.</b>	<b>Cum. &lt;</b>
<b>um</b>	<b>Volume</b>	<b>Diff.</b>	<b>Diff.</b>	<b>Volume</b>
	<b>%</b>	<b>Volume</b>	<b>Volume</b>	<b>%</b>
		<b>%</b>	<b>%</b>	
0.393	0.12	0.11	0.13	0
0.431	0.21	0.2	0.22	0.12

0.474	0.31	0.29	0.33	0.33
0.52	0.44	0.42	0.46	0.64
0.571	0.55	0.53	0.57	1.07
0.627	0.65	0.63	0.67	1.62
0.688	0.74	0.72	0.75	2.27
0.755	0.83	0.81	0.84	3.01
0.829	0.91	0.89	0.93	3.84
0.91	0.98	0.94	1.01	4.74
0.999	1.04	0.99	1.08	5.72
1.097	1.09	1.03	1.15	6.75
1.204	1.15	1.08	1.22	7.85
1.321	1.21	1.13	1.28	9
1.451	1.26	1.19	1.34	10.2
1.592	1.32	1.25	1.39	11.5
1.748	1.38	1.32	1.45	12.8
1.919	1.45	1.4	1.5	14.2
2.107	1.53	1.49	1.56	15.6
2.313	1.6	1.58	1.62	17.2
2.539	1.68	1.65	1.71	18.8
2.787	1.76	1.72	1.8	20.4
3.059	1.84	1.79	1.9	22.2
3.358	1.93	1.86	1.99	24
3.687	2.01	1.94	2.08	26
4.047	2.09	2.02	2.16	28
4.443	2.16	2.09	2.24	30.1
4.877	2.24	2.17	2.3	32.2
5.354	2.3	2.25	2.36	34.5
5.878	2.37	2.32	2.42	36.8
6.452	2.43	2.39	2.46	39.1
7.083	2.48	2.45	2.51	41.6
7.775	2.52	2.48	2.56	44
8.536	2.57	2.51	2.63	46.6
9.37	2.61	2.53	2.69	49.1
10.29	2.67	2.57	2.76	51.7
11.29	2.72	2.63	2.82	54.4
12.4	2.77	2.67	2.86	57.1
13.61	2.81	2.7	2.91	59.9
14.94	2.84	2.71	2.97	62.7
16.4	2.87	2.72	3.02	65.5
18	2.89	2.75	3.03	68.4
19.76	2.88	2.79	2.97	71.3
21.69	2.82	2.78	2.85	74.2
23.81	2.71	2.63	2.8	77
26.14	2.61	2.54	2.69	79.7

28.7	2.57	2.53	2.6	82.3
31.5	2.59	2.37	2.81	84.9
34.58	2.65	2.28	3.01	87.5
37.97	2.64	2.27	3.02	90.1
41.68	2.47	2.26	2.67	92.8
45.75	2.06	1.82	2.3	95.2
50.22	1.45	0.85	2.05	97.3
55.13	0.81	0.083	1.54	98.7
60.52	0.33	0	0.87	99.6
66.44	0.093	0	0.32	99.9
72.94	0.014	0	0.057	99.98
80.07	0.00091	0	0.0041	99.999
87.9	0	0	0	100
96.49	0	0	0	100
105.9	0	0	0	100
116.3	0	0	0	100
127.6	0	0	0	100
140.1	0	0	0	100
153.8	0	0	0	100
168.9	0	0	0	100
185.4	0	0	0	100
203.5	0	0	0	100
223.4	0	0	0	100
245.2	0	0	0	100
269.2	0	0	0	100
295.5	0	0	0	100
324.4	0	0	0	100
356.1	0	0	0	100
390.9	0	0	0	100
429.2	0	0	0	100
471.1	0	0	0	100
517.2	0	0	0	100
567.7	0	0	0	100
623.3	0	0	0	100
684.2	0	0	0	100
751.1	0	0	0	100
824.5	0	0	0	100
905.1	0	0	0	100
993.6	0	0	0	100
1091	0	0	0	100
1197	0	0	0	100
1314	0	0	0	100
1443	0	0	0	100
1584	0	0	0	100

1739	0	0	0	100
1909	0	0	0	100

**Site 1: Ice Type B (6)**

<b>Channel Diameter</b>	<b>Diff.</b>	<b>-2 S.D.</b>	<b>+2 S.D.</b>	<b>Cum. &lt;</b>
<b>µm</b>	<b>Volume</b>	<b>Diff.</b>	<b>Diff.</b>	<b>Volume</b>
	<b>%</b>	<b>Volume</b>	<b>Volume</b>	<b>%</b>
		<b>%</b>	<b>%</b>	
0.393	0.12	0.12	0.12	0
0.431	0.21	0.21	0.21	0.12
0.474	0.31	0.3	0.31	0.33
0.52	0.44	0.43	0.45	0.64
0.571	0.55	0.54	0.56	1.08
0.627	0.65	0.64	0.66	1.63
0.688	0.74	0.73	0.75	2.28
0.755	0.84	0.83	0.85	3.03
0.829	0.92	0.91	0.93	3.86
0.91	0.99	0.98	1	4.78
0.999	1.05	1.04	1.07	5.77
1.097	1.11	1.1	1.13	6.83
1.204	1.17	1.15	1.18	7.94
1.321	1.22	1.2	1.24	9.11
1.451	1.27	1.25	1.29	10.3
1.592	1.32	1.3	1.34	11.6
1.748	1.38	1.36	1.4	12.9
1.919	1.44	1.42	1.46	14.3
2.107	1.5	1.48	1.52	15.7
2.313	1.57	1.54	1.59	17.2
2.539	1.64	1.61	1.66	18.8
2.787	1.71	1.68	1.74	20.4
3.059	1.79	1.76	1.82	22.2
3.358	1.86	1.83	1.89	23.9
3.687	1.94	1.91	1.97	25.8
4.047	2.02	1.98	2.05	27.7
4.443	2.1	2.06	2.13	29.8
4.877	2.17	2.14	2.2	31.9
5.354	2.24	2.21	2.27	34

5.878	2.31	2.28	2.34	36.3
6.452	2.38	2.35	2.41	38.6
7.083	2.44	2.41	2.47	40.9
7.775	2.5	2.47	2.53	43.4
8.536	2.55	2.52	2.59	45.9
9.37	2.61	2.57	2.65	48.4
10.29	2.66	2.62	2.71	51.1
11.29	2.72	2.67	2.77	53.7
12.4	2.76	2.71	2.81	56.4
13.61	2.79	2.73	2.85	59.2
14.94	2.81	2.75	2.87	62
16.4	2.84	2.77	2.91	64.8
18	2.87	2.8	2.93	67.6
19.76	2.88	2.84	2.91	70.5
21.69	2.83	2.82	2.85	73.4
23.81	2.73	2.67	2.78	76.2
26.14	2.59	2.53	2.65	78.9
28.7	2.49	2.47	2.5	81.5
31.5	2.47	2.4	2.53	84
34.58	2.53	2.39	2.67	86.5
37.97	2.61	2.47	2.76	89
41.68	2.57	2.52	2.63	91.6
45.75	2.3	2.18	2.43	94.2
50.22	1.78	1.48	2.08	96.5
55.13	1.09	0.66	1.51	98.3
60.52	0.48	0.12	0.83	99.4
66.44	0.12	0	0.31	99.9
72.94	0.017	0	0.055	99.98
80.07	0.00081	0	0.0036	99.999
87.9	0	0	0	100
96.49	0	0	0	100
105.9	0	0	0	100
116.3	0	0	0	100
127.6	0	0	0	100
140.1	0	0	0	100
153.8	0	0	0	100
168.9	0	0	0	100
185.4	0	0	0	100
203.5	0	0	0	100
223.4	0	0	0	100
245.2	0	0	0	100
269.2	0	0	0	100
295.5	0	0	0	100
324.4	0	0	0	100

356.1	0	0	0	100
390.9	0	0	0	100
429.2	0	0	0	100
471.1	0	0	0	100
517.2	0	0	0	100
567.7	0	0	0	100
623.3	0	0	0	100
684.2	0	0	0	100
751.1	0	0	0	100
824.5	0	0	0	100
905.1	0	0	0	100
993.6	0	0	0	100
1091	0	0	0	100
1197	0	0	0	100
1314	0	0	0	100
1443	0	0	0	100
1584	0	0	0	100
1739	0	0	0	100
1909	0	0	0	100

**Site 2: Ice Type D**

<b>Channel Diameter</b>	<b>Diff.</b>	<b>-2 S.D.</b>	<b>+2 S.D.</b>	<b>Cum. &lt;</b>
<b>µm</b>	<b>Volume</b>	<b>Diff.</b>	<b>Diff.</b>	<b>Volume</b>
	<b>%</b>	<b>Volume</b>	<b>Volume</b>	<b>%</b>
		<b>%</b>	<b>%</b>	
0.393	0.16	0.15	0.17	0
0.431	0.29	0.27	0.3	0.16
0.474	0.42	0.4	0.44	0.45
0.52	0.59	0.56	0.62	0.87
0.571	0.73	0.7	0.76	1.46
0.627	0.84	0.81	0.88	2.19
0.688	0.94	0.9	0.98	3.04
0.755	1.03	0.99	1.07	3.98
0.829	1.09	1.05	1.13	5
0.91	1.13	1.1	1.17	6.1
0.999	1.15	1.12	1.19	7.23
1.097	1.16	1.13	1.19	8.39
1.204	1.16	1.13	1.19	9.55
1.321	1.15	1.12	1.18	10.7
1.451	1.14	1.11	1.17	11.9
1.592	1.13	1.1	1.16	13
1.748	1.12	1.09	1.15	14.1

1.919	1.13	1.09	1.16	15.2
2.107	1.14	1.1	1.17	16.4
2.313	1.15	1.11	1.19	17.5
2.539	1.18	1.13	1.22	18.7
2.787	1.21	1.16	1.25	19.8
3.059	1.24	1.2	1.29	21
3.358	1.29	1.24	1.34	22.3
3.687	1.33	1.28	1.38	23.6
4.047	1.38	1.33	1.43	24.9
4.443	1.43	1.37	1.48	26.3
4.877	1.48	1.42	1.54	27.7
5.354	1.53	1.47	1.59	29.2
5.878	1.58	1.52	1.64	30.7
6.452	1.63	1.56	1.69	32.3
7.083	1.67	1.61	1.74	33.9
7.775	1.72	1.65	1.78	35.6
8.536	1.76	1.69	1.82	37.3
9.37	1.8	1.74	1.86	39.1
10.29	1.84	1.78	1.91	40.9
11.29	1.88	1.82	1.95	42.7
12.4	1.91	1.85	1.97	44.6
13.61	1.91	1.85	1.97	46.5
14.94	1.89	1.83	1.94	48.4
16.4	1.85	1.79	1.9	50.3
18	1.81	1.75	1.87	52.2
19.76	1.78	1.72	1.84	54
21.69	1.76	1.69	1.82	55.8
23.81	1.73	1.67	1.8	57.5
26.14	1.7	1.64	1.75	59.2
28.7	1.64	1.59	1.69	60.9
31.5	1.57	1.53	1.61	62.6
34.58	1.5	1.47	1.53	64.1
37.97	1.44	1.42	1.47	65.6
41.68	1.4	1.38	1.42	67.1
45.75	1.37	1.34	1.39	68.5
50.22	1.33	1.3	1.37	69.9
55.13	1.3	1.26	1.33	71.2
60.52	1.25	1.21	1.28	72.5
66.44	1.19	1.16	1.21	73.7
72.94	1.12	1.09	1.14	74.9
80.07	1.03	0.99	1.06	76
87.9	0.93	0.88	0.97	77.1
96.49	0.82	0.77	0.87	78
105.9	0.72	0.67	0.76	78.8

116.3	0.64	0.6	0.68	79.5
127.6	0.59	0.55	0.62	80.2
140.1	0.55	0.52	0.57	80.8
153.8	0.5	0.49	0.51	81.3
168.9	0.43	0.42	0.44	81.8
185.4	0.34	0.32	0.35	82.2
203.5	0.26	0.24	0.28	82.6
223.4	0.24	0.21	0.27	82.8
245.2	0.31	0.26	0.36	83.1
269.2	0.48	0.41	0.56	83.4
295.5	0.75	0.64	0.87	83.9
324.4	1.07	0.93	1.2	84.6
356.1	1.33	1.21	1.44	85.7
390.9	1.48	1.42	1.53	87
429.2	1.52	1.35	1.69	88.5
471.1	1.5	1.18	1.82	90
517.2	1.46	1.07	1.86	91.5
567.7	1.5	1.19	1.8	93
623.3	1.6	1.56	1.65	94.5
684.2	1.68	0.95	2.41	96.1
751.1	1.34	0.21	2.47	97.7
824.5	0.72	0	1.69	99.1
905.1	0.17	0	0.45	99.8
993.6	0.019	0	0.052	99.98
1091	0	0	0	100
1197	0	0	0	100
1314	0	0	0	100
1443	0	0	0	100
1584	0	0	0	100
1739	0	0	0	100
1909	0	0	0	100

**Site 2: Ice Type B**

<b>Channel Diameter</b>	<b>Diff.</b>	<b>-2 S.D.</b>	<b>+2 S.D.</b>	<b>Cum. &lt;</b>
<b>µm</b>	<b>Volume</b>	<b>Diff.</b>	<b>Diff.</b>	<b>Volume</b>
	<b>%</b>	<b>Volume</b>	<b>Volume</b>	<b>%</b>
		<b>%</b>	<b>%</b>	
0.393	0.094	0.09	0.098	0
0.431	0.17	0.16	0.17	0.094

0.474	0.24	0.24	0.25	0.26
0.52	0.35	0.34	0.36	0.51
0.571	0.43	0.42	0.45	0.85
0.627	0.51	0.5	0.52	1.29
0.688	0.57	0.56	0.59	1.8
0.755	0.64	0.62	0.66	2.37
0.829	0.69	0.67	0.72	3.01
0.91	0.74	0.71	0.77	3.7
0.999	0.77	0.73	0.81	4.44
1.097	0.8	0.75	0.85	5.21
1.204	0.83	0.78	0.89	6.02
1.321	0.86	0.8	0.92	6.85
1.451	0.88	0.82	0.94	7.71
1.592	0.91	0.85	0.97	8.59
1.748	0.94	0.89	0.99	9.5
1.919	0.98	0.94	1.02	10.4
2.107	1.02	0.99	1.05	11.4
2.313	1.07	1.05	1.09	12.4
2.539	1.12	1.11	1.13	13.5
2.787	1.18	1.17	1.19	14.6
3.059	1.24	1.23	1.26	15.8
3.358	1.31	1.3	1.33	17.1
3.687	1.39	1.37	1.4	18.4
4.047	1.46	1.44	1.48	19.8
4.443	1.54	1.52	1.56	21.2
4.877	1.62	1.6	1.64	22.8
5.354	1.7	1.67	1.73	24.4
5.878	1.78	1.74	1.82	26.1
6.452	1.86	1.81	1.92	27.9
7.083	1.95	1.87	2.02	29.7
7.775	2.03	1.94	2.12	31.7
8.536	2.11	2	2.22	33.7
9.37	2.2	2.08	2.31	35.8
10.29	2.28	2.16	2.4	38
11.29	2.37	2.25	2.49	40.3
12.4	2.46	2.34	2.58	42.7
13.61	2.54	2.42	2.66	45.1
14.94	2.61	2.49	2.73	47.6
16.4	2.67	2.54	2.79	50.3
18	2.71	2.58	2.85	52.9
19.76	2.76	2.6	2.93	55.6
21.69	2.82	2.61	3.02	58.4
23.81	2.87	2.63	3.12	61.2
26.14	2.93	2.68	3.17	64.1

28.7	2.96	2.78	3.13	67
31.5	2.95	2.9	3.01	70
34.58	2.91	2.84	2.98	72.9
37.97	2.83	2.71	2.95	75.8
41.68	2.75	2.71	2.78	78.7
45.75	2.69	2.51	2.87	81.4
50.22	2.67	2.25	3.1	84.1
55.13	2.67	2.12	3.23	86.8
60.52	2.63	2.23	3.03	89.5
66.44	2.46	2.35	2.57	92.1
72.94	2.11	1.44	2.79	94.5
80.07	1.59	0.44	2.75	96.7
87.9	1.02	0	2.22	98.3
96.49	0.51	0	1.31	99.3
105.9	0.18	0	0.5	99.8
116.3	0.032	0	0.093	99.97
127.6	0.0024	0	0.007	99.998
140.1	0	0	0	100
153.8	0	0	0	100
168.9	0	0	0	100
185.4	0	0	0	100
203.5	0	0	0	100
223.4	0	0	0	100
245.2	0	0	0	100
269.2	0	0	0	100
295.5	0	0	0	100
324.4	0	0	0	100
356.1	0	0	0	100
390.9	0	0	0	100
429.2	0	0	0	100
471.1	0	0	0	100
517.2	0	0	0	100
567.7	0	0	0	100
623.3	0	0	0	100
684.2	0	0	0	100
751.1	0	0	0	100
824.5	0	0	0	100
905.1	0	0	0	100
993.6	0	0	0	100
1091	0	0	0	100
1197	0	0	0	100
1314	0	0	0	100
1443	0	0	0	100
1584	0	0	0	100

1739	0	0	0	100
1909	0	0	0	100

**Site 2: Proglacial Sediments (1)**

<b>Channel Diameter</b>	<b>Diff.</b>	<b>-2 S.D.</b>	<b>+2 S.D.</b>	<b>Cum. &lt;</b>
<b>µm</b>	<b>Volume</b>	<b>Diff.</b>	<b>Diff.</b>	<b>Volume</b>
	<b>%</b>	<b>Volume</b>	<b>Volume</b>	<b>%</b>
		<b>%</b>	<b>%</b>	
0.393	0.07	0.063	0.076	0
0.431	0.12	0.11	0.13	0.07
0.474	0.18	0.17	0.2	0.19
0.52	0.26	0.24	0.28	0.37
0.571	0.32	0.29	0.34	0.63
0.627	0.37	0.34	0.4	0.95
0.688	0.42	0.39	0.44	1.32
0.755	0.46	0.43	0.49	1.74
0.829	0.5	0.47	0.52	2.2
0.91	0.52	0.5	0.55	2.7
0.999	0.54	0.52	0.56	3.22
1.097	0.56	0.54	0.58	3.76
1.204	0.57	0.55	0.59	4.32
1.321	0.58	0.56	0.6	4.89
1.451	0.6	0.58	0.62	5.47
1.592	0.61	0.59	0.64	6.07
1.748	0.64	0.61	0.67	6.68
1.919	0.67	0.63	0.7	7.31
2.107	0.7	0.66	0.75	7.98
2.313	0.74	0.69	0.8	8.68
2.539	0.8	0.73	0.86	9.43
2.787	0.86	0.78	0.93	10.2
3.059	0.93	0.84	1.01	11.1
3.358	1	0.91	1.09	12
3.687	1.08	0.99	1.18	13
4.047	1.17	1.07	1.28	14.1
4.443	1.27	1.16	1.38	15.3
4.877	1.37	1.25	1.48	16.5
5.354	1.47	1.35	1.58	17.9

5.878	1.57	1.45	1.68	19.4
6.452	1.67	1.55	1.78	20.9
7.083	1.77	1.65	1.88	22.6
7.775	1.86	1.75	1.98	24.4
8.536	1.96	1.85	2.06	26.2
9.37	2.04	1.94	2.15	28.2
10.29	2.13	2.03	2.23	30.2
11.29	2.21	2.11	2.3	32.4
12.4	2.27	2.19	2.36	34.6
13.61	2.33	2.25	2.4	36.8
14.94	2.37	2.31	2.43	39.2
16.4	2.41	2.36	2.45	41.5
18	2.44	2.41	2.48	43.9
19.76	2.49	2.46	2.53	46.4
21.69	2.56	2.52	2.6	48.9
23.81	2.64	2.58	2.69	51.4
26.14	2.72	2.64	2.8	54.1
28.7	2.8	2.7	2.9	56.8
31.5	2.85	2.74	2.96	59.6
34.58	2.88	2.78	2.99	62.4
37.97	2.87	2.78	2.95	65.3
41.68	2.8	2.73	2.86	68.2
45.75	2.68	2.63	2.73	71
50.22	2.52	2.48	2.55	73.7
55.13	2.33	2.29	2.38	76.2
60.52	2.14	2.07	2.22	78.5
66.44	1.96	1.85	2.07	80.7
72.94	1.79	1.65	1.94	82.6
80.07	1.63	1.45	1.81	84.4
87.9	1.47	1.26	1.69	86
96.49	1.31	1.08	1.55	87.5
105.9	1.15	0.93	1.37	88.8
116.3	0.99	0.83	1.16	90
127.6	0.85	0.79	0.91	91
140.1	0.74	0.62	0.86	91.8
153.8	0.69	0.43	0.95	92.6
168.9	0.7	0.35	1.04	93.3
185.4	0.76	0.39	1.13	94
203.5	0.83	0.42	1.23	94.7
223.4	0.84	0.31	1.37	95.5
245.2	0.76	0.12	1.41	96.4
269.2	0.6	0	1.24	97.1
295.5	0.4	0	0.91	97.7
324.4	0.26	0	0.77	98.1

356.1	0.21	0	0.84	98.4
390.9	0.22	0	0.96	98.6
429.2	0.25	0	1.09	98.8
471.1	0.27	0	1.22	99.1
517.2	0.28	0	1.25	99.4
567.7	0.22	0	0.98	99.6
623.3	0.12	0	0.53	99.8
684.2	0.029	0	0.13	99.97
751.1	0.0032	0	0.014	99.997
824.5	0	0	0	100
905.1	0	0	0	100
993.6	0	0	0	100
1091	0	0	0	100
1197	0	0	0	100
1314	0	0	0	100
1443	0	0	0	100
1584	0	0	0	100
1739	0	0	0	100
1909	0	0	0	100

**Site 2: Proglacial Sediments (2)**

<b>Channel Diameter</b>	<b>Diff.</b>	<b>-2 S.D.</b>	<b>+2 S.D.</b>	<b>Cum. &lt;</b>
<b>µm</b>	<b>Volume</b>	<b>Diff.</b>	<b>Diff.</b>	<b>Volume</b>
	<b>%</b>	<b>Volume</b>	<b>Volume</b>	<b>%</b>
		<b>%</b>	<b>%</b>	
0.393	0.071	0.07	0.072	0
0.431	0.13	0.13	0.13	0.071
0.474	0.19	0.18	0.19	0.2
0.52	0.27	0.26	0.27	0.39
0.571	0.33	0.33	0.33	0.65
0.627	0.38	0.38	0.39	0.98
0.688	0.43	0.43	0.44	1.37
0.755	0.48	0.47	0.49	1.8
0.829	0.52	0.51	0.53	2.28
0.91	0.55	0.54	0.55	2.8
0.999	0.57	0.56	0.58	3.35
1.097	0.58	0.58	0.59	3.92
1.204	0.6	0.59	0.61	4.5
1.321	0.61	0.6	0.62	5.1
1.451	0.62	0.61	0.63	5.71
1.592	0.63	0.62	0.64	6.32
1.748	0.65	0.64	0.65	6.95

1.919	0.67	0.66	0.68	7.6
2.107	0.7	0.69	0.71	8.27
2.313	0.73	0.72	0.74	8.96
2.539	0.78	0.77	0.79	9.69
2.787	0.83	0.82	0.85	10.5
3.059	0.9	0.88	0.92	11.3
3.358	0.98	0.96	0.99	12.2
3.687	1.06	1.04	1.08	13.2
4.047	1.16	1.14	1.18	14.2
4.443	1.27	1.24	1.29	15.4
4.877	1.38	1.35	1.4	16.7
5.354	1.5	1.47	1.52	18
5.878	1.62	1.59	1.65	19.5
6.452	1.75	1.72	1.78	21.2
7.083	1.88	1.85	1.9	22.9
7.775	2	1.98	2.03	24.8
8.536	2.13	2.1	2.16	26.8
9.37	2.25	2.22	2.28	28.9
10.29	2.36	2.32	2.4	31.2
11.29	2.46	2.42	2.51	33.5
12.4	2.55	2.49	2.6	36
13.61	2.61	2.54	2.67	38.5
14.94	2.64	2.56	2.71	41.2
16.4	2.64	2.56	2.73	43.8
18	2.63	2.53	2.72	46.4
19.76	2.6	2.51	2.7	49.1
21.69	2.58	2.48	2.67	51.7
23.81	2.55	2.46	2.64	54.2
26.14	2.53	2.44	2.62	56.8
28.7	2.5	2.42	2.59	59.3
31.5	2.47	2.39	2.54	61.8
34.58	2.41	2.34	2.47	64.3
37.97	2.32	2.26	2.38	66.7
41.68	2.19	2.14	2.24	69
45.75	2.03	1.98	2.07	71.2
50.22	1.84	1.81	1.88	73.2
55.13	1.66	1.63	1.7	75.1
60.52	1.51	1.48	1.53	76.7
66.44	1.37	1.35	1.39	78.2
72.94	1.26	1.23	1.29	79.6
80.07	1.15	1.11	1.19	80.9
87.9	1.03	0.98	1.08	82
96.49	0.9	0.85	0.94	83.1
105.9	0.77	0.74	0.8	83.9

116.3	0.68	0.65	0.7	84.7
127.6	0.63	0.59	0.68	85.4
140.1	0.64	0.57	0.72	86
153.8	0.69	0.58	0.8	86.7
168.9	0.75	0.59	0.9	87.4
185.4	0.78	0.58	0.98	88.1
203.5	0.79	0.54	1.04	88.9
223.4	0.77	0.48	1.06	89.7
245.2	0.74	0.46	1.02	90.5
269.2	0.72	0.49	0.94	91.2
295.5	0.71	0.59	0.83	91.9
324.4	0.72	0.67	0.76	92.6
356.1	0.71	0.55	0.87	93.3
390.9	0.68	0.43	0.93	94
429.2	0.63	0.36	0.91	94.7
471.1	0.59	0.33	0.85	95.4
517.2	0.56	0.34	0.79	95.9
567.7	0.6	0.39	0.8	96.5
623.3	0.69	0.48	0.91	97.1
684.2	0.85	0.57	1.13	97.8
751.1	0.76	0.49	1.03	98.6
824.5	0.46	0.29	0.64	99.4
905.1	0.12	0.071	0.16	99.9
993.6	0.013	0.0079	0.019	99.99
1091	0	0	0	100
1197	0	0	0	100
1314	0	0	0	100
1443	0	0	0	100
1584	0	0	0	100
1739	0	0	0	100
1909	0	0	0	100

**Site 3: Ice Type A (1)**

<b>Channel Diameter</b>	<b>Diff.</b>	<b>-2 S.D.</b>	<b>+2 S.D.</b>	<b>Cum. &lt;</b>
<b>µm</b>	<b>Volume</b>	<b>Diff.</b>	<b>Diff.</b>	<b>Volume</b>
	<b>%</b>	<b>Volume</b>	<b>Volume</b>	<b>%</b>
		<b>%</b>	<b>%</b>	
0.393	0.044	0.043	0.045	0
0.431	0.079	0.076	0.081	0.044
0.474	0.12	0.11	0.12	0.12
0.52	0.16	0.16	0.17	0.24
0.571	0.2	0.2	0.21	0.4
0.627	0.24	0.23	0.25	0.61

0.688	0.27	0.26	0.28	0.85
0.755	0.3	0.29	0.31	1.12
0.829	0.32	0.32	0.33	1.42
0.91	0.34	0.33	0.35	1.74
0.999	0.35	0.35	0.36	2.08
1.097	0.36	0.35	0.37	2.43
1.204	0.36	0.36	0.37	2.79
1.321	0.37	0.36	0.37	3.16
1.451	0.36	0.36	0.37	3.52
1.592	0.36	0.36	0.36	3.89
1.748	0.36	0.35	0.36	4.25
1.919	0.36	0.35	0.36	4.6
2.107	0.36	0.35	0.36	4.96
2.313	0.36	0.35	0.36	5.32
2.539	0.36	0.36	0.37	5.67
2.787	0.37	0.37	0.38	6.04
3.059	0.39	0.38	0.39	6.41
3.358	0.4	0.4	0.41	6.8
3.687	0.43	0.42	0.44	7.2
4.047	0.45	0.44	0.47	7.63
4.443	0.49	0.47	0.5	8.08
4.877	0.52	0.51	0.54	8.57
5.354	0.56	0.55	0.58	9.09
5.878	0.61	0.59	0.63	9.66
6.452	0.66	0.64	0.68	10.3
7.083	0.72	0.7	0.74	10.9
7.775	0.79	0.77	0.81	11.7
8.536	0.86	0.84	0.88	12.4
9.37	0.94	0.92	0.96	13.3
10.29	1.04	1.01	1.06	14.2
11.29	1.15	1.12	1.17	15.3
12.4	1.27	1.25	1.3	16.4
13.61	1.42	1.39	1.44	17.7
14.94	1.58	1.56	1.61	19.1
16.4	1.77	1.75	1.79	20.7
18	1.98	1.96	2.01	22.5
19.76	2.22	2.2	2.25	24.5
21.69	2.48	2.46	2.5	26.7
23.81	2.76	2.74	2.78	29.2
26.14	3.04	3.03	3.06	31.9
28.7	3.34	3.33	3.35	35
31.5	3.65	3.64	3.65	38.3
34.58	3.95	3.95	3.96	41.9
37.97	4.24	4.23	4.25	45.9

41.68	4.47	4.46	4.48	50.1
45.75	4.62	4.6	4.64	54.6
50.22	4.67	4.64	4.69	59.2
55.13	4.62	4.59	4.65	63.9
60.52	4.51	4.48	4.55	68.5
66.44	4.4	4.37	4.42	73
72.94	4.29	4.27	4.31	77.4
80.07	4.19	4.17	4.2	81.7
87.9	3.99	3.97	4.02	85.9
96.49	3.59	3.53	3.65	89.9
105.9	2.92	2.82	3.02	93.5
116.3	2.04	1.91	2.16	96.4
127.6	1.09	0.99	1.2	98.4
140.1	0.4	0.35	0.46	99.5
153.8	0.074	0.061	0.087	99.9
168.9	0.0056	0.0043	0.0069	99.99
185.4	0	0	0	100
203.5	0	0	0	100
223.4	0	0	0	100
245.2	0	0	0	100
269.2	0	0	0	100
295.5	0	0	0	100
324.4	0	0	0	100
356.1	0	0	0	100
390.9	0	0	0	100
429.2	0	0	0	100
471.1	0	0	0	100
517.2	0	0	0	100
567.7	0	0	0	100
623.3	0	0	0	100
684.2	0	0	0	100
751.1	0	0	0	100
824.5	0	0	0	100
905.1	0	0	0	100
993.6	0	0	0	100
1091	0	0	0	100
1197	0	0	0	100
1314	0	0	0	100
1443	0	0	0	100
1584	0	0	0	100
1739	0	0	0	100
1909	0	0	0	100

**Site 3: Ice Type A (2)**

<b>Channel Diameter</b>	<b>Diff.</b>	<b>-2 S.D.</b>	<b>+2 S.D.</b>	<b>Cum. &lt;</b>
<b>µm</b>	<b>Volume</b>	<b>Diff.</b>	<b>Diff.</b>	<b>Volume</b>
	<b>%</b>	<b>Volume</b>	<b>Volume</b>	<b>%</b>
		<b>%</b>	<b>%</b>	
0.393	0.044	0.044	0.044	0
0.431	0.079	0.078	0.079	0.044
0.474	0.12	0.12	0.12	0.12
0.52	0.17	0.16	0.17	0.24
0.571	0.21	0.2	0.21	0.4
0.627	0.24	0.24	0.24	0.61
0.688	0.27	0.27	0.27	0.85
0.755	0.3	0.3	0.3	1.12
0.829	0.33	0.32	0.33	1.42
0.91	0.34	0.34	0.35	1.75
0.999	0.36	0.35	0.36	2.09
1.097	0.36	0.36	0.37	2.45
1.204	0.37	0.37	0.37	2.81
1.321	0.37	0.37	0.38	3.18
1.451	0.37	0.37	0.37	3.55
1.592	0.37	0.36	0.37	3.92
1.748	0.37	0.36	0.37	4.29
1.919	0.37	0.36	0.37	4.66
2.107	0.37	0.36	0.37	5.02
2.313	0.37	0.37	0.37	5.39
2.539	0.37	0.37	0.38	5.75
2.787	0.38	0.38	0.39	6.13
3.059	0.4	0.39	0.4	6.51
3.358	0.41	0.41	0.42	6.91
3.687	0.43	0.43	0.44	7.32
4.047	0.46	0.45	0.46	7.75
4.443	0.49	0.48	0.5	8.21
4.877	0.53	0.52	0.53	8.7
5.354	0.57	0.55	0.58	9.23
5.878	0.61	0.6	0.62	9.79

6.452	0.66	0.64	0.68	10.4
7.083	0.72	0.7	0.74	11.1
7.775	0.78	0.76	0.8	11.8
8.536	0.85	0.83	0.88	12.6
9.37	0.93	0.9	0.96	13.4
10.29	1.03	1	1.06	14.3
11.29	1.14	1.1	1.17	15.4
12.4	1.26	1.23	1.29	16.5
13.61	1.41	1.37	1.44	17.8
14.94	1.57	1.54	1.61	19.2
16.4	1.76	1.73	1.8	20.7
18	1.98	1.95	2.01	22.5
19.76	2.23	2.2	2.26	24.5
21.69	2.49	2.46	2.52	26.7
23.81	2.77	2.74	2.8	29.2
26.14	3.07	3.04	3.1	32
28.7	3.4	3.37	3.42	35.1
31.5	3.74	3.71	3.76	38.4
34.58	4.07	4.06	4.09	42.2
37.97	4.37	4.37	4.37	46.3
41.68	4.59	4.58	4.6	50.6
45.75	4.69	4.67	4.71	55.2
50.22	4.7	4.68	4.72	59.9
55.13	4.66	4.65	4.66	64.6
60.52	4.64	4.61	4.67	69.3
66.44	4.69	4.62	4.75	73.9
72.94	4.75	4.67	4.83	78.6
80.07	4.69	4.65	4.73	83.3
87.9	4.31	4.27	4.36	88
96.49	3.51	3.36	3.67	92.3
105.9	2.4	2.17	2.63	95.9
116.3	1.23	1.03	1.44	98.3
127.6	0.42	0.31	0.54	99.5
140.1	0.073	0.047	0.1	99.9
153.8	0.0048	0.0021	0.0075	99.995
168.9	0	0	0	100
185.4	0	0	0	100
203.5	0	0	0	100
223.4	0	0	0	100
245.2	0	0	0	100
269.2	0	0	0	100
295.5	0	0	0	100
324.4	0	0	0	100
356.1	0	0	0	100

390.9	0	0	0	100
429.2	0	0	0	100
471.1	0	0	0	100
517.2	0	0	0	100
567.7	0	0	0	100
623.3	0	0	0	100
684.2	0	0	0	100
751.1	0	0	0	100
824.5	0	0	0	100
905.1	0	0	0	100
993.6	0	0	0	100
1091	0	0	0	100
1197	0	0	0	100
1314	0	0	0	100
1443	0	0	0	100
1584	0	0	0	100
1739	0	0	0	100
1909	0	0	0	100

**Site 3: Ice Type A (3)**

<b>Channel Diameter</b>	<b>Diff.</b>	<b>-2 S.D.</b>	<b>+2 S.D.</b>	<b>Cum. &lt;</b>
<b>µm</b>	<b>Volume</b>	<b>Diff.</b>	<b>Diff.</b>	<b>Volume</b>
	<b>%</b>	<b>Volume</b>	<b>Volume</b>	<b>%</b>
		<b>%</b>	<b>%</b>	
0.393	0.042	0.038	0.046	0
0.431	0.075	0.068	0.082	0.042
0.474	0.11	0.1	0.12	0.12
0.52	0.16	0.14	0.17	0.23
0.571	0.2	0.18	0.21	0.39
0.627	0.23	0.21	0.25	0.58
0.688	0.26	0.24	0.28	0.81
0.755	0.29	0.27	0.31	1.07
0.829	0.32	0.3	0.33	1.37
0.91	0.33	0.32	0.35	1.68
0.999	0.35	0.33	0.36	2.02
1.097	0.36	0.35	0.37	2.36
1.204	0.36	0.36	0.37	2.72
1.321	0.37	0.36	0.37	3.09
1.451	0.37	0.36	0.37	3.45
1.592	0.36	0.36	0.37	3.82
1.748	0.36	0.36	0.36	4.18
1.919	0.36	0.35	0.36	4.54

2.107	0.35	0.35	0.36	4.9
2.313	0.35	0.35	0.36	5.25
2.539	0.36	0.35	0.37	5.6
2.787	0.36	0.35	0.38	5.96
3.059	0.37	0.35	0.39	6.32
3.358	0.39	0.36	0.41	6.7
3.687	0.4	0.38	0.43	7.08
4.047	0.43	0.4	0.46	7.49
4.443	0.46	0.43	0.49	7.92
4.877	0.49	0.46	0.53	8.38
5.354	0.54	0.5	0.57	8.87
5.878	0.58	0.55	0.61	9.41
6.452	0.64	0.61	0.66	9.99
7.083	0.69	0.67	0.72	10.6
7.775	0.76	0.74	0.79	11.3
8.536	0.83	0.81	0.86	12.1
9.37	0.92	0.89	0.94	12.9
10.29	1.01	0.99	1.04	13.8
11.29	1.12	1.09	1.15	14.8
12.4	1.25	1.22	1.28	16
13.61	1.39	1.35	1.43	17.2
14.94	1.55	1.51	1.59	18.6
16.4	1.74	1.7	1.78	20.2
18	1.95	1.91	1.99	21.9
19.76	2.19	2.15	2.23	23.8
21.69	2.45	2.41	2.49	26
23.81	2.73	2.69	2.78	28.5
26.14	3.04	2.98	3.09	31.2
28.7	3.35	3.29	3.41	34.2
31.5	3.68	3.63	3.73	37.6
34.58	4	3.97	4.03	41.3
37.97	4.29	4.27	4.31	45.3
41.68	4.52	4.5	4.54	49.6
45.75	4.66	4.64	4.68	54.1
50.22	4.7	4.64	4.77	58.7
55.13	4.66	4.53	4.79	63.4
60.52	4.59	4.43	4.76	68.1
66.44	4.54	4.38	4.7	72.7
72.94	4.51	4.4	4.62	77.2
80.07	4.46	4.39	4.54	81.8
87.9	4.25	4.15	4.35	86.2
96.49	3.74	3.6	3.87	90.5
105.9	2.88	2.69	3.07	94.2
116.3	1.81	1.52	2.09	97.1

127.6	0.83	0.57	1.1	98.9
140.1	0.24	0.092	0.39	99.7
153.8	0.035	0.0011	0.07	99.96
168.9	0.0016	0	0.0047	99.998
185.4	0	0	0	100
203.5	0	0	0	100
223.4	0	0	0	100
245.2	0	0	0	100
269.2	0	0	0	100
295.5	0	0	0	100
324.4	0	0	0	100
356.1	0	0	0	100
390.9	0	0	0	100
429.2	0	0	0	100
471.1	0	0	0	100
517.2	0	0	0	100
567.7	0	0	0	100
623.3	0	0	0	100
684.2	0	0	0	100
751.1	0	0	0	100
824.5	0	0	0	100
905.1	0	0	0	100
993.6	0	0	0	100
1091	0	0	0	100
1197	0	0	0	100
1314	0	0	0	100
1443	0	0	0	100
1584	0	0	0	100
1739	0	0	0	100
1909	0	0	0	100

### Site 3: Proglacial Sediments

<b>Channel Diameter</b>	<b>Cum. &lt;</b>	<b>Diff.</b>	<b>-2 S.D.</b>	<b>+2 S.D.</b>
<b>µm</b>	<b>Volume</b>	<b>Volume</b>	<b>Diff.</b>	<b>Diff.</b>
	<b>%</b>	<b>%</b>	<b>Volume</b>	<b>Volume</b>
			<b>%</b>	<b>%</b>
0.393	0	0.036	0.032	0.039
0.431	0.036	0.063	0.057	0.07
0.474	0.099	0.093	0.084	0.1
0.52	0.19	0.13	0.12	0.14
0.571	0.33	0.16	0.15	0.18
0.627	0.49	0.19	0.18	0.21

0.688	0.68	0.22	0.2	0.23
0.755	0.9	0.24	0.22	0.26
0.829	1.14	0.26	0.24	0.28
0.91	1.4	0.27	0.26	0.29
0.999	1.67	0.28	0.27	0.3
1.097	1.96	0.29	0.28	0.3
1.204	2.25	0.29	0.28	0.3
1.321	2.54	0.3	0.29	0.3
1.451	2.84	0.3	0.29	0.3
1.592	3.13	0.29	0.29	0.3
1.748	3.42	0.29	0.28	0.3
1.919	3.72	0.3	0.28	0.31
2.107	4.01	0.3	0.28	0.31
2.313	4.31	0.3	0.28	0.32
2.539	4.61	0.31	0.28	0.33
2.787	4.92	0.32	0.29	0.35
3.059	5.24	0.33	0.3	0.36
3.358	5.57	0.35	0.31	0.38
3.687	5.92	0.37	0.32	0.41
4.047	6.28	0.39	0.34	0.43
4.443	6.67	0.41	0.37	0.46
4.877	7.08	0.44	0.39	0.49
5.354	7.53	0.48	0.42	0.53
5.878	8	0.51	0.45	0.57
6.452	8.51	0.55	0.49	0.61
7.083	9.06	0.59	0.53	0.65
7.775	9.65	0.63	0.57	0.7
8.536	10.3	0.68	0.62	0.74
9.37	11	0.73	0.67	0.8
10.29	11.7	0.79	0.72	0.86
11.29	12.5	0.85	0.78	0.92
12.4	13.3	0.92	0.84	1
13.61	14.3	0.99	0.91	1.07
14.94	15.3	1.06	0.98	1.15
16.4	16.3	1.14	1.06	1.23
18	17.5	1.23	1.15	1.32
19.76	18.7	1.33	1.25	1.41
21.69	20	1.45	1.37	1.52
23.81	21.5	1.57	1.51	1.64
26.14	23	1.72	1.66	1.77
28.7	24.8	1.88	1.84	1.93
31.5	26.6	2.07	2.03	2.1
34.58	28.7	2.28	2.26	2.3
37.97	31	2.53	2.51	2.54

41.68	33.5	2.8	2.79	2.82
45.75	36.3	3.11	3.1	3.13
50.22	39.4	3.46	3.43	3.48
55.13	42.9	3.82	3.79	3.86
60.52	46.7	4.2	4.17	4.24
66.44	50.9	4.58	4.55	4.6
72.94	55.5	4.9	4.86	4.94
80.07	60.4	5.14	5.05	5.23
87.9	65.5	5.24	5.1	5.38
96.49	70.8	5.19	5.01	5.37
105.9	76	4.98	4.78	5.17
116.3	81	4.61	4.42	4.8
127.6	85.6	4.1	3.93	4.28
140.1	89.7	3.48	3.3	3.65
153.8	93.2	2.75	2.57	2.93
168.9	95.9	1.98	1.78	2.18
185.4	97.9	1.25	1.03	1.46
203.5	99.1	0.62	0.45	0.78
223.4	99.7	0.21	0.13	0.3
245.2	99.96	0.038	0.018	0.059
269.2	99.997	0.0028	0.00063	0.005
295.5	100	0	0	0
324.4	100	0	0	0
356.1	100	0	0	0
390.9	100	0	0	0
429.2	100	0	0	0
471.1	100	0	0	0
517.2	100	0	0	0
567.7	100	0	0	0
623.3	100	0	0	0
684.2	100	0	0	0
751.1	100	0	0	0
824.5	100	0	0	0
905.1	100	0	0	0
993.6	100	0	0	0
1091	100	0	0	0
1197	100	0	0	0
1314	100	0	0	0
1443	100	0	0	0
1584	100	0	0	0
1739	100	0	0	0
1909	100	0	0	0

**Site 3: Minor Outwash Fan**

<b>Channel Diameter</b>	<b>Diff.</b>	<b>-2 S.D.</b>	<b>+2 S.D.</b>	<b>Cum. &lt;</b>
<b>µm</b>	<b>Volume</b>	<b>Diff.</b>	<b>Diff.</b>	<b>Volume</b>
	<b>%</b>	<b>Volume</b>	<b>Volume</b>	<b>%</b>
		<b>%</b>	<b>%</b>	
0.393	0.031	0.029	0.032	0
0.431	0.055	0.053	0.057	0.031
0.474	0.081	0.078	0.084	0.086
0.52	0.11	0.11	0.12	0.17
0.571	0.14	0.14	0.15	0.28
0.627	0.17	0.16	0.17	0.42
0.688	0.19	0.18	0.19	0.59
0.755	0.21	0.2	0.21	0.78
0.829	0.22	0.22	0.23	0.99
0.91	0.23	0.23	0.24	1.21
0.999	0.24	0.24	0.25	1.44
1.097	0.25	0.24	0.26	1.69
1.204	0.25	0.24	0.26	1.93
1.321	0.25	0.24	0.26	2.19
1.451	0.25	0.24	0.26	2.44
1.592	0.25	0.24	0.26	2.69
1.748	0.25	0.24	0.26	2.95
1.919	0.26	0.25	0.26	3.2
2.107	0.26	0.25	0.27	3.46
2.313	0.27	0.26	0.27	3.72
2.539	0.27	0.27	0.28	3.98
2.787	0.28	0.28	0.29	4.26
3.059	0.3	0.29	0.3	4.54
3.358	0.31	0.3	0.32	4.84
3.687	0.33	0.32	0.34	5.15
4.047	0.35	0.34	0.36	5.48
4.443	0.37	0.36	0.39	5.83
4.877	0.4	0.38	0.41	6.2
5.354	0.43	0.41	0.45	6.6
5.878	0.46	0.43	0.48	7.03
6.452	0.49	0.46	0.52	7.48
7.083	0.52	0.48	0.56	7.97
7.775	0.56	0.51	0.61	8.49
8.536	0.6	0.54	0.65	9.05
9.37	0.64	0.57	0.7	9.65
10.29	0.68	0.61	0.75	10.3
11.29	0.73	0.65	0.81	11
12.4	0.78	0.7	0.87	11.7
13.61	0.84	0.75	0.93	12.5
14.94	0.9	0.81	0.99	13.3

16.4	0.96	0.87	1.06	14.2
18	1.03	0.94	1.13	15.2
19.76	1.12	1.03	1.21	16.2
21.69	1.22	1.13	1.3	17.3
23.81	1.32	1.25	1.4	18.6
26.14	1.44	1.37	1.51	19.9
28.7	1.57	1.51	1.63	21.3
31.5	1.71	1.65	1.77	22.9
34.58	1.86	1.8	1.93	24.6
37.97	2.04	1.97	2.11	26.5
41.68	2.25	2.18	2.32	28.5
45.75	2.49	2.41	2.56	30.7
50.22	2.75	2.68	2.82	33.2
55.13	3.04	2.98	3.1	36
60.52	3.36	3.3	3.41	39
66.44	3.69	3.64	3.74	42.4
72.94	4.03	3.98	4.09	46.1
80.07	4.34	4.28	4.41	50.1
87.9	4.6	4.51	4.69	54.4
96.49	4.77	4.66	4.88	59.1
105.9	4.82	4.69	4.94	63.8
116.3	4.72	4.6	4.84	68.6
127.6	4.48	4.37	4.59	73.4
140.1	4.08	4	4.17	77.8
153.8	3.55	3.48	3.61	81.9
168.9	2.89	2.85	2.93	85.5
185.4	2.17	2.15	2.18	88.4
203.5	1.46	1.43	1.49	90.5
223.4	0.86	0.79	0.93	92
245.2	0.46	0.36	0.56	92.8
269.2	0.27	0.17	0.38	93.3
295.5	0.24	0.14	0.33	93.6
324.4	0.3	0.23	0.37	93.8
356.1	0.41	0.36	0.46	94.1
390.9	0.49	0.4	0.58	94.5
429.2	0.51	0.36	0.66	95
471.1	0.47	0.29	0.65	95.5
517.2	0.4	0.22	0.58	96
567.7	0.34	0.18	0.5	96.4
623.3	0.3	0.16	0.44	96.7
684.2	0.3	0.15	0.44	97
751.1	0.31	0.12	0.5	97.3
824.5	0.36	0.1	0.62	97.6
905.1	0.44	0.11	0.77	98

993.6	0.57	0.2	0.94	98.4
1091	0.54	0.25	0.83	99
1197	0.34	0.19	0.49	99.6
1314	0.09	0.056	0.12	99.9
1443	0.011	0.0074	0.014	99.99
1584	0	0	0	100
1739	0	0	0	100
1909	0	0	0	100

**Site 4: Ice Type B (1)**

<b>Channel Diameter</b>	<b>Diff.</b>	<b>-2 S.D.</b>	<b>+2 S.D.</b>	<b>Cum. &lt;</b>
<b>µm</b>	<b>Volume</b>	<b>Diff.</b>	<b>Diff.</b>	<b>Volume</b>
	<b>%</b>	<b>Volume</b>	<b>Volume</b>	<b>%</b>
		<b>%</b>	<b>%</b>	
0.393	0.071	0.068	0.073	0
0.431	0.13	0.12	0.13	0.071
0.474	0.19	0.18	0.19	0.2
0.52	0.27	0.26	0.27	0.38
0.571	0.33	0.32	0.34	0.65
0.627	0.39	0.37	0.4	0.98
0.688	0.44	0.43	0.46	1.37
0.755	0.49	0.47	0.51	1.81
0.829	0.54	0.52	0.55	2.3
0.91	0.57	0.55	0.59	2.84
0.999	0.6	0.57	0.62	3.41
1.097	0.62	0.59	0.64	4
1.204	0.63	0.61	0.66	4.62
1.321	0.64	0.62	0.67	5.25
1.451	0.65	0.62	0.67	5.89
1.592	0.65	0.63	0.68	6.54
1.748	0.66	0.64	0.68	7.19
1.919	0.67	0.64	0.69	7.85
2.107	0.68	0.65	0.7	8.52
2.313	0.69	0.66	0.71	9.2
2.539	0.71	0.68	0.73	9.88
2.787	0.73	0.7	0.76	10.6
3.059	0.76	0.73	0.79	11.3
3.358	0.8	0.77	0.83	12.1
3.687	0.84	0.81	0.87	12.9
4.047	0.89	0.86	0.92	13.7
4.443	0.95	0.92	0.99	14.6
4.877	1.02	0.98	1.06	15.6

5.354	1.09	1.06	1.13	16.6
5.878	1.17	1.13	1.21	17.7
6.452	1.26	1.22	1.3	18.9
7.083	1.35	1.31	1.4	20.1
7.775	1.45	1.4	1.5	21.5
8.536	1.56	1.5	1.61	22.9
9.37	1.67	1.61	1.72	24.5
10.29	1.78	1.72	1.84	26.1
11.29	1.9	1.83	1.96	27.9
12.4	2.02	1.95	2.09	29.8
13.61	2.13	2.06	2.2	31.8
14.94	2.24	2.16	2.32	34
16.4	2.34	2.26	2.42	36.2
18	2.44	2.36	2.52	38.6
19.76	2.53	2.44	2.62	41
21.69	2.61	2.52	2.7	43.5
23.81	2.68	2.59	2.77	46.1
26.14	2.73	2.64	2.83	48.8
28.7	2.77	2.67	2.87	51.6
31.5	2.81	2.7	2.91	54.3
34.58	2.83	2.73	2.94	57.1
37.97	2.85	2.75	2.95	60
41.68	2.85	2.76	2.95	62.8
45.75	2.83	2.74	2.91	65.7
50.22	2.76	2.68	2.83	68.5
55.13	2.64	2.56	2.71	71.2
60.52	2.47	2.39	2.55	73.9
66.44	2.27	2.19	2.36	76.4
72.94	2.05	1.95	2.16	78.6
80.07	1.82	1.7	1.95	80.7
87.9	1.6	1.47	1.74	82.5
96.49	1.4	1.27	1.54	84.1
105.9	1.23	1.11	1.34	85.5
116.3	1.06	0.98	1.14	86.7
127.6	0.87	0.81	0.93	87.8
140.1	0.65	0.59	0.71	88.7
153.8	0.41	0.36	0.46	89.3
168.9	0.2	0.17	0.23	89.7
185.4	0.066	0.055	0.076	89.9
203.5	0.011	0.0084	0.013	90
223.4	0.00072	0.0004	0.001	90
245.2	0.00094	0	0.0026	90
269.2	0.015	0	0.037	90
295.5	0.094	0	0.2	90

324.4	0.3	0.097	0.5	90.1
356.1	0.62	0.36	0.88	90.4
390.9	0.94	0.73	1.16	91
429.2	1.16	1.01	1.32	92
471.1	1.25	1.11	1.39	93.1
517.2	1.23	1.01	1.44	94.4
567.7	1.17	0.84	1.5	95.6
623.3	1.14	0.72	1.57	96.8
684.2	1.01	0.35	1.68	97.9
751.1	0.69	0	1.43	99
824.5	0.29	0	0.88	99.6
905.1	0.061	0	0.23	99.9
993.6	0.0058	0	0.026	99.99
1091	0	0	0	100
1197	0	0	0	100
1314	0	0	0	100
1443	0	0	0	100
1584	0	0	0	100
1739	0	0	0	100
1909	0	0	0	100

**Site 4: Ice Type B (2)**

<b>Channel Diameter</b>	<b>Diff.</b>	<b>-2 S.D.</b>	<b>+2 S.D.</b>	<b>Cum. &lt;</b>
<b>µm</b>	<b>Volume</b>	<b>Diff.</b>	<b>Diff.</b>	<b>Volume</b>
	<b>%</b>	<b>Volume</b>	<b>Volume</b>	<b>%</b>
		<b>%</b>	<b>%</b>	
0.393	0.038	0.036	0.041	0
0.431	0.068	0.064	0.073	0.038
0.474	0.1	0.094	0.11	0.11
0.52	0.14	0.14	0.15	0.21
0.571	0.18	0.17	0.19	0.35
0.627	0.21	0.2	0.22	0.53
0.688	0.24	0.23	0.25	0.74
0.755	0.26	0.26	0.27	0.98
0.829	0.29	0.28	0.29	1.24
0.91	0.3	0.3	0.31	1.53
0.999	0.32	0.31	0.32	1.83
1.097	0.33	0.32	0.33	2.15
1.204	0.33	0.33	0.34	2.47
1.321	0.34	0.33	0.34	2.81
1.451	0.34	0.33	0.35	3.15
1.592	0.34	0.33	0.35	3.49

1.748	0.34	0.34	0.35	3.83
1.919	0.35	0.34	0.35	4.17
2.107	0.35	0.35	0.35	4.52
2.313	0.36	0.35	0.36	4.87
2.539	0.36	0.36	0.37	5.22
2.787	0.38	0.36	0.39	5.59
3.059	0.39	0.37	0.41	5.96
3.358	0.41	0.39	0.43	6.35
3.687	0.43	0.41	0.45	6.76
4.047	0.45	0.43	0.48	7.19
4.443	0.48	0.46	0.51	7.64
4.877	0.52	0.49	0.54	8.13
5.354	0.55	0.53	0.58	8.65
5.878	0.59	0.57	0.61	9.2
6.452	0.64	0.62	0.66	9.79
7.083	0.68	0.67	0.7	10.4
7.775	0.73	0.72	0.75	11.1
8.536	0.79	0.78	0.79	11.8
9.37	0.84	0.84	0.85	12.6
10.29	0.9	0.9	0.91	13.5
11.29	0.97	0.96	0.98	14.4
12.4	1.04	1.02	1.05	15.4
13.61	1.11	1.09	1.12	16.4
14.94	1.18	1.16	1.19	17.5
16.4	1.25	1.23	1.27	18.7
18	1.32	1.3	1.34	19.9
19.76	1.39	1.37	1.42	21.2
21.69	1.47	1.44	1.5	22.6
23.81	1.55	1.51	1.58	24.1
26.14	1.63	1.59	1.67	25.6
28.7	1.72	1.67	1.77	27.3
31.5	1.81	1.76	1.87	29
34.58	1.92	1.86	1.99	30.8
37.97	2.04	1.97	2.11	32.7
41.68	2.16	2.09	2.24	34.8
45.75	2.28	2.2	2.37	36.9
50.22	2.39	2.3	2.48	39.2
55.13	2.49	2.4	2.58	41.6
60.52	2.58	2.5	2.67	44.1
66.44	2.67	2.59	2.75	46.7
72.94	2.74	2.67	2.81	49.3
80.07	2.79	2.73	2.85	52.1
87.9	2.82	2.76	2.87	54.9
96.49	2.81	2.77	2.85	57.7

105.9	2.77	2.73	2.82	60.5
116.3	2.73	2.67	2.79	63.3
127.6	2.67	2.59	2.75	66
140.1	2.61	2.52	2.7	68.7
153.8	2.52	2.44	2.6	71.3
168.9	2.39	2.31	2.46	73.8
185.4	2.2	2.12	2.28	76.2
203.5	1.98	1.88	2.08	78.4
223.4	1.76	1.65	1.87	80.4
245.2	1.58	1.5	1.67	82.1
269.2	1.47	1.43	1.51	83.7
295.5	1.41	1.38	1.44	85.2
324.4	1.39	1.32	1.45	86.6
356.1	1.36	1.28	1.45	88
390.9	1.31	1.23	1.39	89.3
429.2	1.23	1.14	1.32	90.6
471.1	1.13	1.02	1.25	91.9
517.2	1.03	0.92	1.14	93
567.7	0.94	0.86	1.02	94
623.3	0.86	0.74	0.99	95
684.2	0.79	0.55	1.03	95.8
751.1	0.72	0.38	1.06	96.6
824.5	0.66	0.29	1.04	97.4
905.1	0.62	0.28	0.96	98
993.6	0.59	0.35	0.84	98.6
1091	0.45	0.33	0.57	99.2
1197	0.25	0.2	0.29	99.7
1314	0.06	0.05	0.07	99.9
1443	0.0066	0.0053	0.0079	99.99
1584	0	0	0	100
1739	0	0	0	100

**Site 4: Ice Type B (3)**

<b>Channel Diameter</b>	<b>Diff.</b>	<b>-2 S.D.</b>	<b>+2 S.D.</b>	<b>Cum. &lt;</b>
<b>µm</b>	<b>Volume</b>	<b>Diff.</b>	<b>Diff.</b>	<b>Volume</b>
	<b>%</b>	<b>Volume</b>	<b>Volume</b>	<b>%</b>
		<b>%</b>	<b>%</b>	
0.393	0.043	0.043	0.043	0
0.431	0.077	0.076	0.077	0.043
0.474	0.11	0.11	0.11	0.12
0.52	0.16	0.16	0.16	0.23
0.571	0.2	0.2	0.2	0.39

0.627	0.23	0.23	0.23	0.59
0.688	0.26	0.26	0.26	0.83
0.755	0.29	0.29	0.29	1.09
0.829	0.32	0.32	0.32	1.38
0.91	0.34	0.33	0.34	1.7
0.999	0.35	0.35	0.35	2.04
1.097	0.36	0.36	0.36	2.39
1.204	0.37	0.36	0.37	2.74
1.321	0.37	0.37	0.37	3.11
1.451	0.37	0.37	0.38	3.48
1.592	0.38	0.37	0.38	3.86
1.748	0.38	0.38	0.38	4.23
1.919	0.38	0.38	0.39	4.61
2.107	0.39	0.39	0.39	4.99
2.313	0.4	0.39	0.4	5.38
2.539	0.41	0.41	0.41	5.78
2.787	0.42	0.42	0.43	6.19
3.059	0.44	0.44	0.45	6.62
3.358	0.47	0.46	0.47	7.06
3.687	0.49	0.49	0.49	7.53
4.047	0.52	0.52	0.52	8.02
4.443	0.56	0.55	0.56	8.54
4.877	0.59	0.59	0.59	9.09
5.354	0.63	0.63	0.64	9.69
5.878	0.68	0.67	0.68	10.3
6.452	0.72	0.72	0.73	11
7.083	0.77	0.77	0.78	11.7
7.775	0.83	0.82	0.83	12.5
8.536	0.88	0.88	0.89	13.3
9.37	0.94	0.93	0.95	14.2
10.29	1	1	1.01	15.1
11.29	1.07	1.06	1.08	16.1
12.4	1.14	1.13	1.15	17.2
13.61	1.2	1.19	1.21	18.4
14.94	1.27	1.25	1.28	19.6
16.4	1.33	1.31	1.35	20.8
18	1.39	1.37	1.41	22.1
19.76	1.45	1.42	1.48	23.5
21.69	1.51	1.47	1.54	25
23.81	1.56	1.52	1.6	26.5
26.14	1.61	1.56	1.66	28.1
28.7	1.66	1.61	1.72	29.7
31.5	1.72	1.66	1.79	31.3
34.58	1.78	1.71	1.86	33.1

37.97	1.85	1.78	1.93	34.8
41.68	1.92	1.84	1.99	36.7
45.75	1.97	1.89	2.05	38.6
50.22	2.02	1.94	2.11	40.6
55.13	2.07	1.98	2.17	42.6
60.52	2.13	2.02	2.23	44.7
66.44	2.19	2.07	2.31	46.8
72.94	2.26	2.14	2.38	49
80.07	2.33	2.21	2.45	51.2
87.9	2.39	2.28	2.5	53.6
96.49	2.43	2.34	2.52	56
105.9	2.47	2.4	2.54	58.4
116.3	2.51	2.45	2.56	60.9
127.6	2.55	2.51	2.59	63.4
140.1	2.59	2.55	2.63	65.9
153.8	2.59	2.53	2.65	68.5
168.9	2.51	2.41	2.61	71.1
185.4	2.35	2.2	2.49	73.6
203.5	2.11	1.92	2.3	76
223.4	1.87	1.65	2.08	78.1
245.2	1.67	1.44	1.9	79.9
269.2	1.55	1.31	1.78	81.6
295.5	1.49	1.28	1.7	83.2
324.4	1.48	1.33	1.63	84.6
356.1	1.46	1.39	1.53	86.1
390.9	1.42	1.32	1.52	87.6
429.2	1.35	1.15	1.54	89
471.1	1.27	1.01	1.52	90.4
517.2	1.19	0.93	1.45	91.6
567.7	1.13	0.88	1.39	92.8
623.3	1.07	0.78	1.37	93.9
684.2	1	0.64	1.37	95
751.1	0.92	0.51	1.32	96
824.5	0.82	0.45	1.19	96.9
905.1	0.73	0.43	1.04	97.8
993.6	0.67	0.34	1	98.5
1091	0.5	0.17	0.82	99.2
1197	0.27	0.05	0.49	99.7
1314	0.066	0.0058	0.13	99.9
1443	0.0072	0	0.014	99.99
1584	0	0	0	100
1739	0	0	0	100
1909	0	0	0	100

**Site 4: Ice Type A (1)**

<b>Channel Diameter</b>	<b>Diff.</b>	<b>-2 S.D.</b>	<b>+2 S.D.</b>	<b>Cum. &lt;</b>
<b>µm</b>	<b>Volume</b>	<b>Diff.</b>	<b>Diff.</b>	<b>Volume</b>
	<b>%</b>	<b>Volume</b>	<b>Volume</b>	<b>%</b>
		<b>%</b>	<b>%</b>	
0.393	0.065	0.064	0.066	0
0.431	0.12	0.11	0.12	0.065
0.474	0.17	0.17	0.17	0.18
0.52	0.25	0.24	0.25	0.35
0.571	0.31	0.3	0.31	0.6
0.627	0.36	0.35	0.36	0.91
0.688	0.41	0.4	0.41	1.26
0.755	0.45	0.45	0.46	1.67
0.829	0.49	0.48	0.5	2.12
0.91	0.52	0.51	0.53	2.61
0.999	0.54	0.53	0.55	3.13
1.097	0.55	0.55	0.56	3.67
1.204	0.57	0.56	0.57	4.23
1.321	0.57	0.56	0.58	4.79
1.451	0.57	0.56	0.58	5.36
1.592	0.57	0.56	0.58	5.93
1.748	0.57	0.56	0.58	6.5
1.919	0.57	0.56	0.58	7.07
2.107	0.57	0.56	0.58	7.63
2.313	0.58	0.57	0.59	8.21
2.539	0.59	0.58	0.6	8.79
2.787	0.62	0.61	0.62	9.38
3.059	0.65	0.64	0.65	9.99
3.358	0.69	0.68	0.7	10.6
3.687	0.74	0.73	0.75	11.3
4.047	0.8	0.79	0.81	12.1
4.443	0.87	0.86	0.89	12.9
4.877	0.96	0.95	0.97	13.7
5.354	1.06	1.05	1.07	14.7
5.878	1.17	1.15	1.18	15.8
6.452	1.29	1.27	1.31	16.9

7.083	1.42	1.4	1.44	18.2
7.775	1.56	1.54	1.58	19.6
8.536	1.71	1.69	1.73	21.2
9.37	1.87	1.85	1.9	22.9
10.29	2.04	2.02	2.07	24.8
11.29	2.22	2.19	2.24	26.8
12.4	2.39	2.37	2.42	29
13.61	2.57	2.54	2.59	31.4
14.94	2.73	2.71	2.75	34
16.4	2.88	2.86	2.9	36.7
18	3.01	3	3.03	39.6
19.76	3.13	3.12	3.14	42.6
21.69	3.22	3.21	3.23	45.8
23.81	3.29	3.29	3.3	49
26.14	3.35	3.34	3.36	52.3
28.7	3.4	3.38	3.41	55.6
31.5	3.43	3.4	3.46	59
34.58	3.45	3.41	3.49	62.5
37.97	3.45	3.4	3.51	65.9
41.68	3.42	3.36	3.47	69.4
45.75	3.34	3.28	3.4	72.8
50.22	3.22	3.16	3.28	76.1
55.13	3.09	3.04	3.14	79.3
60.52	2.98	2.93	3.03	82.4
66.44	2.89	2.85	2.93	85.4
72.94	2.8	2.77	2.83	88.3
80.07	2.64	2.61	2.66	91.1
87.9	2.32	2.27	2.37	93.7
96.49	1.83	1.74	1.92	96.1
105.9	1.22	1.11	1.34	97.9
116.3	0.63	0.53	0.72	99.1
127.6	0.22	0.17	0.27	99.7
140.1	0.038	0.027	0.05	99.96
153.8	0.0027	0.0016	0.0038	99.997
168.9	0	0	0	100
185.4	0	0	0	100
203.5	0	0	0	100
223.4	0	0	0	100
245.2	0	0	0	100
269.2	0	0	0	100
295.5	0	0	0	100
324.4	0	0	0	100
356.1	0	0	0	100
390.9	0	0	0	100

429.2	0	0	0	100
471.1	0	0	0	100
517.2	0	0	0	100
567.7	0	0	0	100
623.3	0	0	0	100
684.2	0	0	0	100
751.1	0	0	0	100
824.5	0	0	0	100
905.1	0	0	0	100
993.6	0	0	0	100
1091	0	0	0	100
1197	0	0	0	100
1314	0	0	0	100
1443	0	0	0	100
1584	0	0	0	100
1739	0	0	0	100
1909	0	0	0	100

**Site 4: Ice Type A (2)**

<b>Channel Diameter</b>	<b>Diff.</b>	<b>-2 S.D.</b>	<b>+2 S.D.</b>	<b>Cum. &lt;</b>
<b>µm</b>	<b>Volume</b>	<b>Diff.</b>	<b>Diff.</b>	<b>Volume</b>
	<b>%</b>	<b>Volume</b>	<b>Volume</b>	<b>%</b>
		<b>%</b>	<b>%</b>	
0.393	0.078	0.074	0.081	0
0.431	0.14	0.13	0.14	0.078
0.474	0.2	0.19	0.21	0.22
0.52	0.29	0.28	0.3	0.42
0.571	0.36	0.34	0.37	0.71
0.627	0.42	0.4	0.44	1.07
0.688	0.48	0.46	0.49	1.49
0.755	0.53	0.51	0.55	1.96
0.829	0.57	0.56	0.59	2.49
0.91	0.61	0.59	0.62	3.06
0.999	0.63	0.61	0.65	3.67
1.097	0.65	0.63	0.67	4.3
1.204	0.66	0.64	0.68	4.95
1.321	0.67	0.65	0.7	5.61
1.451	0.68	0.66	0.7	6.29
1.592	0.69	0.67	0.71	6.97
1.748	0.69	0.67	0.71	7.65
1.919	0.71	0.69	0.72	8.35
2.107	0.72	0.7	0.74	9.05

2.313	0.74	0.72	0.76	9.77
2.539	0.76	0.74	0.79	10.5
2.787	0.79	0.77	0.82	11.3
3.059	0.83	0.8	0.86	12.1
3.358	0.88	0.85	0.91	12.9
3.687	0.93	0.9	0.97	13.8
4.047	1	0.96	1.04	14.7
4.443	1.07	1.03	1.11	15.7
4.877	1.15	1.11	1.2	16.8
5.354	1.25	1.2	1.29	17.9
5.878	1.35	1.3	1.39	19.2
6.452	1.45	1.41	1.5	20.5
7.083	1.57	1.53	1.62	22
7.775	1.7	1.65	1.74	23.6
8.536	1.83	1.78	1.88	25.3
9.37	1.97	1.92	2.03	27.1
10.29	2.12	2.06	2.18	29.1
11.29	2.28	2.22	2.34	31.2
12.4	2.44	2.37	2.5	33.5
13.61	2.59	2.52	2.66	35.9
14.94	2.74	2.66	2.81	38.5
16.4	2.86	2.78	2.94	41.2
18	2.96	2.87	3.05	44.1
19.76	3.06	2.96	3.17	47
21.69	3.17	3.05	3.29	50.1
23.81	3.29	3.16	3.42	53.3
26.14	3.4	3.28	3.52	56.6
28.7	3.48	3.4	3.57	60
31.5	3.5	3.47	3.53	63.5
34.58	3.44	3.41	3.48	67
37.97	3.34	3.26	3.42	70.4
41.68	3.26	3.18	3.35	73.7
45.75	3.26	3.16	3.36	77
50.22	3.37	3.21	3.54	80.3
55.13	3.53	3.33	3.73	83.6
60.52	3.58	3.48	3.69	87.2
66.44	3.35	3.24	3.47	90.8
72.94	2.76	2.37	3.14	94.1
80.07	1.85	1.21	2.5	96.9
87.9	0.93	0.35	1.51	98.7
96.49	0.3	0	0.63	99.6
105.9	0.051	0	0.12	99.9
116.3	0.0033	0	0.0095	99.997
127.6	0	0	0	100

140.1	0	0	0	100
153.8	0	0	0	100
168.9	0	0	0	100
185.4	0	0	0	100
203.5	0	0	0	100
223.4	0	0	0	100
245.2	0	0	0	100
269.2	0	0	0	100
295.5	0	0	0	100
324.4	0	0	0	100
356.1	0	0	0	100
390.9	0	0	0	100
429.2	0	0	0	100
471.1	0	0	0	100
517.2	0	0	0	100
567.7	0	0	0	100
623.3	0	0	0	100
684.2	0	0	0	100
751.1	0	0	0	100
824.5	0	0	0	100
905.1	0	0	0	100
993.6	0	0	0	100
1091	0	0	0	100
1197	0	0	0	100
1314	0	0	0	100
1443	0	0	0	100
1584	0	0	0	100
1739	0	0	0	100
1909	0	0	0	100

**Site 4: Ice Type A (3)**

<b>Channel Diameter</b>	<b>Diff.</b>	<b>-2 S.D.</b>	<b>+2 S.D.</b>	<b>Cum. &lt;</b>
<b>µm</b>	<b>Volume</b>	<b>Diff.</b>	<b>Diff.</b>	<b>Volume</b>
	<b>%</b>	<b>Volume</b>	<b>Volume</b>	<b>%</b>
		<b>%</b>	<b>%</b>	
0.393	0.08	0.076	0.084	0
0.431	0.14	0.13	0.15	0.08
0.474	0.21	0.2	0.22	0.22
0.52	0.3	0.29	0.31	0.43
0.571	0.37	0.36	0.38	0.73
0.627	0.43	0.42	0.45	1.1
0.688	0.49	0.48	0.5	1.53

0.755	0.55	0.54	0.55	2.03
0.829	0.59	0.58	0.6	2.57
0.91	0.63	0.61	0.64	3.16
0.999	0.65	0.64	0.67	3.79
1.097	0.67	0.65	0.69	4.44
1.204	0.69	0.66	0.71	5.11
1.321	0.7	0.67	0.73	5.8
1.451	0.71	0.68	0.73	6.5
1.592	0.71	0.69	0.74	7.2
1.748	0.72	0.7	0.74	7.92
1.919	0.74	0.72	0.75	8.64
2.107	0.75	0.74	0.77	9.38
2.313	0.78	0.76	0.79	10.1
2.539	0.8	0.78	0.83	10.9
2.787	0.84	0.8	0.87	11.7
3.059	0.88	0.84	0.92	12.5
3.358	0.93	0.88	0.98	13.4
3.687	0.99	0.94	1.04	14.4
4.047	1.05	1	1.11	15.3
4.443	1.13	1.08	1.18	16.4
4.877	1.22	1.17	1.26	17.5
5.354	1.31	1.27	1.36	18.7
5.878	1.42	1.38	1.45	20.1
6.452	1.53	1.5	1.56	21.5
7.083	1.65	1.62	1.68	23
7.775	1.78	1.74	1.82	24.7
8.536	1.92	1.87	1.96	26.4
9.37	2.06	2.01	2.12	28.4
10.29	2.22	2.16	2.27	30.4
11.29	2.38	2.32	2.44	32.6
12.4	2.54	2.48	2.6	35
13.61	2.71	2.64	2.77	37.6
14.94	2.85	2.78	2.92	40.3
16.4	2.98	2.89	3.07	43.1
18	3.09	2.98	3.21	46.1
19.76	3.22	3.08	3.35	49.2
21.69	3.35	3.2	3.5	52.4
23.81	3.48	3.34	3.62	55.8
26.14	3.57	3.47	3.67	59.2
28.7	3.58	3.54	3.62	62.8
31.5	3.51	3.49	3.54	66.4
34.58	3.39	3.35	3.44	69.9
37.97	3.3	3.27	3.34	73.3
41.68	3.3	3.18	3.43	76.6

45.75	3.42	3.17	3.67	79.9
50.22	3.59	3.27	3.91	83.3
55.13	3.65	3.41	3.88	86.9
60.52	3.42	3.33	3.51	90.6
66.44	2.81	2.46	3.16	94
72.94	1.89	1.24	2.55	96.8
80.07	0.95	0.34	1.56	98.7
87.9	0.31	0	0.66	99.6
96.49	0.053	0	0.13	99.9
105.9	0.0036	0	0.01	99.996
116.3	0	0	0	100
127.6	0	0	0	100
140.1	0	0	0	100
153.8	0	0	0	100
168.9	0	0	0	100
185.4	0	0	0	100
203.5	0	0	0	100
223.4	0	0	0	100
245.2	0	0	0	100
269.2	0	0	0	100
295.5	0	0	0	100
324.4	0	0	0	100
356.1	0	0	0	100
390.9	0	0	0	100
429.2	0	0	0	100
471.1	0	0	0	100
517.2	0	0	0	100
567.7	0	0	0	100
623.3	0	0	0	100
684.2	0	0	0	100
751.1	0	0	0	100
824.5	0	0	0	100
905.1	0	0	0	100
993.6	0	0	0	100
1091	0	0	0	100
1197	0	0	0	100
1314	0	0	0	100
1443	0	0	0	100
1584	0	0	0	100
1739	0	0	0	100
1909	0	0	0	100

**Site 4: Minor Outwash Fan**

<b>Channel Diameter</b>	<b>Diff.</b>	<b>-2 S.D.</b>	<b>+2 S.D.</b>	<b>Cum. &lt;</b>
<b>µm</b>	<b>Volume</b>	<b>Diff.</b>	<b>Diff.</b>	<b>Volume</b>
	<b>%</b>	<b>Volume</b>	<b>Volume</b>	<b>%</b>
		<b>%</b>	<b>%</b>	
0.393	0.048	0.041	0.054	0
0.431	0.085	0.074	0.096	0.048
0.474	0.12	0.11	0.14	0.13
0.52	0.18	0.16	0.2	0.26
0.571	0.22	0.19	0.24	0.43
0.627	0.25	0.23	0.28	0.65
0.688	0.29	0.26	0.31	0.91
0.755	0.32	0.29	0.34	1.19
0.829	0.34	0.32	0.36	1.51
0.91	0.36	0.34	0.37	1.85
0.999	0.37	0.35	0.38	2.2
1.097	0.37	0.36	0.38	2.57
1.204	0.38	0.37	0.39	2.94
1.321	0.38	0.38	0.39	3.32
1.451	0.38	0.38	0.39	3.7
1.592	0.38	0.37	0.39	4.09
1.748	0.39	0.37	0.4	4.47
1.919	0.39	0.37	0.41	4.86
2.107	0.4	0.37	0.42	5.25
2.313	0.41	0.38	0.44	5.64
2.539	0.42	0.38	0.46	6.05
2.787	0.44	0.39	0.49	6.48
3.059	0.46	0.41	0.51	6.92
3.358	0.49	0.43	0.55	7.38
3.687	0.52	0.46	0.58	7.87
4.047	0.56	0.5	0.62	8.39
4.443	0.6	0.54	0.66	8.95
4.877	0.65	0.58	0.71	9.55
5.354	0.7	0.64	0.76	10.2
5.878	0.76	0.7	0.81	10.9
6.452	0.82	0.76	0.87	11.7
7.083	0.88	0.83	0.93	12.5
7.775	0.96	0.91	1	13.4
8.536	1.03	0.99	1.07	14.3
9.37	1.12	1.08	1.15	15.3
10.29	1.2	1.17	1.24	16.5
11.29	1.3	1.26	1.34	17.7
12.4	1.4	1.36	1.44	19
13.61	1.49	1.45	1.54	20.4
14.94	1.59	1.54	1.63	21.9

16.4	1.67	1.63	1.72	23.4
18	1.75	1.71	1.8	25.1
19.76	1.83	1.78	1.87	26.9
21.69	1.89	1.84	1.94	28.7
23.81	1.94	1.89	1.99	30.6
26.14	1.98	1.92	2.03	32.5
28.7	2.01	1.94	2.07	34.5
31.5	2.03	1.95	2.11	36.5
34.58	2.06	1.97	2.16	38.5
37.97	2.09	1.98	2.19	40.6
41.68	2.11	2	2.22	42.7
45.75	2.12	2.01	2.22	44.8
50.22	2.11	2.02	2.21	46.9
55.13	2.1	2.02	2.18	49
60.52	2.09	2.01	2.16	51.1
66.44	2.07	2	2.15	53.2
72.94	2.06	1.98	2.14	55.3
80.07	2.04	1.95	2.12	57.3
87.9	2	1.92	2.09	59.4
96.49	1.95	1.87	2.03	61.4
105.9	1.89	1.82	1.96	63.3
116.3	1.84	1.78	1.9	65.2
127.6	1.8	1.72	1.87	67.1
140.1	1.76	1.65	1.87	68.9
153.8	1.71	1.56	1.86	70.6
168.9	1.6	1.42	1.78	72.3
185.4	1.42	1.25	1.59	73.9
203.5	1.21	1.09	1.33	75.4
223.4	1.02	0.98	1.07	76.6
245.2	0.91	0.86	0.97	77.6
269.2	0.91	0.77	1.05	78.5
295.5	1	0.8	1.2	79.4
324.4	1.15	0.92	1.38	80.4
356.1	1.29	1.07	1.52	81.6
390.9	1.39	1.19	1.6	82.8
429.2	1.43	1.17	1.69	84.2
471.1	1.43	1.06	1.81	85.7
517.2	1.43	0.96	1.89	87.1
567.7	1.43	0.93	1.93	88.5
623.3	1.44	0.96	1.92	90
684.2	1.45	1.04	1.86	91.4
751.1	1.43	1.1	1.76	92.9
824.5	1.39	1.14	1.64	94.3
905.1	1.34	1.16	1.52	95.7

993.6	1.3	1.13	1.48	97
1091	0.99	0.84	1.14	98.3
1197	0.55	0.45	0.64	99.3
1314	0.13	0.11	0.16	99.9
1443	0.015	0.012	0.017	99.99
1584	0	0	0	100
1739	0	0	0	100
1909	0	0	0	100

**Site 4: Moraine**

<b>Channel Diameter</b>	<b>Diff.</b>	<b>-2 S.D.</b>	<b>+2 S.D.</b>	<b>Cum. &lt;</b>
<b>µm</b>	<b>Volume</b>	<b>Diff.</b>	<b>Diff.</b>	<b>Volume</b>
	<b>%</b>	<b>Volume</b>	<b>Volume</b>	<b>%</b>
		<b>%</b>	<b>%</b>	
0.393	0.14	0.13	0.14	0
0.431	0.24	0.24	0.24	0.14
0.474	0.35	0.35	0.36	0.38
0.52	0.5	0.5	0.51	0.73
0.571	0.63	0.62	0.63	1.23
0.627	0.73	0.73	0.74	1.86
0.688	0.83	0.82	0.83	2.59
0.755	0.92	0.92	0.93	3.42
0.829	1	0.99	1	4.34
0.91	1.06	1.05	1.06	5.34
0.999	1.1	1.09	1.1	6.39
1.097	1.13	1.13	1.14	7.49
1.204	1.16	1.15	1.16	8.62
1.321	1.18	1.17	1.18	9.78
1.451	1.19	1.18	1.19	11
1.592	1.2	1.19	1.2	12.1
1.748	1.21	1.2	1.21	13.3
1.919	1.23	1.22	1.23	14.6
2.107	1.24	1.24	1.25	15.8
2.313	1.27	1.26	1.27	17
2.539	1.3	1.29	1.3	18.3
2.787	1.33	1.33	1.34	19.6
3.059	1.38	1.37	1.39	20.9
3.358	1.43	1.42	1.44	22.3
3.687	1.49	1.48	1.49	23.7
4.047	1.56	1.55	1.56	25.2
4.443	1.63	1.63	1.63	26.8
4.877	1.71	1.71	1.71	28.4

5.354	1.79	1.79	1.8	30.1
5.878	1.88	1.88	1.89	31.9
6.452	1.97	1.97	1.98	33.8
7.083	2.07	2.07	2.08	35.8
7.775	2.17	2.16	2.17	37.8
8.536	2.27	2.26	2.27	40
9.37	2.36	2.36	2.36	42.3
10.29	2.46	2.46	2.46	44.6
11.29	2.56	2.56	2.56	47.1
12.4	2.66	2.65	2.66	49.7
13.61	2.74	2.73	2.74	52.3
14.94	2.79	2.79	2.8	55.1
16.4	2.84	2.83	2.86	57.8
18	2.9	2.88	2.93	60.7
19.76	2.99	2.95	3.02	63.6
21.69	3.08	3.05	3.11	66.6
23.81	3.15	3.13	3.17	69.7
26.14	3.14	3.13	3.15	72.8
28.7	3.04	3.03	3.04	75.9
31.5	2.88	2.87	2.89	79
34.58	2.72	2.68	2.76	81.9
37.97	2.62	2.54	2.7	84.6
41.68	2.59	2.49	2.69	87.2
45.75	2.57	2.48	2.66	89.8
50.22	2.45	2.41	2.48	92.4
55.13	2.14	2.09	2.19	94.8
60.52	1.61	1.5	1.73	96.9
66.44	0.95	0.78	1.12	98.6
72.94	0.4	0.25	0.54	99.5
80.07	0.091	0.017	0.16	99.9
87.9	0.0099	0	0.025	99.99
96.49	0.00022	0	0.001	100
105.9	0	0	0	100
116.3	0	0	0	100
127.6	0	0	0	100
140.1	0	0	0	100
153.8	0	0	0	100
168.9	0	0	0	100
185.4	0	0	0	100
203.5	0	0	0	100
223.4	0	0	0	100
245.2	0	0	0	100
269.2	0	0	0	100
295.5	0	0	0	100

324.4	0	0	0	100
356.1	0	0	0	100
390.9	0	0	0	100
429.2	0	0	0	100
471.1	0	0	0	100
517.2	0	0	0	100
567.7	0	0	0	100
623.3	0	0	0	100
684.2	0	0	0	100
751.1	0	0	0	100
824.5	0	0	0	100
905.1	0	0	0	100
993.6	0	0	0	100
1091	0	0	0	100
1197	0	0	0	100
1314	0	0	0	100
1443	0	0	0	100
1584	0	0	0	100
1739	0	0	0	100
1909	0	0	0	100

#### Site 4: Proglacial Sediments

<b>Channel Diameter</b>	<b>Diff.</b>	<b>-2 S.D.</b>	<b>+2 S.D.</b>	<b>Cum. &lt;</b>
<b>µm</b>	<b>Volume</b>	<b>Diff.</b>	<b>Diff.</b>	<b>Volume</b>
	<b>%</b>	<b>Volume</b>	<b>Volume</b>	<b>%</b>
		<b>%</b>	<b>%</b>	
0.393	0.11	0.1	0.12	0
0.431	0.19	0.18	0.21	0.11
0.474	0.28	0.26	0.3	0.3
0.52	0.4	0.38	0.42	0.58
0.571	0.49	0.47	0.52	0.98
0.627	0.57	0.55	0.59	1.47
0.688	0.64	0.63	0.66	2.04
0.755	0.71	0.7	0.71	2.69
0.829	0.76	0.75	0.77	3.39
0.91	0.8	0.78	0.82	4.15
0.999	0.83	0.8	0.86	4.95
1.097	0.85	0.81	0.9	5.78
1.204	0.88	0.83	0.93	6.63
1.321	0.9	0.85	0.95	7.51
1.451	0.92	0.87	0.97	8.4
1.592	0.95	0.91	0.99	9.33

1.748	0.98	0.95	1.02	10.3
1.919	1.03	1	1.05	11.3
2.107	1.08	1.06	1.09	12.3
2.313	1.13	1.1	1.15	13.4
2.539	1.19	1.15	1.22	14.5
2.787	1.25	1.2	1.3	15.7
3.059	1.31	1.26	1.37	16.9
3.358	1.38	1.32	1.44	18.2
3.687	1.45	1.39	1.51	19.6
4.047	1.52	1.46	1.58	21.1
4.443	1.6	1.55	1.66	22.6
4.877	1.68	1.63	1.74	24.2
5.354	1.76	1.72	1.81	25.9
5.878	1.85	1.8	1.89	27.6
6.452	1.93	1.88	1.97	29.5
7.083	2	1.95	2.06	31.4
7.775	2.08	2.02	2.14	33.4
8.536	2.15	2.07	2.22	35.5
9.37	2.22	2.14	2.31	37.6
10.29	2.3	2.21	2.39	39.9
11.29	2.39	2.3	2.47	42.2
12.4	2.46	2.38	2.54	44.6
13.61	2.52	2.43	2.6	47
14.94	2.54	2.45	2.63	49.5
16.4	2.55	2.44	2.66	52.1
18	2.57	2.45	2.69	54.6
19.76	2.61	2.49	2.73	57.2
21.69	2.68	2.56	2.79	59.8
23.81	2.75	2.65	2.84	62.5
26.14	2.78	2.71	2.86	65.2
28.7	2.76	2.7	2.81	68
31.5	2.66	2.61	2.71	70.8
34.58	2.51	2.46	2.56	73.4
37.97	2.33	2.27	2.38	75.9
41.68	2.14	2.08	2.2	78.3
45.75	1.97	1.9	2.03	80.4
50.22	1.8	1.75	1.86	82.4
55.13	1.64	1.61	1.68	84.2
60.52	1.47	1.46	1.48	85.8
66.44	1.28	1.24	1.31	87.3
72.94	1.06	1	1.13	88.6
80.07	0.85	0.76	0.93	89.6
87.9	0.65	0.56	0.74	90.5
96.49	0.5	0.42	0.58	91.1

105.9	0.41	0.35	0.46	91.6
116.3	0.37	0.34	0.41	92
127.6	0.37	0.34	0.4	92.4
140.1	0.37	0.32	0.41	92.8
153.8	0.32	0.29	0.36	93.1
168.9	0.23	0.21	0.25	93.4
185.4	0.14	0.046	0.24	93.7
203.5	0.099	0	0.26	93.8
223.4	0.13	0	0.38	93.9
245.2	0.21	0	0.62	94
269.2	0.34	0	0.96	94.3
295.5	0.45	0	1.24	94.6
324.4	0.48	0	1.32	95
356.1	0.36	0	0.99	95.5
390.9	0.17	0	0.48	95.9
429.2	0.038	0	0.11	96.1
471.1	0.013	0.00014	0.025	96.1
517.2	0.058	0.014	0.1	96.1
567.7	0.33	0.077	0.59	96.2
623.3	0.94	0.21	1.68	96.5
684.2	1.28	0.27	2.29	97.5
751.1	0.96	0.2	1.72	98.7
824.5	0.27	0.058	0.49	99.7
905.1	0.033	0.0071	0.059	99.97
993.6	0	0	0	100
1091	0	0	0	100
1197	0	0	0	100
1314	0	0	0	100
1443	0	0	0	100
1584	0	0	0	100
1739	0	0	0	100
1909	0	0	0	100

**Site 5: Ice Type B**

<b>Channel Diameter</b>	<b>Diff.</b>	<b>-2 S.D.</b>	<b>+2 S.D.</b>	<b>Cum. &lt;</b>
<b>µm</b>	<b>Volume</b>	<b>Diff.</b>	<b>Diff.</b>	<b>Volume</b>
	<b>%</b>	<b>Volume</b>	<b>Volume</b>	<b>%</b>
		<b>%</b>	<b>%</b>	
0.393	0.094	0.09	0.098	0
0.431	0.17	0.16	0.17	0.094
0.474	0.24	0.23	0.25	0.26
0.52	0.35	0.33	0.36	0.51

0.571	0.43	0.42	0.45	0.85
0.627	0.5	0.49	0.52	1.28
0.688	0.57	0.55	0.59	1.79
0.755	0.63	0.61	0.65	2.36
0.829	0.67	0.65	0.69	2.98
0.91	0.71	0.69	0.73	3.66
0.999	0.73	0.71	0.75	4.37
1.097	0.75	0.73	0.76	5.1
1.204	0.76	0.74	0.77	5.84
1.321	0.76	0.75	0.78	6.6
1.451	0.76	0.75	0.78	7.36
1.592	0.76	0.75	0.77	8.13
1.748	0.76	0.75	0.78	8.89
1.919	0.77	0.76	0.78	9.65
2.107	0.78	0.77	0.79	10.4
2.313	0.79	0.78	0.8	11.2
2.539	0.81	0.8	0.82	12
2.787	0.84	0.83	0.85	12.8
3.059	0.87	0.86	0.88	13.6
3.358	0.91	0.9	0.92	14.5
3.687	0.96	0.94	0.97	15.4
4.047	1	0.99	1.02	16.4
4.443	1.06	1.04	1.07	17.4
4.877	1.12	1.1	1.13	18.4
5.354	1.18	1.16	1.19	19.6
5.878	1.24	1.22	1.26	20.7
6.452	1.31	1.29	1.32	22
7.083	1.38	1.36	1.39	23.3
7.775	1.45	1.44	1.46	24.7
8.536	1.52	1.52	1.53	26.1
9.37	1.6	1.6	1.61	27.6
10.29	1.69	1.69	1.7	29.2
11.29	1.79	1.78	1.79	30.9
12.4	1.89	1.88	1.9	32.7
13.61	1.99	1.98	2	34.6
14.94	2.1	2.08	2.11	36.6
16.4	2.2	2.18	2.22	38.7
18	2.32	2.3	2.33	40.9
19.76	2.44	2.43	2.45	43.2
21.69	2.56	2.55	2.57	45.7
23.81	2.67	2.64	2.7	48.2
26.14	2.76	2.73	2.79	50.9
28.7	2.83	2.8	2.85	53.6
31.5	2.87	2.86	2.88	56.5

34.58	2.9	2.86	2.94	59.3
37.97	2.92	2.87	2.98	62.2
41.68	2.93	2.88	2.99	65.2
45.75	2.92	2.89	2.95	68.1
50.22	2.86	2.86	2.87	71
55.13	2.77	2.73	2.8	73.9
60.52	2.63	2.58	2.68	76.6
66.44	2.47	2.44	2.5	79.3
72.94	2.28	2.27	2.3	81.7
80.07	2.09	2.04	2.14	84
87.9	1.91	1.84	1.97	86.1
96.49	1.73	1.68	1.78	88
105.9	1.57	1.53	1.6	89.8
116.3	1.43	1.36	1.5	91.3
127.6	1.32	1.22	1.42	92.8
140.1	1.22	1.11	1.32	94.1
153.8	1.11	1.02	1.2	95.3
168.9	0.96	0.89	1.04	96.4
185.4	0.78	0.7	0.85	97.4
203.5	0.58	0.48	0.68	98.1
223.4	0.4	0.26	0.53	98.7
245.2	0.26	0.12	0.41	99.1
269.2	0.19	0.063	0.31	99.4
295.5	0.15	0.07	0.23	99.6
324.4	0.13	0.084	0.18	99.7
356.1	0.095	0.046	0.14	99.8
390.9	0.049	0.0073	0.09	99.9
429.2	0.013	0	0.03	99.99
471.1	0.0016	0	0.0047	99.998
517.2	0.000036	0	0.00016	100
567.7	0	0	0	100
623.3	0	0	0	100
684.2	0	0	0	100
751.1	0	0	0	100
824.5	0	0	0	100
905.1	0	0	0	100
993.6	0	0	0	100
1091	0	0	0	100
1197	0	0	0	100
1314	0	0	0	100
1443	0	0	0	100
1584	0	0	0	100
1739	0	0	0	100
1909	0	0	0	100

**Site 5: Ice Type A**

<b>Channel Diameter</b>	<b>Diff.</b>	<b>-2 S.D.</b>	<b>+2 S.D.</b>	<b>Cum. &lt;</b>
<b>µm</b>	<b>Volume</b>	<b>Diff.</b>	<b>Diff.</b>	<b>Volume</b>
	<b>%</b>	<b>Volume</b>	<b>Volume</b>	<b>%</b>
		<b>%</b>	<b>%</b>	
0.393	0.16	0.15	0.17	0
0.431	0.28	0.26	0.3	0.16
0.474	0.42	0.39	0.44	0.44
0.52	0.6	0.57	0.63	0.86
0.571	0.75	0.72	0.78	1.46
0.627	0.89	0.86	0.91	2.21
0.688	1.02	0.99	1.04	3.1
0.755	1.14	1.11	1.18	4.11
0.829	1.26	1.21	1.31	5.26
0.91	1.37	1.3	1.43	6.52
0.999	1.46	1.37	1.55	7.89
1.097	1.55	1.43	1.66	9.34
1.204	1.63	1.5	1.76	10.9
1.321	1.71	1.58	1.84	12.5
1.451	1.78	1.66	1.91	14.2
1.592	1.85	1.74	1.96	16
1.748	1.92	1.83	2.01	17.9
1.919	1.98	1.92	2.04	19.8
2.107	2.04	2	2.07	21.8
2.313	2.08	2.06	2.1	23.8
2.539	2.12	2.08	2.15	25.9
2.787	2.14	2.09	2.19	28
3.059	2.15	2.09	2.21	30.1
3.358	2.15	2.08	2.21	32.3
3.687	2.13	2.07	2.2	34.4
4.047	2.11	2.06	2.17	36.6
4.443	2.08	2.04	2.13	38.7
4.877	2.05	2.02	2.08	40.8
5.354	2.01	2	2.03	42.8
5.878	1.98	1.97	1.99	44.8
6.452	1.95	1.94	1.96	46.8
7.083	1.92	1.9	1.94	48.8
7.775	1.9	1.86	1.93	50.7
8.536	1.89	1.84	1.93	52.6
9.37	1.89	1.85	1.94	54.5

10.29	1.93	1.89	1.97	56.4
11.29	1.99	1.96	2.02	58.3
12.4	2.05	2.02	2.07	60.3
13.61	2.1	2.06	2.15	62.3
14.94	2.17	2.07	2.26	64.4
16.4	2.26	2.09	2.42	66.6
18	2.36	2.16	2.57	68.8
19.76	2.47	2.29	2.65	71.2
21.69	2.52	2.45	2.6	73.7
23.81	2.51	2.44	2.58	76.2
26.14	2.44	2.29	2.6	78.7
28.7	2.39	2.28	2.5	81.2
31.5	2.4	2.33	2.47	83.5
34.58	2.48	2.17	2.8	85.9
37.97	2.59	2.1	3.08	88.4
41.68	2.58	2.13	3.03	91
45.75	2.36	2.19	2.53	93.6
50.22	1.89	1.6	2.18	95.9
55.13	1.23	0.52	1.94	97.8
60.52	0.63	0	1.43	99.1
66.44	0.23	0	0.78	99.7
72.94	0.064	0	0.27	99.9
80.07	0.01	0	0.045	99.99
87.9	0.00061	0	0.0027	99.999
96.49	0	0	0	100
105.9	0	0	0	100
116.3	0	0	0	100
127.6	0	0	0	100
140.1	0	0	0	100
153.8	0	0	0	100
168.9	0	0	0	100
185.4	0	0	0	100
203.5	0	0	0	100
223.4	0	0	0	100
245.2	0	0	0	100
269.2	0	0	0	100
295.5	0	0	0	100
324.4	0	0	0	100
356.1	0	0	0	100
390.9	0	0	0	100
429.2	0	0	0	100
471.1	0	0	0	100
517.2	0	0	0	100
567.7	0	0	0	100

623.3	0	0	0	100
684.2	0	0	0	100
751.1	0	0	0	100
824.5	0	0	0	100
905.1	0	0	0	100
993.6	0	0	0	100
1091	0	0	0	100
1197	0	0	0	100
1314	0	0	0	100
1443	0	0	0	100
1584	0	0	0	100
1739	0	0	0	100
1909	0	0	0	100

### Site 5: Proglacial Sediments

<b>Channel Diameter</b>	<b>Diff.</b>	<b>-2 S.D.</b>	<b>+2 S.D.</b>	<b>Cum. &lt;</b>
<b>µm</b>	<b>Volume</b>	<b>Diff.</b>	<b>Diff.</b>	<b>Volume</b>
	<b>%</b>	<b>Volume</b>	<b>Volume</b>	<b>%</b>
		<b>%</b>	<b>%</b>	
0.393	0.08	0.079	0.082	0
0.431	0.14	0.14	0.15	0.08
0.474	0.21	0.21	0.21	0.22
0.52	0.3	0.29	0.3	0.43
0.571	0.37	0.36	0.38	0.73
0.627	0.43	0.42	0.44	1.1
0.688	0.48	0.48	0.49	1.53
0.755	0.53	0.53	0.54	2.01
0.829	0.58	0.57	0.58	2.55
0.91	0.6	0.59	0.61	3.12
0.999	0.62	0.61	0.63	3.73
1.097	0.64	0.63	0.65	4.35
1.204	0.65	0.64	0.66	4.99
1.321	0.65	0.64	0.66	5.64
1.451	0.65	0.64	0.66	6.29
1.592	0.65	0.64	0.66	6.94
1.748	0.66	0.64	0.67	7.59
1.919	0.66	0.65	0.68	8.25
2.107	0.67	0.66	0.69	8.91
2.313	0.69	0.67	0.7	9.58
2.539	0.71	0.69	0.72	10.3
2.787	0.73	0.71	0.75	11
3.059	0.76	0.74	0.78	11.7

3.358	0.8	0.77	0.82	12.5
3.687	0.84	0.81	0.86	13.3
4.047	0.88	0.86	0.91	14.1
4.443	0.93	0.91	0.96	15
4.877	0.99	0.97	1.01	15.9
5.354	1.05	1.03	1.07	16.9
5.878	1.11	1.09	1.13	18
6.452	1.17	1.16	1.19	19.1
7.083	1.24	1.23	1.26	20.2
7.775	1.31	1.3	1.33	21.5
8.536	1.38	1.37	1.4	22.8
9.37	1.46	1.45	1.47	24.2
10.29	1.54	1.53	1.56	25.6
11.29	1.63	1.61	1.65	27.2
12.4	1.71	1.69	1.73	28.8
13.61	1.8	1.77	1.82	30.5
14.94	1.87	1.84	1.91	32.3
16.4	1.95	1.92	1.99	34.2
18	2.04	2	2.07	36.1
19.76	2.12	2.09	2.16	38.2
21.69	2.2	2.16	2.24	40.3
23.81	2.27	2.22	2.31	42.5
26.14	2.33	2.27	2.39	44.8
28.7	2.39	2.31	2.47	47.1
31.5	2.46	2.38	2.55	49.5
34.58	2.55	2.47	2.63	52
37.97	2.64	2.58	2.7	54.5
41.68	2.71	2.68	2.74	57.2
45.75	2.72	2.71	2.72	59.9
50.22	2.66	2.64	2.69	62.6
55.13	2.56	2.52	2.6	65.2
60.52	2.44	2.36	2.52	67.8
66.44	2.33	2.21	2.44	70.2
72.94	2.25	2.1	2.39	72.6
80.07	2.19	2.02	2.35	74.8
87.9	2.12	1.95	2.29	77
96.49	2.01	1.84	2.19	79.1
105.9	1.84	1.64	2.04	81.1
116.3	1.61	1.38	1.85	83
127.6	1.37	1.12	1.63	84.6
140.1	1.17	0.93	1.41	86
153.8	1.02	0.82	1.23	87.1
168.9	0.93	0.76	1.1	88.2
185.4	0.85	0.7	1	89.1

203.5	0.77	0.67	0.87	89.9
223.4	0.68	0.54	0.82	90.7
245.2	0.6	0.34	0.86	91.4
269.2	0.57	0.23	0.92	92
295.5	0.6	0.26	0.94	92.6
324.4	0.66	0.42	0.91	93.2
356.1	0.73	0.67	0.78	93.8
390.9	0.75	0.59	0.92	94.5
429.2	0.73	0.42	1.05	95.3
471.1	0.7	0.29	1.1	96
517.2	0.67	0.25	1.1	96.7
567.7	0.69	0.28	1.1	97.4
623.3	0.75	0.4	1.1	98.1
684.2	0.65	0.41	0.88	98.8
751.1	0.39	0.27	0.51	99.5
824.5	0.1	0.071	0.13	99.9
905.1	0.012	0.0078	0.015	99.99
993.6	0	0	0	100
1091	0	0	0	100
1197	0	0	0	100
1314	0	0	0	100
1443	0	0	0	100
1584	0	0	0	100
1739	0	0	0	100
1909	0	0	0	100

**Site 5: Minor Outwash Fan**

<b>Channel Diameter</b>	<b>Diff.</b>	<b>-2 S.D.</b>	<b>+2 S.D.</b>	<b>Cum. &lt;</b>
<b>µm</b>	<b>Volume</b>	<b>Diff.</b>	<b>Diff.</b>	<b>Volume</b>
	<b>%</b>	<b>Volume</b>	<b>Volume</b>	<b>%</b>
		<b>%</b>	<b>%</b>	
0.393	0.05	0.045	0.055	0
0.431	0.089	0.081	0.097	0.05
0.474	0.13	0.12	0.14	0.14
0.52	0.19	0.17	0.2	0.27
0.571	0.23	0.21	0.25	0.46
0.627	0.27	0.24	0.29	0.68
0.688	0.3	0.27	0.32	0.95
0.755	0.33	0.3	0.35	1.25
0.829	0.35	0.32	0.38	1.58
0.91	0.37	0.34	0.39	1.93
0.999	0.38	0.35	0.4	2.29

1.097	0.38	0.35	0.41	2.67
1.204	0.38	0.35	0.42	3.05
1.321	0.38	0.35	0.42	3.43
1.451	0.38	0.35	0.41	3.81
1.592	0.38	0.34	0.41	4.19
1.748	0.38	0.35	0.41	4.57
1.919	0.38	0.35	0.41	4.95
2.107	0.39	0.36	0.41	5.33
2.313	0.39	0.36	0.42	5.71
2.539	0.4	0.37	0.44	6.11
2.787	0.42	0.39	0.45	6.51
3.059	0.44	0.4	0.48	6.93
3.358	0.46	0.42	0.5	7.37
3.687	0.49	0.45	0.53	7.83
4.047	0.52	0.47	0.56	8.32
4.443	0.55	0.51	0.59	8.84
4.877	0.59	0.55	0.63	9.39
5.354	0.63	0.59	0.67	9.98
5.878	0.67	0.63	0.71	10.6
6.452	0.72	0.68	0.76	11.3
7.083	0.77	0.73	0.81	12
7.775	0.83	0.79	0.86	12.8
8.536	0.89	0.85	0.93	13.6
9.37	0.96	0.91	1	14.5
10.29	1.03	0.99	1.08	15.4
11.29	1.12	1.07	1.17	16.5
12.4	1.22	1.16	1.27	17.6
13.61	1.32	1.27	1.38	18.8
14.94	1.44	1.38	1.5	20.1
16.4	1.56	1.5	1.63	21.6
18	1.7	1.63	1.77	23.1
19.76	1.85	1.78	1.92	24.8
21.69	2	1.92	2.07	26.7
23.81	2.15	2.07	2.22	28.7
26.14	2.28	2.2	2.36	30.8
28.7	2.39	2.31	2.47	33.1
31.5	2.49	2.41	2.57	35.5
34.58	2.57	2.49	2.64	38
37.97	2.64	2.55	2.72	40.5
41.68	2.7	2.62	2.79	43.2
45.75	2.77	2.67	2.87	45.9
50.22	2.83	2.72	2.93	48.7
55.13	2.87	2.76	2.99	51.5
60.52	2.89	2.78	3	54.4

66.44	2.87	2.76	2.98	57.2
72.94	2.8	2.69	2.91	60.1
80.07	2.68	2.58	2.78	62.9
87.9	2.52	2.43	2.61	65.6
96.49	2.33	2.25	2.41	68.1
105.9	2.14	2.05	2.22	70.4
116.3	1.95	1.87	2.04	72.6
127.6	1.79	1.7	1.88	74.5
140.1	1.65	1.56	1.73	76.3
153.8	1.52	1.45	1.59	78
168.9	1.4	1.35	1.45	79.5
185.4	1.29	1.25	1.32	80.9
203.5	1.2	1.15	1.24	82.2
223.4	1.14	1.09	1.19	83.4
245.2	1.12	1.07	1.17	84.5
269.2	1.14	1.1	1.18	85.6
295.5	1.17	1.14	1.21	86.8
324.4	1.19	1.14	1.23	87.9
356.1	1.15	1.07	1.23	89.1
390.9	1.06	0.94	1.19	90.3
429.2	0.95	0.79	1.11	91.3
471.1	0.84	0.68	1.01	92.3
517.2	0.77	0.63	0.91	93.1
567.7	0.74	0.66	0.83	93.9
623.3	0.75	0.69	0.81	94.6
684.2	0.77	0.59	0.95	95.4
751.1	0.76	0.43	1.09	96.1
824.5	0.74	0.26	1.23	96.9
905.1	0.71	0.096	1.33	97.6
993.6	0.7	0	1.42	98.4
1091	0.55	0	1.16	99.1
1197	0.31	0	0.66	99.6
1314	0.076	0	0.16	99.9
1443	0.0086	0	0.018	99.99
1584	0	0	0	100
1739	0	0	0	100
1909	0	0	0	100

**Site 5: Moraine**

<b>Channel Diameter</b>	<b>Diff.</b>	<b>-2 S.D.</b>	<b>+2 S.D.</b>	<b>Cum. &lt;</b>
<b>µm</b>	<b>Volume</b>	<b>Diff.</b>	<b>Diff.</b>	<b>Volume</b>
	<b>%</b>	<b>Volume</b>	<b>Volume</b>	<b>%</b>
		<b>%</b>	<b>%</b>	
0.393	0.096	0.083	0.11	0
0.431	0.17	0.15	0.19	0.096
0.474	0.25	0.22	0.28	0.27
0.52	0.36	0.31	0.4	0.52
0.571	0.44	0.39	0.49	0.87
0.627	0.51	0.46	0.57	1.31
0.688	0.58	0.52	0.63	1.82
0.755	0.63	0.57	0.69	2.4
0.829	0.68	0.62	0.74	3.03
0.91	0.71	0.66	0.77	3.72
0.999	0.74	0.69	0.79	4.43
1.097	0.75	0.71	0.8	5.17
1.204	0.76	0.72	0.81	5.92
1.321	0.77	0.73	0.81	6.69
1.451	0.77	0.73	0.82	7.46
1.592	0.78	0.73	0.82	8.23
1.748	0.79	0.74	0.83	9.01
1.919	0.8	0.74	0.86	9.79
2.107	0.82	0.75	0.88	10.6
2.313	0.84	0.76	0.92	11.4
2.539	0.86	0.77	0.96	12.2
2.787	0.9	0.79	1	13.1
3.059	0.94	0.82	1.05	14
3.358	0.98	0.86	1.11	14.9
3.687	1.03	0.9	1.16	15.9
4.047	1.09	0.95	1.22	17
4.443	1.14	1	1.29	18
4.877	1.21	1.07	1.35	19.2
5.354	1.28	1.13	1.42	20.4
5.878	1.35	1.21	1.48	21.7
6.452	1.42	1.28	1.55	23
7.083	1.5	1.37	1.63	24.4
7.775	1.58	1.46	1.7	25.9
8.536	1.66	1.55	1.78	27.5
9.37	1.75	1.64	1.86	29.2
10.29	1.85	1.74	1.96	30.9

11.29	1.95	1.83	2.06	32.8
12.4	2.05	1.93	2.17	34.7
13.61	2.14	2.02	2.26	36.8
14.94	2.22	2.1	2.34	38.9
16.4	2.3	2.18	2.42	41.1
18	2.37	2.25	2.49	43.4
19.76	2.44	2.31	2.57	45.8
21.69	2.51	2.38	2.65	48.2
23.81	2.58	2.44	2.72	50.7
26.14	2.62	2.48	2.76	53.3
28.7	2.65	2.51	2.78	55.9
31.5	2.65	2.53	2.77	58.6
34.58	2.64	2.54	2.75	61.2
37.97	2.63	2.54	2.72	63.9
41.68	2.61	2.52	2.69	66.5
45.75	2.58	2.49	2.66	69.1
50.22	2.53	2.44	2.62	71.7
55.13	2.46	2.36	2.57	74.2
60.52	2.37	2.27	2.48	76.7
66.44	2.26	2.16	2.36	79.1
72.94	2.12	2.03	2.21	81.3
80.07	1.96	1.88	2.04	83.4
87.9	1.77	1.69	1.85	85.4
96.49	1.58	1.51	1.66	87.2
105.9	1.4	1.32	1.48	88.8
116.3	1.23	1.14	1.32	90.2
127.6	1.06	0.93	1.18	91.4
140.1	0.86	0.71	1.01	92.4
153.8	0.63	0.48	0.77	93.3
168.9	0.4	0.26	0.54	93.9
185.4	0.21	0.048	0.37	94.3
203.5	0.11	0	0.31	94.5
223.4	0.086	0	0.35	94.6
245.2	0.11	0	0.47	94.7
269.2	0.13	0	0.58	94.8
295.5	0.14	0	0.56	95
324.4	0.15	0	0.37	95.1
356.1	0.22	0	0.46	95.3
390.9	0.38	0	0.99	95.5
429.2	0.57	0	1.55	95.9
471.1	0.74	0	2.05	96.4
517.2	0.83	0	2.32	97.2
567.7	0.76	0	2.08	98
623.3	0.61	0	1.79	98.7

684.2	0.38	0	1.45	99.4
751.1	0.2	0	0.87	99.7
824.5	0.051	0	0.23	99.9
905.1	0.0057	0	0.025	99.99
993.6	0	0	0	100
1091	0	0	0	100
1197	0	0	0	100
1314	0	0	0	100
1443	0	0	0	100
1584	0	0	0	100
1739	0	0	0	100
1909	0	0	0	100

**Site 5: Sediment Rich Stream**

<b>Channel Diameter</b>	<b>Diff.</b>	<b>-2 S.D.</b>	<b>+2 S.D.</b>	<b>Cum. &lt;</b>
<b>µm</b>	<b>Volume</b>	<b>Diff.</b>	<b>Diff.</b>	<b>Volume</b>
	<b>%</b>	<b>Volume</b>	<b>Volume</b>	<b>%</b>
		<b>%</b>	<b>%</b>	
0.393	0.082	0.077	0.088	0
0.431	0.15	0.14	0.16	0.082
0.474	0.21	0.2	0.23	0.23
0.52	0.3	0.29	0.32	0.44
0.571	0.38	0.36	0.4	0.75
0.627	0.44	0.42	0.46	1.13
0.688	0.49	0.47	0.52	1.57
0.755	0.55	0.52	0.57	2.06
0.829	0.59	0.56	0.61	2.61
0.91	0.62	0.6	0.64	3.19
0.999	0.64	0.62	0.66	3.81
1.097	0.65	0.64	0.67	4.45
1.204	0.67	0.65	0.68	5.11
1.321	0.67	0.66	0.69	5.77
1.451	0.68	0.67	0.69	6.45
1.592	0.68	0.68	0.69	7.13
1.748	0.69	0.68	0.7	7.81
1.919	0.7	0.69	0.71	8.5
2.107	0.71	0.7	0.72	9.2
2.313	0.73	0.71	0.74	9.92
2.539	0.75	0.73	0.76	10.6
2.787	0.77	0.74	0.79	11.4
3.059	0.79	0.76	0.82	12.2
3.358	0.81	0.78	0.85	12.9

3.687	0.84	0.8	0.88	13.8
4.047	0.87	0.82	0.91	14.6
4.443	0.9	0.85	0.94	15.5
4.877	0.93	0.88	0.97	16.4
5.354	0.95	0.91	1	17.3
5.878	0.98	0.94	1.03	18.2
6.452	1.01	0.97	1.06	19.2
7.083	1.04	1	1.08	20.2
7.775	1.07	1.04	1.1	21.3
8.536	1.09	1.07	1.11	22.3
9.37	1.12	1.1	1.13	23.4
10.29	1.14	1.12	1.16	24.6
11.29	1.17	1.13	1.21	25.7
12.4	1.19	1.12	1.26	26.9
13.61	1.2	1.09	1.3	28
14.94	1.2	1.06	1.33	29.2
16.4	1.2	1.04	1.37	30.4
18	1.24	1.06	1.42	31.6
19.76	1.33	1.15	1.51	32.9
21.69	1.47	1.32	1.62	34.2
23.81	1.63	1.55	1.72	35.7
26.14	1.78	1.76	1.81	37.3
28.7	1.87	1.73	2.02	39.1
31.5	1.89	1.65	2.12	41
34.58	1.83	1.58	2.08	42.9
37.97	1.74	1.57	1.9	44.7
41.68	1.65	1.64	1.66	46.4
45.75	1.61	1.4	1.81	48.1
50.22	1.63	1.3	1.96	49.7
55.13	1.72	1.4	2.03	51.3
60.52	1.86	1.74	1.97	53
66.44	2.01	1.81	2.2	54.9
72.94	2.12	1.63	2.6	56.9
80.07	2.15	1.56	2.73	59
87.9	2.09	1.67	2.5	61.2
96.49	1.99	1.91	2.07	63.2
105.9	1.94	1.61	2.27	65.2
116.3	1.99	1.48	2.5	67.2
127.6	2.15	1.73	2.56	69.2
140.1	2.33	2.19	2.46	71.3
153.8	2.4	2.06	2.75	73.6
168.9	2.29	1.76	2.81	76
185.4	2	1.55	2.45	78.3
203.5	1.69	1.42	1.97	80.3

223.4	1.52	1.28	1.76	82
245.2	1.54	1.29	1.79	83.5
269.2	1.73	1.58	1.88	85.1
295.5	1.97	1.87	2.08	86.8
324.4	2.09	1.86	2.32	88.8
356.1	1.94	1.68	2.2	90.9
390.9	1.52	1.28	1.75	92.8
429.2	0.97	0.65	1.28	94.3
471.1	0.53	0.12	0.93	95.3
517.2	0.32	0	0.71	95.8
567.7	0.33	0.0021	0.66	96.2
623.3	0.51	0.21	0.81	96.5
684.2	0.79	0.45	1.13	97
751.1	0.95	0.55	1.36	97.8
824.5	0.77	0.43	1.1	98.7
905.1	0.39	0.21	0.58	99.5
993.6	0.092	0.047	0.14	99.9
1091	0.0089	0.0041	0.014	99.99
1197	0	0	0	100
1314	0	0	0	100
1443	0	0	0	100
1584	0	0	0	100
1739	0	0	0	100
1909	0	0	0	100

**Site 5: Supraglacial**

<b>Channel Diameter</b>	<b>Diff.</b>	<b>-2 S.D.</b>	<b>+2 S.D.</b>	<b>Cum. &lt;</b>
<b>µm</b>	<b>Volume</b>	<b>Diff.</b>	<b>Diff.</b>	<b>Volume</b>
	<b>%</b>	<b>Volume</b>	<b>Volume</b>	<b>%</b>
		<b>%</b>	<b>%</b>	
0.393	0.065	0.048	0.082	0
0.431	0.11	0.085	0.14	0.065
0.474	0.17	0.12	0.21	0.18
0.52	0.24	0.18	0.3	0.35
0.571	0.3	0.22	0.37	0.58
0.627	0.34	0.26	0.43	0.88
0.688	0.39	0.29	0.48	1.22
0.755	0.43	0.32	0.53	1.61
0.829	0.46	0.35	0.57	2.04
0.91	0.48	0.37	0.6	2.5
0.999	0.5	0.39	0.62	2.98
1.097	0.51	0.4	0.63	3.48

1.204	0.53	0.41	0.65	3.99
1.321	0.54	0.41	0.66	4.52
1.451	0.54	0.42	0.67	5.06
1.592	0.55	0.42	0.68	5.6
1.748	0.56	0.43	0.7	6.15
1.919	0.58	0.43	0.73	6.72
2.107	0.6	0.44	0.75	7.3
2.313	0.61	0.45	0.78	7.89
2.539	0.64	0.46	0.81	8.51
2.787	0.66	0.47	0.85	9.14
3.059	0.68	0.48	0.88	9.8
3.358	0.71	0.5	0.91	10.5
3.687	0.73	0.51	0.95	11.2
4.047	0.76	0.53	0.98	11.9
4.443	0.78	0.55	1.02	12.7
4.877	0.81	0.57	1.05	13.5
5.354	0.84	0.59	1.09	14.3
5.878	0.87	0.61	1.12	15.1
6.452	0.89	0.63	1.15	16
7.083	0.92	0.66	1.19	16.9
7.775	0.96	0.69	1.22	17.8
8.536	0.99	0.72	1.25	18.7
9.37	1.02	0.76	1.29	19.7
10.29	1.07	0.8	1.34	20.8
11.29	1.11	0.84	1.39	21.8
12.4	1.16	0.88	1.45	22.9
13.61	1.2	0.92	1.49	24.1
14.94	1.24	0.95	1.53	25.3
16.4	1.27	0.98	1.57	26.5
18	1.31	1.02	1.6	27.8
19.76	1.35	1.05	1.64	29.1
21.69	1.38	1.09	1.68	30.5
23.81	1.42	1.12	1.72	31.9
26.14	1.44	1.14	1.75	33.3
28.7	1.46	1.15	1.77	34.7
31.5	1.47	1.16	1.78	36.2
34.58	1.47	1.16	1.78	37.6
37.97	1.47	1.17	1.77	39.1
41.68	1.45	1.17	1.73	40.6
45.75	1.41	1.16	1.67	42
50.22	1.36	1.13	1.6	43.5
55.13	1.32	1.1	1.54	44.8
60.52	1.3	1.08	1.52	46.1
66.44	1.32	1.09	1.55	47.4

72.94	1.36	1.12	1.61	48.8
80.07	1.42	1.16	1.68	50.1
87.9	1.46	1.21	1.71	51.5
96.49	1.46	1.24	1.68	53
105.9	1.44	1.26	1.62	54.5
116.3	1.41	1.27	1.55	55.9
127.6	1.4	1.31	1.5	57.3
140.1	1.43	1.36	1.5	58.7
153.8	1.47	1.43	1.52	60.1
168.9	1.52	1.49	1.55	61.6
185.4	1.57	1.55	1.59	63.1
203.5	1.62	1.61	1.64	64.7
223.4	1.7	1.67	1.72	66.3
245.2	1.79	1.73	1.84	68
269.2	1.88	1.79	1.97	69.8
295.5	1.95	1.82	2.07	71.7
324.4	1.96	1.78	2.13	73.6
356.1	1.92	1.65	2.18	75.6
390.9	1.84	1.46	2.22	77.5
429.2	1.77	1.29	2.25	79.4
471.1	1.72	1.17	2.27	81.1
517.2	1.69	1.1	2.29	82.9
567.7	1.68	1.08	2.29	84.5
623.3	1.68	1.09	2.26	86.2
684.2	1.67	1.11	2.23	87.9
751.1	1.67	1.14	2.2	89.6
824.5	1.67	1.17	2.16	91.2
905.1	1.64	1.14	2.15	92.9
993.6	1.55	0.87	2.24	94.6
1091	1.35	0.25	2.45	96.1
1197	1.04	0	2.52	97.5
1314	0.75	0	2.45	98.5
1443	0.46	0	1.87	99.3
1584	0.23	0	1	99.7
1739	0.054	0	0.24	99.9
1909	0.0057	0	0.025	99.99

**Site 6: Ice Type B (1)**

<b>Channel Diameter</b>	<b>Diff.</b>	<b>-2 S.D.</b>	<b>+2 S.D.</b>	<b>Cum. &lt;</b>
<b>µm</b>	<b>Volume</b>	<b>Diff.</b>	<b>Diff.</b>	<b>Volume</b>
	<b>%</b>	<b>Volume</b>	<b>Volume</b>	<b>%</b>
		<b>%</b>	<b>%</b>	
0.393	0.032	0.028	0.036	0
0.431	0.057	0.05	0.064	0.032
0.474	0.084	0.074	0.095	0.089
0.52	0.12	0.1	0.14	0.17
0.571	0.15	0.13	0.17	0.29
0.627	0.18	0.15	0.2	0.44
0.688	0.2	0.17	0.22	0.62
0.755	0.22	0.19	0.25	0.82
0.829	0.24	0.2	0.27	1.04
0.91	0.25	0.22	0.29	1.27
0.999	0.26	0.22	0.3	1.53
1.097	0.27	0.23	0.31	1.79
1.204	0.28	0.23	0.32	2.06
1.321	0.28	0.24	0.32	2.34
1.451	0.28	0.24	0.33	2.62
1.592	0.28	0.24	0.33	2.9
1.748	0.28	0.24	0.33	3.18
1.919	0.29	0.25	0.33	3.47
2.107	0.29	0.25	0.33	3.75
2.313	0.29	0.25	0.33	4.04
2.539	0.29	0.26	0.33	4.33
2.787	0.3	0.26	0.34	4.63
3.059	0.31	0.27	0.35	4.93
3.358	0.32	0.27	0.36	5.23
3.687	0.32	0.28	0.37	5.55
4.047	0.34	0.29	0.38	5.87
4.443	0.35	0.3	0.4	6.21
4.877	0.36	0.31	0.42	6.56
5.354	0.38	0.32	0.44	6.92
5.878	0.39	0.33	0.46	7.3
6.452	0.41	0.34	0.48	7.69
7.083	0.42	0.35	0.5	8.1
7.775	0.44	0.36	0.52	8.53
8.536	0.45	0.37	0.54	8.96
9.37	0.47	0.38	0.55	9.42
10.29	0.48	0.39	0.57	9.89

11.29	0.49	0.4	0.59	10.4
12.4	0.51	0.41	0.6	10.9
13.61	0.52	0.43	0.61	11.4
14.94	0.53	0.44	0.62	11.9
16.4	0.54	0.45	0.63	12.4
18	0.55	0.46	0.64	13
19.76	0.57	0.48	0.65	13.5
21.69	0.58	0.5	0.66	14.1
23.81	0.59	0.51	0.67	14.7
26.14	0.6	0.53	0.68	15.3
28.7	0.62	0.54	0.69	15.9
31.5	0.63	0.55	0.7	16.5
34.58	0.65	0.57	0.72	17.1
37.97	0.67	0.6	0.75	17.7
41.68	0.71	0.63	0.79	18.4
45.75	0.76	0.68	0.84	19.1
50.22	0.82	0.73	0.91	19.9
55.13	0.89	0.8	0.99	20.7
60.52	0.98	0.87	1.08	21.6
66.44	1.08	0.96	1.2	22.6
72.94	1.2	1.06	1.35	23.7
80.07	1.36	1.18	1.54	24.9
87.9	1.54	1.33	1.76	26.2
96.49	1.77	1.51	2.03	27.8
105.9	2.02	1.72	2.31	29.5
116.3	2.28	1.95	2.6	31.5
127.6	2.53	2.19	2.87	33.8
140.1	2.75	2.4	3.09	36.4
153.8	2.92	2.56	3.27	39.1
168.9	3.02	2.65	3.39	42
185.4	3.07	2.7	3.45	45
203.5	3.08	2.72	3.44	48.1
223.4	3.06	2.74	3.39	51.2
245.2	3.05	2.78	3.32	54.3
269.2	3.05	2.82	3.29	57.3
295.5	3.06	2.82	3.29	60.4
324.4	3.04	2.77	3.31	63.4
356.1	2.96	2.62	3.31	66.5
390.9	2.81	2.37	3.26	69.4
429.2	2.61	2.05	3.17	72.2
471.1	2.38	1.72	3.03	74.8
517.2	2.17	1.46	2.88	77.2
567.7	2.03	1.31	2.76	79.4
623.3	1.97	1.29	2.65	81.4

684.2	1.96	1.39	2.53	83.4
751.1	1.96	1.55	2.38	85.4
824.5	1.94	1.64	2.25	87.3
905.1	1.88	1.31	2.45	89.3
993.6	1.78	0.68	2.88	91.1
1091	1.65	0	3.47	92.9
1197	1.58	0	4.06	94.6
1314	1.59	0	4.49	96.2
1443	1.3	0	3.72	97.7
1584	0.75	0	2.13	99
1739	0.19	0	0.54	99.8
1909	0.021	0	0.059	99.98

**Site 6: Ice Type B (2)**

<b>Channel Diameter</b>	<b>Diff.</b>	<b>-2 S.D.</b>	<b>+2 S.D.</b>	<b>Cum. &lt;</b>
<b>um</b>	<b>Volume</b>	<b>Diff.</b>	<b>Diff.</b>	<b>Volume</b>
	<b>%</b>	<b>Volume</b>	<b>Volume</b>	<b>%</b>
		<b>%</b>	<b>%</b>	
0.393	0.067	0.062	0.073	0
0.431	0.12	0.11	0.13	0.067
0.474	0.17	0.16	0.19	0.19
0.52	0.24	0.23	0.26	0.36
0.571	0.3	0.28	0.32	0.6
0.627	0.35	0.33	0.36	0.91
0.688	0.39	0.37	0.4	1.25
0.755	0.42	0.41	0.44	1.64
0.829	0.45	0.43	0.47	2.06
0.91	0.47	0.44	0.49	2.51
0.999	0.47	0.44	0.51	2.98
1.097	0.48	0.44	0.52	3.45
1.204	0.48	0.44	0.52	3.93
1.321	0.49	0.44	0.53	4.41
1.451	0.49	0.45	0.53	4.9
1.592	0.49	0.45	0.53	5.39
1.748	0.5	0.47	0.53	5.88
1.919	0.51	0.48	0.54	6.38
2.107	0.52	0.5	0.55	6.89
2.313	0.54	0.51	0.57	7.41
2.539	0.56	0.52	0.59	7.95
2.787	0.57	0.54	0.61	8.51
3.059	0.59	0.55	0.63	9.08
3.358	0.61	0.57	0.65	9.67

3.687	0.62	0.58	0.66	10.3
4.047	0.64	0.6	0.68	10.9
4.443	0.66	0.62	0.7	11.5
4.877	0.68	0.64	0.71	12.2
5.354	0.7	0.66	0.73	12.9
5.878	0.72	0.68	0.75	13.6
6.452	0.73	0.7	0.77	14.3
7.083	0.75	0.72	0.79	15
7.775	0.77	0.74	0.8	15.8
8.536	0.78	0.76	0.81	16.5
9.37	0.8	0.78	0.83	17.3
10.29	0.82	0.8	0.85	18.1
11.29	0.84	0.82	0.87	18.9
12.4	0.86	0.83	0.89	19.8
13.61	0.87	0.84	0.89	20.7
14.94	0.86	0.83	0.89	21.5
16.4	0.85	0.82	0.88	22.4
18	0.84	0.81	0.87	23.2
19.76	0.84	0.81	0.87	24.1
21.69	0.83	0.8	0.86	24.9
23.81	0.82	0.79	0.85	25.7
26.14	0.79	0.76	0.83	26.6
28.7	0.76	0.73	0.8	27.4
31.5	0.72	0.69	0.76	28.1
34.58	0.69	0.65	0.73	28.8
37.97	0.66	0.62	0.71	29.5
41.68	0.64	0.6	0.69	30.2
45.75	0.63	0.58	0.67	30.8
50.22	0.62	0.57	0.66	31.5
55.13	0.61	0.57	0.65	32.1
60.52	0.61	0.57	0.65	32.7
66.44	0.63	0.59	0.66	33.3
72.94	0.66	0.64	0.69	33.9
80.07	0.73	0.7	0.75	34.6
87.9	0.83	0.79	0.86	35.3
96.49	0.97	0.91	1.02	36.1
105.9	1.15	1.08	1.22	37.1
116.3	1.38	1.28	1.48	38.2
127.6	1.65	1.52	1.78	39.6
140.1	1.93	1.77	2.09	41.3
153.8	2.18	1.99	2.36	43.2
168.9	2.37	2.19	2.55	45.4
185.4	2.49	2.35	2.64	47.7
203.5	2.56	2.49	2.64	50.2

223.4	2.61	2.57	2.65	52.8
245.2	2.66	2.51	2.81	55.4
269.2	2.73	2.46	3	58.1
295.5	2.8	2.42	3.18	60.8
324.4	2.86	2.4	3.32	63.6
356.1	2.87	2.39	3.36	66.5
390.9	2.84	2.41	3.28	69.3
429.2	2.77	2.45	3.1	72.2
471.1	2.69	2.49	2.89	75
517.2	2.61	2.38	2.85	77.6
567.7	2.56	2.17	2.95	80.3
623.3	2.54	2.01	3.07	82.8
684.2	2.51	1.9	3.12	85.4
751.1	2.47	1.86	3.08	87.9
824.5	2.37	1.87	2.88	90.3
905.1	2.2	1.88	2.52	92.7
993.6	1.94	1.82	2.06	94.9
1091	1.57	1.32	1.83	96.8
1197	1.01	0.69	1.33	98.4
1314	0.46	0.24	0.69	99.4
1443	0.1	0.04	0.16	99.9
1584	0.0097	0.0023	0.017	99.99
1739	0	0	0	100
1909	0	0	0	100

**Site 6: Ice Type B (3)**

<b>Channel Diameter</b>	<b>Diff.</b>	<b>-2 S.D.</b>	<b>+2 S.D.</b>	<b>Cum. &lt;</b>
<b>um</b>	<b>Volume</b>	<b>Diff.</b>	<b>Diff.</b>	<b>Volume</b>
	<b>%</b>	<b>Volume</b>	<b>Volume</b>	<b>%</b>
		<b>%</b>	<b>%</b>	
0.393	0.16	0.16	0.16	0
0.431	0.28	0.28	0.29	0.16
0.474	0.42	0.41	0.42	0.44
0.52	0.6	0.59	0.6	0.86
0.571	0.74	0.73	0.75	1.46
0.627	0.87	0.86	0.88	2.2
0.688	0.98	0.97	0.99	3.07
0.755	1.09	1.08	1.1	4.05
0.829	1.18	1.17	1.19	5.14
0.91	1.25	1.24	1.26	6.32
0.999	1.3	1.29	1.31	7.57
1.097	1.34	1.33	1.35	8.87

1.204	1.37	1.35	1.38	10.2
1.321	1.39	1.37	1.4	11.6
1.451	1.4	1.38	1.41	13
1.592	1.4	1.39	1.42	14.4
1.748	1.41	1.4	1.43	15.8
1.919	1.42	1.41	1.44	17.2
2.107	1.44	1.42	1.45	18.6
2.313	1.45	1.44	1.47	20
2.539	1.47	1.46	1.49	21.5
2.787	1.5	1.49	1.51	23
3.059	1.53	1.52	1.54	24.5
3.358	1.57	1.55	1.58	26
3.687	1.61	1.59	1.62	27.6
4.047	1.66	1.64	1.67	29.2
4.443	1.71	1.69	1.72	30.8
4.877	1.76	1.74	1.78	32.5
5.354	1.82	1.8	1.84	34.3
5.878	1.88	1.85	1.9	36.1
6.452	1.94	1.91	1.96	38
7.083	2	1.97	2.03	39.9
7.775	2.06	2.03	2.09	41.9
8.536	2.12	2.09	2.16	44
9.37	2.19	2.15	2.22	46.1
10.29	2.25	2.21	2.29	48.3
11.29	2.31	2.28	2.35	50.6
12.4	2.37	2.33	2.4	52.9
13.61	2.4	2.37	2.44	55.2
14.94	2.42	2.39	2.46	57.6
16.4	2.43	2.4	2.46	60.1
18	2.43	2.4	2.47	62.5
19.76	2.44	2.4	2.48	64.9
21.69	2.44	2.4	2.48	67.4
23.81	2.42	2.39	2.46	69.8
26.14	2.37	2.35	2.4	72.2
28.7	2.3	2.29	2.31	74.6
31.5	2.21	2.2	2.22	76.9
34.58	2.12	2.1	2.14	79.1
37.97	2.04	2.01	2.06	81.2
41.68	1.95	1.92	1.97	83.3
45.75	1.84	1.83	1.86	85.2
50.22	1.72	1.71	1.73	87.1
55.13	1.57	1.56	1.58	88.8
60.52	1.43	1.4	1.45	90.3
66.44	1.32	1.28	1.35	91.8

72.94	1.25	1.2	1.31	93.1
80.07	1.22	1.14	1.3	94.3
87.9	1.19	1.08	1.3	95.6
96.49	1.11	0.97	1.25	96.8
105.9	0.93	0.79	1.08	97.9
116.3	0.67	0.54	0.8	98.8
127.6	0.36	0.28	0.45	99.5
140.1	0.13	0.095	0.17	99.8
153.8	0.024	0.016	0.032	99.97
168.9	0.0017	0.00098	0.0024	99.998
185.4	0	0	0	100
203.5	0	0	0	100
223.4	0	0	0	100
245.2	0	0	0	100
269.2	0	0	0	100
295.5	0	0	0	100
324.4	0	0	0	100
356.1	0	0	0	100
390.9	0	0	0	100
429.2	0	0	0	100
471.1	0	0	0	100
517.2	0	0	0	100
567.7	0	0	0	100
623.3	0	0	0	100
684.2	0	0	0	100
751.1	0	0	0	100
824.5	0	0	0	100
905.1	0	0	0	100
993.6	0	0	0	100
1091	0	0	0	100
1197	0	0	0	100
1314	0	0	0	100
1443	0	0	0	100
1584	0	0	0	100
1739	0	0	0	100
1909	0	0	0	100

**Site 6: Ice Type D (1)**

<b>Channel Diameter</b>	<b>Diff.</b>	<b>-2 S.D.</b>	<b>+2 S.D.</b>	<b>Cum. &lt;</b>
<b>µm</b>	<b>Volume</b>	<b>Diff.</b>	<b>Diff.</b>	<b>Volume</b>
	<b>%</b>	<b>Volume</b>	<b>Volume</b>	<b>%</b>
		<b>%</b>	<b>%</b>	
0.393	0.011	0.0095	0.012	0
0.431	0.02	0.018	0.022	0.011
0.474	0.033	0.03	0.036	0.03
0.52	0.045	0.041	0.049	0.063
0.571	0.055	0.05	0.061	0.11
0.627	0.064	0.058	0.07	0.16
0.688	0.072	0.065	0.078	0.23
0.755	0.077	0.071	0.084	0.3
0.829	0.081	0.074	0.088	0.38
0.91	0.083	0.077	0.09	0.46
0.999	0.084	0.078	0.09	0.54
1.097	0.084	0.079	0.09	0.63
1.204	0.084	0.079	0.089	0.71
1.321	0.084	0.079	0.088	0.79
1.451	0.084	0.079	0.088	0.88
1.592	0.085	0.08	0.089	0.96
1.748	0.087	0.082	0.091	1.05
1.919	0.09	0.085	0.094	1.13
2.107	0.094	0.089	0.099	1.22
2.313	0.099	0.093	0.1	1.32
2.539	0.1	0.098	0.11	1.41
2.787	0.11	0.1	0.12	1.52
3.059	0.12	0.11	0.13	1.63
3.358	0.13	0.11	0.14	1.75
3.687	0.13	0.12	0.15	1.87
4.047	0.14	0.12	0.16	2.01
4.443	0.15	0.13	0.17	2.15
4.877	0.15	0.13	0.18	2.29
5.354	0.16	0.14	0.19	2.45
5.878	0.17	0.14	0.2	2.61
6.452	0.18	0.15	0.2	2.78
7.083	0.18	0.15	0.21	2.96
7.775	0.19	0.16	0.22	3.14
8.536	0.2	0.16	0.23	3.33
9.37	0.2	0.17	0.24	3.53
10.29	0.21	0.18	0.24	3.73

11.29	0.22	0.18	0.25	3.94
12.4	0.22	0.18	0.26	4.15
13.61	0.22	0.19	0.26	4.37
14.94	0.22	0.19	0.25	4.6
16.4	0.22	0.19	0.25	4.82
18	0.21	0.19	0.24	5.03
19.76	0.21	0.19	0.24	5.25
21.69	0.22	0.2	0.24	5.46
23.81	0.22	0.2	0.25	5.68
26.14	0.23	0.21	0.25	5.9
28.7	0.22	0.2	0.24	6.13
31.5	0.21	0.2	0.23	6.35
34.58	0.2	0.19	0.21	6.57
37.97	0.19	0.19	0.19	6.76
41.68	0.19	0.19	0.19	6.95
45.75	0.19	0.19	0.19	7.14
50.22	0.19	0.18	0.19	7.33
55.13	0.19	0.18	0.19	7.52
60.52	0.21	0.2	0.22	7.7
66.44	0.28	0.27	0.29	7.91
72.94	0.42	0.4	0.43	8.19
80.07	0.64	0.62	0.66	8.6
87.9	1	0.95	1.05	9.24
96.49	1.57	1.5	1.65	10.2
105.9	2.42	2.32	2.52	11.8
116.3	3.53	3.41	3.65	14.2
127.6	4.8	4.66	4.94	17.8
140.1	6.04	5.88	6.21	22.6
153.8	7.07	6.88	7.26	28.6
168.9	7.72	7.51	7.92	35.7
185.4	7.88	7.69	8.07	43.4
203.5	7.55	7.4	7.7	51.3
223.4	6.84	6.74	6.95	58.8
245.2	5.92	5.82	6.02	65.7
269.2	4.92	4.79	5.04	71.6
295.5	3.94	3.83	4.06	76.5
324.4	3.09	3.04	3.14	80.5
356.1	2.4	2.35	2.46	83.5
390.9	1.88	1.73	2.04	85.9
429.2	1.5	1.3	1.71	87.8
471.1	1.22	1.02	1.41	89.3
517.2	1.01	0.87	1.14	90.5
567.7	0.85	0.77	0.92	91.6
623.3	0.69	0.56	0.82	92.4

684.2	0.53	0.37	0.7	93.1
751.1	0.45	0.31	0.59	93.6
824.5	0.46	0.37	0.54	94.1
905.1	0.44	0.4	0.49	94.5
993.6	0.4	0.37	0.43	95
1091	0.4	0.38	0.42	95.4
1197	0.48	0.46	0.5	95.8
1314	0.57	0.49	0.66	96.3
1443	0.67	0.52	0.83	96.8
1584	0.77	0.55	0.98	97.5
1739	0.85	0.58	1.11	98.3
1909	0.88	0.59	1.18	99.1

**Site 6: Ice Type D (2)**

<b>Channel Diameter</b>	<b>Diff.</b>	<b>-2 S.D.</b>	<b>+2 S.D.</b>	<b>Cum. &lt;</b>
<b>um</b>	<b>Volume</b>	<b>Diff.</b>	<b>Diff.</b>	<b>Volume</b>
	<b>%</b>	<b>Volume</b>	<b>Volume</b>	<b>%</b>
		<b>%</b>	<b>%</b>	
0.393	0.011	0.0098	0.011	0
0.431	0.02	0.019	0.022	0.011
0.474	0.033	0.031	0.036	0.031
0.52	0.045	0.042	0.049	0.064
0.571	0.056	0.052	0.06	0.11
0.627	0.065	0.061	0.069	0.17
0.688	0.073	0.068	0.077	0.23
0.755	0.079	0.074	0.083	0.3
0.829	0.083	0.078	0.087	0.38
0.91	0.085	0.081	0.09	0.46
0.999	0.087	0.083	0.091	0.55
1.097	0.087	0.084	0.091	0.64
1.204	0.088	0.085	0.09	0.72
1.321	0.088	0.085	0.09	0.81
1.451	0.088	0.086	0.091	0.9
1.592	0.089	0.087	0.092	0.99
1.748	0.092	0.089	0.094	1.08
1.919	0.095	0.091	0.098	1.17
2.107	0.099	0.095	0.1	1.26
2.313	0.1	0.099	0.11	1.36
2.539	0.11	0.1	0.11	1.46
2.787	0.11	0.11	0.12	1.57
3.059	0.12	0.11	0.13	1.69
3.358	0.13	0.12	0.13	1.81

3.687	0.13	0.12	0.14	1.93
4.047	0.14	0.13	0.15	2.07
4.443	0.14	0.13	0.16	2.2
4.877	0.15	0.13	0.16	2.35
5.354	0.15	0.14	0.17	2.49
5.878	0.16	0.14	0.17	2.65
6.452	0.16	0.14	0.18	2.8
7.083	0.16	0.14	0.18	2.96
7.775	0.17	0.14	0.19	3.13
8.536	0.17	0.15	0.19	3.29
9.37	0.17	0.15	0.19	3.46
10.29	0.17	0.15	0.19	3.63
11.29	0.17	0.15	0.2	3.8
12.4	0.18	0.15	0.2	3.97
13.61	0.18	0.16	0.2	4.15
14.94	0.18	0.16	0.2	4.33
16.4	0.17	0.15	0.19	4.5
18	0.17	0.15	0.18	4.68
19.76	0.16	0.15	0.18	4.84
21.69	0.16	0.15	0.17	5
23.81	0.16	0.15	0.18	5.16
26.14	0.16	0.15	0.17	5.33
28.7	0.16	0.15	0.17	5.49
31.5	0.15	0.14	0.16	5.65
34.58	0.14	0.14	0.15	5.79
37.97	0.14	0.13	0.14	5.94
41.68	0.14	0.13	0.14	6.07
45.75	0.14	0.13	0.14	6.21
50.22	0.13	0.13	0.13	6.35
55.13	0.13	0.12	0.13	6.48
60.52	0.15	0.14	0.15	6.61
66.44	0.21	0.2	0.21	6.75
72.94	0.33	0.33	0.34	6.96
80.07	0.55	0.54	0.55	7.29
87.9	0.9	0.87	0.92	7.84
96.49	1.46	1.41	1.51	8.73
105.9	2.31	2.23	2.38	10.2
116.3	3.42	3.33	3.52	12.5
127.6	4.73	4.62	4.85	15.9
140.1	6.07	5.92	6.22	20.7
153.8	7.21	7.02	7.4	26.7
168.9	7.97	7.75	8.18	33.9
185.4	8.2	7.97	8.43	41.9
203.5	7.91	7.68	8.14	50.1

223.4	7.19	6.96	7.42	58
245.2	6.23	5.99	6.46	65.2
269.2	5.17	4.93	5.41	71.4
295.5	4.14	3.92	4.36	76.6
324.4	3.24	3.07	3.41	80.7
356.1	2.51	2.41	2.61	84
390.9	1.95	1.9	2	86.5
429.2	1.51	1.47	1.54	88.4
471.1	1.15	1.13	1.18	89.9
517.2	0.89	0.87	0.91	91.1
567.7	0.73	0.67	0.78	92
623.3	0.6	0.52	0.68	92.7
684.2	0.45	0.4	0.49	93.3
751.1	0.37	0.32	0.43	93.8
824.5	0.42	0.34	0.5	94.1
905.1	0.41	0.33	0.49	94.6
993.6	0.29	0.19	0.39	95
1091	0.27	0.13	0.4	95.3
1197	0.38	0.19	0.56	95.5
1314	0.5	0.27	0.74	95.9
1443	0.66	0.35	0.97	96.4
1584	0.87	0.44	1.31	97.1
1739	1.03	0.48	1.58	97.9
1909	1.03	0.44	1.62	99

**Site 6: Ice Type D (3)**

<b>Channel Diameter</b>	<b>Diff.</b>	<b>-2 S.D.</b>	<b>+2 S.D.</b>	<b>Cum. &lt;</b>
<b>µm</b>	<b>Volume</b>	<b>Diff.</b>	<b>Diff.</b>	<b>Volume</b>
	<b>%</b>	<b>Volume</b>	<b>Volume</b>	<b>%</b>
		<b>%</b>	<b>%</b>	
0.393	0.015	0.011	0.019	0
0.431	0.028	0.02	0.036	0.015
0.474	0.047	0.034	0.059	0.043
0.52	0.063	0.047	0.079	0.09
0.571	0.077	0.059	0.096	0.15
0.627	0.089	0.07	0.11	0.23
0.688	0.098	0.08	0.12	0.32
0.755	0.11	0.089	0.12	0.42
0.829	0.11	0.096	0.12	0.52
0.91	0.11	0.1	0.12	0.63
0.999	0.11	0.11	0.12	0.74
1.097	0.11	0.11	0.12	0.86

1.204	0.11	0.11	0.12	0.97
1.321	0.11	0.11	0.12	1.08
1.451	0.12	0.11	0.12	1.2
1.592	0.12	0.11	0.13	1.31
1.748	0.13	0.11	0.14	1.43
1.919	0.13	0.12	0.15	1.56
2.107	0.14	0.12	0.16	1.69
2.313	0.15	0.12	0.18	1.83
2.539	0.16	0.12	0.19	1.98
2.787	0.16	0.13	0.2	2.14
3.059	0.17	0.14	0.2	2.3
3.358	0.18	0.14	0.21	2.47
3.687	0.18	0.15	0.22	2.65
4.047	0.19	0.16	0.23	2.83
4.443	0.2	0.16	0.24	3.02
4.877	0.21	0.17	0.25	3.22
5.354	0.21	0.17	0.26	3.43
5.878	0.22	0.18	0.27	3.64
6.452	0.23	0.18	0.27	3.86
7.083	0.23	0.19	0.28	4.09
7.775	0.24	0.2	0.28	4.32
8.536	0.24	0.2	0.28	4.56
9.37	0.25	0.21	0.28	4.8
10.29	0.25	0.22	0.28	5.04
11.29	0.26	0.22	0.29	5.29
12.4	0.26	0.22	0.3	5.55
13.61	0.26	0.22	0.31	5.81
14.94	0.26	0.22	0.31	6.08
16.4	0.26	0.22	0.29	6.34
18	0.25	0.22	0.27	6.6
19.76	0.24	0.22	0.26	6.84
21.69	0.24	0.22	0.26	7.08
23.81	0.24	0.21	0.27	7.32
26.14	0.24	0.2	0.28	7.56
28.7	0.22	0.19	0.26	7.8
31.5	0.2	0.18	0.22	8.03
34.58	0.18	0.17	0.19	8.22
37.97	0.17	0.16	0.18	8.4
41.68	0.18	0.15	0.2	8.57
45.75	0.18	0.14	0.21	8.75
50.22	0.16	0.14	0.17	8.92
55.13	0.13	0.12	0.14	9.08
60.52	0.14	0.12	0.16	9.21
66.44	0.22	0.21	0.23	9.36

72.94	0.39	0.34	0.43	9.58
80.07	0.65	0.59	0.71	9.97
87.9	1.05	1.01	1.1	10.6
96.49	1.69	1.66	1.72	11.7
105.9	2.64	2.61	2.66	13.4
116.3	3.87	3.81	3.92	16
127.6	5.24	5.12	5.36	19.9
140.1	6.56	6.37	6.75	25.1
153.8	7.6	7.33	7.86	31.7
168.9	8.18	7.85	8.52	39.3
185.4	8.21	7.84	8.59	47.4
203.5	7.73	7.35	8.1	55.7
223.4	6.89	6.53	7.25	63.4
245.2	5.91	5.58	6.23	70.3
269.2	4.89	4.67	5.12	76.2
295.5	3.93	3.77	4.09	81.1
324.4	3.11	2.81	3.41	85
356.1	2.48	2.09	2.87	88.1
390.9	1.99	1.62	2.36	90.6
429.2	1.53	1.25	1.81	92.6
471.1	1.08	0.94	1.22	94.1
517.2	0.8	0.64	0.95	95.2
567.7	0.78	0.6	0.95	96
623.3	0.81	0.56	1.05	96.8
684.2	0.57	0.14	1	97.6
751.1	0.37	0	1	98.2
824.5	0.4	0	1.12	98.5
905.1	0.35	0	0.98	98.9
993.6	0.16	0	0.45	99.3
1091	0.12	0	0.34	99.4
1197	0.2	0	0.55	99.6
1314	0.14	0	0.42	99.8
1443	0.057	0	0.23	99.9
1584	0.033	0	0.15	99.96
1739	0.005	0	0.022	99.99
1909	0	0	0	100

**Site 6: Ice Type E (1)**

<b>Channel Diameter</b>	<b>Diff.</b>	<b>-2 S.D.</b>	<b>+2 S.D.</b>	<b>Cum. &lt;</b>
<b>µm</b>	<b>Volume</b>	<b>Diff.</b>	<b>Diff.</b>	<b>Volume</b>
	<b>%</b>	<b>Volume</b>	<b>Volume</b>	<b>%</b>
		<b>%</b>	<b>%</b>	

0.393	0.046	0.045	0.048	0
0.431	0.083	0.081	0.085	0.046
0.474	0.12	0.12	0.12	0.13
0.52	0.17	0.17	0.18	0.25
0.571	0.22	0.21	0.22	0.43
0.627	0.26	0.25	0.26	0.64
0.688	0.29	0.29	0.29	0.9
0.755	0.32	0.32	0.33	1.19
0.829	0.35	0.35	0.35	1.51
0.91	0.37	0.37	0.38	1.86
0.999	0.39	0.38	0.39	2.23
1.097	0.4	0.39	0.41	2.62
1.204	0.41	0.4	0.42	3.02
1.321	0.41	0.4	0.42	3.43
1.451	0.41	0.4	0.42	3.84
1.592	0.41	0.4	0.41	4.25
1.748	0.41	0.4	0.41	4.66
1.919	0.4	0.4	0.41	5.06
2.107	0.4	0.39	0.41	5.47
2.313	0.4	0.39	0.41	5.87
2.539	0.4	0.38	0.42	6.27
2.787	0.4	0.38	0.43	6.67
3.059	0.41	0.38	0.44	7.07
3.358	0.42	0.39	0.46	7.48
3.687	0.44	0.41	0.48	7.91
4.047	0.47	0.43	0.5	8.35
4.443	0.5	0.46	0.53	8.82
4.877	0.54	0.51	0.57	9.32
5.354	0.59	0.56	0.62	9.86
5.878	0.65	0.63	0.68	10.4
6.452	0.72	0.71	0.74	11.1
7.083	0.81	0.8	0.82	11.8
7.775	0.91	0.91	0.91	12.6
8.536	1.03	1.02	1.04	13.5
9.37	1.16	1.14	1.18	14.6
10.29	1.32	1.29	1.35	15.7
11.29	1.51	1.47	1.54	17.1
12.4	1.73	1.69	1.77	18.6
13.61	1.99	1.93	2.04	20.3
14.94	2.27	2.2	2.34	22.3
16.4	2.59	2.5	2.68	24.5
18	2.95	2.85	3.04	27.1
19.76	3.35	3.26	3.44	30.1
21.69	3.78	3.7	3.87	33.4

23.81	4.22	4.14	4.3	37.2
26.14	4.62	4.54	4.7	41.4
28.7	4.96	4.87	5.06	46.1
31.5	5.26	5.12	5.4	51
34.58	5.55	5.35	5.75	56.3
37.97	5.86	5.59	6.14	61.8
41.68	6.17	5.83	6.51	67.7
45.75	6.33	5.99	6.66	73.9
50.22	6.12	5.91	6.32	80.2
55.13	5.38	5.33	5.43	86.3
60.52	4.13	3.79	4.46	91.7
66.44	2.58	1.93	3.22	95.8
72.94	1.19	0.59	1.79	98.4
80.07	0.35	0.015	0.69	99.6
87.9	0.055	0	0.13	99.9
96.49	0.0032	0	0.0091	99.997
105.9	0	0	0	100
116.3	0	0	0	100
127.6	0	0	0	100
140.1	0	0	0	100
153.8	0	0	0	100
168.9	0	0	0	100
185.4	0	0	0	100
203.5	0	0	0	100
223.4	0	0	0	100
245.2	0	0	0	100
269.2	0	0	0	100
295.5	0	0	0	100
324.4	0	0	0	100
356.1	0	0	0	100
390.9	0	0	0	100
429.2	0	0	0	100
471.1	0	0	0	100
517.2	0	0	0	100
567.7	0	0	0	100
623.3	0	0	0	100
684.2	0	0	0	100
751.1	0	0	0	100
824.5	0	0	0	100
905.1	0	0	0	100
993.6	0	0	0	100
1091	0	0	0	100
1197	0	0	0	100
1314	0	0	0	100

1443	0	0	0	100
1584	0	0	0	100
1739	0	0	0	100
1909	0	0	0	100

**Site 6: Ice Type E (2)**

<b>Channel Diameter</b>	<b>Diff.</b>	<b>-2 S.D.</b>	<b>+2 S.D.</b>	<b>Cum. &lt;</b>
<b>um</b>	<b>Volume</b>	<b>Diff.</b>	<b>Diff.</b>	<b>Volume</b>
	<b>%</b>	<b>Volume</b>	<b>Volume</b>	<b>%</b>
		<b>%</b>	<b>%</b>	
0.393	0.048	0.045	0.05	0
0.431	0.085	0.081	0.09	0.048
0.474	0.13	0.12	0.13	0.13
0.52	0.18	0.17	0.19	0.26
0.571	0.22	0.21	0.23	0.44
0.627	0.26	0.25	0.27	0.66
0.688	0.3	0.29	0.31	0.92
0.755	0.33	0.32	0.34	1.22
0.829	0.36	0.35	0.37	1.55
0.91	0.38	0.38	0.39	1.91
0.999	0.4	0.39	0.4	2.3
1.097	0.41	0.41	0.41	2.69
1.204	0.42	0.41	0.42	3.1
1.321	0.42	0.42	0.42	3.52
1.451	0.42	0.42	0.42	3.94
1.592	0.42	0.41	0.42	4.36
1.748	0.41	0.41	0.42	4.78
1.919	0.41	0.4	0.42	5.2
2.107	0.41	0.39	0.42	5.61
2.313	0.41	0.38	0.43	6.01
2.539	0.41	0.38	0.43	6.42
2.787	0.41	0.37	0.44	6.83
3.059	0.42	0.38	0.46	7.23
3.358	0.43	0.39	0.47	7.65
3.687	0.45	0.4	0.49	8.08
4.047	0.47	0.42	0.52	8.53
4.443	0.51	0.45	0.56	9
4.877	0.55	0.5	0.6	9.51
5.354	0.6	0.55	0.65	10.1
5.878	0.66	0.62	0.7	10.7
6.452	0.73	0.7	0.77	11.3
7.083	0.82	0.79	0.85	12

7.775	0.92	0.9	0.95	12.9
8.536	1.04	1.03	1.05	13.8
9.37	1.18	1.17	1.18	14.8
10.29	1.34	1.32	1.35	16
11.29	1.54	1.52	1.56	17.3
12.4	1.77	1.74	1.8	18.9
13.61	2.04	2	2.08	20.7
14.94	2.33	2.28	2.38	22.7
16.4	2.66	2.62	2.71	25
18	3.04	3.02	3.07	27.7
19.76	3.47	3.42	3.51	30.7
21.69	3.9	3.84	3.97	34.2
23.81	4.3	4.25	4.35	38.1
26.14	4.64	4.62	4.66	42.4
28.7	4.93	4.83	5.04	47
31.5	5.27	5.09	5.45	52
34.58	5.72	5.49	5.95	57.2
37.97	6.28	6.03	6.54	63
41.68	6.78	6.54	7.02	69.2
45.75	6.91	6.74	7.08	76
50.22	6.38	6.32	6.43	82.9
55.13	5.1	4.98	5.23	89.3
60.52	3.35	3.08	3.61	94.4
66.44	1.63	1.38	1.88	97.8
72.94	0.51	0.37	0.66	99.4
80.07	0.082	0.047	0.12	99.9
87.9	0.0046	0.0011	0.008	99.995
96.49	0	0	0	100
105.9	0	0	0	100
116.3	0	0	0	100
127.6	0	0	0	100
140.1	0	0	0	100
153.8	0	0	0	100
168.9	0	0	0	100
185.4	0	0	0	100
203.5	0	0	0	100
223.4	0	0	0	100
245.2	0	0	0	100
269.2	0	0	0	100
295.5	0	0	0	100
324.4	0	0	0	100
356.1	0	0	0	100
390.9	0	0	0	100
429.2	0	0	0	100

471.1	0	0	0	100
517.2	0	0	0	100
567.7	0	0	0	100
623.3	0	0	0	100
684.2	0	0	0	100
751.1	0	0	0	100
824.5	0	0	0	100
905.1	0	0	0	100
993.6	0	0	0	100
1091	0	0	0	100
1197	0	0	0	100
1314	0	0	0	100
1443	0	0	0	100
1584	0	0	0	100
1739	0	0	0	100
1909	0	0	0	100

**Site 6: Ice Type E (3)**

<b>Channel Diameter</b>	<b>Diff.</b>	<b>-2 S.D.</b>	<b>+2 S.D.</b>	<b>Cum. &lt;</b>
<b>um</b>	<b>Volume</b>	<b>Diff.</b>	<b>Diff.</b>	<b>Volume</b>
	<b>%</b>	<b>Volume</b>	<b>Volume</b>	<b>%</b>
		<b>%</b>	<b>%</b>	
0.393	0.047	0.045	0.049	0
0.431	0.083	0.08	0.087	0.047
0.474	0.12	0.12	0.13	0.13
0.52	0.18	0.17	0.18	0.25
0.571	0.22	0.21	0.23	0.43
0.627	0.26	0.25	0.26	0.65
0.688	0.29	0.28	0.3	0.9
0.755	0.33	0.32	0.33	1.2
0.829	0.35	0.35	0.36	1.52
0.91	0.38	0.37	0.38	1.88
0.999	0.39	0.39	0.4	2.25
1.097	0.4	0.4	0.41	2.65
1.204	0.41	0.41	0.42	3.05
1.321	0.42	0.41	0.42	3.46
1.451	0.42	0.41	0.42	3.88
1.592	0.42	0.41	0.42	4.3
1.748	0.41	0.4	0.42	4.71
1.919	0.41	0.4	0.42	5.13
2.107	0.41	0.39	0.42	5.54
2.313	0.41	0.39	0.42	5.95

2.539	0.41	0.38	0.43	6.35
2.787	0.41	0.38	0.44	6.76
3.059	0.42	0.38	0.45	7.17
3.358	0.43	0.39	0.47	7.58
3.687	0.45	0.41	0.49	8.01
4.047	0.47	0.43	0.51	8.46
4.443	0.5	0.46	0.55	8.93
4.877	0.54	0.5	0.59	9.43
5.354	0.6	0.55	0.64	9.98
5.878	0.65	0.62	0.69	10.6
6.452	0.73	0.7	0.76	11.2
7.083	0.81	0.78	0.84	12
7.775	0.91	0.89	0.93	12.8
8.536	1.03	1.01	1.04	13.7
9.37	1.16	1.14	1.18	14.7
10.29	1.32	1.29	1.34	15.9
11.29	1.51	1.48	1.54	17.2
12.4	1.73	1.7	1.77	18.7
13.61	1.99	1.94	2.03	20.4
14.94	2.27	2.22	2.33	22.4
16.4	2.59	2.54	2.65	24.7
18	2.96	2.91	3	27.3
19.76	3.36	3.31	3.42	30.2
21.69	3.79	3.73	3.86	33.6
23.81	4.2	4.15	4.25	37.4
26.14	4.56	4.55	4.57	41.6
28.7	4.88	4.79	4.96	46.1
31.5	5.21	5.07	5.35	51
34.58	5.63	5.47	5.79	56.2
37.97	6.13	5.97	6.29	61.9
41.68	6.61	6.45	6.77	68
45.75	6.82	6.7	6.94	74.6
50.22	6.46	6.43	6.49	81.4
55.13	5.4	5.24	5.56	87.9
60.52	3.8	3.51	4.1	93.3
66.44	2.03	1.76	2.31	97.1
72.94	0.74	0.58	0.89	99.1
80.07	0.13	0.097	0.17	99.9
87.9	0.0098	0.0058	0.014	99.99
96.49	0	0	0	100
105.9	0	0	0	100
116.3	0	0	0	100
127.6	0	0	0	100
140.1	0	0	0	100

153.8	0	0	0	100
168.9	0	0	0	100
185.4	0	0	0	100
203.5	0	0	0	100
223.4	0	0	0	100
245.2	0	0	0	100
269.2	0	0	0	100
295.5	0	0	0	100
324.4	0	0	0	100
356.1	0	0	0	100
390.9	0	0	0	100
429.2	0	0	0	100
471.1	0	0	0	100
517.2	0	0	0	100
567.7	0	0	0	100
623.3	0	0	0	100
684.2	0	0	0	100
751.1	0	0	0	100
824.5	0	0	0	100
905.1	0	0	0	100
993.6	0	0	0	100
1091	0	0	0	100
1197	0	0	0	100
1314	0	0	0	100
1443	0	0	0	100
1584	0	0	0	100
1739	0	0	0	100
1909	0	0	0	100

**Site 6: Moraine 0-30cm**

<b>Channel Diameter</b>	<b>Diff.</b>	<b>-2 S.D.</b>	<b>+2 S.D.</b>	<b>Cum. &lt;</b>
<b>um</b>	<b>Volume</b>	<b>Diff.</b>	<b>Diff.</b>	<b>Volume</b>
	<b>%</b>	<b>Volume</b>	<b>Volume</b>	<b>%</b>
		<b>%</b>	<b>%</b>	
0.393	0.026	0.024	0.028	0
0.431	0.046	0.043	0.05	0.026
0.474	0.068	0.064	0.073	0.073
0.52	0.097	0.09	0.1	0.14
0.571	0.12	0.11	0.13	0.24
0.627	0.14	0.13	0.15	0.36
0.688	0.16	0.14	0.17	0.5
0.755	0.17	0.16	0.19	0.65

0.829	0.19	0.17	0.21	0.83
0.91	0.19	0.17	0.22	1.01
0.999	0.2	0.18	0.23	1.21
1.097	0.2	0.18	0.23	1.41
1.204	0.21	0.18	0.23	1.61
1.321	0.21	0.18	0.24	1.82
1.451	0.21	0.18	0.24	2.03
1.592	0.21	0.18	0.23	2.23
1.748	0.21	0.18	0.23	2.44
1.919	0.21	0.18	0.23	2.65
2.107	0.21	0.19	0.24	2.85
2.313	0.22	0.19	0.24	3.07
2.539	0.22	0.2	0.25	3.28
2.787	0.23	0.21	0.25	3.5
3.059	0.24	0.22	0.27	3.74
3.358	0.26	0.23	0.28	3.98
3.687	0.27	0.24	0.3	4.24
4.047	0.29	0.26	0.33	4.51
4.443	0.31	0.27	0.36	4.8
4.877	0.34	0.29	0.39	5.12
5.354	0.36	0.31	0.42	5.45
5.878	0.39	0.33	0.46	5.82
6.452	0.43	0.35	0.5	6.21
7.083	0.46	0.37	0.55	6.64
7.775	0.5	0.4	0.59	7.1
8.536	0.53	0.42	0.64	7.59
9.37	0.57	0.45	0.69	8.13
10.29	0.62	0.49	0.74	8.7
11.29	0.66	0.53	0.8	9.32
12.4	0.71	0.57	0.85	9.98
13.61	0.76	0.62	0.89	10.7
14.94	0.8	0.66	0.94	11.4
16.4	0.84	0.71	0.98	12.2
18	0.89	0.76	1.02	13.1
19.76	0.94	0.81	1.07	14
21.69	0.99	0.87	1.12	14.9
23.81	1.05	0.93	1.17	15.9
26.14	1.11	1	1.22	17
28.7	1.17	1.07	1.27	18.1
31.5	1.23	1.14	1.31	19.2
34.58	1.29	1.21	1.36	20.5
37.97	1.34	1.28	1.4	21.8
41.68	1.39	1.33	1.45	23.1
45.75	1.45	1.39	1.5	24.5

50.22	1.5	1.45	1.56	25.9
55.13	1.56	1.51	1.62	27.4
60.52	1.64	1.59	1.68	29
66.44	1.72	1.68	1.76	30.6
72.94	1.81	1.78	1.84	32.4
80.07	1.9	1.87	1.92	34.2
87.9	1.99	1.96	2.01	36.1
96.49	2.07	2.04	2.1	38
105.9	2.15	2.11	2.19	40.1
116.3	2.22	2.17	2.27	42.3
127.6	2.29	2.23	2.35	44.5
140.1	2.34	2.26	2.42	46.8
153.8	2.37	2.25	2.48	49.1
168.9	2.36	2.21	2.5	51.5
185.4	2.31	2.15	2.48	53.8
203.5	2.25	2.07	2.43	56.1
223.4	2.19	2.02	2.36	58.4
245.2	2.16	2.02	2.3	60.6
269.2	2.16	2.06	2.25	62.7
295.5	2.18	2.11	2.25	64.9
324.4	2.2	2.12	2.28	67.1
356.1	2.19	2.09	2.3	69.3
390.9	2.16	2.06	2.26	71.5
429.2	2.1	2.01	2.2	73.6
471.1	2.04	1.88	2.2	75.7
517.2	1.99	1.74	2.25	77.8
567.7	1.98	1.62	2.33	79.8
623.3	1.98	1.56	2.41	81.7
684.2	2	1.54	2.46	83.7
751.1	2.01	1.56	2.47	85.7
824.5	2	1.56	2.43	87.7
905.1	1.94	1.54	2.35	89.7
993.6	1.84	1.47	2.22	91.7
1091	1.72	1.39	2.04	93.5
1197	1.58	1.34	1.82	95.3
1314	1.43	1.29	1.57	96.8
1443	1.05	0.97	1.12	98.3
1584	0.55	0.5	0.6	99.3
1739	0.13	0.12	0.15	99.9
1909	0.014	0.012	0.016	99.99

**Site 6: Moraine 30-60cm**

<b>Channel Diameter</b>	<b>Diff.</b>	<b>-2 S.D.</b>	<b>+2 S.D.</b>	<b>Cum. &lt;</b>
<b>µm</b>	<b>Volume</b>	<b>Diff.</b>	<b>Diff.</b>	<b>Volume</b>
	<b>%</b>	<b>Volume</b>	<b>Volume</b>	<b>%</b>
		<b>%</b>	<b>%</b>	
0.393	0.026	0.024	0.027	0
0.431	0.046	0.043	0.048	0.026
0.474	0.067	0.064	0.07	0.071
0.52	0.096	0.091	0.1	0.14
0.571	0.12	0.11	0.12	0.23
0.627	0.14	0.13	0.15	0.35
0.688	0.16	0.15	0.16	0.49
0.755	0.17	0.17	0.18	0.65
0.829	0.19	0.18	0.2	0.82
0.91	0.2	0.19	0.21	1.01
0.999	0.2	0.19	0.21	1.21
1.097	0.21	0.2	0.22	1.41
1.204	0.21	0.2	0.22	1.62
1.321	0.21	0.2	0.22	1.83
1.451	0.21	0.2	0.22	2.05
1.592	0.21	0.2	0.22	2.26
1.748	0.21	0.2	0.22	2.47
1.919	0.21	0.2	0.22	2.68
2.107	0.21	0.2	0.23	2.89
2.313	0.21	0.2	0.23	3.11
2.539	0.22	0.2	0.23	3.32
2.787	0.22	0.2	0.24	3.54
3.059	0.23	0.21	0.25	3.76
3.358	0.24	0.22	0.27	3.99
3.687	0.26	0.23	0.28	4.23
4.047	0.27	0.24	0.3	4.49
4.443	0.29	0.26	0.32	4.76
4.877	0.31	0.28	0.35	5.05
5.354	0.34	0.3	0.37	5.36
5.878	0.36	0.32	0.4	5.7
6.452	0.4	0.35	0.44	6.06
7.083	0.43	0.38	0.47	6.46
7.775	0.47	0.42	0.51	6.89
8.536	0.51	0.46	0.56	7.35
9.37	0.55	0.5	0.6	7.86
10.29	0.6	0.55	0.65	8.41
11.29	0.66	0.61	0.71	9.01
12.4	0.72	0.67	0.76	9.67

13.61	0.78	0.74	0.83	10.4
14.94	0.86	0.81	0.9	11.2
16.4	0.93	0.89	0.97	12
18	1.02	0.97	1.06	13
19.76	1.11	1.06	1.16	14
21.69	1.21	1.15	1.28	15.1
23.81	1.32	1.24	1.4	16.3
26.14	1.44	1.34	1.53	17.6
28.7	1.56	1.45	1.68	19.1
31.5	1.7	1.56	1.83	20.6
34.58	1.83	1.67	1.99	22.3
37.97	1.96	1.77	2.14	24.2
41.68	2.08	1.87	2.28	26.1
45.75	2.18	1.95	2.4	28.2
50.22	2.26	2.02	2.49	30.4
55.13	2.31	2.07	2.55	32.6
60.52	2.35	2.11	2.59	34.9
66.44	2.37	2.13	2.6	37.3
72.94	2.36	2.14	2.59	39.7
80.07	2.34	2.13	2.56	42
87.9	2.3	2.09	2.52	44.4
96.49	2.24	2.03	2.46	46.7
105.9	2.17	1.96	2.39	48.9
116.3	2.09	1.88	2.31	51.1
127.6	2.01	1.8	2.22	53.2
140.1	1.93	1.73	2.14	55.2
153.8	1.84	1.64	2.05	57.1
168.9	1.74	1.54	1.94	59
185.4	1.61	1.42	1.8	60.7
203.5	1.49	1.31	1.66	62.3
223.4	1.39	1.24	1.54	63.8
245.2	1.35	1.21	1.48	65.2
269.2	1.37	1.24	1.49	66.5
295.5	1.44	1.32	1.57	67.9
324.4	1.56	1.42	1.71	69.4
356.1	1.68	1.49	1.88	70.9
390.9	1.78	1.49	2.07	72.6
429.2	1.84	1.44	2.24	74.4
471.1	1.87	1.39	2.35	76.2
517.2	1.87	1.37	2.37	78.1
567.7	1.87	1.42	2.32	80
623.3	1.87	1.52	2.21	81.8
684.2	1.87	1.59	2.14	83.7
751.1	1.86	1.48	2.25	85.6

824.5	1.85	1.26	2.43	87.4
905.1	1.82	1.05	2.6	89.3
993.6	1.78	0.86	2.71	91.1
1091	1.73	0.71	2.75	92.9
1197	1.68	0.6	2.76	94.6
1314	1.62	0.51	2.73	96.3
1443	1.25	0.35	2.14	97.9
1584	0.68	0.17	1.18	99.1
1739	0.17	0.04	0.29	99.8
1909	0.018	0.0038	0.032	99.98

**Site 6: Moraine 60-100cm**

<b>Channel Diameter</b>	<b>Diff.</b>	<b>-2 S.D.</b>	<b>+2 S.D.</b>	<b>Cum. &lt;</b>
<b>µm</b>	<b>Volume</b>	<b>Diff.</b>	<b>Diff.</b>	<b>Volume</b>
	<b>%</b>	<b>Volume</b>	<b>Volume</b>	<b>%</b>
		<b>%</b>	<b>%</b>	
0.393	0.037	0.035	0.04	0
0.431	0.067	0.063	0.071	0.037
0.474	0.098	0.093	0.1	0.1
0.52	0.14	0.13	0.15	0.2
0.571	0.17	0.16	0.18	0.34
0.627	0.2	0.19	0.22	0.52
0.688	0.23	0.22	0.24	0.72
0.755	0.25	0.24	0.27	0.95
0.829	0.27	0.26	0.29	1.2
0.91	0.29	0.27	0.31	1.48
0.999	0.3	0.28	0.32	1.77
1.097	0.3	0.28	0.32	2.06
1.204	0.31	0.29	0.33	2.37
1.321	0.31	0.29	0.33	2.68
1.451	0.31	0.28	0.33	2.98
1.592	0.3	0.28	0.32	3.29
1.748	0.3	0.28	0.32	3.59
1.919	0.3	0.28	0.32	3.89
2.107	0.3	0.27	0.32	4.19
2.313	0.3	0.27	0.32	4.49
2.539	0.3	0.28	0.33	4.79
2.787	0.31	0.28	0.33	5.09
3.059	0.32	0.29	0.35	5.4
3.358	0.33	0.3	0.36	5.72
3.687	0.35	0.32	0.38	6.05
4.047	0.37	0.34	0.41	6.4

4.443	0.4	0.36	0.44	6.77
4.877	0.43	0.39	0.48	7.17
5.354	0.47	0.42	0.52	7.6
5.878	0.51	0.45	0.56	8.07
6.452	0.55	0.49	0.61	8.58
7.083	0.6	0.54	0.66	9.13
7.775	0.65	0.59	0.72	9.73
8.536	0.71	0.64	0.79	10.4
9.37	0.78	0.71	0.86	11.1
10.29	0.86	0.78	0.94	11.9
11.29	0.95	0.86	1.03	12.7
12.4	1.04	0.95	1.13	13.7
13.61	1.15	1.05	1.24	14.7
14.94	1.26	1.17	1.36	15.9
16.4	1.39	1.29	1.49	17.1
18	1.53	1.43	1.63	18.5
19.76	1.67	1.57	1.78	20.1
21.69	1.83	1.72	1.93	21.7
23.81	1.98	1.88	2.09	23.6
26.14	2.15	2.04	2.26	25.5
28.7	2.32	2.21	2.43	27.7
31.5	2.5	2.39	2.61	30
34.58	2.68	2.56	2.79	32.5
37.97	2.84	2.73	2.96	35.2
41.68	2.99	2.87	3.11	38
45.75	3.12	2.99	3.24	41
50.22	3.22	3.09	3.35	44.1
55.13	3.3	3.16	3.43	47.4
60.52	3.35	3.22	3.49	50.7
66.44	3.38	3.25	3.51	54
72.94	3.37	3.25	3.5	57.4
80.07	3.32	3.21	3.42	60.8
87.9	3.21	3.12	3.29	64.1
96.49	3.05	2.98	3.11	67.3
105.9	2.85	2.8	2.9	70.3
116.3	2.62	2.58	2.67	73.2
127.6	2.38	2.35	2.41	75.8
140.1	2.12	2.09	2.15	78.2
153.8	1.84	1.81	1.87	80.3
168.9	1.55	1.52	1.58	82.1
185.4	1.27	1.25	1.3	83.7
203.5	1.04	1.02	1.05	85
223.4	0.87	0.86	0.87	86
245.2	0.78	0.76	0.79	86.9

269.2	0.76	0.74	0.78	87.6
295.5	0.8	0.79	0.82	88.4
324.4	0.88	0.87	0.89	89.2
356.1	0.94	0.94	0.95	90.1
390.9	0.98	0.95	1.01	91
429.2	0.98	0.92	1.05	92
471.1	0.96	0.85	1.07	93
517.2	0.93	0.77	1.08	94
567.7	0.89	0.7	1.08	94.9
623.3	0.84	0.62	1.06	95.8
684.2	0.77	0.51	1.03	96.6
751.1	0.69	0.37	1.01	97.4
824.5	0.6	0.17	1.02	98.1
905.1	0.51	0	1.06	98.7
993.6	0.41	0	1.06	99.2
1091	0.27	0	0.82	99.6
1197	0.12	0	0.47	99.8
1314	0.028	0	0.12	99.97
1443	0.003	0	0.013	99.997
1584	0	0	0	100
1739	0	0	0	100
1909	0	0	0	100

**Site 7: Ice Type C (1)**

<b>Channel Diameter</b>	<b>Diff.</b>	<b>-2 S.D.</b>	<b>+2 S.D.</b>	<b>Cum. &lt;</b>
<b>µm</b>	<b>Volume</b>	<b>Diff.</b>	<b>Diff.</b>	<b>Volume</b>
	<b>%</b>	<b>Volume</b>	<b>Volume</b>	<b>%</b>
		<b>%</b>	<b>%</b>	
0.393	0.13	0.12	0.14	0
0.431	0.23	0.21	0.24	0.13
0.474	0.33	0.31	0.35	0.35
0.52	0.47	0.44	0.5	0.68
0.571	0.59	0.55	0.62	1.16
0.627	0.69	0.66	0.73	1.74
0.688	0.78	0.75	0.82	2.44
0.755	0.87	0.84	0.9	3.22
0.829	0.95	0.93	0.97	4.09
0.91	1.01	1	1.03	5.04
0.999	1.06	1.05	1.08	6.05
1.097	1.11	1.09	1.12	7.11
1.204	1.15	1.13	1.17	8.22
1.321	1.19	1.16	1.22	9.37

1.451	1.22	1.19	1.26	10.6
1.592	1.26	1.23	1.3	11.8
1.748	1.31	1.28	1.34	13
1.919	1.37	1.34	1.39	14.4
2.107	1.43	1.41	1.45	15.7
2.313	1.5	1.49	1.52	17.2
2.539	1.59	1.57	1.61	18.7
2.787	1.69	1.66	1.71	20.3
3.059	1.79	1.76	1.82	21.9
3.358	1.91	1.87	1.94	23.7
3.687	2.03	1.98	2.07	25.6
4.047	2.16	2.11	2.2	27.7
4.443	2.29	2.24	2.33	29.8
4.877	2.42	2.37	2.46	32.1
5.354	2.54	2.5	2.59	34.5
5.878	2.66	2.62	2.7	37.1
6.452	2.78	2.75	2.81	39.7
7.083	2.88	2.87	2.9	42.5
7.775	2.97	2.96	2.99	45.4
8.536	3.05	3.01	3.08	48.4
9.37	3.11	3.05	3.17	51.4
10.29	3.16	3.08	3.24	54.5
11.29	3.18	3.08	3.27	57.7
12.4	3.17	3.06	3.28	60.8
13.61	3.14	3.01	3.26	64
14.94	3.08	2.95	3.22	67.2
16.4	3.02	2.89	3.14	70.2
18	2.93	2.85	3.01	73.3
19.76	2.81	2.77	2.85	76.2
21.69	2.64	2.57	2.72	79
23.81	2.45	2.36	2.54	81.6
26.14	2.28	2.26	2.31	84.1
28.7	2.18	2.08	2.29	86.4
31.5	2.16	1.91	2.42	88.6
34.58	2.18	1.85	2.51	90.7
37.97	2.13	1.85	2.41	92.9
41.68	1.91	1.78	2.05	95
45.75	1.51	1.28	1.74	96.9
50.22	0.95	0.52	1.39	98.4
55.13	0.44	0.028	0.86	99.4
60.52	0.13	0	0.37	99.8
66.44	0.021	0	0.075	99.98
72.94	0.0014	0	0.0062	99.999
80.07	0	0	0	100

87.9	0	0	0	100
96.49	0	0	0	100
105.9	0	0	0	100
116.3	0	0	0	100
127.6	0	0	0	100
140.1	0	0	0	100
153.8	0	0	0	100
168.9	0	0	0	100
185.4	0	0	0	100
203.5	0	0	0	100
223.4	0	0	0	100
245.2	0	0	0	100
269.2	0	0	0	100
295.5	0	0	0	100
324.4	0	0	0	100
356.1	0	0	0	100
390.9	0	0	0	100
429.2	0	0	0	100
471.1	0	0	0	100
517.2	0	0	0	100
567.7	0	0	0	100
623.3	0	0	0	100
684.2	0	0	0	100
751.1	0	0	0	100
824.5	0	0	0	100
905.1	0	0	0	100
993.6	0	0	0	100
1091	0	0	0	100
1197	0	0	0	100
1314	0	0	0	100
1443	0	0	0	100
1584	0	0	0	100
1739	0	0	0	100
1909	0	0	0	100

**Site 7: Ice Type C (2)**

<b>Channel Diameter</b>	<b>Diff.</b>	<b>-2 S.D.</b>	<b>+2 S.D.</b>	<b>Cum. &lt;</b>
<b>um</b>	<b>Volume</b>	<b>Diff.</b>	<b>Diff.</b>	<b>Volume</b>
	<b>%</b>	<b>Volume</b>	<b>Volume</b>	<b>%</b>
		<b>%</b>	<b>%</b>	
0.393	0.11	0.11	0.11	0
0.431	0.2	0.19	0.2	0.11
0.474	0.29	0.29	0.3	0.31
0.52	0.41	0.41	0.42	0.6
0.571	0.52	0.51	0.53	1.01
0.627	0.61	0.6	0.62	1.53
0.688	0.69	0.68	0.7	2.14
0.755	0.77	0.75	0.78	2.82
0.829	0.83	0.82	0.85	3.59
0.91	0.89	0.88	0.9	4.42
0.999	0.93	0.92	0.94	5.31
1.097	0.97	0.96	0.98	6.25
1.204	1.01	1	1.02	7.22
1.321	1.04	1.03	1.05	8.23
1.451	1.07	1.07	1.08	9.27
1.592	1.11	1.1	1.12	10.3
1.748	1.15	1.14	1.16	11.5
1.919	1.2	1.19	1.21	12.6
2.107	1.25	1.24	1.26	13.8
2.313	1.32	1.3	1.33	15.1
2.539	1.39	1.37	1.4	16.4
2.787	1.47	1.45	1.49	17.8
3.059	1.56	1.54	1.58	19.2
3.358	1.66	1.64	1.68	20.8
3.687	1.76	1.74	1.78	22.4
4.047	1.87	1.85	1.89	24.2
4.443	1.98	1.96	2.01	26.1
4.877	2.1	2.07	2.12	28.1
5.354	2.21	2.18	2.23	30.2
5.878	2.31	2.29	2.34	32.4
6.452	2.42	2.4	2.44	34.7
7.083	2.51	2.49	2.53	37.1
7.775	2.6	2.58	2.62	39.6
8.536	2.67	2.66	2.69	42.2
9.37	2.74	2.72	2.75	44.9
10.29	2.78	2.77	2.8	47.6
11.29	2.81	2.8	2.83	50.4
12.4	2.82	2.8	2.84	53.2
13.61	2.8	2.78	2.83	56
14.94	2.76	2.73	2.78	58.8

16.4	2.69	2.66	2.73	61.6
18	2.63	2.59	2.66	64.3
19.76	2.57	2.53	2.61	66.9
21.69	2.51	2.48	2.55	69.5
23.81	2.46	2.44	2.49	72
26.14	2.4	2.39	2.41	74.5
28.7	2.32	2.31	2.33	76.9
31.5	2.23	2.2	2.25	79.2
34.58	2.13	2.09	2.17	81.4
37.97	2.03	1.99	2.07	83.5
41.68	1.92	1.88	1.95	85.6
45.75	1.79	1.76	1.81	87.5
50.22	1.63	1.62	1.64	89.3
55.13	1.45	1.45	1.45	90.9
60.52	1.26	1.26	1.27	92.3
66.44	1.08	1.06	1.09	93.6
72.94	0.9	0.87	0.94	94.7
80.07	0.74	0.69	0.79	95.6
87.9	0.59	0.53	0.65	96.3
96.49	0.47	0.41	0.52	96.9
105.9	0.37	0.33	0.41	97.4
116.3	0.32	0.29	0.34	97.8
127.6	0.3	0.28	0.31	98.1
140.1	0.3	0.29	0.31	98.4
153.8	0.3	0.29	0.32	98.7
168.9	0.29	0.26	0.31	99
185.4	0.24	0.22	0.27	99.3
203.5	0.18	0.15	0.22	99.5
223.4	0.13	0.079	0.18	99.7
245.2	0.083	0.023	0.14	99.8
269.2	0.053	0	0.11	99.9
295.5	0.032	0	0.081	99.9
324.4	0.015	0	0.045	99.98
356.1	0.0048	0	0.017	99.99
390.9	0.00081	0	0.0033	99.999
429.2	0.000051	0	0.00023	100
471.1	0	0	0	100
517.2	0	0	0	100
567.7	0	0	0	100
623.3	0	0	0	100
684.2	0	0	0	100
751.1	0	0	0	100
824.5	0	0	0	100
905.1	0	0	0	100

993.6	0	0	0	100
1091	0	0	0	100
1197	0	0	0	100
1314	0	0	0	100
1443	0	0	0	100
1584	0	0	0	100
1739	0	0	0	100
1909	0	0	0	100

**Site 7: Ice Type C (3)**

<b>Channel Diameter</b>	<b>Diff.</b>	<b>-2 S.D.</b>	<b>+2 S.D.</b>	<b>Cum. &lt;</b>
<b>µm</b>	<b>Volume</b>	<b>Diff.</b>	<b>Diff.</b>	<b>Volume</b>
	<b>%</b>	<b>Volume</b>	<b>Volume</b>	<b>%</b>
		<b>%</b>	<b>%</b>	
0.393	0.093	0.091	0.095	0
0.431	0.17	0.16	0.17	0.093
0.474	0.24	0.24	0.25	0.26
0.52	0.35	0.34	0.35	0.5
0.571	0.43	0.42	0.44	0.85
0.627	0.51	0.5	0.51	1.28
0.688	0.57	0.56	0.58	1.78
0.755	0.64	0.63	0.65	2.35
0.829	0.69	0.68	0.7	2.99
0.91	0.74	0.73	0.75	3.68
0.999	0.77	0.76	0.78	4.42
1.097	0.8	0.79	0.81	5.19
1.204	0.83	0.82	0.84	6
1.321	0.86	0.85	0.87	6.83
1.451	0.88	0.87	0.89	7.68
1.592	0.9	0.89	0.91	8.56
1.748	0.93	0.92	0.95	9.47
1.919	0.97	0.96	0.98	10.4
2.107	1.01	1	1.02	11.4
2.313	1.06	1.04	1.07	12.4
2.539	1.11	1.1	1.13	13.4
2.787	1.18	1.16	1.19	14.6
3.059	1.25	1.23	1.26	15.7
3.358	1.32	1.3	1.34	17
3.687	1.4	1.38	1.42	18.3
4.047	1.49	1.47	1.51	19.7
4.443	1.58	1.56	1.6	21.2
4.877	1.67	1.65	1.69	22.8

5.354	1.76	1.74	1.79	24.4
5.878	1.85	1.83	1.88	26.2
6.452	1.94	1.92	1.97	28.1
7.083	2.03	2.01	2.05	30
7.775	2.11	2.09	2.14	32
8.536	2.19	2.17	2.22	34.1
9.37	2.26	2.24	2.29	36.3
10.29	2.33	2.3	2.35	38.6
11.29	2.38	2.35	2.41	40.9
12.4	2.42	2.39	2.45	43.3
13.61	2.44	2.41	2.48	45.7
14.94	2.45	2.42	2.48	48.2
16.4	2.44	2.41	2.47	50.6
18	2.43	2.4	2.46	53.1
19.76	2.44	2.41	2.46	55.5
21.69	2.49	2.46	2.51	57.9
23.81	2.57	2.56	2.59	60.4
26.14	2.68	2.67	2.7	63
28.7	2.77	2.75	2.79	65.7
31.5	2.81	2.79	2.84	68.4
34.58	2.8	2.75	2.84	71.3
37.97	2.75	2.7	2.8	74
41.68	2.73	2.68	2.78	76.8
45.75	2.79	2.74	2.85	79.5
50.22	2.96	2.89	3.03	82.3
55.13	3.15	3.07	3.24	85.3
60.52	3.23	3.15	3.32	88.4
66.44	3.04	2.95	3.12	91.7
72.94	2.48	2.38	2.59	94.7
80.07	1.67	1.54	1.8	97.2
87.9	0.83	0.72	0.95	98.8
96.49	0.27	0.21	0.33	99.7
105.9	0.044	0.03	0.059	99.95
116.3	0.0026	0.0012	0.0039	99.997
127.6	0	0	0	100
140.1	0	0	0	100
153.8	0	0	0	100
168.9	0	0	0	100
185.4	0	0	0	100
203.5	0	0	0	100
223.4	0	0	0	100
245.2	0	0	0	100
269.2	0	0	0	100
295.5	0	0	0	100

324.4	0	0	0	100
356.1	0	0	0	100
390.9	0	0	0	100
429.2	0	0	0	100
471.1	0	0	0	100
517.2	0	0	0	100
567.7	0	0	0	100
623.3	0	0	0	100
684.2	0	0	0	100
751.1	0	0	0	100
824.5	0	0	0	100
905.1	0	0	0	100
993.6	0	0	0	100
1091	0	0	0	100
1197	0	0	0	100
1314	0	0	0	100
1443	0	0	0	100
1584	0	0	0	100
1739	0	0	0	100
1909	0	0	0	100

**Site 7: Ice Type C (4)**

<b>Channel Diameter</b>	<b>Diff.</b>	<b>-2 S.D.</b>	<b>+2 S.D.</b>	<b>Cum. &lt;</b>
<b>µm</b>	<b>Volume</b>	<b>Diff.</b>	<b>Diff.</b>	<b>Volume</b>
	<b>%</b>	<b>Volume</b>	<b>Volume</b>	<b>%</b>
		<b>%</b>	<b>%</b>	
0.393	0.12	0.12	0.12	0
0.431	0.22	0.22	0.22	0.12
0.474	0.32	0.32	0.33	0.34
0.52	0.46	0.45	0.47	0.66
0.571	0.58	0.57	0.59	1.13
0.627	0.68	0.67	0.69	1.7
0.688	0.78	0.77	0.79	2.38
0.755	0.88	0.86	0.89	3.16
0.829	0.96	0.95	0.97	4.04
0.91	1.03	1.02	1.05	5
0.999	1.1	1.09	1.11	6.03
1.097	1.16	1.14	1.17	7.13
1.204	1.22	1.2	1.23	8.29
1.321	1.27	1.25	1.28	9.51
1.451	1.32	1.31	1.33	10.8
1.592	1.37	1.36	1.38	12.1
1.748	1.43	1.42	1.44	13.5

1.919	1.49	1.48	1.5	14.9
2.107	1.56	1.55	1.57	16.4
2.313	1.64	1.63	1.65	17.9
2.539	1.72	1.71	1.74	19.6
2.787	1.82	1.8	1.84	21.3
3.059	1.92	1.91	1.94	23.1
3.358	2.03	2.01	2.05	25
3.687	2.14	2.12	2.16	27.1
4.047	2.26	2.23	2.28	29.2
4.443	2.37	2.35	2.4	31.5
4.877	2.49	2.46	2.51	33.9
5.354	2.59	2.56	2.62	36.3
5.878	2.69	2.66	2.71	38.9
6.452	2.77	2.74	2.8	41.6
7.083	2.85	2.82	2.88	44.4
7.775	2.91	2.88	2.94	47.2
8.536	2.95	2.93	2.98	50.1
9.37	2.97	2.95	2.99	53.1
10.29	2.97	2.95	2.99	56.1
11.29	2.95	2.93	2.97	59
12.4	2.9	2.88	2.92	62
13.61	2.82	2.8	2.84	64.9
14.94	2.71	2.69	2.74	67.7
16.4	2.59	2.56	2.62	70.4
18	2.48	2.44	2.52	73
19.76	2.39	2.35	2.42	75.5
21.69	2.29	2.27	2.31	77.9
23.81	2.17	2.16	2.19	80.2
26.14	2.03	1.99	2.07	82.3
28.7	1.9	1.87	1.93	84.4
31.5	1.82	1.81	1.84	86.3
34.58	1.84	1.78	1.9	88.1
37.97	1.94	1.85	2.03	89.9
41.68	2.04	1.98	2.1	91.9
45.75	2.01	1.97	2.05	93.9
50.22	1.76	1.59	1.93	95.9
55.13	1.29	1.01	1.57	97.7
60.52	0.71	0.46	0.97	99
66.44	0.27	0.12	0.41	99.7
72.94	0.049	0.015	0.084	99.9
80.07	0.0036	0.00006	0.0072	99.996
87.9	0	0	0	100
96.49	0	0	0	100
105.9	0	0	0	100

116.3	0	0	0	100
127.6	0	0	0	100
140.1	0	0	0	100
153.8	0	0	0	100
168.9	0	0	0	100
185.4	0	0	0	100
203.5	0	0	0	100
223.4	0	0	0	100
245.2	0	0	0	100
269.2	0	0	0	100
295.5	0	0	0	100
324.4	0	0	0	100
356.1	0	0	0	100
390.9	0	0	0	100
429.2	0	0	0	100
471.1	0	0	0	100
517.2	0	0	0	100
567.7	0	0	0	100
623.3	0	0	0	100
684.2	0	0	0	100
751.1	0	0	0	100
824.5	0	0	0	100
905.1	0	0	0	100
993.6	0	0	0	100
1091	0	0	0	100
1197	0	0	0	100
1314	0	0	0	100
1443	0	0	0	100
1584	0	0	0	100
1739	0	0	0	100
1909	0	0	0	100

**Site 7: Ice Type C (5)**

<b>Channel Diameter</b>	<b>Diff.</b>	<b>-2 S.D.</b>	<b>+2 S.D.</b>	<b>Cum. &lt;</b>
<b>µm</b>	<b>Volume</b>	<b>Diff.</b>	<b>Diff.</b>	<b>Volume</b>
	<b>%</b>	<b>Volume</b>	<b>Volume</b>	<b>%</b>
		<b>%</b>	<b>%</b>	
0.393	0.13	0.13	0.13	0
0.431	0.22	0.22	0.23	0.13
0.474	0.33	0.33	0.33	0.35
0.52	0.47	0.47	0.47	0.68
0.571	0.58	0.58	0.59	1.15
0.627	0.68	0.68	0.69	1.74
0.688	0.77	0.77	0.78	2.42
0.755	0.86	0.86	0.87	3.2
0.829	0.94	0.93	0.94	4.06
0.91	1	0.99	1	4.99
0.999	1.05	1.04	1.05	5.99
1.097	1.09	1.09	1.09	7.04
1.204	1.13	1.13	1.14	8.12
1.321	1.17	1.17	1.18	9.26
1.451	1.21	1.21	1.22	10.4
1.592	1.26	1.25	1.27	11.6
1.748	1.31	1.31	1.32	12.9
1.919	1.38	1.37	1.39	14.2
2.107	1.45	1.45	1.46	15.6
2.313	1.53	1.53	1.54	17
2.539	1.63	1.62	1.63	18.6
2.787	1.73	1.72	1.73	20.2
3.059	1.83	1.83	1.84	21.9
3.358	1.94	1.93	1.95	23.8
3.687	2.05	2.04	2.06	25.7
4.047	2.16	2.15	2.17	27.8
4.443	2.27	2.26	2.28	29.9
4.877	2.37	2.36	2.38	32.2
5.354	2.46	2.45	2.47	34.6
5.878	2.53	2.53	2.54	37
6.452	2.6	2.59	2.6	39.6
7.083	2.65	2.64	2.65	42.1
7.775	2.68	2.68	2.69	44.8
8.536	2.7	2.69	2.7	47.5
9.37	2.69	2.68	2.7	50.2
10.29	2.67	2.66	2.69	52.9
11.29	2.64	2.63	2.65	55.5
12.4	2.58	2.57	2.59	58.2
13.61	2.5	2.49	2.5	60.8
14.94	2.39	2.38	2.39	63.3

16.4	2.27	2.26	2.27	65.6
18	2.16	2.15	2.16	67.9
19.76	2.08	2.07	2.09	70.1
21.69	2.02	2.01	2.04	72.1
23.81	1.99	1.97	2	74.2
26.14	1.95	1.94	1.96	76.2
28.7	1.89	1.88	1.9	78.1
31.5	1.82	1.8	1.84	80
34.58	1.73	1.7	1.76	81.8
37.97	1.64	1.6	1.68	83.5
41.68	1.55	1.51	1.6	85.2
45.75	1.46	1.43	1.5	86.7
50.22	1.37	1.34	1.39	88.2
55.13	1.27	1.26	1.28	89.6
60.52	1.16	1.16	1.17	90.8
66.44	1.06	1.05	1.07	92
72.94	0.95	0.91	0.99	93.1
80.07	0.82	0.75	0.89	94
87.9	0.67	0.57	0.77	94.8
96.49	0.52	0.41	0.63	95.5
105.9	0.4	0.3	0.5	96
116.3	0.33	0.26	0.4	96.4
127.6	0.31	0.28	0.35	96.7
140.1	0.33	0.32	0.34	97.1
153.8	0.35	0.32	0.37	97.4
168.9	0.34	0.29	0.38	97.7
185.4	0.3	0.24	0.36	98.1
203.5	0.26	0.18	0.33	98.4
223.4	0.23	0.16	0.31	98.6
245.2	0.24	0.15	0.33	98.9
269.2	0.26	0.14	0.37	99.1
295.5	0.25	0.13	0.38	99.4
324.4	0.21	0.099	0.31	99.6
356.1	0.12	0.054	0.19	99.8
390.9	0.047	0.018	0.075	99.9
429.2	0.0088	0.0029	0.015	99.99
471.1	0.00063	0.00013	0.0011	99.999
517.2	0	0	0	100
567.7	0	0	0	100
623.3	0	0	0	100
684.2	0	0	0	100
751.1	0	0	0	100
824.5	0	0	0	100
905.1	0	0	0	100

993.6	0	0	0	100
1091	0	0	0	100
1197	0	0	0	100
1314	0	0	0	100
1443	0	0	0	100
1584	0	0	0	100
1739	0	0	0	100
1909	0	0	0	100

**Site 7: Ice Type C (6)**

<b>Channel Diameter</b>	<b>Diff.</b>	<b>-2 S.D.</b>	<b>+2 S.D.</b>	<b>Cum. &lt;</b>
<b>µm</b>	<b>Volume</b>	<b>Diff.</b>	<b>Diff.</b>	<b>Volume</b>
	<b>%</b>	<b>Volume</b>	<b>Volume</b>	<b>%</b>
		<b>%</b>	<b>%</b>	
0.393	0.14	0.14	0.14	0
0.431	0.25	0.25	0.25	0.14
0.474	0.37	0.36	0.37	0.39
0.52	0.52	0.52	0.53	0.76
0.571	0.65	0.65	0.66	1.28
0.627	0.77	0.76	0.77	1.93
0.688	0.87	0.87	0.88	2.7
0.755	0.98	0.97	0.99	3.57
0.829	1.07	1.06	1.08	4.55
0.91	1.15	1.14	1.16	5.62
0.999	1.21	1.2	1.23	6.76
1.097	1.28	1.26	1.29	7.97
1.204	1.34	1.32	1.35	9.25
1.321	1.4	1.38	1.41	10.6
1.451	1.45	1.44	1.47	12
1.592	1.52	1.5	1.53	13.4
1.748	1.59	1.57	1.6	15
1.919	1.67	1.65	1.69	16.5
2.107	1.76	1.74	1.77	18.2
2.313	1.85	1.83	1.87	20
2.539	1.96	1.94	1.98	21.8
2.787	2.07	2.05	2.09	23.8
3.059	2.19	2.17	2.21	25.8
3.358	2.31	2.29	2.33	28
3.687	2.43	2.41	2.45	30.3
4.047	2.55	2.53	2.58	32.8
4.443	2.67	2.65	2.69	35.3
4.877	2.78	2.75	2.8	38
5.354	2.88	2.85	2.9	40.8

5.878	2.96	2.93	2.99	43.6
6.452	3.03	3	3.06	46.6
7.083	3.09	3.05	3.12	49.6
7.775	3.12	3.09	3.15	52.7
8.536	3.13	3.09	3.17	55.8
9.37	3.12	3.08	3.17	59
10.29	3.09	3.05	3.13	62.1
11.29	3.03	2.99	3.07	65.2
12.4	2.94	2.9	2.98	68.2
13.61	2.82	2.77	2.87	71.2
14.94	2.68	2.63	2.73	74
16.4	2.53	2.49	2.57	76.7
18	2.37	2.36	2.38	79.2
19.76	2.19	2.15	2.24	81.6
21.69	2.02	1.95	2.1	83.8
23.81	1.88	1.81	1.95	85.8
26.14	1.78	1.76	1.81	87.7
28.7	1.76	1.7	1.82	89.4
31.5	1.78	1.65	1.9	91.2
34.58	1.79	1.66	1.91	93
37.97	1.7	1.66	1.74	94.8
41.68	1.47	1.35	1.58	96.5
45.75	1.09	0.84	1.34	97.9
50.22	0.64	0.33	0.94	99
55.13	0.27	0.036	0.5	99.7
60.52	0.067	0	0.17	99.9
66.44	0.0085	0	0.029	99.99
72.94	0.00036	0	0.0016	100
80.07	0	0	0	100
87.9	0	0	0	100
96.49	0	0	0	100
105.9	0	0	0	100
116.3	0	0	0	100
127.6	0	0	0	100
140.1	0	0	0	100
153.8	0	0	0	100
168.9	0	0	0	100
185.4	0	0	0	100
203.5	0	0	0	100
223.4	0	0	0	100
245.2	0	0	0	100
269.2	0	0	0	100
295.5	0	0	0	100
324.4	0	0	0	100

356.1	0	0	0	100
390.9	0	0	0	100
429.2	0	0	0	100
471.1	0	0	0	100
517.2	0	0	0	100
567.7	0	0	0	100
623.3	0	0	0	100
684.2	0	0	0	100
751.1	0	0	0	100
824.5	0	0	0	100
905.1	0	0	0	100
993.6	0	0	0	100
1091	0	0	0	100
1197	0	0	0	100
1314	0	0	0	100
1443	0	0	0	100
1584	0	0	0	100
1739	0	0	0	100
1909	0	0	0	100

**Site 7: Minor Outwash Fan (1)**

<b>Channel Diameter</b>	<b>Diff.</b>	<b>-2 S.D.</b>	<b>+2 S.D.</b>	<b>Cum. &lt;</b>
<b>µm</b>	<b>Volume</b>	<b>Diff.</b>	<b>Diff.</b>	<b>Volume</b>
	<b>%</b>	<b>Volume</b>	<b>Volume</b>	<b>%</b>
		<b>%</b>	<b>%</b>	
0.393	0.093	0.089	0.097	0
0.431	0.17	0.16	0.17	0.093
0.474	0.24	0.23	0.25	0.26
0.52	0.35	0.33	0.36	0.5
0.571	0.43	0.41	0.44	0.85
0.627	0.5	0.48	0.51	1.28
0.688	0.56	0.54	0.57	1.77
0.755	0.61	0.6	0.63	2.33
0.829	0.66	0.64	0.67	2.94
0.91	0.68	0.68	0.69	3.6
0.999	0.7	0.69	0.7	4.28
1.097	0.71	0.71	0.71	4.98
1.204	0.71	0.71	0.71	5.69
1.321	0.71	0.71	0.71	6.4
1.451	0.71	0.71	0.71	7.11
1.592	0.71	0.7	0.71	7.82
1.748	0.71	0.71	0.72	8.53
1.919	0.73	0.72	0.73	9.24

2.107	0.75	0.74	0.76	9.97
2.313	0.79	0.78	0.81	10.7
2.539	0.85	0.83	0.87	11.5
2.787	0.92	0.9	0.94	12.4
3.059	1.01	0.99	1.04	13.3
3.358	1.13	1.1	1.15	14.3
3.687	1.26	1.23	1.29	15.4
4.047	1.41	1.38	1.44	16.7
4.443	1.59	1.56	1.61	18.1
4.877	1.78	1.75	1.8	19.7
5.354	1.98	1.95	2	21.5
5.878	2.19	2.17	2.21	23.4
6.452	2.41	2.39	2.43	25.6
7.083	2.64	2.62	2.65	28
7.775	2.86	2.84	2.87	30.7
8.536	3.07	3.05	3.09	33.5
9.37	3.27	3.25	3.3	36.6
10.29	3.46	3.43	3.5	39.9
11.29	3.63	3.58	3.67	43.3
12.4	3.75	3.7	3.81	47
13.61	3.84	3.77	3.9	50.7
14.94	3.88	3.81	3.95	54.6
16.4	3.88	3.82	3.95	58.4
18	3.86	3.81	3.91	62.3
19.76	3.8	3.77	3.83	66.2
21.69	3.7	3.68	3.72	70
23.81	3.56	3.54	3.58	73.7
26.14	3.41	3.37	3.44	77.2
28.7	3.28	3.23	3.33	80.6
31.5	3.17	3.11	3.24	83.9
34.58	3.07	3.02	3.12	87.1
37.97	2.89	2.86	2.91	90.2
41.68	2.54	2.51	2.58	93
45.75	2.02	1.93	2.11	95.6
50.22	1.37	1.26	1.49	97.6
55.13	0.72	0.62	0.81	99
60.52	0.26	0.21	0.31	99.7
66.44	0.046	0.035	0.058	99.95
72.94	0.0034	0.0022	0.0045	99.997
80.07	0	0	0	100
87.9	0	0	0	100
96.49	0	0	0	100
105.9	0	0	0	100
116.3	0	0	0	100

127.6	0	0	0	100
140.1	0	0	0	100
153.8	0	0	0	100
168.9	0	0	0	100
185.4	0	0	0	100
203.5	0	0	0	100
223.4	0	0	0	100
245.2	0	0	0	100
269.2	0	0	0	100
295.5	0	0	0	100
324.4	0	0	0	100
356.1	0	0	0	100
390.9	0	0	0	100
429.2	0	0	0	100
471.1	0	0	0	100
517.2	0	0	0	100
567.7	0	0	0	100
623.3	0	0	0	100
684.2	0	0	0	100
751.1	0	0	0	100
824.5	0	0	0	100
905.1	0	0	0	100
993.6	0	0	0	100
1091	0	0	0	100
1197	0	0	0	100
1314	0	0	0	100
1443	0	0	0	100
1584	0	0	0	100
1739	0	0	0	100
1909	0	0	0	100

**Site 7: Minor Outwash Fan (2)**

<b>Channel Diameter</b>	<b>Diff.</b>	<b>-2 S.D.</b>	<b>+2 S.D.</b>	<b>Cum. &lt;</b>
<b>µm</b>	<b>Volume</b>	<b>Diff.</b>	<b>Diff.</b>	<b>Volume</b>
	<b>%</b>	<b>Volume</b>	<b>Volume</b>	<b>%</b>
		<b>%</b>	<b>%</b>	
0.393	0.036	0.036	0.036	0
0.431	0.064	0.064	0.065	0.036
0.474	0.095	0.094	0.095	0.1
0.52	0.13	0.13	0.14	0.2
0.571	0.17	0.17	0.17	0.33
0.627	0.2	0.19	0.2	0.5
0.688	0.22	0.22	0.22	0.69

0.755	0.25	0.24	0.25	0.92
0.829	0.26	0.26	0.27	1.16
0.91	0.28	0.28	0.28	1.43
0.999	0.29	0.28	0.29	1.7
1.097	0.29	0.29	0.3	1.99
1.204	0.3	0.29	0.3	2.28
1.321	0.3	0.29	0.3	2.58
1.451	0.29	0.29	0.3	2.87
1.592	0.29	0.28	0.29	3.17
1.748	0.28	0.28	0.29	3.45
1.919	0.28	0.28	0.28	3.74
2.107	0.28	0.27	0.28	4.02
2.313	0.28	0.27	0.28	4.29
2.539	0.28	0.28	0.28	4.57
2.787	0.28	0.28	0.29	4.85
3.059	0.29	0.29	0.3	5.13
3.358	0.31	0.3	0.31	5.43
3.687	0.33	0.32	0.33	5.73
4.047	0.35	0.35	0.35	6.06
4.443	0.38	0.38	0.39	6.41
4.877	0.42	0.42	0.42	6.79
5.354	0.46	0.46	0.47	7.21
5.878	0.52	0.51	0.52	7.68
6.452	0.58	0.57	0.59	8.19
7.083	0.64	0.63	0.66	8.77
7.775	0.72	0.7	0.74	9.41
8.536	0.81	0.78	0.83	10.1
9.37	0.9	0.87	0.93	10.9
10.29	1.01	0.98	1.04	11.8
11.29	1.13	1.09	1.17	12.9
12.4	1.26	1.21	1.31	14
13.61	1.39	1.33	1.45	15.2
14.94	1.53	1.46	1.6	16.6
16.4	1.67	1.58	1.75	18.2
18	1.8	1.7	1.9	19.8
19.76	1.92	1.81	2.03	21.6
21.69	2.03	1.91	2.15	23.5
23.81	2.14	2.01	2.26	25.6
26.14	2.23	2.1	2.36	27.7
28.7	2.32	2.18	2.45	29.9
31.5	2.4	2.26	2.54	32.3
34.58	2.47	2.32	2.62	34.7
37.97	2.53	2.37	2.69	37.1
41.68	2.57	2.4	2.74	39.7

45.75	2.59	2.41	2.77	42.2
50.22	2.6	2.42	2.78	44.8
55.13	2.6	2.43	2.78	47.4
60.52	2.61	2.44	2.78	50
66.44	2.63	2.46	2.8	52.6
72.94	2.64	2.45	2.82	55.3
80.07	2.62	2.42	2.82	57.9
87.9	2.56	2.34	2.78	60.5
96.49	2.46	2.23	2.68	63.1
105.9	2.32	2.1	2.53	65.5
116.3	2.16	1.97	2.35	67.8
127.6	2	1.85	2.16	70
140.1	1.84	1.72	1.96	72
153.8	1.68	1.58	1.77	73.9
168.9	1.5	1.42	1.58	75.5
185.4	1.32	1.23	1.4	77
203.5	1.15	1.06	1.24	78.4
223.4	1.03	0.93	1.13	79.5
245.2	0.97	0.88	1.06	80.5
269.2	0.96	0.88	1.05	81.5
295.5	1	0.89	1.12	82.5
324.4	1.06	0.88	1.23	83.5
356.1	1.1	0.86	1.33	84.5
390.9	1.11	0.84	1.38	85.6
429.2	1.1	0.83	1.38	86.7
471.1	1.09	0.85	1.33	87.8
517.2	1.08	0.91	1.25	88.9
567.7	1.08	0.96	1.2	90
623.3	1.09	0.91	1.27	91.1
684.2	1.11	0.81	1.42	92.2
751.1	1.15	0.72	1.58	93.3
824.5	1.21	0.64	1.79	94.4
905.1	1.29	0.55	2.03	95.6
993.6	1.33	0.2	2.45	96.9
1091	1.04	0	2.19	98.3
1197	0.56	0	1.36	99.3
1314	0.13	0	0.35	99.9
1443	0.015	0	0.04	99.99
1584	0	0	0	100
1739	0	0	0	100
1909	0	0	0	100

**Frazil Sample (1)**

<b>Channel Diameter</b>	<b>Diff.</b>	<b>-2 S.D.</b>	<b>+2 S.D.</b>	<b>Cum. &lt;</b>
<b>µm</b>	<b>Volume</b>	<b>Diff.</b>	<b>Diff.</b>	<b>Volume</b>
	<b>%</b>	<b>Volume</b>	<b>Volume</b>	<b>%</b>
		<b>%</b>	<b>%</b>	
0.393	0.11	0.11	0.12	0
0.431	0.2	0.2	0.21	0.11
0.474	0.3	0.3	0.3	0.32
0.52	0.43	0.42	0.43	0.62
0.571	0.53	0.53	0.53	1.05
0.627	0.62	0.61	0.62	1.58
0.688	0.69	0.69	0.7	2.19
0.755	0.77	0.76	0.77	2.89
0.829	0.83	0.82	0.83	3.66
0.91	0.87	0.87	0.88	4.48
0.999	0.9	0.9	0.91	5.35
1.097	0.93	0.92	0.93	6.25
1.204	0.95	0.94	0.95	7.18
1.321	0.97	0.96	0.97	8.13
1.451	0.98	0.98	0.99	9.1
1.592	1.01	1.01	1.02	10.1
1.748	1.05	1.05	1.06	11.1
1.919	1.11	1.1	1.11	12.1
2.107	1.18	1.17	1.19	13.2
2.313	1.28	1.27	1.28	14.4
2.539	1.4	1.39	1.41	15.7
2.787	1.55	1.54	1.56	17.1
3.059	1.73	1.72	1.74	18.7
3.358	1.94	1.93	1.95	20.4
3.687	2.18	2.16	2.19	22.3
4.047	2.44	2.42	2.46	24.5
4.443	2.72	2.7	2.74	26.9
4.877	3.02	3	3.03	29.7
5.354	3.31	3.29	3.33	32.7
5.878	3.6	3.58	3.62	36
6.452	3.89	3.87	3.91	39.6
7.083	4.16	4.14	4.18	43.5
7.775	4.39	4.38	4.4	47.6
8.536	4.57	4.56	4.58	52
9.37	4.69	4.68	4.7	56.6
10.29	4.75	4.74	4.75	61.3
11.29	4.72	4.71	4.72	66
12.4	4.57	4.55	4.58	70.8
13.61	4.29	4.28	4.31	75.3
14.94	3.93	3.93	3.94	79.6

16.4	3.55	3.54	3.57	83.5
18	3.21	3.17	3.24	87.1
19.76	2.87	2.85	2.89	90.3
21.69	2.47	2.46	2.49	93.2
23.81	1.96	1.9	2.02	95.6
26.14	1.35	1.25	1.45	97.6
28.7	0.72	0.63	0.81	99
31.5	0.27	0.22	0.31	99.7
34.58	0.049	0.038	0.061	99.9
37.97	0.0037	0.0025	0.005	99.996
41.68	0	0	0	100
45.75	0	0	0	100
50.22	0	0	0	100
55.13	0	0	0	100
60.52	0	0	0	100
66.44	0	0	0	100
72.94	0	0	0	100
80.07	0	0	0	100
87.9	0	0	0	100
96.49	0	0	0	100
105.9	0	0	0	100
116.3	0	0	0	100
127.6	0	0	0	100
140.1	0	0	0	100
153.8	0	0	0	100
168.9	0	0	0	100
185.4	0	0	0	100
203.5	0	0	0	100
223.4	0	0	0	100
245.2	0	0	0	100
269.2	0	0	0	100
295.5	0	0	0	100
324.4	0	0	0	100
356.1	0	0	0	100
390.9	0	0	0	100
429.2	0	0	0	100
471.1	0	0	0	100
517.2	0	0	0	100
567.7	0	0	0	100
623.3	0	0	0	100
684.2	0	0	0	100
751.1	0	0	0	100
824.5	0	0	0	100
905.1	0	0	0	100

993.6	0	0	0	100
1091	0	0	0	100
1197	0	0	0	100
1314	0	0	0	100
1443	0	0	0	100
1584	0	0	0	100
1739	0	0	0	100
1909	0	0	0	100

**Frazil Sample (2)**

<b>Channel Diameter</b>	<b>Diff.</b>	<b>-2 S.D.</b>	<b>+2 S.D.</b>	<b>Cum. &lt;</b>
<b>µm</b>	<b>Volume</b>	<b>Diff.</b>	<b>Diff.</b>	<b>Volume</b>
	<b>%</b>	<b>Volume</b>	<b>Volume</b>	<b>%</b>
		<b>%</b>	<b>%</b>	
0.393	0.12	0.11	0.13	0
0.431	0.21	0.2	0.22	0.12
0.474	0.31	0.3	0.33	0.33
0.52	0.44	0.42	0.46	0.64
0.571	0.55	0.52	0.57	1.09
0.627	0.64	0.61	0.66	1.63
0.688	0.71	0.69	0.74	2.27
0.755	0.79	0.77	0.81	2.98
0.829	0.84	0.83	0.86	3.77
0.91	0.89	0.87	0.9	4.61
0.999	0.91	0.91	0.92	5.5
1.097	0.94	0.93	0.94	6.41
1.204	0.96	0.96	0.96	7.35
1.321	0.98	0.98	0.98	8.31
1.451	1	1	1	9.29
1.592	1.03	1.03	1.04	10.3
1.748	1.08	1.07	1.08	11.3
1.919	1.14	1.13	1.15	12.4
2.107	1.22	1.2	1.24	13.5
2.313	1.32	1.3	1.35	14.8
2.539	1.46	1.43	1.48	16.1
2.787	1.61	1.58	1.64	17.5
3.059	1.8	1.77	1.83	19.1
3.358	2.01	1.98	2.04	20.9
3.687	2.25	2.22	2.28	23
4.047	2.51	2.48	2.55	25.2
4.443	2.8	2.77	2.83	27.7
4.877	3.09	3.06	3.12	30.5
5.354	3.39	3.36	3.42	33.6

5.878	3.68	3.64	3.71	37
6.452	3.96	3.93	4	40.7
7.083	4.22	4.19	4.26	44.6
7.775	4.44	4.41	4.47	48.9
8.536	4.6	4.59	4.62	53.3
9.37	4.71	4.69	4.72	57.9
10.29	4.74	4.73	4.75	62.6
11.29	4.67	4.64	4.7	67.4
12.4	4.47	4.4	4.55	72
13.61	4.13	3.99	4.28	76.5
14.94	3.71	3.52	3.91	80.6
16.4	3.29	3.1	3.49	84.3
18	2.94	2.78	3.1	87.6
19.76	2.64	2.56	2.73	90.6
21.69	2.32	2.31	2.33	93.2
23.81	1.9	1.86	1.95	95.5
26.14	1.37	1.29	1.45	97.5
28.7	0.78	0.68	0.89	98.8
31.5	0.32	0.23	0.4	99.6
34.58	0.07	0.023	0.12	99.9
37.97	0.0073	0	0.017	99.99
41.68	0.00014	0	0.00061	100
45.75	0	0	0	100
50.22	0	0	0	100
55.13	0	0	0	100
60.52	0	0	0	100
66.44	0	0	0	100
72.94	0	0	0	100
80.07	0	0	0	100
87.9	0	0	0	100
96.49	0	0	0	100
105.9	0	0	0	100
116.3	0	0	0	100
127.6	0	0	0	100
140.1	0	0	0	100
153.8	0	0	0	100
168.9	0	0	0	100
185.4	0	0	0	100
203.5	0	0	0	100
223.4	0	0	0	100
245.2	0	0	0	100
269.2	0	0	0	100
295.5	0	0	0	100
324.4	0	0	0	100

356.1	0	0	0	100
390.9	0	0	0	100
429.2	0	0	0	100
471.1	0	0	0	100
517.2	0	0	0	100
567.7	0	0	0	100
623.3	0	0	0	100
684.2	0	0	0	100
751.1	0	0	0	100
824.5	0	0	0	100
905.1	0	0	0	100
993.6	0	0	0	100
1091	0	0	0	100
1197	0	0	0	100
1314	0	0	0	100
1443	0	0	0	100
1584	0	0	0	100
1739	0	0	0	100
1909	0	0	0	100

### Frazil Sample (3)

<b>Channel Diameter</b>	<b>Diff.</b>	<b>-2 S.D.</b>	<b>+2 S.D.</b>	<b>Cum. &lt;</b>
<b>µm</b>	<b>Volume</b>	<b>Diff.</b>	<b>Diff.</b>	<b>Volume</b>
	<b>%</b>	<b>Volume</b>	<b>Volume</b>	<b>%</b>
		<b>%</b>	<b>%</b>	
0.393	0.12	0.11	0.12	0
0.431	0.21	0.2	0.22	0.12
0.474	0.31	0.29	0.32	0.33
0.52	0.44	0.42	0.45	0.63
0.571	0.54	0.52	0.56	1.07
0.627	0.63	0.61	0.65	1.61
0.688	0.7	0.69	0.72	2.23
0.755	0.78	0.76	0.79	2.94
0.829	0.83	0.82	0.85	3.71
0.91	0.88	0.87	0.88	4.55
0.999	0.9	0.9	0.91	5.42
1.097	0.93	0.92	0.93	6.33
1.204	0.95	0.94	0.96	7.26
1.321	0.97	0.95	0.98	8.2
1.451	0.98	0.97	1	9.17
1.592	1.01	1	1.02	10.2
1.748	1.05	1.04	1.07	11.2
1.919	1.11	1.1	1.12	12.2

2.107	1.19	1.18	1.2	13.3
2.313	1.29	1.29	1.3	14.5
2.539	1.42	1.41	1.42	15.8
2.787	1.57	1.57	1.58	17.2
3.059	1.76	1.75	1.76	18.8
3.358	1.97	1.96	1.98	20.6
3.687	2.2	2.19	2.21	22.5
4.047	2.46	2.45	2.47	24.7
4.443	2.74	2.73	2.75	27.2
4.877	3.03	3.02	3.04	29.9
5.354	3.32	3.31	3.33	33
5.878	3.61	3.6	3.61	36.3
6.452	3.88	3.88	3.89	39.9
7.083	4.14	4.13	4.14	43.8
7.775	4.36	4.34	4.38	47.9
8.536	4.54	4.51	4.56	52.3
9.37	4.65	4.62	4.69	56.8
10.29	4.69	4.65	4.72	61.4
11.29	4.64	4.59	4.68	66.1
12.4	4.48	4.43	4.53	70.8
13.61	4.2	4.15	4.26	75.2
14.94	3.8	3.74	3.87	79.5
16.4	3.31	3.24	3.38	83.3
18	2.79	2.72	2.86	86.6
19.76	2.33	2.26	2.39	89.4
21.69	1.96	1.89	2.03	91.7
23.81	1.69	1.62	1.75	93.6
26.14	1.46	1.42	1.5	95.3
28.7	1.22	1.17	1.26	96.8
31.5	0.93	0.82	1.04	98
34.58	0.61	0.45	0.77	98.9
37.97	0.32	0.15	0.48	99.5
41.68	0.12	0.0064	0.23	99.9
45.75	0.026	0	0.068	99.97
50.22	0.0029	0	0.01	99.997
55.13	0.0001	0	0.00045	100
60.52	0	0	0	100
66.44	0	0	0	100
72.94	0	0	0	100
80.07	0	0	0	100
87.9	0	0	0	100
96.49	0	0	0	100
105.9	0	0	0	100
116.3	0	0	0	100

127.6	0	0	0	100
140.1	0	0	0	100
153.8	0	0	0	100
168.9	0	0	0	100
185.4	0	0	0	100
203.5	0	0	0	100
223.4	0	0	0	100
245.2	0	0	0	100
269.2	0	0	0	100
295.5	0	0	0	100
324.4	0	0	0	100
356.1	0	0	0	100
390.9	0	0	0	100
429.2	0	0	0	100
471.1	0	0	0	100
517.2	0	0	0	100
567.7	0	0	0	100
623.3	0	0	0	100
684.2	0	0	0	100
751.1	0	0	0	100
824.5	0	0	0	100
905.1	0	0	0	100
993.6	0	0	0	100
1091	0	0	0	100
1197	0	0	0	100
1314	0	0	0	100
1443	0	0	0	100
1584	0	0	0	100
1739	0	0	0	100
1909	0	0	0	100

**Storglaciären: Sample S1**

<b>Channel Diameter</b>	<b>Diff.</b>	<b>-2 S.D.</b>	<b>+2 S.D.</b>	<b>Cum. &lt;</b>
<b>µm</b>	<b>Volume</b>	<b>Diff.</b>	<b>Diff.</b>	<b>Volume</b>
	<b>%</b>	<b>Volume</b>	<b>Volume</b>	<b>%</b>
		<b>%</b>	<b>%</b>	
0.393	0.11	0.11	0.11	0
0.431	0.19	0.19	0.2	0.11
0.474	0.29	0.28	0.29	0.3
0.52	0.41	0.4	0.41	0.59
0.571	0.5	0.5	0.51	0.99
0.627	0.58	0.58	0.59	1.5
0.688	0.65	0.65	0.66	2.08

0.755	0.72	0.71	0.73	2.73
0.829	0.77	0.76	0.78	3.45
0.91	0.8	0.79	0.81	4.22
0.999	0.82	0.81	0.83	5.03
1.097	0.83	0.82	0.84	5.85
1.204	0.83	0.82	0.84	6.67
1.321	0.82	0.81	0.83	7.5
1.451	0.8	0.79	0.81	8.31
1.592	0.78	0.77	0.79	9.11
1.748	0.77	0.76	0.78	9.89
1.919	0.75	0.75	0.76	10.7
2.107	0.75	0.74	0.76	11.4
2.313	0.75	0.74	0.76	12.2
2.539	0.76	0.75	0.77	12.9
2.787	0.78	0.77	0.79	13.7
3.059	0.81	0.8	0.82	14.4
3.358	0.85	0.85	0.86	15.3
3.687	0.91	0.9	0.91	16.1
4.047	0.97	0.96	0.98	17
4.443	1.04	1.03	1.05	18
4.877	1.13	1.12	1.14	19
5.354	1.22	1.21	1.23	20.2
5.878	1.32	1.31	1.33	21.4
6.452	1.42	1.41	1.43	22.7
7.083	1.54	1.53	1.55	24.1
7.775	1.66	1.65	1.67	25.7
8.536	1.79	1.78	1.79	27.3
9.37	1.92	1.92	1.93	29.1
10.29	2.07	2.06	2.08	31
11.29	2.23	2.22	2.24	33.1
12.4	2.4	2.39	2.41	35.3
13.61	2.58	2.57	2.59	37.7
14.94	2.77	2.76	2.78	40.3
16.4	2.96	2.95	2.98	43.1
18	3.17	3.15	3.19	46
19.76	3.4	3.38	3.43	49.2
21.69	3.64	3.6	3.68	52.6
23.81	3.85	3.8	3.9	56.3
26.14	4.01	3.98	4.05	60.1
28.7	4.11	4.1	4.12	64.1
31.5	4.15	4.11	4.18	68.2
34.58	4.15	4.09	4.22	72.4
37.97	4.14	4.06	4.22	76.5
41.68	4.09	4	4.17	80.7

45.75	3.94	3.85	4.02	84.8
50.22	3.61	3.55	3.67	88.7
55.13	3.04	3.02	3.07	92.3
60.52	2.28	2.18	2.38	95.3
66.44	1.43	1.25	1.61	97.6
72.94	0.69	0.52	0.85	99.1
80.07	0.22	0.13	0.32	99.7
87.9	0.037	0.014	0.059	99.96
96.49	0.0023	0	0.0046	99.998
105.9	0	0	0	100
116.3	0	0	0	100
127.6	0	0	0	100
140.1	0	0	0	100
153.8	0	0	0	100
168.9	0	0	0	100
185.4	0	0	0	100
203.5	0	0	0	100
223.4	0	0	0	100
245.2	0	0	0	100
269.2	0	0	0	100
295.5	0	0	0	100
324.4	0	0	0	100
356.1	0	0	0	100
390.9	0	0	0	100
429.2	0	0	0	100
471.1	0	0	0	100
517.2	0	0	0	100
567.7	0	0	0	100
623.3	0	0	0	100
684.2	0	0	0	100
751.1	0	0	0	100
824.5	0	0	0	100
905.1	0	0	0	100
993.6	0	0	0	100
1091	0	0	0	100
1197	0	0	0	100
1314	0	0	0	100
1443	0	0	0	100
1584	0	0	0	100
1739	0	0	0	100
1909	0	0	0	100

**Storglaciären: Sample S2**

<b>Channel Diameter</b>	<b>Diff.</b>	<b>-2 S.D.</b>	<b>+2 S.D.</b>	<b>Cum. &lt;</b>
<b>µm</b>	<b>Volume</b>	<b>Diff.</b>	<b>Diff.</b>	<b>Volume</b>
	<b>%</b>	<b>Volume</b>	<b>Volume</b>	<b>%</b>
		<b>%</b>	<b>%</b>	
0.393	0.11	0.11	0.11	0
0.431	0.2	0.2	0.2	0.11
0.474	0.29	0.29	0.3	0.31
0.52	0.42	0.42	0.42	0.6
0.571	0.52	0.52	0.53	1.02
0.627	0.62	0.61	0.62	1.55
0.688	0.7	0.7	0.71	2.17
0.755	0.79	0.78	0.8	2.87
0.829	0.86	0.84	0.88	3.66
0.91	0.92	0.9	0.94	4.52
0.999	0.97	0.94	0.99	5.44
1.097	1.01	0.98	1.03	6.41
1.204	1.04	1.01	1.07	7.41
1.321	1.06	1.04	1.09	8.45
1.451	1.08	1.06	1.1	9.52
1.592	1.09	1.08	1.11	10.6
1.748	1.1	1.09	1.11	11.7
1.919	1.11	1.1	1.12	12.8
2.107	1.12	1.1	1.14	13.9
2.313	1.13	1.09	1.17	15
2.539	1.14	1.09	1.19	16.2
2.787	1.16	1.09	1.22	17.3
3.059	1.17	1.09	1.25	18.5
3.358	1.19	1.1	1.28	19.6
3.687	1.22	1.12	1.31	20.8
4.047	1.25	1.15	1.34	22
4.443	1.28	1.19	1.38	23.3
4.877	1.33	1.25	1.42	24.6
5.354	1.39	1.32	1.46	25.9
5.878	1.46	1.41	1.52	27.3
6.452	1.55	1.52	1.59	28.7
7.083	1.66	1.65	1.67	30.3
7.775	1.79	1.77	1.8	32
8.536	1.95	1.91	1.99	33.7
9.37	2.15	2.09	2.22	35.7
10.29	2.4	2.31	2.48	37.9
11.29	2.68	2.59	2.77	40.3
12.4	3.01	2.92	3.1	42.9
13.61	3.4	3.31	3.49	45.9
14.94	3.82	3.73	3.9	49.3

16.4	4.23	4.16	4.29	53.2
18	4.59	4.55	4.64	57.4
19.76	4.88	4.82	4.94	62
21.69	5.09	4.95	5.23	66.9
23.81	5.22	4.95	5.49	71.9
26.14	5.22	4.82	5.62	77.2
28.7	5	4.58	5.41	82.4
31.5	4.45	4.18	4.72	87.4
34.58	3.58	3.55	3.61	91.8
37.97	2.49	2.18	2.8	95.4
41.68	1.38	0.86	1.91	97.9
45.75	0.56	0.12	1	99.3
50.22	0.14	0	0.36	99.8
55.13	0.018	0	0.063	99.98
60.52	0.00092	0	0.0041	99.999
66.44	0	0	0	100
72.94	0	0	0	100
80.07	0	0	0	100
87.9	0	0	0	100
96.49	0	0	0	100
105.9	0	0	0	100
116.3	0	0	0	100
127.6	0	0	0	100
140.1	0	0	0	100
153.8	0	0	0	100
168.9	0	0	0	100
185.4	0	0	0	100
203.5	0	0	0	100
223.4	0	0	0	100
245.2	0	0	0	100
269.2	0	0	0	100
295.5	0	0	0	100
324.4	0	0	0	100
356.1	0	0	0	100
390.9	0	0	0	100
429.2	0	0	0	100
471.1	0	0	0	100
517.2	0	0	0	100
567.7	0	0	0	100
623.3	0	0	0	100
684.2	0	0	0	100
751.1	0	0	0	100
824.5	0	0	0	100
905.1	0	0	0	100

993.6	0	0	0	100
1091	0	0	0	100
1197	0	0	0	100
1314	0	0	0	100
1443	0	0	0	100
1584	0	0	0	100
1739	0	0	0	100
1909	0	0	0	100

**Storglaciären: Sample S3**

<b>Channel Diameter</b>	<b>Diff.</b>	<b>-2 S.D.</b>	<b>+2 S.D.</b>	<b>Cum. &lt;</b>
<b>µm</b>	<b>Volume</b>	<b>Diff.</b>	<b>Diff.</b>	<b>Volume</b>
	<b>%</b>	<b>Volume</b>	<b>Volume</b>	<b>%</b>
		<b>%</b>	<b>%</b>	
0.393	0.12	0.11	0.13	0
0.431	0.22	0.2	0.23	0.12
0.474	0.32	0.3	0.34	0.34
0.52	0.45	0.43	0.48	0.66
0.571	0.56	0.53	0.59	1.11
0.627	0.65	0.62	0.68	1.67
0.688	0.73	0.7	0.75	2.32
0.755	0.8	0.78	0.82	3.05
0.829	0.85	0.84	0.86	3.85
0.91	0.89	0.89	0.89	4.7
0.999	0.91	0.9	0.92	5.59
1.097	0.92	0.89	0.94	6.5
1.204	0.92	0.88	0.96	7.42
1.321	0.91	0.87	0.95	8.33
1.451	0.9	0.85	0.95	9.24
1.592	0.88	0.84	0.93	10.1
1.748	0.88	0.83	0.92	11
1.919	0.87	0.83	0.91	11.9
2.107	0.88	0.85	0.91	12.8
2.313	0.89	0.87	0.9	13.7
2.539	0.91	0.9	0.91	14.5
2.787	0.94	0.93	0.95	15.5
3.059	0.98	0.96	1	16.4
3.358	1.02	0.99	1.05	17.4
3.687	1.08	1.04	1.11	18.4
4.047	1.14	1.1	1.18	19.5
4.443	1.21	1.16	1.25	20.6
4.877	1.28	1.24	1.32	21.8
5.354	1.36	1.32	1.39	23.1

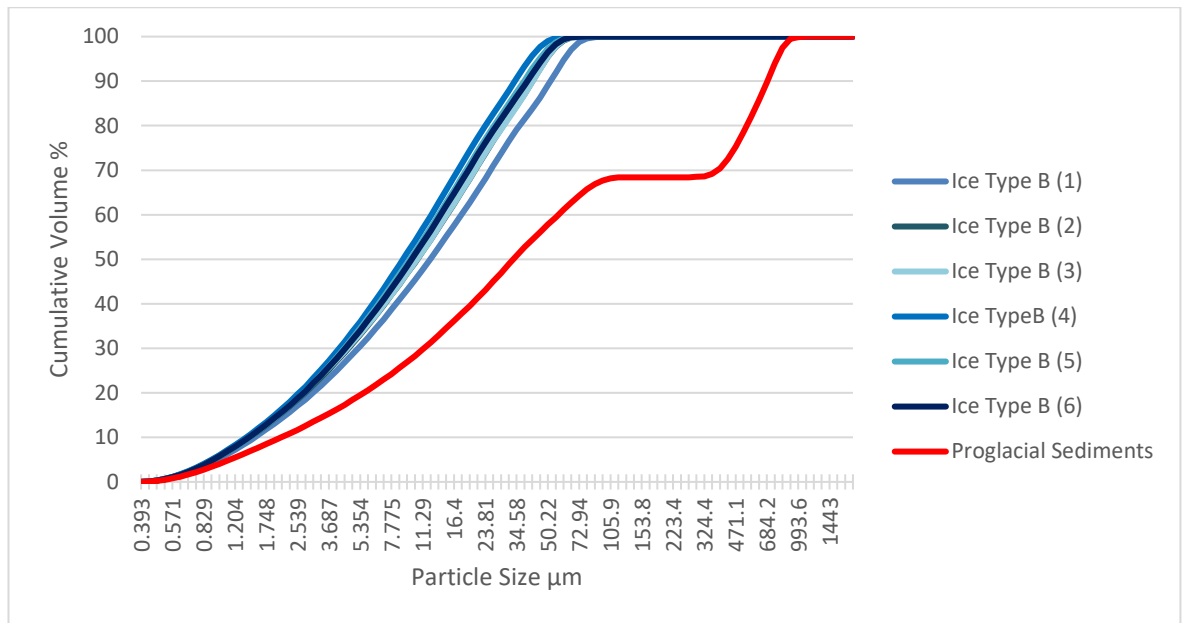
5.878	1.44	1.4	1.47	24.4
6.452	1.52	1.49	1.55	25.9
7.083	1.61	1.6	1.62	27.4
7.775	1.7	1.69	1.71	29
8.536	1.79	1.77	1.81	30.7
9.37	1.89	1.86	1.93	32.5
10.29	2.01	1.96	2.06	34.4
11.29	2.15	2.08	2.21	36.4
12.4	2.28	2.2	2.37	38.6
13.61	2.42	2.31	2.53	40.8
14.94	2.57	2.45	2.69	43.3
16.4	2.77	2.64	2.89	45.8
18	3	2.9	3.11	48.6
19.76	3.23	3.17	3.29	51.6
21.69	3.4	3.38	3.41	54.8
23.81	3.46	3.42	3.49	58.2
26.14	3.45	3.42	3.49	61.7
28.7	3.49	3.45	3.53	65.1
31.5	3.69	3.54	3.83	68.6
34.58	4.08	3.81	4.35	72.3
37.97	4.57	4.23	4.9	76.4
41.68	4.9	4.64	5.17	81
45.75	4.8	4.73	4.87	85.9
50.22	4.11	3.84	4.39	90.7
55.13	2.94	2.44	3.45	94.8
60.52	1.59	1.11	2.06	97.7
66.44	0.58	0.3	0.85	99.3
72.94	0.11	0.038	0.17	99.9
80.07	0.0076	0.00055	0.015	99.99
87.9	0	0	0	100
96.49	0	0	0	100
105.9	0	0	0	100
116.3	0	0	0	100
127.6	0	0	0	100
140.1	0	0	0	100
153.8	0	0	0	100
168.9	0	0	0	100
185.4	0	0	0	100
203.5	0	0	0	100
223.4	0	0	0	100
245.2	0	0	0	100
269.2	0	0	0	100
295.5	0	0	0	100
324.4	0	0	0	100

356.1	0	0	0	100
390.9	0	0	0	100
429.2	0	0	0	100
471.1	0	0	0	100
517.2	0	0	0	100
567.7	0	0	0	100
623.3	0	0	0	100
684.2	0	0	0	100
751.1	0	0	0	100
824.5	0	0	0	100
905.1	0	0	0	100
993.6	0	0	0	100
1091	0	0	0	100
1197	0	0	0	100
1314	0	0	0	100
1443	0	0	0	100
1584	0	0	0	100
1739	0	0	0	100
1909	0	0	0	100

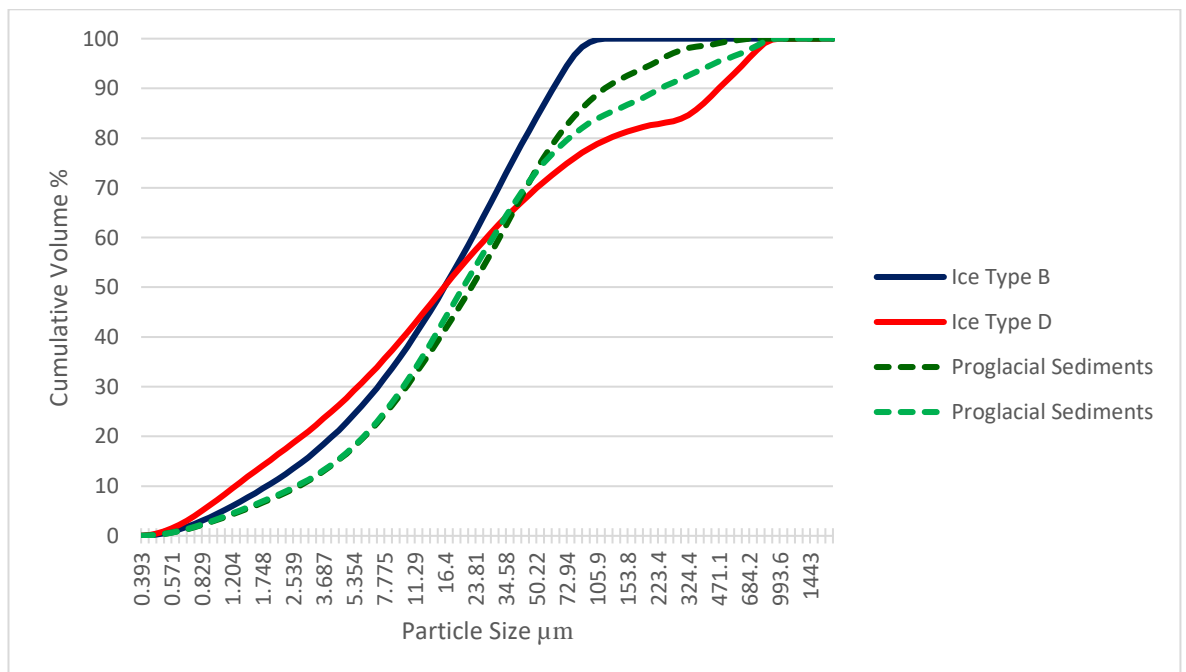
## Appendix B: Cumulative Volume Graphs

### APPENDIX B: CUMULATIVE GRAIN SIZE GRAPHS

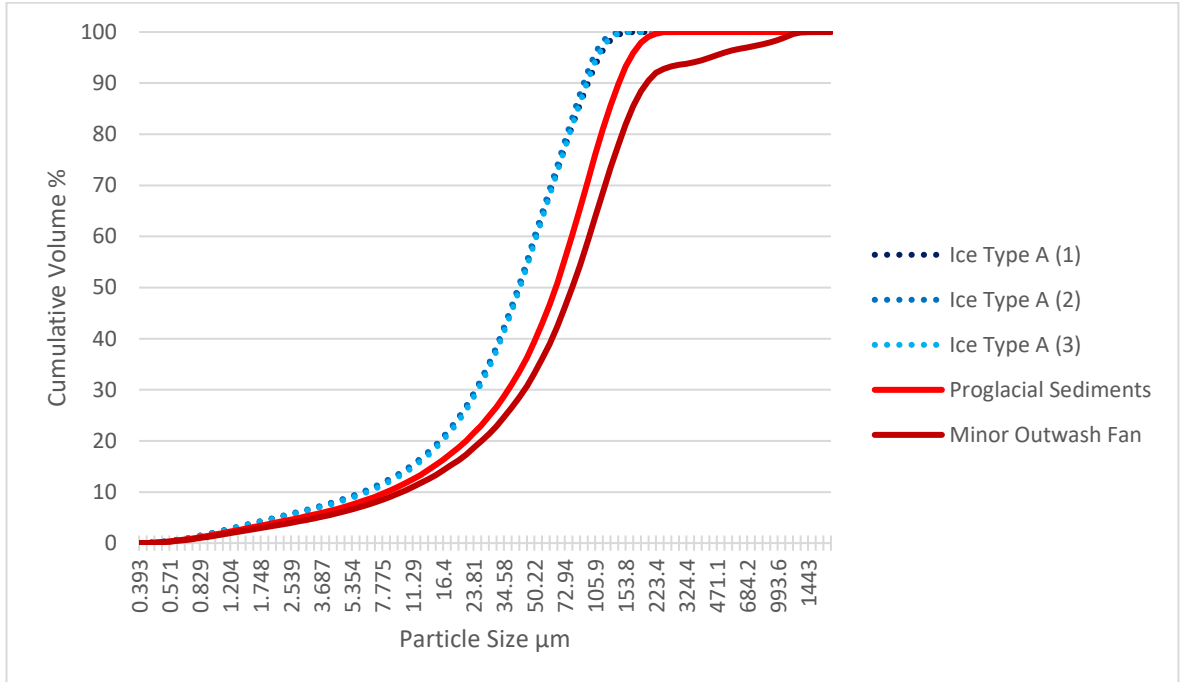
#### Site 1



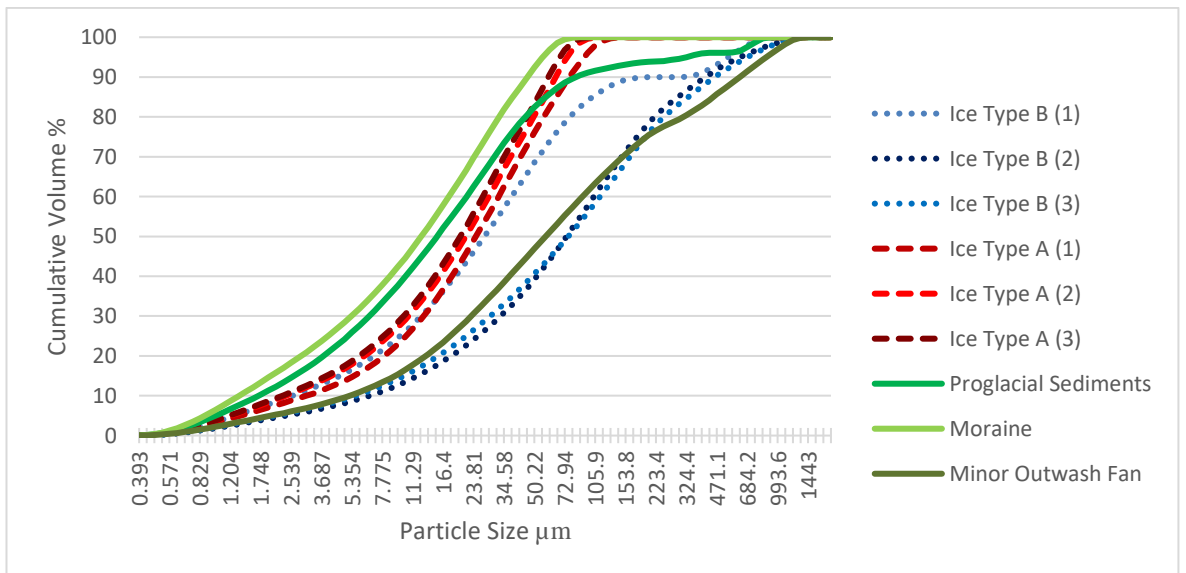
#### Site 2



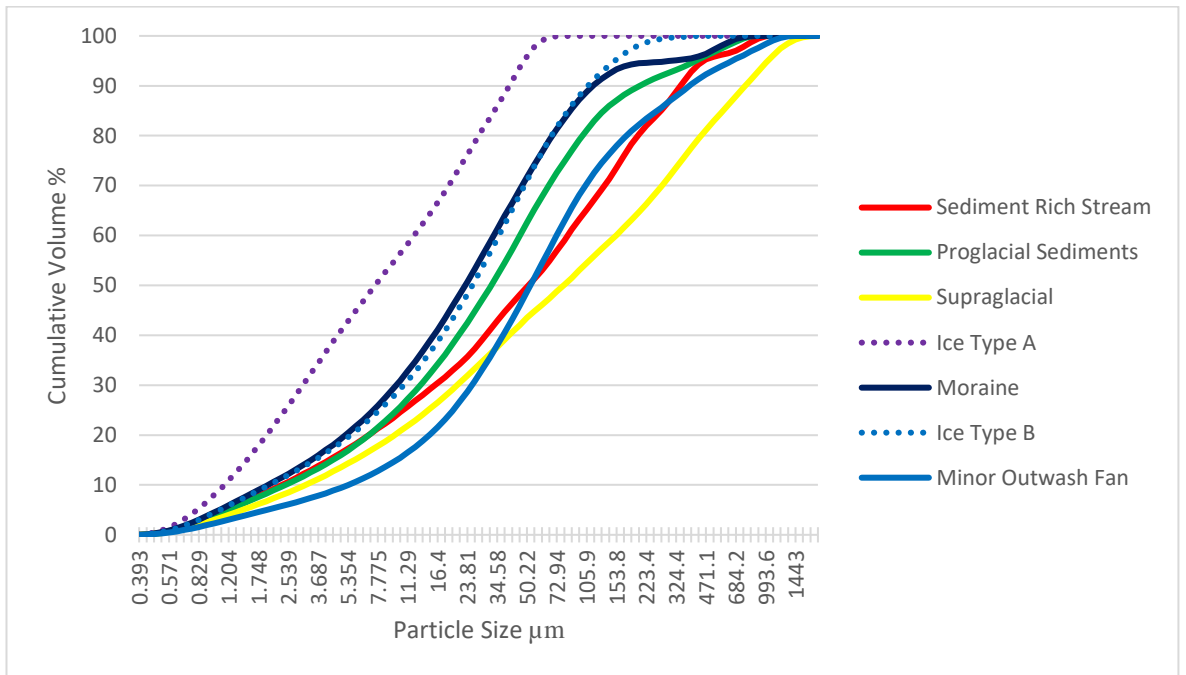
**Site 3**



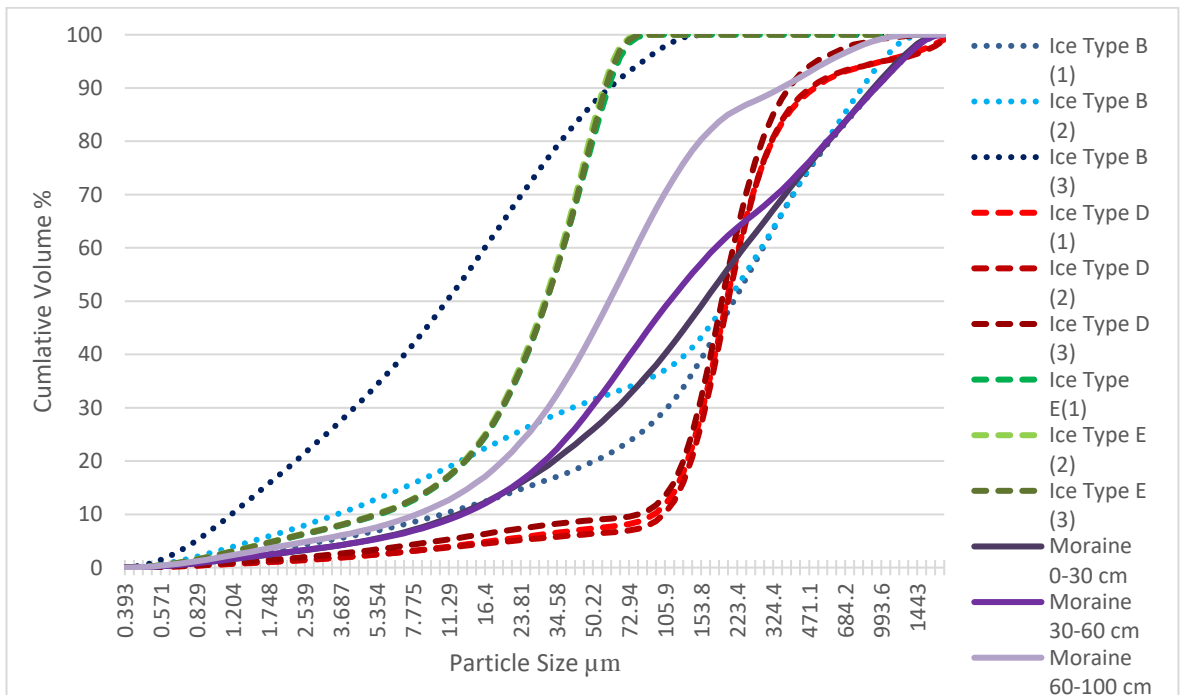
**Site 4**



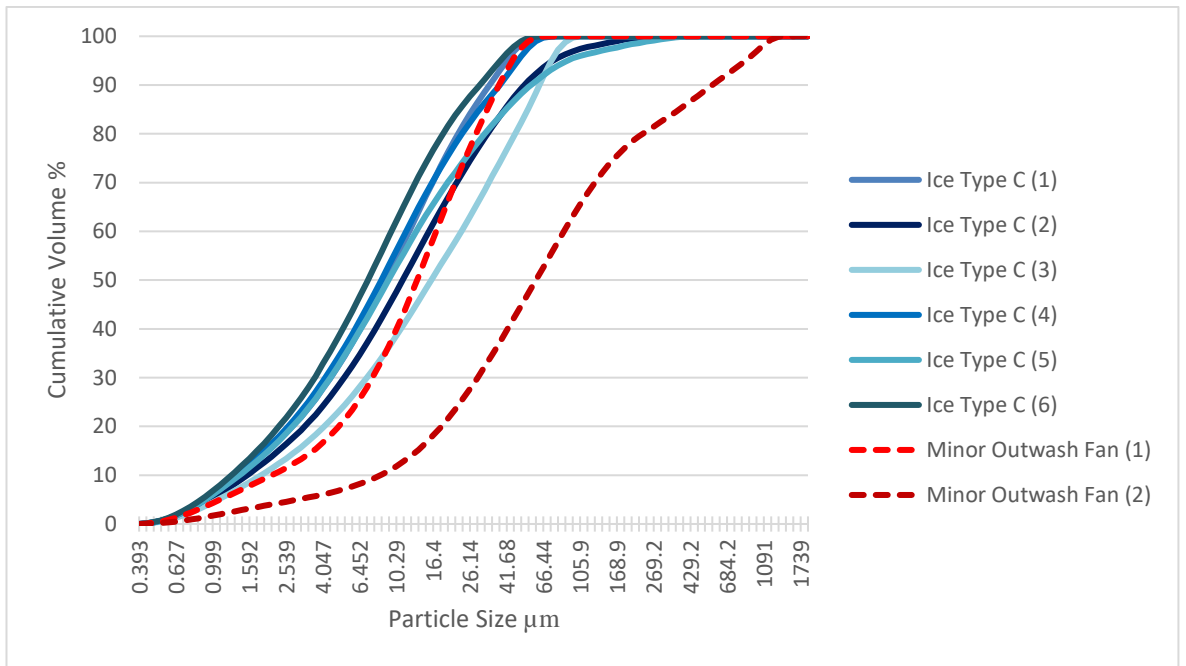
**Site 5**



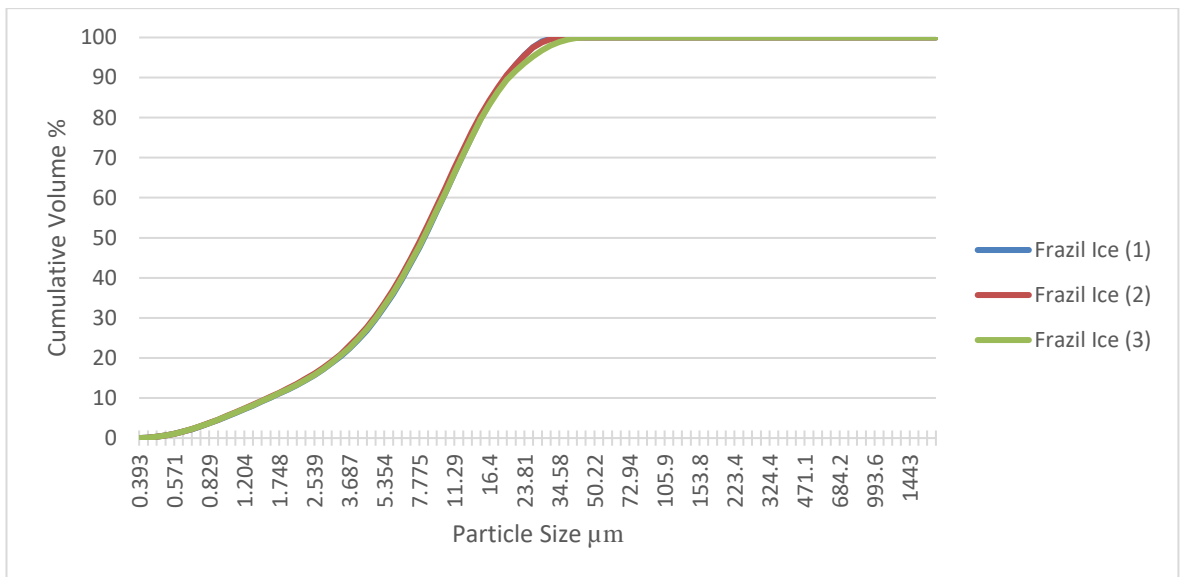
**Site 6**



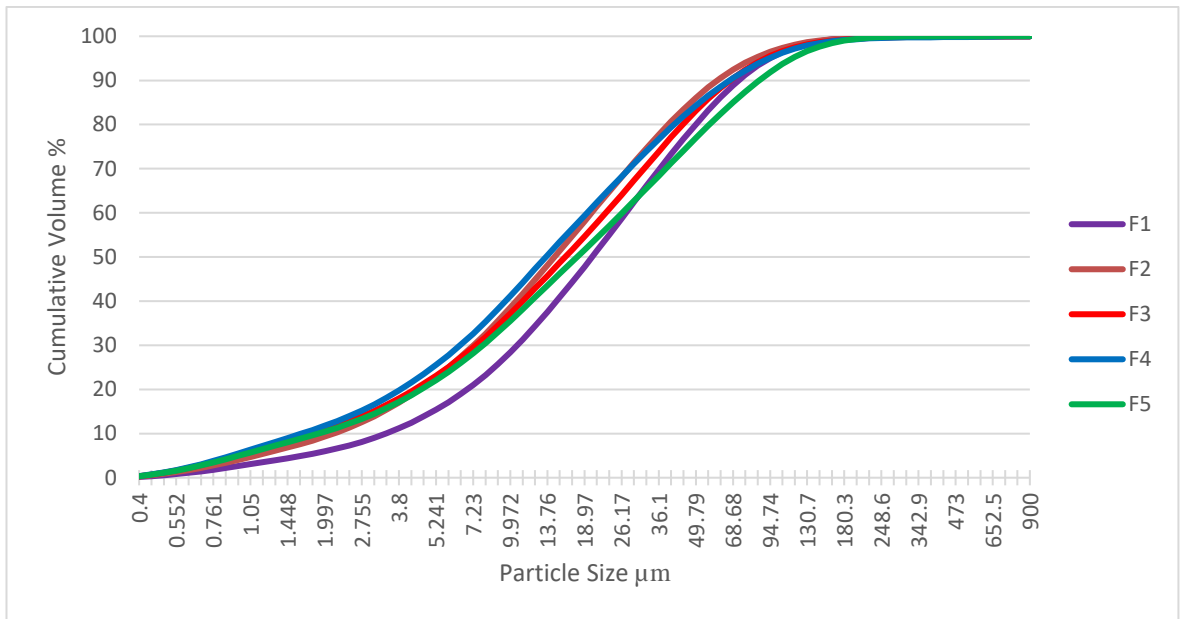
**Site 7**



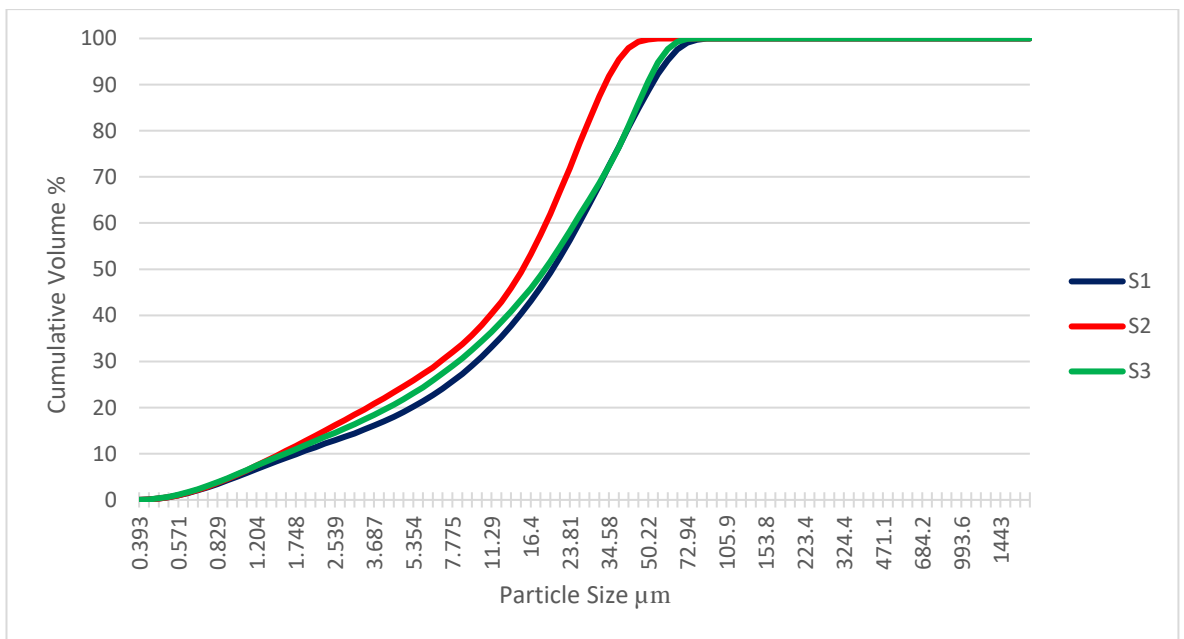
**Site 8**



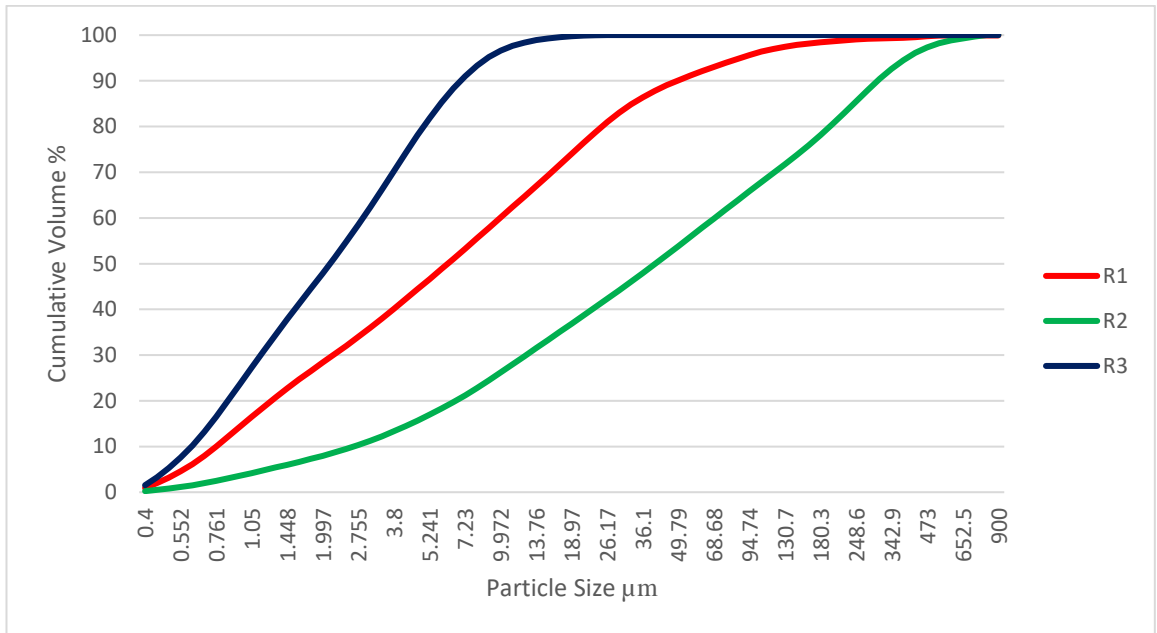
## Ferpècle



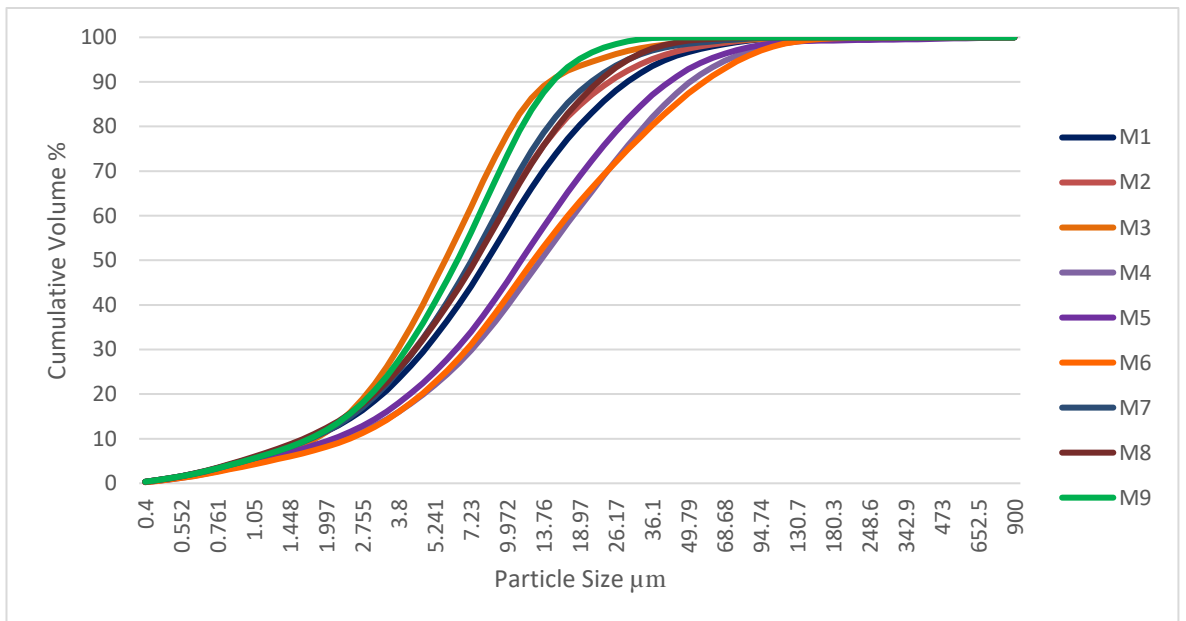
## Storglaciären



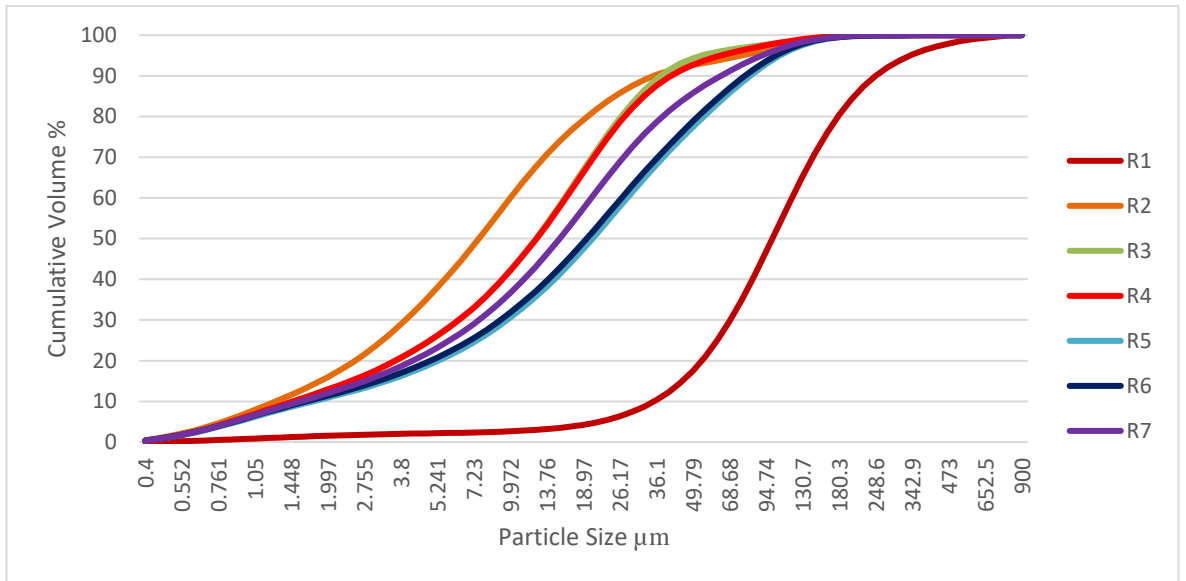
### Root Glacier



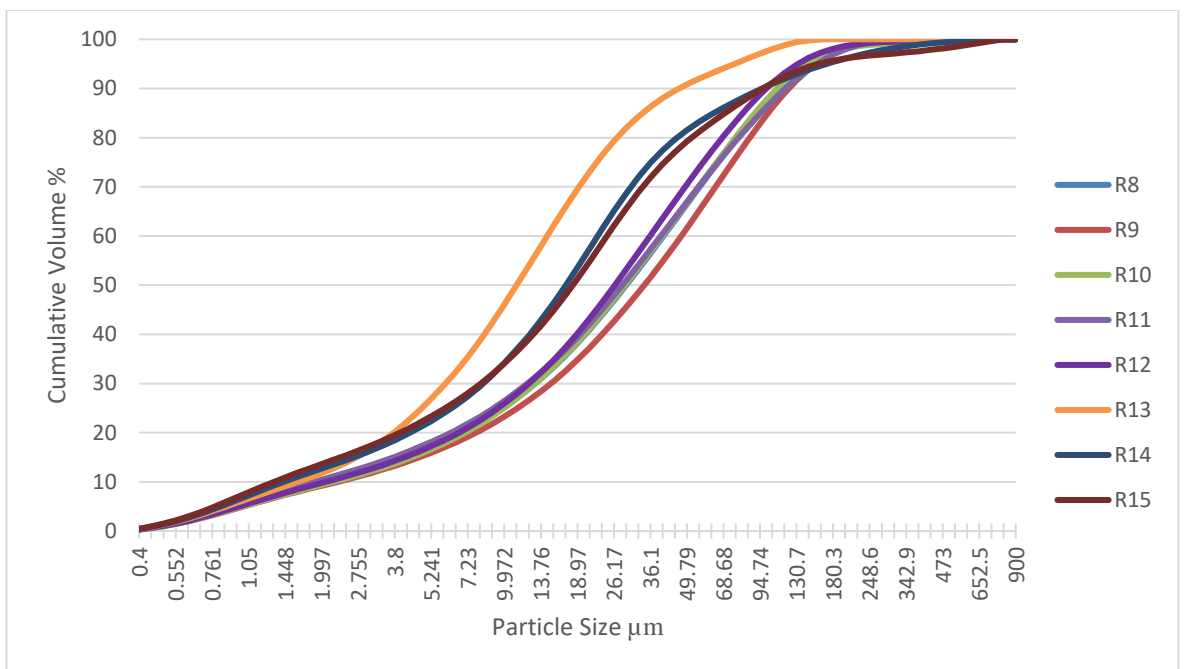
### Matanuska Glacier



**Russell Glacier Graph 1**



**Russell Glacier Graph 2**



## Skeiðarárjökull

